Molecular and physiological assessment of metabolic health

Adipose tissue, Transcriptome analysis and Challenge tests

Loes P.M. Duivenvoorde

Thesis committee

Promotor
Prof. Dr J. Keijer
Professor of Human and Animal Physiology
Wageningen University

Co-promotor
Dr E.M. van Schothorst
Assistant professor, Human and Animal Physiology
Wageningen University

Other members
Dr G. Goossens, Maastricht University
Prof. Dr A.H. Kersten, Wageningen University
Prof. Dr S. Klaus, German Institute of Human Nutrition, Potsdam, Germany
Dr P.Y. Wielinga, TNO-Metabolic Health Research, Leiden

This research was conducted under the auspices of the Graduate School of Wageningen Institute of Animal Sciences (WIAS)

Molecular and physiological assessment of metabolic health

Adipose tissue, Transcriptome analysis and Challenge tests

Loes P.M. Duivenvoorde

Thesis

submitted in fulfilment of the requirements for the degree of doctor
at Wageningen University
by the authority of the Rector Magnificus
Prof. Dr M.J. Kropff,
in the presence of the
Thesis Committee appointed by the Academic Board
to be defended in public
on Tuesday 26 May 2015
at 11 a.m. in the Aula.

Loes P.M. Duivenvoorde
Molecular and physiological assessment of metabolic health - Adipose tissue, Transcriptome analysis and Challenge tests,
186 pages.

PhD thesis, Wageningen University, Wageningen, NL (2015)
With references, with summaries in Dutch and English

ISBN 978-94-6257-301-7

Contents

Chapter 1

General introduction

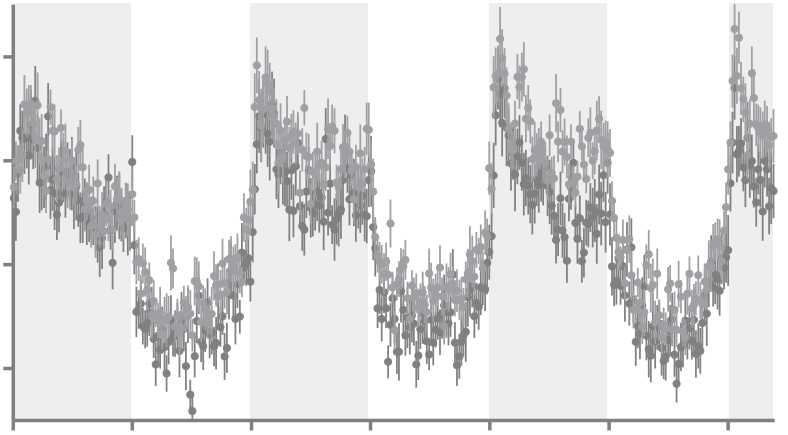

Metabolic health and metabolic flexibility

Metabolic health can be defined as the ability to properly adapt metabolism to variations in environmental and nutritional circumstances. A reduction in metabolic health can lead to several serious diseases, such as type 2 diabetes mellitus, gallbladder disease, coronary heart disease, dyslipidaemia, and osteoarthritis (33, 34, 38). Overweight and obesity are major risk factors for impaired metabolic health. The prevalence of obesity has increased dramatically over the past decades, probably because of the increased abundance of easily accessible, energy-dense food products and the increase in sedentary life-styles. As a result, about 35% of the world population is now classified as being overweight (15) and it is estimated that around 300,000 US adults die of causes attributable to obesity each year (31). Next to obesity, metabolic health can decline due to aging (36), physical inactivity (19) or by genetic predisposition (26).

Metabolic health can be measured as metabolic flexibility, which is the capacity to match substrate oxidation to substrate availability (24, 47). A subject that displays metabolic flexibility e.g. increases fat storage in adipose tissue when circulating fat levels are elevated and increases fat oxidation during fasting. Furthermore, in healthy individuals, insulin inhibits fatty acid oxidation and glucose oxidation is inhibited when fatty acid oxidation increases, which ensures predominantly fat oxidation during fasting and glucose oxidation during food intake or during vigorous physical activity (30, 41). Adequate regulation of glucose and fat oxidation prevents excessive accumulation of stored lipids and preserves glucose for essential tasks, such as intense physical exercise or brain functioning.

The high prevalence of obesity, but also the increase in mean life span in most developed countries (27), highly increased the proportion of humans that are at risk for impaired metabolic health. Research to better understand the factors that influence metabolic health may offer opportunities to confine this threat to human health worldwide.

White adipose tissue and metabolic health

White adipose tissue (WAT) plays an important role in energy homeostasis and maintenance of metabolic health. WAT mainly consists of lipid-loaded adipocytes, but also contains macrophages, pre-adipocytes, and neuronal, endothelial and epithelial cells. Adipocytes not only store excess energy in the form of triglycerides, but also have an important endocrine function. Adipocytes communicate with other organs via adipokines and lipokines, which are signalling molecules that are released in the circulation (1, 8, 50). Adipokines influence many other metabolic organs, such as the liver, muscle tissue and the hypothalamus, and can e.g. regulate appetite and energy expenditure, but also immune response, fertility, depression and anxiety (reviewed in 9, 23). Dysregulation of adipokine secretion is associated with reduced metabolic health. Leptin, for example, which is the first identified (59) and probably the best known

adipokine, is thought to be involved in the development of obesity and insulin resistance. In healthy subjects, leptin decreases appetite and increases energy expenditure (55), preventing further adipose mass expansion. In obese individuals, however, circulating leptin levels are elevated (12), but this does not lead to inhibition of appetite and the subsequent WAT expansion. Such deviations in adipokine signalling occur, in the first place, when adipose tissue mass expands. Leptin secretion simply increases when adipose mass, and therefore the productive capacity of the organ, increases (45). An increase in circulating adipokine levels may decrease sensitivity to the cytokine (35), which decreases the potential of WAT to regulate whole-body energy balance. Second, WAT functionality can be affected by internal factors, such as tissue inflammation. Obesity is, in fact, associated with chronic low-grade inflammation in adipose tissue (2, 14). WAT inflammation increases the release of inflammatory cytokines, such as tumor necrosis factor alpha (TNFα) and interleukin 6 (IL6) (58) and decreases the secretion of anti-inflammatory and insulin-sensitising adipokines, such as adiponectin (56). WAT inflammation is expected to play a causal role in the development of metabolic diseases, such as insulin resistance and other associated pathologies of obesity (22, 57) and might arise from local oxygen depletion (hypoxia) in WAT. Local hypoxia in WAT probably occurs because during WAT expansion, parts of the tissue become remote from the vascular supply, which leads to limitation of oxygen availability (51). Alternatively, WAT hypoxia may occur due to the enlargement of adipocytes (hypertrophy), reaching the diffusion limit for oxygen (48).

Excessive adipocyte hypertrophy also increases cell death and subsequent macrophage infiltration in WAT (10). WAT macrophages are recruited to phagocytose dying adipocytes and can be divided into two categories: pro-inflammatory M1 macrophages that are associated with obesity, and anti-inflammatory M2 macrophages that are more prevalent in healthy adipose tissue (28). Clusters of macrophages around death or dying adipocytes can be visualized with immunohistochemistry and are called crown like structures (CLSs, Figure 1).

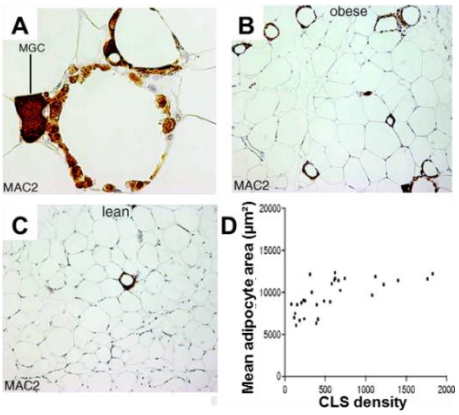

Figure 1 WAT macrophages and crown-like structures. Crown-like structures (CLSs) are clusters of macrophages around dying adipocytes. CLSs can be visualised with light microscopy and MAC-2 immunoreactive stainings (A). The number of CLSs in WAT is higher in obese mice (B) than in lean mice (C). White adipocyte size in mice positively correlates ($r = 0.72$, $P < 0.0001$) with the amount of CLSs in the fat depot (D). (adapted from (10) and (33))

The occurrence of enlarged adipocytes, moreover, indicates a reduced capacity to recruit new adipocytes via adipogenesis, which decreases the storage capacity of the tissue and promotes lipid storage in other organs, such as muscle tissue or the liver (21). Lipid accumulation in muscle and liver, or ectopic lipid accumulation, is associated with severe metabolic dysfunction (44).

To summarize, altered adipokine secretion, WAT inflammation and adipocyte hypertrophy indicate WAT dysfunction. WAT dysfunction is positively correlated with metabolic inflexibility and is, therefore, seen as an important hallmark of reduced metabolic health.

Mitochondrial function and metabolic health

To further understand the factors that influence metabolic health and metabolic flexibility, we should first focus on the cell organelle that stands at the basis of substrate selection and oxidation: the mitochondrion. Mitochondria are dynamic organelles that are essential for energy metabolism and also play an important role in apoptosis (54) and heat production (32). Mitochondria are responsible for efficient ATP production from acetyl-CoA, which can be derived from fat, sugar or protein catabolism (Figure 2). Mitochondria are surrounded by an inner and outer membrane; the inner membrane contains the respiratory complexes that are responsible for oxidative phosphorylation and ATP production. The mitochondrial matrix can be found inside the inner membrane and contains enzymes for i.e. the tricarboxylic acid (TCA) cycle, fatty acid oxidation and decarboxylation of pyruvate (from glucose or amino acid catabolism) (46). The conversion of fatty acids to acetyl-CoA during β-oxidation results in the formation of nicotinamide adenine dinucleotide (NADH) and flavin adenine dinucleotide ($FADH_2$). The conversion of acetyl-CoA to citrate and further oxidation to oxaloacetate in the TCA cycle (also known as the citric acid cycle or Krebs cycle) also results in the formation of NADH and $FADH_2$. NADH and $FADH_2$ are co-factors that carry hydrogens and electrons to the electron transport chain (ETC), or respiratory chain. Electrons can also be transferred directly from β-oxidation to the ETC via electron transfer flavoproteins. In the ETC, electrons are used to pump protons from the matrix to the intermembrane space, generating a potential difference across the inner mitochondrial membrane. The membrane potential is used to drive the synthesis of ATP in the final step of oxidative phosphorylation at complex V.

Oxygen is essential for the functioning of the ECT because it captures the electrons that emerge from the ETC. When oxygen availability is limited, the mitochondrial membrane potential increases and electrons may leak from the ETC, which results in the formation of reactive oxygen species (ROS) (Figure 3) (6). High levels of ROS cause cellular oxidative damage and are associated with metabolic disorders, such as insulin resistance and obesity (17, 43).

Mitochondria play an important role in metabolic flexibility because they can sense the cellular energy status and match ATP synthesis, metabolism, and other physiological

processes to energy requirements. Due to their capacity to complete either fat, sugar or protein oxidation, and their interconversions, mitochondria are crucial for cellular substrate selection. Mitochondrial β-oxidation and pyruvate oxidation, for example, directly respond to changes in mitochondrial fatty acid levels (40). Alterations in mitochondrial function and substrate switching are associated with several metabolic disorders, such as obesity and type 2 diabetes (25, 37).

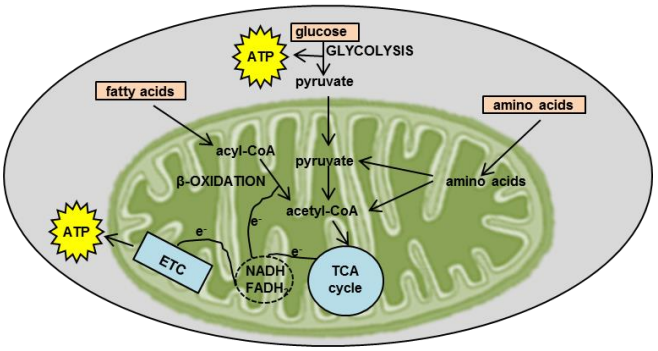

Figure 2 Cellular conversion of nutrients to ATP. Fatty acids, glucose and amino acids can be catabolised to acetyl-CoA, which is oxidized to carbon dioxide in the TCA cycle in the mitochondrial matrix. Both the TCA cycle and β-oxidation provide electrons and hydrogens to the electron transport chain (ETC) where ATP is produced through oxidative phosphorylation. A smaller amount of ATP is produced cytoplasmic by glycolysis of glucose into pyruvate.

Analysis of metabolic health

Metabolic health can be studied with various tools and methods. The choice for a certain method depends on the focus and aim of the study; there is no biomarker or test that singly defines metabolic health. Metabolic health can be studied directly in humans, but also other species can be used as a model for human health. Model organisms, such as laboratory mice or rats, are often used to study the molecular and physiological aspects of diseases, including obesity. Like humans, mice can become obese and display metabolic inflexibility when supplied with high-energy diets and the possibility to exercise is reduced (18, 49). Moreover, like many other mammals, metabolic health of mice greatly improves with dietary restriction, which is one of the best known methods to promote healthy aging in a variety of species (4). During dietary restriction, an animal receives only a proportion of its normal dietary intake, generally between 50 and 90%, which has been shown to improve metabolic health in mice, rats, nematodes, insects, fish, spiders (reviewed in 39) and, possibly, primates (11, 29). Although the best 'model' to study human metabolic health is generally considered to be the human itself, a big advantage of the use of model organisms is that most confounding factors, such as life style, education, dietary habits, social interactions, and physical activity, that highly influence health status can be levelled out or fully controlled. Mouse models are, therefore, a useful tool to characterize molecular and physiological aspects of metabolic health.

The methods to study metabolic health in mice can roughly be divided into two categories: methods that assess static parameters and methods that measure adaptive responses in the form of a challenge test.

Static measurements of metabolic health can focus on a single analyte, such as circulating insulin, glucose or adipokine levels during fasting. Also adipocyte size, the occurrence of CLSs in WAT and the level of ectopic lipid storage can be seen as static parameters to analyse metabolic health. Static measurements can, however, also involve analysis of multiple analytes in a single assay, e.g. with metabolomics, measuring metabolites, or with transcriptomics, measuring gene expression by its transcripts levels. The -omics approach is valuable since it extends the scale and depth of understanding biological processes.

Challenge tests measure the response to an environmental or nutritional stressor and are frequently used in nutritional research because they enlarge the effect of a nutritional intervention (52). Early diet-induced health effects are, in fact, often hidden under static conditions, but can be revealed under challenged conditions.

In this thesis we used whole-genome micro-arrays to study gene expression in WAT and evaluated and developed several challenge tests to measure metabolic flexibility in mice. Both approaches and the rationale to use those methods will now be explained in more detail.

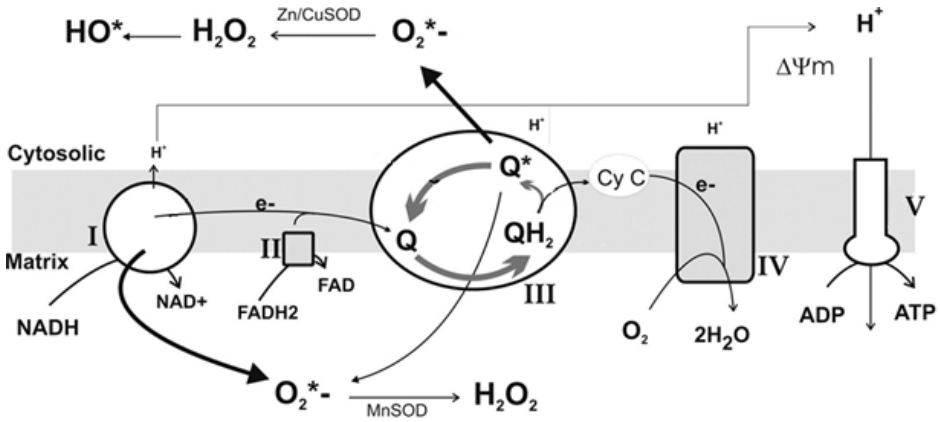

Figure 3 ROS formation in the electron transport chain. Reactive oxygen species (ROS) are continuously made as a side product of electron transport during oxidative phosphorylation. Oxidative stress may occur when ROS formation increases (when oxygen availability is either low or high or when the mitochondrial membrane potential (ΔΨm) increases or when antioxidant defences are hampered. Metabolic pathways supply electrons (e^-) and hydrogens (H^+) to complex I and II of the electron transport chain, where electrons are used to create a membrane potential that drives ATP synthesis via ATP synthase (complex V). Occasionally, electrons are transferred to oxygen to form superoxide (O_2^-) . O_2^- is mainly formed in complex I and III and is a precursor of most other reactive oxygen species, such as hydrogen peroxide (H_2O_2) by the enzyme superoxide dismutase (SOD), and the hydroxyl radical (OH) from the reduction of H_2O_2 by catalase or glutathione peroxidase (adapted from (7)).

Analysis of metabolic health with whole-genome analysis

With whole-genome gene expression analysis, mRNA levels of all known genes in a specific tissue can be measured within a single assay. The comparison between different (dietary) treatments and a control group indicates the impact of the treatment on gene expression. Changes in gene expression appear relatively short after exposure

to a treatment. Food consumption after a period of fasting, for example, increases the expression of several genes involved in protein synthesis already 1.5 hours after food provision (13). Gene expression, therefore, displays acute metabolic adaptation. An increase in gene expression mostly leads to an increase in protein abundance of the encoded protein (53), revealing which (metabolic) process is mostly affected by the treatment. Transcriptome analysis, moreover, does not only reveal which genes respond to a certain (dietary) treatment, but also reveals when a treatment group fails to respond to the treatment, which can either implicate health improvement or health deterioration. Mice fed a low-calorie diet, for example, have a different transcriptomic profile compared with mice fed a high-calorie diet. High-caloric intake e.g. increases lipid metabolism and mitochondrial oxidative phosphorylation in liver, but this profile is shifted back towards the low-calorie profile when the high-calorie diet is supplemented with a substance that improves metabolic health, such as resveratrol (3).

The enormous amount of data that results from transcriptome analysis can be used as a strategy to 'fish' for results, in which new candidate biomarker genes or pathways for a certain treatment or condition can be identified, or as a strategy to 'hunt' for results, in which the effect of a treatment on one or several specific metabolic genes or pathways is requested. The possibility to measure thousands of end points in one single assay, makes transcriptome analysis very suitable to study the effect of dietary or environmental treatments on metabolic health, especially when combined with additional assays that link the molecular response to a relevant physiological response.

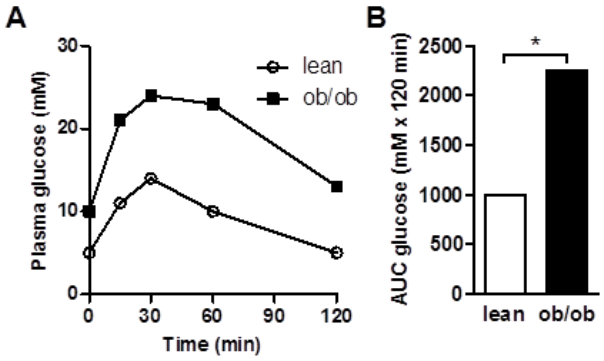

Figure 4 Glucose tolerance of lean and obese mice. Example of an oral glucose tolerance test in lean and genetically obese (ob/ob) mice. The time course following glucose administration (A) represents uptake of glucose to and from the blood stream. The curve of blood glucose levels can also be expressed as the area under the curve (AUC) (B), in which glucose intolerant mice have a larger AUC (data from (5)).

Analysis of metabolic health with challenge tests

Transcriptome analysis reveals all changes in gene expression that are affected by an experimental intervention in a specific organ. Metabolic health, however, also highly depends on the adaptive capacity of the body as a whole. This thesis, therefore, also focusses on the development and characterization of challenge tests to study metabolic health at whole body-level. Challenge tests disrupt homeostasis with an environmental or nutritional stressor, which triggers an animal to change its metabolism and prevent accumulation of harmful substances or other unfavourable physiological states.

Animals that are metabolically healthy and flexible can adequately adapt to the challenge test and maintain homeostasis. Individuals that are less flexible cannot adapt adequately and will display an aberrant response. One of the best-known challenge tests to measure metabolic flexibility is the oral glucose tolerance test (OGTT; Figure 4). For an OGTT, mice are fasted and receive an oral dose of glucose. Baseline (fasting) blood glucose measurements are taken before glucose administration, and further measurements are made at regular intervals thereafter. An OGTT reveals the rate of glucose uptake in the intestine and the release of glucose to and from the bloodstream, but especially the insulin-stimulated uptake in peripheral organs like muscle and adipose tissue. This depends on the release of insulin from the pancreas in response to circulating glucose and on the sensitivity of target tissues to insulin.

Challenge tests are, indeed, helpful to reveal relevant impairments in energy homeostasis. A disadvantage of many used challenge tests, however, is the requirement of invasive methods, such as injection, blood sampling or oral gavage. These invasive methods induce stress and modify the physiological status, which does not only affect animal wellbeing but also increases variability of experimental data and reduces data quality and reproducibility. For this thesis we, therefore, aimed to identify and evaluate non-invasive methods to assess metabolic flexibility in mice. For this purpose we used indirect calorimetry (InCa) to monitor the response to a challenge. Three InCa-based challenge tests were used: a challenge with glucose consumption, fasting followed by re-feeding, and an environmental challenge with oxygen restriction. Each challenge test and the principle of InCa will now be described in more detail.

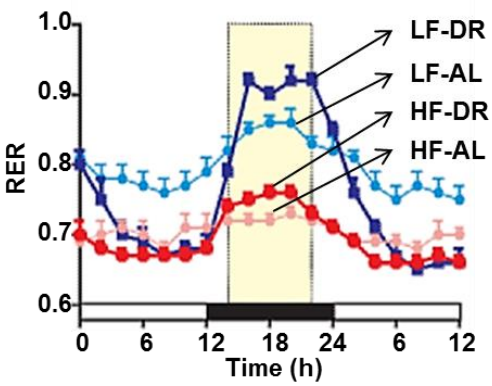

Figure 5 RER during restricted or *ad libitum* feeding of a high- or low-fat diet. The RER after food consumption depends on diet composition. High-fat or high-calorie rodent diets generally contain less carbohydrates than low-fat or low-calorie diets. Consequently, mice that receive a low-fat-diet *ad libitum* (LF-AL) or restricted (LF-DR) reach higher mean RER values than mice that receive a high-fat diet at *ad libitum* (HF-AL) or dietary restricted (HF-DR) basis. (adapted from (20)). Restricted feed is accessible during time frame indicated in yellow.

Indirect calorimetry and non-invasive challenge tests

Indirect calorimetry is a non-invasive method to estimate energy metabolism based on oxygen consumption and carbon dioxide production. InCa can be used to calculate real-time energy expenditure and substrate use (reviewed by 16). Rodent InCa systems have evolved over the past decades towards a system in which mice can remain in their home cage and only the cage lid is replaced to enable controlled air flow and air sampling from the cage. Energy expenditure depends on metabolic rate, diet-induced

thermogenesis and physical activity (42). The ratio of carbon dioxide production over oxygen consumption, also known as the respiratory quotient (RQ) at the cellular level; or respiratory exchange ratio (RER) at whole body level, displays which macronutrient is mainly being oxidized. Fat oxidation requires, compared with glucose oxidation, more oxygen per mole carbon dioxide produced. The RQ or RER depends on mitochondrial substrate selection and equals 1 for primarily glucose oxidation and 0.7 for primarily fat oxidation. In normal subjects, protein catabolism only contributes around 1% to the total energy expenditure and increases only during prolonged starvation. Therefore, when fat and glycogen stores are not depleted, fatty acids, glucose and oxygen form the principal substrates for mitochondrial energy production. Restriction or rather (re)-supplementation of either of these mitochondrial substrates requires metabolic adaptation and forms the basis of most InCa-based challenge tests. Fasting, for example, causes RER values to decrease towards 0.7 in mice, whereas re-feeding increases the RER, in which the amplitude of the increase depends on the carbohydrate content of the diet (Figure 5). The higher the carbohydrate content of the meal consumed, the larger the increase in RER should be - if metabolism adapts properly. This principle forms the basis of most nutrient-based challenge tests in the InCa system, in which mice are fasted and then re-supplied with feed. Re-feeding can occur with a single nutrient, such as glucose, or a combination of nutrients, such as rodent chow. A delay, reduction or absence in the response to re-feeding indicates an incapacity to switch from fat oxidation during fasting to carbohydrate oxidation during feeding, which is an important hallmark of metabolic inflexibility.

Next to nutrient-based challenge tests, InCa can also be used to assess the response to an environmental challenge, e.g. a change in ambient temperature, humidity, duration of the light-dark cycle or in oxygen levels.

In this thesis a reduction in oxygen availability (oxygen restriction; OxR) was used as a novel non-invasive InCa-based challenge test. During OxR, mice remain in a fasted state but the possibility to maintain ATP production via mitochondrial oxidation is reduced. Strategies to match energy metabolism to oxygen availability and possible deviations in the capacity to respond to oxygen restriction are largely unknown, which motivated the design and validation of a metabolic challenge test based on OxR. An adequate response to OxR may include a reduction of total metabolic rate or changes in mitochondrial substrate use or in total mitochondrial activity.

Aims and outline of this thesis

Detailed understanding of the factors that influence metabolic health will contribute to the development of interventions that improve metabolic health and thus to a decrease in the prevalence of metabolic diseases. Transcriptome analysis is a well-established method to evaluate genome-wide gene expression and can be used to increase the scale and depth of understanding biological processes underlying metabolic health. Challenge tests are able to detect physiological differences before static (health)

markers are changed and physical differences that are obscured under static conditions. We, therefore, aim to assess metabolic health using transcriptome analysis and non-invasive challenge tests. Special focus is on the development and validation of InCa-based non-invasive challenge tests. Next to the validation of two nutrient-based challenge tests (based on fasting and re-feeding, and fasting and glucose consumption), this thesis introduces a novel challenge test that is based on exposure to OxR.

Chapter 2 aimed to assess metabolic health effects of dietary restriction of a high fat diet and to identify associated molecular changes in WAT. Metabolic health was analysed with several conventional health markers, such as oral glucose tolerance and circulating glucose and adipokine levels. Whole genome gene expression in WAT was used to identify the molecular changes underlying alterations in metabolic health. **Chapter 3** aimed to assess whether InCa could be used to measure age-impaired metabolic health in mice. The aging-model was used as a first validation of OxR as a novel, non-nutrient based challenge test in comparison to two other InCa-based health assessment approaches. **Chapter 4** continues with the OxR challenge and aimed to assess whether OxR can be used to distinguish changes in metabolic health that are caused by short term overfeeding. Metabolic flexibility was measured in mice that were either fed a moderate high-fat diet or a low-fat diet for only five days. The potential to use OxR to detect early health effects decreases costs and may facilitate health improvement strategies. After the promising effects in chapter 3 and 4, the OxR challenge was used in **chapter 5** to assess differences in metabolic health of two isocaloric high fat diets differing only in fatty acid profile. In addition to the OxR challenge, metabolic flexibility was tested with a fasting and re-feeding challenge and several conventional methods to analyse metabolic health, such as the analysis of body composition, glucose tolerance and WAT health, which enabled us to make a direct comparison. Finally, **chapter 6** aimed to increase our understanding of the OxR challenge by analysis of whole genome gene expression in WAT and by analysis of WAT and circulating metabolites. **Chapter 7** consists of a discussion of the research presented in this thesis.

References

1. Ahima RS, Flier JS Adipose tissue as an endocrine organ. Trends in Endocrinology and Metabolism. 2000;11: 327-332.
2. Bastard JP, Jardel C, Bruckert E, Blondy P, Capeau J, Laville M*, et al.* Elevated levels of interleukin 6 are reduced in serum and subcutaneous adipose tissue of obese women after weight loss. Journal of Clinical Endocrinology & Metabolism. 2000;85: 3338-3342.
3. Baur JA, Pearson KJ, Price NL, Jamieson HA, Lerin C, Kalra A*, et al.* Resveratrol improves health and survival of mice on a high-calorie diet. Nature. 2006;444: 337-342.
4. Bordone L, Guarente L Calorie restriction, SIRT1 and metabolism: understanding longevity. Nat Rev Mol Cell Biol. 2005;6: 298-305.
5. Bowe JE, Franklin ZJ, Hauge-Evans AC, King AJ, Persaud SJ, Jones PM METABOLIC PHENOTYPING GUIDELINES Assessing glucose homeostasis in rodent models. Journal of Endocrinology. 2014;222: G13-G25.
6. Brand MD, Affourtit C, Esteves TC, Green K, Lambert AJ, Miwa S*, et al.* Mitochondrial superoxide: Production, biological effects, and activation of uncoupling proteins. Free Radical Biology and Medicine. 2004;37: 755-767.
7. Camello-Almaraz C, Gomez-Pinilla PJ, Pozo MJ, Camello PJ Mitochondrial reactive oxygen species and Ca2+ signaling. American Journal of Physiology-Cell Physiology. 2006;291: C1082-C1088.
8. Cao H, Gerhold K, Mayers JR, Wiest MM, Watkins SM, Hotamisligil GS Identification of a lipokine, a lipid hormone linking adipose tissue to systemic metabolism. Cell. 2008;134: 933-944.
9. Cao HM Adipocytokines in obesity and metabolic disease. Journal of Endocrinology. 2014;220: T47-T59.
10. Cinti S, Mitchell G, Barbatelli G, Murano I, Ceresi E, Faloia E*, et al.* Adipocyte death defines macrophage localization and function in adipose tissue of obese mice and humans. J Lipid Res. 2005;46: 2347-2355.
11. Colman RJ, Beasley TM, Kemnitz JW, Johnson SC, Weindruch R, Anderson RM Caloric restriction reduces age-related and all-cause mortality in rhesus monkeys. Nat Commun. 2014;5: 3557.
12. Considine RV, Sinha MK, Heiman ML, Kriauciunas A, Stephens TW, Nyce MR*, et al.* Serum immunoreactive-leptin concentrations in normal-weight and obese humans. N Engl J Med. 1996;334: 292-295.
13. Dhahbi JM, Cao SX, Mote PL, Rowley BC, Wingo JE, Spindler SR Postprandial induction of chaperone gene expression is rapid in mice. J Nutr. 2002;132: 31-37.
14. Festa A, D'Agostino R, Williams K, Karter AJ, Mayer-Davis EJ, Tracy RP*, et al.* The relation of body fat mass and distribution to markers of chronic inflammation. International Journal of Obesity. 2001;25: 1407-1415.
15. Finucane MM, Stevens GA, Cowan MJ, Danaei G, Lin JK, Paciorek CJ*, et al.* National, regional, and global trends in body-mass index since 1980: systematic analysis of health examination surveys and epidemiological studies with 960 country-years and 9.1 million participants. Lancet. 2011;377: 557-567.
16. Frankenfield DC On heat, respiration, and calorimetry. Nutrition. 2010;26: 939-950.
17. Furukawa S, Fujita T, Shimabukuro M, Iwaki M, Yamada Y, Nakajima Y*, et al.* Increased oxidative stress in obesity and its impact on metabolic syndrome. J Clin Invest. 2004;114: 1752-1761.
18. Gallou-Kabani C, Vige A, Gross MS, Rabes JP, Boileau C, Larue-Achagiotis C*, et al.* C57BL/6J and A/J mice fed a high-fat diet delineate components of metabolic syndrome. Obesity (Silver Spring). 2007;15: 1996-2005.
19. Hamburg NM, McMackin CJ, Huang AL, Shenouda SM, Widlansky ME, Schulz E*, et al.* Physical inactivity rapidly induces insulin resistance and microvascular dysfunction in healthy volunteers. Arterioscler Thromb Vasc Biol. 2007;27: 2650-2656.
20. Hatori M, Vollmers C, Zarrinpar A, DiTacchio L, Bushong EA, Gill S*, et al.* Time-Restricted Feeding without Reducing Caloric Intake Prevents Metabolic Diseases in Mice Fed a High-Fat Diet. Cell Metab. 2012;15: 848-860.

21. Heilbronn L, Smith SR, Ravussin E Failure of fat cell proliferation, mitochondrial function and fat oxidation results in ectopic fat storage, insulin resistance and type II diabetes mellitus. Int J Obes Relat Metab Disord. 2004;28 Suppl 4: S12-21.
22. Hotamisligil GS Inflammatory pathways and insulin action. International Journal of Obesity. 2003;27: S53-S55.
23. Houseknecht KL, Baile CA, Matteri RL, Spurlock ME The biology of leptin: A review. Journal of Animal Science. 1998;76: 1405-1420.
24. Kelley DE, Mandarino LJ Fuel selection in human skeletal muscle in insulin resistance - A reexamination. Diabetes. 2000;49: 677-683.
25. Koves TR, Ussher JR, Noland RC, Slentz D, Mosedale M, Ilkayeva O*, et al.* Mitochondrial overload and incomplete fatty acid oxidation contribute to skeletal muscle insulin resistance. Cell Metab. 2008;7: 45-56.
26. Kraja AT, Chasman DI, North KE, Reiner AP, Yanek LR, Kilpelainen TO*, et al.* Pleiotropic genes for metabolic syndrome and inflammation. Mol Genet Metab. 2014;112: 317-338.
27. Leon DA Trends in European life expectancy: a salutary view. Int J Epidemiol. 2011;40: 271-277.
28. Lumeng CN, Bodzin JL, Saltiel AR Obesity induces a phenotypic switch in adipose tissue macrophage polarization. Journal of Clinical Investigation. 2007;117: 175-184.
29. Mattison JA, Roth GS, Beasley TM, Tilmont EM, Handy AM, Herbert RL*, et al.* Impact of caloric restriction on health and survival in rhesus monkeys from the NIA study. Nature. 2012;489: 318-321.
30. McGarry JD Dysregulation of fatty acid metabolism in the etiology of type 2 diabetes. Diabetes. 2002;51: 7-18.
31. Mokdad AH, Serdula MK, Dietz WH, Bowman BA, Marks JS, Koplan JP The continuing epidemic of obesity in the United States. JAMA. 2000;284: 1650-1651.
32. Mozo J, Emre Y, Bouillaud F, Ricquier D, Criscuolo F Thermoregulation: what role for UCPs in mammals and birds? Biosci Rep. 2005;25: 227-249.
33. Murano I, Barbatelli G, Parisani V, Latini C, Muzzonigro G, Castellucci M*, et al.* Dead adipocytes, detected as crown-like structures, are prevalent in visceral fat depots of genetically obese mice. J Lipid Res. 2008;49: 1562-1568.
34. Must A, Spadano J, Coakley EH, Field AE, Colditz G, Dietz WH The disease burden associated with overweight and obesity. JAMA. 1999;282: 1523-1529.
35. Myers MG, Cowley MA, Munzberg H Mechanisms of leptin action and leptin resistance. Annu Rev Physiol. 2008;70: 537-556.
36. Petersen KF, Befroy D, Dufour S, Dziura J, Ariyan C, Rothman DL*, et al.* Mitochondrial dysfunction in the elderly: possible role in insulin resistance. Science. 2003;300: 1140-1142.
37. Peterson LR, Herrero P, Schechtman KB, Racette SB, Waggoner AD, Kisrieva-Ware Z*, et al.* Effect of obesity and insulin resistance on myocardial substrate metabolism and efficiency in young women. Circulation. 2004;109: 2191-2196.
38. Poirier P, Giles TD, Bray GA, Hong Y, Stern JS, Pi-Sunyer FX*, et al.* Obesity and cardiovascular disease: pathophysiology, evaluation, and effect of weight loss: an update of the 1997 American Heart Association Scientific Statement on Obesity and Heart Disease from the Obesity Committee of the Council on Nutrition, Physical Activity, and Metabolism. Circulation. 2006;113: 898-918.
39. Ramsey JJ, Harper ME, Weindruch R Restriction of energy intake, energy expenditure, and aging. Free Radic Biol Med. 2000;29: 946-968.
40. Randle PJ Regulatory interactions between lipids and carbohydrates: the glucose fatty acid cycle after 35 years. Diabetes-Metabolism Reviews. 1998;14: 263-283.
41. Randle PJ Regulatory interactions between lipids and carbohydrates: The glucose fatty acid cycle after 35 years. Diabetes-Metabolism Reviews. 1998;14: 263-283.
42. Ravussin E, Lillioja S, Anderson TE, Christin L, Bogardus C Determinants of 24-Hour Energy-Expenditure in Man - Methods and Results Using a Respiratory Chamber. Journal of Clinical Investigation. 1986;78: 1568-1578.
43. Rudich A, Tirosh A, Potashnik R, Hemi R, Kanety H, Bashan N Prolonged oxidative stress impairs insulin-induced GLUT4 translocation in 3T3-L1 adipocytes. Diabetes. 1998;47: 1562-1569.
44. Savage DB, Petersen KF, Shulman GI Disordered lipid metabolism and the pathogenesis of insulin resistance. Physiological Reviews. 2007;87: 507-520.

45. Shimizu H, Shimomura Y, Hayashi R, Ohtani K, Sato N, Futawatari T, *et al.* Serum leptin concentration is associated with total body fat mass, but not abdominal fat distribution. International Journal of Obesity. 1997;21: 536-541.
46. Srere PA The Infrastructure of the Mitochondrial Matrix. Trends in Biochemical Sciences. 1980;5: 120-121.
47. Storlien L, Oakes ND, Kelley DE Metabolic flexibility. Proceedings of the Nutrition Society. 2004;63: 363-368.
48. Sun K, Kusminski CM, Scherer PE Adipose tissue remodeling and obesity. Journal of Clinical Investigation. 2011;121: 2094-2101.
49. Surwit RS, Kuhn CM, Cochrane C, McCubbin JA, Feinglos MN Diet-induced type II diabetes in C57BL/6J mice. Diabetes. 1988;37: 1163-1167.
50. Trayhurn P, Beattie JH Physiological role of adipose tissue: white adipose tissue as an endocrine and secretory organ. Proceedings of the Nutrition Society. 2001;60: 329-339.
51. Trayhurn P, Wood IS Adipokines: inflammation and the pleiotropic role of white adipose tissue. British Journal of Nutrition. 2004;92: 347-355.
52. van Ommen B, Keijer J, Heil SG, Kaput J Challenging homeostasis to define biomarkers for nutrition related health. Mol Nutr Food Res. 2009;53: 795-804.
53. Vogel C, Marcotte EM Insights into the regulation of protein abundance from proteomic and transcriptomic analyses. Nat Rev Genet. 2012;13: 227-232.
54. Wang X The expanding role of mitochondria in apoptosis. Genes Dev. 2001;15: 2922-2933.
55. Williams KW, Scott MM, Elmquist JK From observation to experimentation: leptin action in the mediobasal hypothalamus. Am J Clin Nutr. 2009;89: 985S-990S.
56. Ye J, Gao Z, Yin J, He Q Hypoxia is a potential risk factor for chronic inflammation and adiponectin reduction in adipose tissue of ob/ob and dietary obese mice. Am J Physiol Endocrinol Metab. 2007;293: E1118-1128.
57. Yudkin JS Adipose tissue, insulin action and vascular disease: inflammatory signals. Int J Obes Relat Metab Disord. 2003;27 Suppl 3: S25-28.
58. Yudkin JS, Stehouwer CD, Emeis JJ, Coppack SW C-reactive protein in healthy subjects: associations with obesity, insulin resistance, and endothelial dysfunction: a potential role for cytokines originating from adipose tissue? Arterioscler Thromb Vasc Biol. 1999;19: 972-978.
59. Zhang YY, Proenca R, Maffei M, Barone M, Leopold L, Friedman JM Positional Cloning of the Mouse Obese Gene and Its Human Homolog. Nature. 1994;372: 425-432.

Chapter 2

Dietary restriction of mice on a high-fat diet induces substrate efficiency and improves metabolic health.

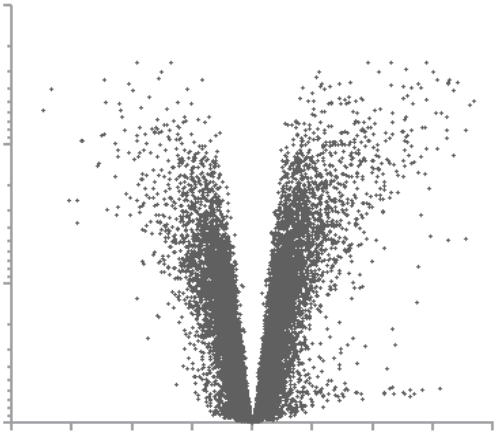

Loes P.M. Duivenvoorde, Evert M. van Schothorst, Annelies Bunschoten, and Jaap Keijer

Published in: Journal of Molecular Endocrinology (2011) 47, 81–97

Abstract

High energy intake and, specifically, high dietary fat intake challenges the mammalian metabolism and correlates with many metabolic disorders, such as obesity and diabetes. Dietary restriction (DR) is, on the other hand, known to prevent the development of metabolic disorders. The current Western diets are highly enriched in fat and it is as yet unclear whether DR on a certain high-fat (HF) diet elicits similar beneficial effects on health. Here, we report that HF-DR improves metabolic health of mice, compared to mice receiving the same diet on an *ad libitum* basis (HF-AL). Already after five weeks of restriction the serum levels of cholesterol and leptin were significantly decreased in HF-DR mice, while their glucose sensitivity and serum adiponectin levels were increased. The body weight and measured serum parameters remained stable in the following 7 weeks of restriction, implying metabolic adaptation. To understand the molecular events associated with this adaptation, we analysed gene expression in white adipose tissue (WAT) with whole genome microarrays. HF-DR strongly influenced gene expression in WAT; in total 8,643 genes were differentially expressed between both groups of mice, with a major role for genes involved in lipid metabolism and mitochondrial functioning. This was confirmed by qRT-PCR and substantiated by an increase in mitochondrial density in WAT of HF-DR mice. These results provide new insights in the metabolic flexibility of dietary restricted animals and suggest the development of substrate efficiency.

Introduction

Obesity is a major health concern that affects millions of people worldwide (26, 42). While white adipose tissue (WAT) plays an important role in mammalian energy homeostasis by preventing lipotoxicity and providing a source of energy in times of need, excess amounts of WAT relate to reduction in the number of mitochondria and inflammation of the tissue (9, 54), subsequently resulting in metabolic dysfunction (23, 58). Obesity is associated with several serious complications; including type 2 diabetes, coronary heart disease, and certain types of cancer; and therefore significantly increases morbidity risks into those affected (55). The current prevalence of obesity most likely resulted from the notable decrease in overall physical activity and increase in consumption of readily available energy dense foods (30). Fast foods, for example, as supplied by some typical outlets, contain an average energy density that is more than twice the energy density of a recommended healthy diet; and the energy density of food highly correlates with the fat content of a meal (48). Consistently, the WHO concluded that, in the period from 2000 to 2003, the average European diet consisted of 35-40% of energy available from fat; in France and Spain this proportion was even higher (67).

Restriction on dietary intake (DR) is known to robustly improve metabolic health (32, 50). Long term DR extends maximum lifespan and opposes the development of a broad array of age-associated biological and pathological changes in a diverse range of organisms (65). Dietary restriction studies in mice and other species have led to detailed descriptions of changes in gene expression in different tissues (15, 31, 32, 37, 63) and various mechanisms that are implicated in the beneficial health effects. Among the DR-related biomarkers are an increase in mitochondrial density in adipocytes (28) and an increase in insulin sensitivity (29). Most studies examining the effects of DR, however, have been performed in standard rodent diets that are characterized by a low fat content (7-9 en%). Only few studies focused on the effect of dietary restriction using high fat diets (HF-DR) (11, 21, 47); which is, in fact, more relevant to the current dietary status in most developed countries.

Here, we therefore examined the effects of DR in the context of a semi-synthetic AIN93 based diet that contains 30 en% of fat and compare metabolic adaptation and metabolic health of mice that received the diet either on a restricted (30%) or *ad libitum* (HF-AL) basis. We show that, although an animal is fed a high-fat (Western) diet, the moderate reduction in the total amount of calories improves metabolic health; as measured by a number of parameters, such as glucose tolerance and serum cholesterol, leptin and adiponectin levels. Whole genome gene expression analysis of WAT revealed a strong upregulation of genes involved in mitochondrial function and lipid metabolism by HF-DR. Relative to results obtained with standard diets, in particularly lipid handling is affected, implying the development of substrate efficiency in

HF-DR mice. Finally, we observed an increase in mitochondrial density in WAT of HF-DR mice.

Materials and methods

Animals and Dietary manipulations

Thirty-six male C57BL/6JOlaHsd mice (Harlan Laboratories, Horst, The Netherlands) aged 10 weeks were used for this study. The experimental protocol was approved by the Animal Welfare Committee of Wageningen University, Wageningen, The Netherlands. Mice were individually housed and maintained under environmentally controlled conditions (temperature 21ºC, 12 h/12 h light–dark cycle, 45% humidity) and had, during the first three weeks (the adaptation phase), *ad-libitum* access to food and water. The food consisted of a palletized diet (Research Diets Services B.V., Wijk bij Duurstede, the Netherlands) with a fat content of 30%, which resembles a Western human diet (Table 1). The amount of lard and corn oil are also based on average human intake levels. The diet that was used for dietary restriction was in ratio supplemented with a vitamin and mineral premix to guarantee the same level of intake as in the non-restricted group to prevent deficiencies. Since the mineral and vitamin premixes contain corn-starch, the HF-DR diet is corrected in the carbohydrate fraction.

Table 1 Diet composition of the HF-AL and HF-DR diets in g/kg of the diet and based on relative intake.

Component	HF-AL (g/kg feed)	HF-DR (g/kg feed)	AL intake HF-AL x1	DR intake HF-DR x0.7
Acid casein	220	220	220	154
L-Cystine	3	3	3	2.1
Starch	336.7	331.3	336.7	231.9
Maltodextrose	112.25	110.4	112.25	77.3
Sucrose	85.5	84.1	85.5	58.9
Cellulose (Arbocel B800)	50	38.3	50	26.8
Lard	101.5	101.5	101.5	71.1
Corn oil	43.5	43.5	43.5	30.5
Mineral premix AIN-93G	35	50	35	35
Vitamin premix AIN-93	10	14.3	10	10
Choline bitartrate	2.5	3.5	2.5	2.5
Energy (kcal/kg)	4375	4375		
en% from fat	30	30		
en% from proteins	20	20		
en% from carbohydrates	50	50		

The HF-AL diet was fed *ad libitum*; the HF-DR animals received 70% energy of the HF-DR diet compared with the HF-AL animals. Both diets were iso-caloric in the lipid, protein, and carbohydrate fraction. The HF-DR diet was adjusted for the amount of vitamins and minerals to ensure a homologous intake between both groups

At t=0 weeks, animals were stratified on body weight and divided into groups of twelve animals. The first treatment group (t=0) was directly culled after the adaptation phase, the high-fat *ad-libitum* (HF-AL) group remained under the same conditions, while the high-fat dietary restriction (HF-DR) group received a dietary restriction of 30%, which

lasted for twelve weeks. The amount of restricted food depended on the amount individual mice consumed at the end of the adaptation phase and remained unchanged during the whole intervention phase. The bodyweight and food intake of individual mice were monitored on a weekly basis. The HF-DR group received a fixed amount of feed on a daily basis. All mice were culled at the end of the twelve week intervention.

WAT and blood collection (at time of section)

The HF-AL and t=0 mice were fasted for two hours before sectioning. To match the level of food intake before sectioning to the HF-AL group, HF-DR mice received the regular (restricted) amount of food on the habitual time in the morning and were sectioned 6 hours afterwards. At the time point of section, mice were anesthetized by inhalation of 5% isoflurane. Blood was sampled after eye extraction and collected in Mini collect serum tubes (Greiner Bio-one, Longwood, USA), and centrifuged for 10 min at 3000 g and 4 °C to obtain serum. Serum samples were aliquoted and stored at –80 °C. After blood collection, mice were killed using cervical dislocation and epididymal white adipose tissue was dissected, weighted and snap frozen in liquid nitrogen and stored at –80 °C.

RNA isolation, cDNA synthesis and microarray hybridization

RNA isolation from WAT was performed as described (62). Briefly, WAT was homogenized in liquid nitrogen using a cooled mortar and pestle. Total RNA was isolated using TRIzol reagent, chloroform, and isoamyl alcohol (PCI) (Invitrogen, Breda, The Netherlands) followed by purification with RNeasy columns (Qiagen, Venlo, The Netherlands) using the instructions of the manufacturer. RNA concentration and purity were measured using the Nanodrop (IsoGen Life Science, Maarsen, The Netherlands). Approximately 30 µg of total RNA was isolated with A260/A280 ratios above 2 and A260/A230 ratios above 1.9 for all samples, indicating good RNA purity. RNA quality was additionally checked on the Experion automated electrophoresis system (Bio-Rad, Veenendaal, The Netherlands) using Experion StdSense chips (Bio-Rad).

For transcriptome analysis, the 4 x 44k Agilent whole-mouse genome microarrays (G4122F, Agilent Technologies Inc., Santa Clara, USA) were used. Preparation of the samples and the microarray hybridizations were carried out according to the manufacturer's protocol with a few modifications as described previously (59, 64). All materials and reagents are from AgilentTechnologies, Palo Alto, USA unless stated otherwise. In brief, cDNA was synthesized for each animal from 1 µg WAT RNA using the Agilent Low-RNA Input Fluorescent Linear Amplification Kit without addition of spikes. Thereafter, samples were split into two equal amounts, to synthesize Cyanine 3-CTP (Cy3) and Cyanine 5-CTP (Cy5) labelled cRNA, using half the amounts per dye as indicated by the manufacturer. Labelled cRNA was purified using RNeasy columns (Qiagen). Yield and Cy–dye incorporation were examined for every sample using the Nanodrop. All samples met the criteria of a cRNA yield higher than 825 ng and a

specific activity of at least 8.0 pmol Cy-dye per µg cRNA. Then, Cy3-labeled cRNA samples were pooled on an equimolar basis and used as a common reference pool. Individual 825-ng Cy5-labeled cRNA and 825-ng pooled Cy3-labeled cRNA were fragmented in 1x fragmentation and 1x blocking agent at 60ºC for 30 min and thereafter mixed with GEx Hybridization Buffer HI-RPM. Individual Cy5-labeled cRNA and pooled Cy3-labeled cRNA were hybridized to the arrays in a 1:1 ratio at 65ºC for 17h in the Agilent Microarray Hybridization Chamber rotating at 10 rpm. Samples were randomly divided over the slides and positions on the slides. After hybridization, slides were washed according to the manufacturer's wash protocol. Arrays were scanned with an Agilent Technologies Scanner G2505B with 10 and 100% laser-power intensities.

Normalization and statistical analysis of microarray data

Signal intensities for each spot were quantified using Feature Extraction version 9.5.3.1 (Agilent Technologies). Median density values and background values of each spot were extracted for both the individual samples (Cy5) and the pooled samples (Cy3). Quality control for every microarray was performed visually by using 'Quality control graphs' from Feature extraction and M-A plots and box plots, which were made using limmaGUI in R (66). Data were imported into GeneMaths XT 2.0 (Applied Maths, Sint-Martens-Latem, Belgium). Spots with an average Cy5 and Cy3 signal twice above background were selected and log transformed. The Cy5 signal was normalized against the Cy3 intensity as described before (45). All arrays are deposited in GEO under number GSE27213. Supervised principal component analysis and heat mapping were performed using GeneMaths XT. Volcano plots were made using GraphPad Prism version 5.03 (Graphpad Software, San Diego, USA). Gene expression levels of the HF-DR versus the HF-AL groups were analysed by Student's t tests using a multiple testing correction according to Benjamini-Hochberg (16). Corrected P-values smaller than 0.01 were considered as statistically significant. Fold change is expressed as the ratio of the HF-DR group over the HF-AL group. For downregulated genes, the fold change is converted to the corresponding negative value. Pathway analysis was performed using MetaCore (GeneGo, St. Joseph, Michigan, USA), GO overrepresentation analysis and literature mining.

Quantitative real-time reverse transcription-polymerase chain reaction (qRT-PCR)

qRT-PCR was performed on individual samples as previously described (10, 61) to validate the microarray data. One microgram of RNA of all individual samples was used for cDNA synthesis using the iScript cDNA synthesis kit (Bio-Rad). qRT-PCR reactions were performed with iQ SYBR Green Supermix (Bio-Rad) using the MyIQ single-colour real-time PCR detection system (Bio-Rad). Each reaction (25 µl) contained 12.5 µl iQ SYBR green supermix, 1 µl forward primer (10 µM), 1 µl reverse primer (10 µM), 8.5 µl RNase-free water and 2 µl 100x diluted cDNA. The following cycles were performed: 1 x 3 min at 95ºC, 40 amplification cycles (40 x 15 s 95ºC, 45 s optimal annealing

temperature, which was followed by 1 x 1 min 95ºC and 1 x 1 min 65ºC and a melting curve was prepared (60 x 10 s 65ºC with an increase of 0.5ºC per 10 s). A standard curve using serial dilutions of pooled sample (cDNA from all samples), a negative control without cDNA template, and a negative control without reverse transcriptase (-RT) were taken along with every assay. Only standard curves with efficiency between 90-110% and a correlation coefficient above 0.99 were accepted. Individual samples were measured in duplicate. Data were normalized against the geometrical mean of the reference genes calnexin (*Canx*), beta-2 microglobulin (*B2m*), ribosomal protein S15 (*Rps15*), and endoplasmic reticulum chaperone SIL1 homolog (*Sil1*), which were chosen based on stable gene expression levels between the mice on the microarray and confirmed with the resulting qRT-PCR data (geNorm, Ghent University Hospital, Ghent, Belgium). Primers were designed using the NCBI Primer-Blast (NCBI Web site) and Beacon designer (Premier Biosoft International, Palo Alto, USA). The primer sequences and PCR annealing temperatures for each gene are summarized in table 2.

Table 2 Primer sequences and PCR annealing temperatures of the primers used for quantitative real-time reverse transcription-PCR (qRT-PCR).

Gene	Forward primer 5' – 3'	Reverse primer 5' – 3'	PCR temp.
Acaca	AGCAGATCCGCAGCTTGGTC	CGGGAAGCTCCTCCTACGTG	60.0ºC
Acly	TGGGCTTCATTGGGCACTACC	AGGGCTCCTGGCTCAGTTACA	62.0ºC
Elovl3	TGTTGAACTGGGAGACACGGC	GTCATGAACCAGCCACCCGA	62.0ºC
Elovl6	GGCACTAAGACCGCAAGGCA	GCTACGTGTTCTCTGCGCCT	60.0ºC
Fasn	AGTTAGAGCAGGACAAGCCCAAG	GTGCAGAGCTGTGCTCCTGA	60.0ºC
Sqle	CCGGAAAGCAGCTATGGCAGA	GCGTGGAGCTCCTTGGTGTC	62.0ºC
Srebf1	TCCAGTGGCAAAGGAGGCAC	CAGCATGCTCATTCGCTGCC	60.0ºC
B2m *	CCCCACTGAGACTGATACATACGC	AGAAACTGGATTTGTAATTAAGCAGGTTC	60.0ºC
Canx *	GCAGCGACCTATGATTGACAACC	GCTCCAAACCAATAGCACTGAAAGG	62.0ºC
Rps15 *	CGGAGATGGTGGGTAGCATGG	ACGGGTTTGTAGGTGATGGAGAAC	62.0ºC
Sil1 *	GGCCGCCTTTTCCAGCAATC	CGGGGAGAGGCTGGTTTGTG	62.0ºC

Genes denoted with an asterisk were used as reference genes

Oral glucose tolerance test (OGTT)

Oral glucose tolerance was tested in all mice of the HF-AL and HF-DR group at t= 5, 8 and 11 weeks of the dietary intervention. At t=0 weeks, before the switch to the different dietary interventions, glucose tolerance was tested in three mice per group. On the days that the OGTTs took place, HF-DR mice received their daily amount of food after the OGTT. Food of all mice was removed at the start of the light phase and 5 hours afterwards tail blood (approximately 50 µl) was collected and partly used to determine the glucose concentration with an automated blood glucose monitoring system (Freestyle, Abbott Diabetes Care, Amersfoort, The Netherlands). Remaining blood was transferred to Mini collect serum tubes (Greiner Bio-one, Longwood, USA), and centrifuged for 10 min at 3000 g and 4 °C to obtain serum; serum samples were stored at –80 °C. Glucose (2 g/kg BW) was given orally by gavage at the start of each experiment. 15, 30, 60, 90, and 120 min after glucose administration, 3 µl of tail blood was collected and used to determine the glucose concentration with the automated

blood glucose monitoring system. The incremental area under the curve (AUC) of the changes in blood glucose over time per mouse was calculated using GraphPad Prism.

Serum measurements

Serum samples of the starting point (t=0 min.) of each of the OGTTs were used to measure serum leptin, insulin and adiponectin in fasted animals with the mouse serum adipokine Lincoplex Kit (Linco Research, Nuclilab, Ede, The Netherlands). Preparation of the samples and binding to the antibody-coupled beads were carried out according to the manufacturer's protocol with a few modifications as described previously (60). In short, sera were diluted 5x in HPE buffer (Sanquin, Amsterdam, The Netherlands), debris was removed by spinning the sample using SpinX columns (Corning, Schiphol-Rijk, The Netherlands), and possible inhibition of the immunological Ig fraction in serum was circumvented by an incubation at gentle shaking for 1 h at room temperature in 96-well Reacti-BindTM protein L-coated plates (Pierce, Rockford, IL, USA) before adipokine assaying. The assays were measured using the Luminex X100 system (Biorad, Veenendaal, The Netherlands) with Starstation software (Applied Cytometry Systems, Dinnington, Sheffield, UK). Sample concentrations were calculated using a standard curve of the metabolite of interest (supplied by the kit). All individual samples were analysed in duplicate and averaged.

Serum total cholesterol, HDL-cholesterol and triglycerides were measured using liquicolor enzymatic colorimetric tests (Human, Wiesbaden, Germany). Measured serum triglyceride concentrations were corrected for free serum glycerol concentrations, using a glycerol colorimetric method (Instruchemie, Delfzijl, The Netherlands). Serum samples (2 µl) were measured in duplicate and averaged. Sample concentrations were calculated using a standard curve of the metabolite of interest (supplied by the kit). Serum LDL-cholesterol concentrations were calculated using the modified (for rodents) Friedewald formula (LDL-cholesterol = Total cholesterol – HDL cholesterol – (triglycerides*0.16)) (13).

Mitochondrial mass measurement

To estimate the mitochondrial density in WAT of HF-AL, HF-DR and t=0 mice, we determined the ratio of mitochondrial DNA to nuclear DNA with qRT-PCR according to Lagouge et al. (27) Total DNA was isolated from 25 mg WAT using the QIAamp DNA minikit (Qiagen). Quality and quantity of DNA in each sample was analysed with the Nanodrop and each sample was diluted to the same concentration. qRT-PCR was performed with mitochondrial DNA and genomic DNA-specific primers (27). A standard curve for both genes was generated using serial dilutions of a pooled sample (DNA from all samples). Only standard curves with an efficiency between 90-110% and a correlation coefficient above 0.99 were accepted. Samples were measured in duplicate. The individual relative mitochondrial density was calculated as the Ct value of the mitochondrial gene compared to the Ct value of the nucleic gene in the same sample.

Statistical analysis of serum samples, WAT weight and OGTT

Data are expressed as mean ± SEM; statistical analyses were performed using GraphPad Prism. All individual measurements within the different treatment groups were checked for normality using the D'Agostino-Pearson normality test. Test results that were not normally distributed were log-transformed. Measurements at single time points between 2 groups were analysed by Student's t tests. Measurements at single time points between 3 groups were analysed by one-way ANOVA and Bonferoni Posthoc analysis. P< 0.05 was considered as statistically significant.

Results

High- fat dietary restriction decreased body weight and WAT weight

Body weight of HF-DR animals declines after the start of the intervention and stabilizes after approximately 5 weeks, while HF-AL fed mice gained weight throughout the study (Fig 1a). At the time point of section, twelve weeks after the adaptation phase, HF-DR mice showed a significant decrease in absolute and relative epididymal WAT, compared to HF-AL mice (Fig 1b+c).

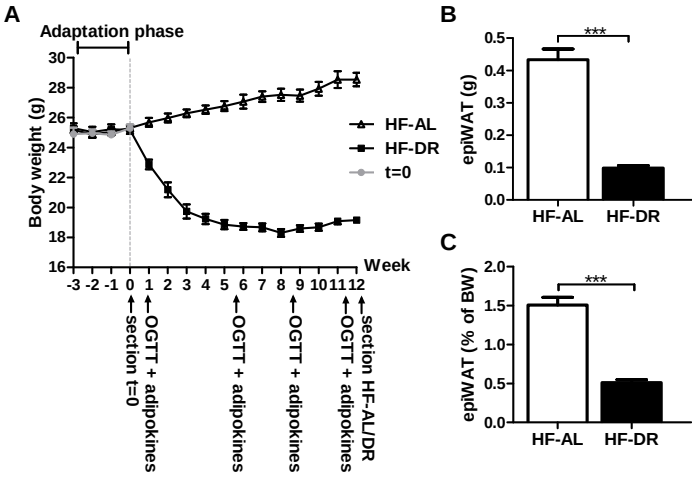

Figure 1 Changes in body and white adipose tissue (WAT) weight of mice fed either a dietary restricted (HF-DR) or *ad libitum* (HF-AL) high-fat diet. During the adaptation phase, HF-AL, HF-DR, and *t=0* mice had similar body weights. During the first 5 weeks of the restriction period, HF-DR mice gradually lost body weight, after which body weight stabilized (A). HF-DR mice exhibit a significant decrease in absolute (B) and relative (C) epididymal WAT weight at the time of section. Data are mean ± S.E.M. of 12 mice. ***P<0.0001.

HF-DR mice performed better on the oral glucose tolerance tests (OGTT) and had decreased fasting glucose and insulin levels

In a fasted state, HF-AL and HF-DR mice differed significantly in serum levels of markers that predict the onset of insulin resistance; at 5, 8, and 11 weeks after the start of the intervention OGTTs indicated that the insulin sensitivity of the HF-DR mice was considerably higher than that of HF-AL mice (Fig. 2a+b). Second, the HF-DR group had significantly lower serum levels of glucose and insulin (Fig 2c+d). It should be noted that insulin levels of most of the HF-DR animals (approximately 9 per measurement)

were below the detection limit of the serum adipokine kit; these values were set to half the value of the detection limit (0.13 nM).

Serum leptin, adiponectin and cholesterol levels were significantly altered in HF-DR mice

Leptin concentrations were significantly lowered in HF-DR animals (Fig. 3a), while serum adiponectin levels were significantly elevated after 5, 8 and 11 weeks of dietary restriction (Fig. 3c). At the end of the dietary intervention, total cholesterol was significantly lowered in HF-DR mice (Fig. 3b). Triglycerides and HDL cholesterol levels remained unchanged between both groups (data not shown). Serum LDL cholesterol was decreased in HF-DR mice at time point of section, which caused a significant increase in the HDL/LDL – cholesterol ratio in these mice (Fig. 3d).

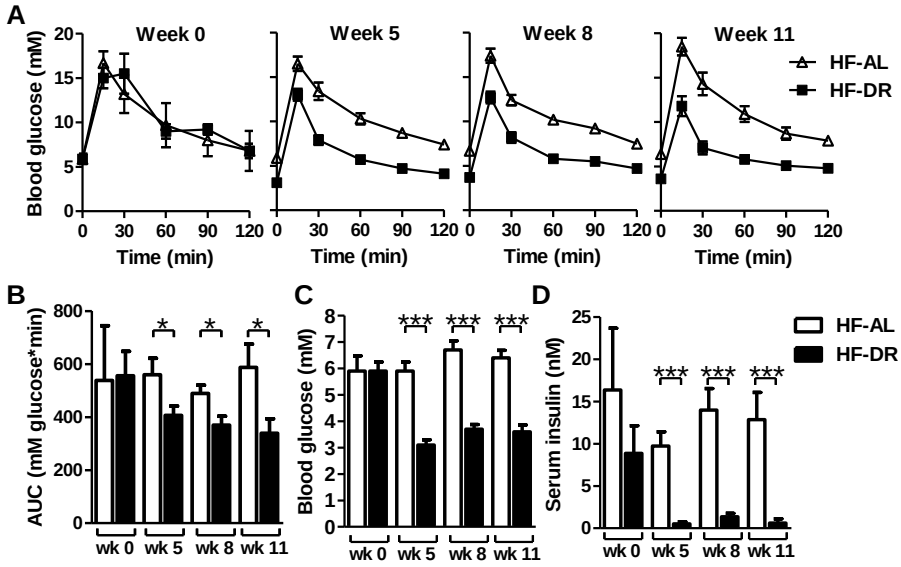

Figure 2 HF-DR improved glucose tolerance and decreased fasted glucose and insulin levels. Oral glucose tolerance was tested at the start of the intervention and after 5, 8, and 11 weeks and improved during the course of the experiment (A). 5, 8, and 11 weeks after the start of the restriction, HF-DR mice had increased glucose sensitivity, as measured by the incremental area under the curve (B). At 5, 8, and 11 weeks, HF-DR mice exhibit a decrease in serum glucose (C) and insulin (D) levels. Data are mean ± S.E.M. of 12 mice. (results of the tests in week 0 are based on three mice per group). *P<0.05; ***P<0.0001.

Gene expression in epididymal white adipose tissue was drastically altered between HF-DR and HF-AL mice

Gene expression in epididymal WAT was measured after 12 weeks of HF-DR or HF-AL diet. Of the more than 43,000 transcripts that were studied, 24,146 transcripts were found to be expressed in WAT (Supplementary Table 1). After filtering the transcripts that encode for the same gene and are similarly regulated, 16,995 genes appeared to be expressed in WAT (Fig 4a), of which 8,643 genes were significantly different

expressed between HF-DR and HF-AL mice ($p<0.01$ Benjamin-Hochberg FDR adjusted). Initially, we focused on the 96 genes that have a p-value $<10^{-11}$ (Table 3). The majority of these 96 genes is involved in lipid metabolism and mitochondrial function. A substantial part is involved in other metabolic processes (particularly in carbohydrate metabolism) and in the cellular response to stress (fig 5). Twenty-four genes have an unknown function. The 96 genes that were differentially expressed between HF-DR and HF-AL mice were not significantly modulated by high-fat feeding on itself, as analysed between HF-AL and t=0 mice (Fig. 4b+c).

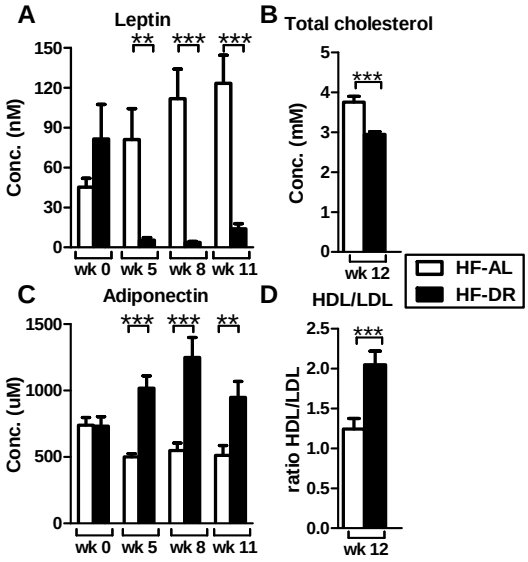

Figure 3 Fasting serum adipokine and cholesterol levels of HF-DR mice altered during dietary restriction. HF-DR mice exhibit decreased leptin (A) and total cholesterol (B) levels and increased adiponectin (C) levels. (D) The dietary intervention elevated the ratio of HDL-cholesterol to LDL-cholesterol in HF-DR animals. Fasting leptin and adiponectin concentrations were determined at the start of the intervention and 5, 8, and 11 weeks afterward. The level of cholesterol was determined at the end of the study. Data are mean ± S.E.M. of 12 mice. ***P*<0.01; ****P*<0.001.

Microarray analysis on highly significantly regulated genes revealed a major role for genes involved in lipid metabolism and mitochondrial functioning

Lipid metabolism

A large proportion of the significantly regulated genes ($p<10^{-11}$) play a role in lipid metabolism. All genes in this group exhibit a strong upregulation compared to the expression in HF-AL mice, except for *BC005764* that serves a function in triglycerides formation and was downregulated. Among the upregulated genes in this group, *Srebf2* functions as a key transcriptional regulator of genes involved in fatty acid and cholesterol synthesis. The majority of the genes in this group are known to be under transcriptional control of *Srebf2* (denoted with asterisks in Table 3). Indeed, all genes involved in cholesterol synthesis (*Cyp51*, *Fdps*, *Hmgcr*, *Insig1*, *Lss*, *Mvd*, *Sqle*, *Tm7sf2*) and fatty acid synthesis and elongation (*Acaca*, *Acly*, *Elovl3*, *Elovl6*, *Pecr*) were significantly upregulated, as was *Me1* which plays a central role in adipose metabolism, linking gluconeogenesis and fatty acid metabolism by producing NADPH. This confirms earlier findings of long and short term DR, although on a low fat diet (15, 63), but is in contrast with short term HF-DR of only 12 days (63). Interestingly, *Sqle* and *Hmgcr* are rate limiting enzymes in cholesterol synthesis, while *Elovl6* controls the first, rate

limiting condensation step of fatty acid elongation (33). The transcription of *Ppara* and *Pparg*, two other key regulators of lipid metabolism, were not altered by the restriction regime (also see Table 4). HF-DR upregulated the expression of two genes encoding lipolysis-related proteins (*Aspg*, *Lpcat3*) and it upregulated the expression of two StAR-related lipid transfer proteins (*Stard4*, *Stard5*) that play a role in the transfer of cholesterol to different cellular compartments, such as the endoplasmic reticulum and the Golgi apparatus (52); and *Rdh11* and *Sorl1* that play a role in the reduction of short-chain (fatty) aldehydes and the uptake of lipoproteins and proteases, respectively.

Mitochondrial functioning

All 8 mitochondrial genes that were highly significantly regulated by HF-DR (with $p<10^{-11}$) seem to promote mitochondrial functioning and biogenesis, except for *C80638*, a mitochondrial sodium/hydrogen exchanger, of which transcription is downregulated by HF-DR. The majority of genes in this group fulfil a role in mitochondrial activity. Transcription of *Fxn*, for example, a gene that promotes mitochondrial function and oxidative phosphorylation was increased by HF-DR. The same holds true for *L2hgdh* and *Slc25a1* that both play a promoting role in the mitochondrial citric acid cycle. Transcription of mitochondrial-localized *Ifi27* protein that is expected to inhibit adipocyte differentiation and mitochondrial biogenesis and function (34), was downregulated.

Since the genes mentioned above are not known as the 'classical' regulators of mitochondrial functioning, we further analysed the complete list of regulated genes ($p<0.01$) for genes that are better established as key regulators in mitochondrial biogenesis, dynamics and autophagy (Table 4). *Ppargc1a, Ppargc1b*, *Esrra*, *Nrf1* and *Tfam*, which are known to be of major importance for mitochondrial biogenesis (53) were indeed all upregulated in HF-DR animals. The same holds true for *Dnm1l*, *Mtfr1*, *March5*, *Mfn1*, *Opa1*, *Oma1* and *Stoml2*, the genes that play an important role in mitochondrial fission and fusion (68). *Mtor*, a transcription factor that is involved in the suppression of autophagy and cell death (20) is upregulated in HF-DR animals. *Ulk2* promotes autophagy and cell death in the absence of *Mtor* and is consistently downregulated. The expression of *Park2* that is involved in the induction of mitophagy and the promotion of cell survival (40) is, on the other hand, increased in these animals; the same holds true for the expression of *Rab7* and *Bnip3l* that are involved in the induction of autophagy (19, 69).

Other metabolic genes

Next to the genes involved in lipid metabolism and mitochondrial function, we found a number of genes that are involved in other metabolic processes. Most of the genes in this category are involved in carbohydrate metabolism. *Pdk1*, for example, inhibits glycolysis and was strongly upregulated by the restriction regime. Similarly, *Ppp1r3b* promoting glycogen synthesis and *Slc2a5* promoting glucose uptake are both increased in HF-DR animals.

Table 3 Categorization and expression profiles of strongly regulated genes (P<10K11) between HF-AL and HF-DR mice.

Gene symbol	*Protein name*	*FC*	*P-value*	*Function*
		Lipid metabolism		
Cyp51 *	Cytochrome P450, family 51	8.0	2.50E-13	Cholesterol synthesis
Fdps	Farnesyl pyrophosphate synthetase	4.3	2.50E-13	Cholesterol synthesis
Hmgcr *	3-hydroxy-3-methylglutaryl-coenzyme A reductase	2.9	2.40E-12	Cholesterol synthesis
Insig1	Insulin-induced gene 1 protein	8.7	7.50E-12	Cholesterol synthesis
Lss	Lanosterol synthase	6.7	7.00E-13	Cholesterol synthesis
Mvd	Diphosphomevalonate decarboxylase	8.4	4.90E-13	Cholesterol synthesis
Sqle *	Squalene epoxidase	7.4	1.10E-13	Cholesterol synthesis
Tm7sf2	Delta(14)-sterol reductase	5.0	7.50E-12	Cholesterol synthesis
BC0057 64	Lipid phosphate phosphatase-related protein type 3	-2.8	2.50E-13	1,2-diacylglycerol synthesis
Elovl3	Elongation of very long chain fatty acids protein 3	28.6	0	Fatty acid elongation
Elovl6 *	Elongation of very long chain fatty acids protein 6	47.2	0	Fatty acid elongation
Pecr	Peroxisomal trans-2-enoyl-CoA reductase	2.8	3.50E-12	Fatty acid elongation
Acaca *	Acetyl-Coenzyme A carboxylase α	5.7	2.30E-12	Fatty acid synthesis
Acly *	ATP-citrate synthase	12.3	3.90E-12	Lipogenesis
Aspg	60 kDa lysophospholipase	12.8	2.70E-12	Lipolysis
Lpcat3	Lysophospholipid acyltransferase 5	2.7	2.10E-12	Lipolysis
Rdh11 *	Retinol dehydrogenase 11	9.6	6.10E-13	Reduction of short-chain aldehydes
Srebf2	Sterol regulatory element-binding protein 2	2.0	7.90E-12	Transcriptional regulation of lipid metabolism
Stard4 *	StAR-related lipid transfer domain containing 4	2.1	3.80E-13	Intracellular transport of cholesterol
Stard5	StAR-related lipid transfer protein 5	3.3	2.80E-12	Intracellular transport of cholesterol
Sorl1 *	Sortilin-related receptor	6.2	9.10E-13	Uptake of lipoproteins and proteases
		Mitochondrial function		
1700020 C11 Rik	Mitochondrial 18 kDa protein	6.3	3.56E-12	Maintenance of the mitochondrial network
C80638	Mitochondrial sodium/hydrogen exchanger	-9.0	0	H+/Na+ exchange across mitochondrial inner membrane
Fxn	Frataxin, mitochondrial	2.3	6.58E-12	Mitochondrial iron transport and respiration
Ifi27	Interferon, alpha-inducible protein 27 like 2A	-11.1	6.15E-12	Adipocyte differentiation and mitochondrial biogenesis
L2hgdh	L-2-hydroxyglutarate dehydrogenase	2.0	2.77E-12	Synthesis of 2-oxoglutarate
Ppif	Peptidyl-prolyl cis-trans isomerase, mitochondrial	3.2	6.42E-12	Inhibition of the mitochondrial permeability transition pore
Slc25a1	Solute carrier family 25 (mitochondrial citrate transporter), 1	8.2	7.59E-12	Citrate transport / Krebs cycle
Timm9	Translocase of inner mitochondrial membrane 9 homolog variant 1	3.1	5.83E-13	Import and insertion of mitochondrial membrane proteins
		Other metabolic genes		
Acp1	Acid phosphatase 1	-5.6	0	Amino acid dephosphorylation
Adh1	Alcohol dehydrogenase 1	2.4	3.30E-12	Alcohol metabolism
Me1	NADP-dependent malic enzyme	9.0	0	Gluconeogenesis
Pdk1	Pyruvate dehydrogenase kinase isozyme 1	5.0	1.12E-13	Gluconeogenesis
Pgk1	Phosphoglycerate kinase 1	2.8	9.36E-13	Glycolysis
Pgp	Phosphoglycolate phosphatase	2.1	2.51E-13	Carbohydrate metabolic process
Ppp1r3b	Protein phosphatase 1 regulatory subunit 3B	17.8	0	Glycogen synthesis

Table 3 continued from page 33

Gene symbol	*Protein name*	*FC*	*P-value*	*Function*
Prei4	Putative glycerophosphodiester phosphodiesterase	2.7	6.70E-13	Carbohydrate/ glycerol metabolic process
Psph	Phosphoserine phosphatase	5.0	7.31E-13	Amino acid biosynthesis
Rorc	Nuclear receptor ROR-gamma	5.7	8.49E-13	Transcriptional regulation of metabolism
Slc2a5	Solute carrier family 2 (facilitated glucose transporter), member 5	35.0	5.69E-12	Glucose uptake
	Cellular response to stress			
Blcap	Bladder cancer-related protein	-4.5	9.77E-12	Regulation of cell proliferation and apoptosis (by similarity)
C8g	Complement component 8, gamma	2.5	3.26E-12	Complement pathway
Egln3	EGL nine homolog 3	7.4	2.36E-12	Cellular response to stress
Fastkd3	FAST kinase domains 3	2.2	6.59E-12	Regulation of apoptosis
Gclm	Glutamate--cysteine ligase regulatory subunit	2.2	8.49E-13	Glutathione metabolism; response to oxidative stress
Klf11	Krueppel-like factor 11	-1.8	4.69E-13	Transcriptional regulation of apoptosis
Tmem49	Transmembrane protein 49	2.1	9.10E-12	Cellular response to stress
Traf4	Tnf receptor associated factor 4	6.0	1.68E-12	Proapoptotic cellular signaling
	Other functions			
Abcc3	ATP-binding cassette, sub-family C	-3.0	4.35E-13	Transmembrane organic anion transport
Ank	Progressive ankylosis	4.3	5.29E-12	Transmembrane inorganic pyrophosphate transport
Atp1a3	Na^+ / K^--transporting ATPase subunit	16.9	0	Transmembrane ion transport
Anxa6	Annexin A6	-2.6	1.12E-13	Transmembrane ion release
Kcne1l	K^- voltage-gated channel, Isk-related family, member 1-like	-4.6	3.52E-12	Transmembrane ion release
Kctd15	K^- channel tetramerisation domain containing 15	-2.4	3.13E-12	Transmembrane ion release
Bmper	BMP-binding endothelial regulator	-3.3	1.95E-12	Cell differentiation
Col1a1	Collagen alpha-1(I) chain	-3.9	8.00E-13	Cell development
Cry1	Cryptochrome 1 (photolyase-like)	3.6	0	Regulation of the circadian rhythm
Dixdc1	DIX domain containing 1	3.1	1.94E-12	Multicellular organismal development
Dock11	Dedicator of cytokinesis 11	-4.6	5.69E-12	Activation of G proteins
Ift122	Intraflagellar transport 122 homolog	-2.7	5.14E-12	Cilia formation
Nnat	Neuronatin, transcript variant 1	-4.0	0	Regulation of insulin secretion
Pcsk4	Proprotein convertase subtilisin/kexin type 4	5.8	1.99E-13	Conversion of secretory precursor proteins
Recql4	RecQ protein-like 4	9.7	4.87E-13	DNA recombination
S100b	S100 protein, beta polypeptide	-4.0	1.17E-12	Regulation of proinflammatory cytokines (in neurons)
Sar1b	SAR1 gene homolog B	2.0	1.43E-12	Protein transport from ER to Golgi
Syngr1	Synaptogyrin 1, transcript variant 1b	3.0	3.30E-12	Protein targeting for synaptic like microvesicles
Tmem41b	Transmembrane protein 41B	2.4	9.71E-13	Transmembrane protein
Tmem79	Transmembrane protein 79	4.5	0	Transmembrane protein
Polr3g	Polymerase (RNA) III polypeptide G	4.1	0	(regulation of) transcription
1500003 O22 Rik	Ribosomal RNA processing 8, methyltransferase, homolog	1.9	2.74E-12	Regulation of transcription
Zbtb20	Zinc finger and BTB domain containing 20	-2.0	3.56E-12	Regulation of transcription
6330548 G22 Rik	Small nuclear ribonucleoprotein 35	1.7	2.21E-12	RNA splicing

Genes are ordered based on function and within functional categories based on alphabetic order.
Genes indicated with an asterisk are transcriptionally regulated by *Srebf2*

Pathway analysis

In addition to analysis of strongly significantly regulated genes, we performed a pathway analysis on the complete set of regulated genes (Table 5). This analysis confirmed that the primary changes in gene expression are related to lipid metabolism and mitochondrial functioning. Of the top 10 named pathways, 8 pathways (Oxidative phosphorylation, Cholesterol biosynthesis, Citric acid cycle (Ubiquinone metabolism), Regulation of lipid metabolism, Mitochondrial fatty acid unsaturated and long chain β-oxidation and Regulation of fatty acid metabolism) are involved in these functions.

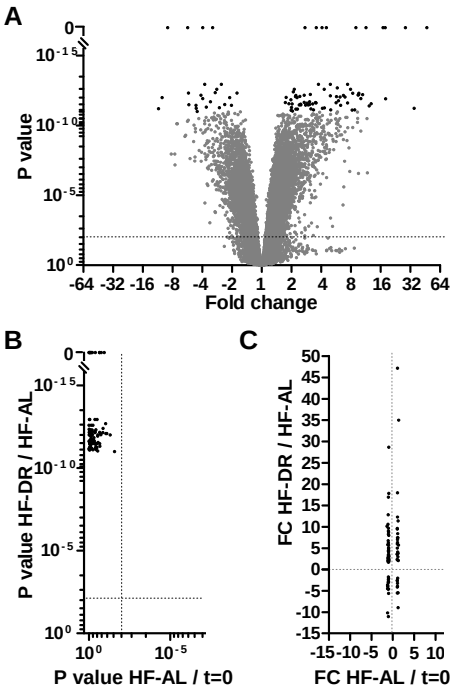

Figure 4 Volcano plot (A) of 16 995 genes expressed in WAT showing the *t*-test statistics *P* value plotted against the fold change of each transcript of the microarray analysis between HF-DR and HF-AL mice. *P* values were corrected for multiple testing using a Benjamini–Hochberg correction. Black dots represent the 96 genes that have a *P* value smaller than 10^{-11}. The dotted line indicates the significance level of 0.01. The 96 genes that were differentially expressed between HF-DR and HF-AL mice as observed by microarray analysis were not modulated between HF-AL and *t=0* mice (based on *P* values (B) of the HF-DR and HF-AL compared to HF-AL and *t=0* mice (the dotted lines indicate a significance level of 0.01) and based on fold changes (FC; C) of HF-DR and HF-AL compared to HF-AL and *t=0* mice).

Microarray results were confirmed with qRT-PCR

qRT-PCR was used to validate the microarray results for 7 genes with an important role in lipid metabolism. This resulted in a significant upregulation of all 7 genes with fold changes ranging between 4.0 and 513.3 (microarray data ranged between 2.0 and 48.0 for these genes) (Fig. 6).

HF-DR mice have higher levels of mitochondrial mass in WAT

Mitochondrial and nuclear DNA content in WAT of HF-AL, HF-DR and t=0 mice was compared with qRT-PCR in order to estimate mitochondrial density. HF-DR mice had a significantly higher mitochondrial DNA content compared to both HF-AL and t=0 mice (Fig. 7). High-fat feeding (HF-AL vs. t=0) reduced mitochondrial density; although non-significantly.

Table 4 Expression profiles of genes that are known to play an important role in mitochondrial function.

Gene symbol	*Gene name*	*FC*	*P-value*	*Function*
	Mitochondrial biogenesis			
Cox4i1 *	cytochrome c oxidase subunit IV isoform 1	1.81	3.45E-05	Formation of respiratory chain complex IV
Cox5b *	cytochrome c oxidase, subunit Vb	2.10	5.36E-07	Formation of respiratory chain complex IV
Esrra *	estrogen related receptor, alpha	2.06	1.64E-06	Regulation of nuclear and mitochondrial respiratory proteins
Gabpa *	GA repeat binding protein, alpha	1.74	9.63E-08	Regulation of nuclear and mitochondrial respiratory proteins
Nrf1 *	nuclear respiratory factor 1	1.25	7.68E-04	Regulation of nuclear and mitochondrial respiratory proteins
Polg	polymerase (DNA directed), gamma	-1.06	2.85E-01	mtDNA maintenance
Ppara	peroxisome proliferator activated receptor alpha	-1.19	2.44E-02	Regulation of fatty acid oxidation
Pparg	peroxisome proliferator activated receptor gamma	-1.13	4.09E-01	Regulation of fatty acid oxidation
Ppargc1a *	peroxisome proliferative activated receptor, gamma, coactivator 1 alpha	2.39	2.13E-06	Regulation of mitochondrial biogenesis
Ppargc1b *	peroxisome proliferative activated receptor, gamma, coactivator 1 beta	1.85	5.70E-05	Regulation of mitochondrial biogenesis
Pprc1	peroxisome proliferative activated receptor, gamma, coactivator-related1	-1.03	7.82E-01	Regulation of mitochondrial biogenesis
Sirt3	sirtuin 3	1.10	1.78E-01	ROS detoxification + mitochondrial biogenesis
Tfam *	transcription factor A, mitochondrial	1.34	9.71E-06	Stabilization + maintenance of the mitochondrial chromosome
	Mitochondrial dynamics			
Dhodh *	dihydroorotate dehydrogenase	1.37	6.65E-07	Regulation of mitochondrial fission
Dnm1l *	dynamin 1-like	1.32	3.46E-06	Mitochondrial fission
Fis1	fission 1	1.16	3.58E-02	Mitochondrial fission
Gdap1l1	ganglioside-induced differentiation-associated protein 1-like 1	-1.14	1.46E-01	Mitochondrial fission
Mtfr1 *	mitochondrial fission regulator 1	1.69	2.02E-08	Mitochondrial fission
March5 *	membrane-associated ring finger (C3HC4) 5	1.65	4.76E-06	Activation of Dnm1l, Fis1 and Mfn2
Mfn1 *	mitofusin 1	1.22	4.70E-04	Outer membrane fusion
Mfn2	mitofusin 2	1.18	9.38E-02	Outer membrane fusion
Oma1 *	OMA1 homolog,zinc Metallopeptidase	1.29	2.21E-05	Activation of OPA1
Opa1 *	optic atrophy 1 homolog	1.42	3.68E-05	Inner membrane fusion
Stoml2 *	stomatin (Epb7.2)-like 2	1.51	6.70E-09	Stress-induced fusion
	(mitochondrial) Autophagy			
Atg13	ATG13 autophagy related 13homolog	1.11	1.93E-01	Induction of autophagy
Becn1	beclin 1, autophagy related	1.14	6.49E-02	Induction of autophagy
Bcl2	B-cell leukemia/lymphoma 2	-1.73	2.97E-08	Inhibition of autophagy
Bnip3	BCL2/adenovirus E1B interacting protein 3	-1.06	6.54E-01	Induction of autophagy, cell death and mitophagy
Bnip3l *	BCL2/adenovirus E1B interacting protein 3-like	1.53	1.28E-05	Induction of autophagy, cell death and mitophagy
Mtor *	mechanistic target of rapamycin	1.34	7.23E-05	Regulation of autophagy
Rab7 *	RAB7, member RAS oncogene family	1.31	4.67E-05	Maturation of autophagic vacuoles
Ulk1	Unc-51 like kinase 1	1.10	1.79E-01	Induction of autophagy
Ulk2 *	Unc-51 like kinase 2	-1.82	2.73E-09	Induction of autophagy
Park2 *	Parkin 2	1.44	2.79E-03	Induction of mitophagy
Pink1	PTEN induced putative kinase 1	-1.12	1.81E-01	Induction of mitophagy

Genes are ordered based on function and within functional category based on alphabetic order. Genes indicated with an asterisk are significantly differently expressed between HF-DR and HF-AL mice.

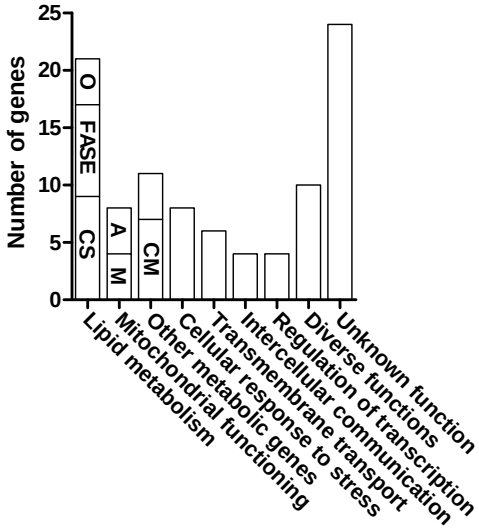

Figure 5 Categorization of the 96 genes that were found to be strongly regulated (*P* value <10^{-11}) between HF-DR and HF-AL mice into functional categories. The majority of genes is involved in lipid metabolism and mitochondrial functioning. Nine genes are involved in cholesterol synthesis (CS), eight are involved in fatty acid synthesis and elongation (FASE), and four genes are involved in other processes in lipid metabolism (O). Four genes are involved in mitochondrial maintenance (M) and four genes are involved in mitochondrial activity (A). Most of the genes involved in other metabolic processes serve a role in carbohydrate metabolism (CM).

Discussion

Dietary restriction of a high-fat diet improves metabolic health and promotes a metabolic adaptation towards lipid metabolism

We demonstrate that dietary restriction of a high-fat diet restores glucose sensitivity, increases the mitochondrial density in WAT, decreases the serum levels of cholesterol and leptin; and increases serum adiponectin levels. The bodyweight and serum parameters of HF-DR mice remained stable during the last 7 weeks of restriction, implying that within 5 weeks HF-DR mice have adapted to the restriction regime and exhibit a steady energy balance. The beneficial effects on health are comparable to previous reports that demonstrate that DR on a standard mouse diet improves health, by enhancing insulin sensitivity (12), decreasing serum cholesterol (6), glucose, and leptin levels (49), and increasing serum adiponectin (7). To our knowledge this is the first study that exclusively reports improvements in markers of the metabolic syndrome by dietary restriction with a high-fat diet. Two previous studies, in fact, reported unfavourable effects in mice that were pair-fed on a high-fat diet to match the caloric intake of mice on a low-fat diet. A certain iso-caloric treatment was found to result in a decrease in insulin sensitivity in the restricted high-fat group (47); whereas a second study reported that high-fat pair-fed mice develop insulin resistance, hepatic steatosis, and obesity (11). The diets used in both studies, however, contained almost twice as much energy available from fat compared to the diet we used in our study (58 and 60en%, compared to 30en%), which might have evoked a different coping strategy. A third study on high-fat dietary restriction in mice, consistently, reported decreased

fasting insulin levels; although it also reported a decrease in serum adiponectin levels and only minor effects of high-fat restriction on inflammations in WAT (21). An important difference with our study is that the authors used a run-in period on the high-fat diet that is much longer than the actual restriction period. In this case, two months of dietary restriction might simply be insufficient to reverse the negative effects of six months *ad libitum* high-fat feeding and to stabilize energy balance, as was seen in our study. The occurrence of beneficial effects of DR with a high-fat diet seems, consequently, to depend on both the duration of restriction and the fat content of the diet.

Table 5 Top ten pathways that are significantly regulated between HF-AL and HF-DR mice.

Pathway	P-value	total # of genes involved in pathway	# of upreg. genes in dataset	# of downreg genes in dataset
1. Oxidative phosphorylation	1.80E-11	114	77	0
2. Cholesterol biosynthesis	1.16E-06	22	20	0
3. Citric acid cycle	2.49E-06	20	18	1
4. Regulation of lipid metabolism via LXR, NF-Y and SREBF	7.75E-06	35	18	9
5. Ubiquinone metabolism	1.03E-05	52	37	0
6. BAD phoshorylation	1.08E-05	88	29	12
7. Mitochondrial long chain fatty acid β-oxidation	1.14E-05	18	14	2
8. EDG3 signaling	3.11E-05	68	13	22
9. Insulin regulation of fatty acid metabolism	5.12E-05	55	25	9
10. Mitochondrial unsaturated fatty acid β-oxidation	5.13E-05	16	13	1

Pathway analysis was performed on the complete set of regulated genes (P<0.01). The top ten pathways (based on P value) consist of several pathways involved in lipid metabolism and mitochondrial function. The table additionally shows the total number of genes that is involved in the pathway and the number of these genes that was either upregulated or downregulated in our dataset.

To additionally examine the molecular events associated with the observed adaptation to HF-DR, we analysed whole genome expression in WAT; the organ that was notably affected by HF-DR (Fig. 1b+c, 3a+c) and is known to play an important role in the development of metabolic complications in obesity (58). Among the drastic shifts in gene expression in WAT, the changes in genes involved in lipid metabolism and mitochondrial function were most pronounced (Table 3, Fig. 5). In our study, the majority of lipid metabolism-related genes plays a role in cholesterol synthesis and fatty acid synthesis and elongation and was upregulated by the restriction regime. For this analysis we initially focused on the functional interpretation of genes with the strongest P-values. To further validate this approach we also conducted a pathway analysis on the complete set of regulated genes, which revealed significant regulation of several pathways involved in both lipid metabolism and mitochondrial function (Table 5), which further supports the functional interpretation of our initial approach. To our surprise, pathway analysis also pointed towards an upregulation of mitochondrial fatty acid

oxidation. A result that seems contradictory to the observed increase in fatty acid synthesis and elongation. Earlier studies to the effects of dietary restriction on gene expression in WAT, however, also reported changes in genes and pathways involved in both storage and usage of energy; although in these studies a standard rodent diet was use for dietary restriction and compared to our results, the effects on lipid metabolism are less pronounced (15, 44). We propose that the HF-DR mice have developed an enhanced substrate efficiency for the abundant fat component in the diet, and that upregulation of both fat storage and release pathways relates to the beneficial effects on metabolic health we observed in this study.

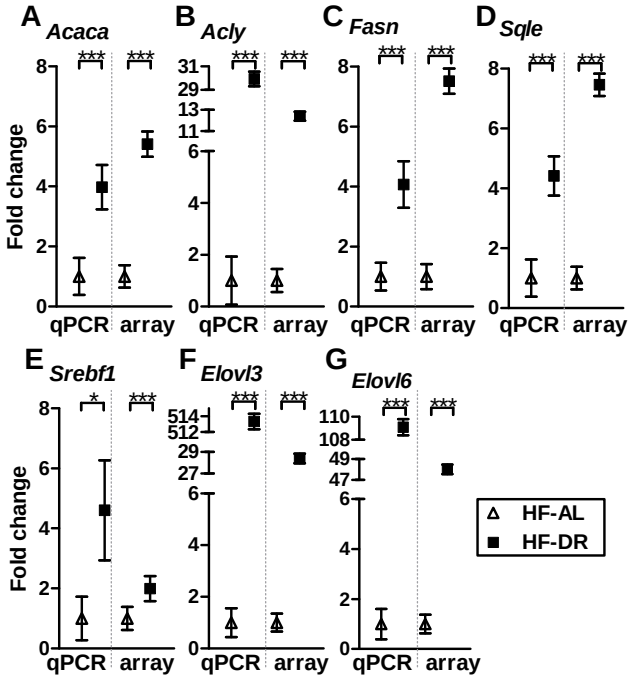

Figure 6 Confirmation of microarray results by real-time qRT-PCR. The expression of *Acaca* (A), *Acly* (B), *Fasn* (C), *Sqle* (D), *Srebf1* (E), *Elovl3* (F), and *Elovl6* (G) in HF-DR and HF-AL mice was analysed by qRT-PCR (left) using stable reference genes *Canx*, *B2m*, *Sil1*, and *Rps15*. Data obtained with microarray are shown for comparison (right). Data represent the mean ± S.E.M. of 12 mice, in which the mean expression of HF-AL mice is set to 1.0. *P<0.05; ***P<0.001.

Since both groups of mice were kept under the same rearing conditions and on diets with equal vitamin and mineral intake and identical macronutrient composition, most plausible alternative explanations for the differences in gene expression between HF-DR and HF-AL can be excluded. It should, nonetheless, be noted that, in order to match the levels of food intake, animals of both groups were treated differently. HF-DR animals received their restricted amount of food at the start of the light phase and were sectioned 6 hours afterwards, while HF-AL animals were sectioned 3 hours after start of the light phase; which might have influenced expression patterns of genes that display a diurnal pattern, such as Bmal, *Cry1*, *Elovl3* and *Elovl6*. Indeed, we found a significant up-regulation of the circadian clock regulator *Bmal* in HF-DR mice (data not shown). However, we found the expression of *Cry1* to be increased, while it is expected

to be stable within the time frame just mentioned (1). Accordingly, the expression level of *Elovl3* is increased instead of decreased, as would be expected if the difference was due to the circadian rhythm of this gene (2). Finally, the increase in expression of Elovl6 is well beyond the increase in expression that is normally seen during this time frame in the light phase (a 2-fold increase that is normally seen, compared to a 47.2-fold increased observed in this study) (8). It seems, therefore, unlikely that the differences observed in the expression of metabolic genes, which is the focus of this study, are primarily due to the differences in feeding and sectioning time.

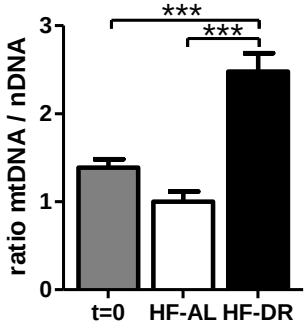

Figure 7 Mitochondrial density in WAT of *t=0*, HF-AL, and HF-DR mice. Mitochondrial density was measured by the mitochondrial DNA copy number versus nuclear DNA and measured with qRT-PCR. Data represent the mean ± S.E.M. of 12 mice, of which the mtDNA/nDNA ratio of HF-AL mice was set to 1.0. ***P<0.001.

Srebf1 and *Srebf2* are expected to play a major role in the adaptation to a high-fat diet in HF-DR animals

Srebf1 and *-2*, play an important role in the regulation of lipid metabolism, and were both higher expressed in HF-DR mice. Although *Srebf1* did not belong to the list of genes with the strongest P-values (Table 3), the same list contains various genes that are under transcriptional control of both *Srebf* isoforms, such as *Elovl6*, *Acly* and *Acaca* (38). SREBPs (the human annotation of *Srebfs*) are known as crucial cellular molecules that mediate adaptive metabolic responses to changing dietary exposures (57). Nuclear translocation of SREBPs is regulated by intracellular fatty acid and sterol levels. When cellular sterols are abundant, SREBPs are inactive in the endoplasmic reticulum membrane. Upon sterol depletion, SREBPs are cleaved by regulated proteolysis to release the mature transcription factor domain, which translocates to the nucleus. SREBPs then bind promoter sterol-regulatory elements (SREs) to activate genes involved in the biosynthesis and uptake of cholesterol and fatty acids (3). The expression of *Ppara* and *Pparg*, two other key regulators of lipid metabolism, is not significantly altered between HF-DR and HF-AL, implying the significance of both *Srebfs* in upregulating lipid metabolism in our study.

Consistently to the upregulation of both *Srebfs,* cholesterol synthesis appeared to be significantly changed in HF-DR mice (Fig. 5), in fact, 20 of the 22 genes that are involved in this metabolic process were upregulated by our treatment. At first sight it might appear strange for HF-DR mice to increase the rate of cholesterol and fatty acid synthesis. The HF-AL mice consumed 3.94 kcal from fat per day; this was 2.76 kcal for

HF-DR mice, while a chow-fed mouse eats about 1.08 kcal form fat per day (5). Second, mice on a standard chow diet receive no cholesterol, while HF-DR mice do consume cholesterol; although to a lesser extent compared to HF-AL mice. It can, therefore, be assumed that both HF-DR and HF-AL mice received enough energy from fat. Similar results on *Srebfs* functioning and upregulation of energy metabolism have, however, earlier been observed in dietary restricted animals. At first, high-fat diets are, known to induce expression of *Srebf1* in the liver (36), and studies in both mice and humans showed that the expression of *SREBPs* is downregulated in obese versus lean subjects (39, 41, 56). These authors subsequently hypothesize that the downregulation of *Srebfs* correlates with the dedifferentiation of adipocytes in obesity, while enhanced differentiation of adipocytes is rather known as a characteristic of dietary restriction (15). Second, it was shown that re-feeding after fasting stimulates the expression of *Srebf1* (35), which implies that the dietary restricted animals in our study are still (6 hours after feeding) in a post-prandial state. A result that is consistent to a study by Bruss *et al.* (4), who noticed that dietary restriction elevates fatty acid synthesis in mice until 4 to 6 hours after food provision compared to normal fed mice as measured by their respiratory exchange ratio. Our study confirms this finding and implicates an important role for *Srebf1* and *Srebf2* in this metabolic adaptation.

Finally, upregulation of metabolic rate has earlier been observed in 'normal' low-fat dietary restriction studies in mice (15), as well as in dietary restricted nematodes (17) and flies (18). The main difference with these studies is, however, that our results primarily point in the direction of lipid metabolism, implying that mice are capable of adjusting their metabolism specifically to their diet. As a result, HF-DR mice seem to be better equipped to deal with the excess of amount of fat in their diet, compared to the HF-AL mice. Several aspects of the micro array results fit within this theory. The upregulation of, for example, mitochondrial fatty acid β-oxidation (Fig. 5), in which acyl-CoA molecules are oxidized to generate acetyl-CoA that can subsequently be used in the citric acid cycle, enables HF-DR animals to synthesize ATP during scarcity of pyruvate. *Pdk1* that was also upregulated by HF-DR complements in this process by protecting carbohydrate stores in muscle (46) and, in this way, stimulating cells to shift to fat utilization and spare carbohydrate stores. Finally, the upregulation of *Stard4* and *Stard5* could make the metabolism of cholesterol more efficient by regulating the transfer of cholesterol to different cellular compartments. Apart from that, by binding, transporting, and positioning dietary cholesterol, STARD4 protein increases cholesteryl ester formation; and is therefore, postulated to play a role in the determination of serum total cholesterol and LDL cholesterol (51), which were found to be significantly decreased in serum of HF-DR mice (Fig. 3).

HF-DR significantly enhanced mitochondrial function and density in WAT

The mitochondrion serves a critical function in the maintenance of cellular energy stores, thermogenesis, and apoptosis. Proper control of mitochondrial function is,

therefore, of major importance for cell survival and the maintenance of metabolic health. In our list of strongly regulated genes we identified several genes that are involved in mitochondrial function (Table 3). The expression patterns of these genes pointed towards an improved mitochondrial function. To further confirm this finding, we analysed our complete set of regulated genes for genes that are better established to play a key role in the regulation of mitochondrial function (Table 4). In the first place we aimed at genes involved in the process of mitochondrial biogenesis. Mitochondrial biogenesis is mainly determined by genes that promote the formation of elements of the respiratory chain and the maintenance of mitochondrial DNA. *Ppargc1a*, *Ppargc1b* and *Esrra* are known as the key transcriptional regulators within this process and were all significantly upregulated in HF-DR animals. *Nrf1*, *Gabpa* and *Tfam* that work as the direct effectors of *Ppargc1a* and stimulated mitochondrial biogenesis (53) were consistently upregulated in these animals. In addition, we found a significant increase in the expression of *CoxIV* and *CoxVb* that are under transcriptional control of *Nrf1* and *Gabpa* and serve a direct function in the formation of the cytochrome oxidase subunits (24).

Second, we looked at genes involved in mitochondrial dynamics, which can be characterized by the degree of fission and fusion of mitochondria. Fission and fusion refers to the formation and breakdown of tubules between mitochondria, which plays an important role in the regulation of mitochondrial morphology. Dysregulation of genes involved in fission and fusion relates to the development of various disorders, such as diabetes (68). In mammals, fission is primarily regulated by *Dnml1* and *Fis1*, which are both upregulated by HF-DR, although the regulation of *Fis1* is only marginally significant. Fusion of mitochondrial tubules is mediated by *Mfn1* and *OPA1*, which are both significantly upregulated in HF-DR mice. *OPA1* is specifically involved in the fusion of the mitochondrial inner membrane and was found to be cleaved and activated by *OMA1*, which is also significantly upregulated in our data set. Finally, we also found a significant upregulation in the expression of *Stoml2* and *Dhodh* that play a role in stress induced fusion and the transcriptional regulation of fission respectively. Under normal conditions, fission and fusion proteins are expressed in response to the mitochondrial activity of the cell. Artificial overexpression of one of either fission or fusion proteins disrupts the balance and disturbs normal cell function (68). *Fis1* overexpression in liver cells, for example, causes mitochondrial fragmentation and impaired glucose stimulated insulin secretion; while overexpression of *Mfn1* causes similar perturbations of the metabolism-secretion coupling of glucose (43). Regarding the improved health status of HF-DR mice, we hypothesize that the upregulation of both fission and fusion proteins relates to the observed improvement of mitochondrial function.

Fission and fusion proteins are, additionally, involved in the regulation of apoptosis by the elimination of damaged mitochondria by autophagy. Selective autophagy of mitochondria, or mitophagy, has extensively been described in yeast, where it is known to play an important role in the determination of cell survival or cell death after oxidative

stress (22). In short, damaged, aged or excess mitochondria are a risk factor for the cell, and proper elimination of such organelles is important to maintain optimal cellular homeostasis. To also investigate the end stage of mitochondrial function we analysed a number of genes involved in mitochondrial autophagy. In mammals, mitophagy is regulated by *Bnip3*, *Bnip3l*, and *Park2* (40, 69), of which the latter two were significantly upregulated in HF-DR mice. Finally we analysed the expression of *mTor,* a serine/threonine protein kinase transcription factor that responds to nutrient starvation, oxidative stress and availability of growth factors. In fact, nutrient starvation and oxidative stress inhibit *mTor* transcription, which stimulates autophagy and apoptosis (20). *mTor* appeared to be significantly higher expressed in HF-DR animals, which implies a decreased prevalence of oxidative damage and apoptosis. The downstream effectors of *mTor*, *Ulk1* and *Ulk2* that initiate apoptosis in the absence of *mTor* were either not regulated or significantly downregulated.

It should be noted that dietary restriction is often related to downregulation of *mTor* (25). An increase in autophagy is in this case seen as strategy to survive low nutrient concentrations by recycling their own cell content. In our study, however the restriction of the high-fat diet still provides the animals with an amount of calories that is similar to the amount of calories that mice consume on a standard low-fat rodent diet: the HF-DR mice received 9.2 kcal/day, while an 'average' male C57BL6/J mouse eats around 10.8 kcal/day (5). It can, therefore, be hypothesised that the HF-DR mice received sufficient nutrients and therefore did not need to switch to salvage pathways such as autophagy.

To summarise, microarray analysis provided us with a convincing amount of evidence for the upregulation of mitochondrial function in HF-DR mice. The increase in the ratio of mitochondrial DNA in WAT of HF-DR mice, which can be seen as an estimation of the mitochondrial density (27), further confirms our findings regarding the upregulation of mitochondrial genes. Although the promotion of mitochondrial biogenesis induced by caloric restriction was recently re-evaluated in an extensive restriction study in rats, in which no changes were found in the amount of mitochondrial proteins in restricted animals (14), improvements of mitochondrial function in WAT were earlier observed in other restricted animals and is thought to be related to the beneficial effects of restriction (15, 37), in which our study is the first to report effects on mitochondrial function in mice restricted on a high-fat diet.

Conclusions

The results of our study prove that dietary restriction can reverse the adverse effects of an, initial unhealthy, high-fat diet. Our treatment had a large influence on gene expression in WAT. An in-depth study on genes with the strongest P-values revealed a major role for genes involved in lipid metabolism and mitochondrial functioning. It is hypothesized that the restriction procedure has forced the metabolism of mice towards the utilization of especially lipids in order to effectively make use of the diet, spare carbohydrates and to create a stable energy balance. The effective use of fat seems to

protect HF-DR mice from the increase in serum cholesterol and leptin levels that were found in HF-AL mice, as well as from the decrease in mitochondrial density in WAT, and decrease in glucose sensitivity and serum adiponectin levels.

Acknowledgements
We thank all members of the Department of Human and Animal Physiology and RIKILT Food Bioactives group for their helpful contributions, especially Melissa Bekkenkamp and Marianne van der Mark for their help with the OGTT and qRT-PCR, and everyone from the animal facility who was involved in this study. The research leading to these results has received funding from the European Union's Seventh Framework Programme FP7 2007-2013 under grant agreement nº 244995 (BIOCLAIMS Project).

References

1. Ando H, Yanagihara H, Hayashi Y, Obi Y, Tsuruoka S, Takamura T*, et al.* Rhythmic messenger ribonucleic acid expression of clock genes and adipocytokines in mouse visceral adipose tissue. Endocrinology. 2005;146: 5631-5636.
2. Anzulovich A, Mir A, Brewer M, Ferreyra G, Vinson C, Baler R Elovl3: a model gene to dissect homeostatic links between the circadian clock and nutritional status. J Lipid Res. 2006;47: 2690-2700.
3. Brown MS, Goldstein JL The SREBP pathway: regulation of cholesterol metabolism by proteolysis of a membrane-bound transcription factor. Cell. 1997;89: 331-340.
4. Bruss MD, Khambatta CF, Ruby MA, Aggarwal I, Hellerstein MK Calorie restriction increases fatty acid synthesis and whole body fat oxidation rates. Am J Physiol Endocrinol Metab. 2010;298: E108-116.
5. Champy MF, Selloum M, Zeitler V, Caradec C, Jung B, Rousseau S*, et al.* Genetic background determines metabolic phenotypes in the mouse. Mamm Genome. 2008;19: 318-331.
6. Choi YS, Goto S, Ikeda I, Sugano M Age-related changes in lipid metabolism in rats: the consequence of moderate food restriction. Biochim Biophys Acta. 1988;963: 237-242.
7. Combs TP, Berg AH, Rajala MW, Klebanov S, Iyengar P, Jimenez-Chillaron JC*, et al.* Sexual differentiation, pregnancy, calorie restriction, and aging affect the adipocyte-specific secretory protein adiponectin. Diabetes. 2003;52: 268-276.
8. Cretenet G, Le Clech M, Gachon F Circadian clock-coordinated 12 Hr period rhythmic activation of the IRE1alpha pathway controls lipid metabolism in mouse liver. Cell Metab. 2010;11: 47-57.
9. Dahlman I, Forsgren M, Sjogren A, Nordstrom EA, Kaaman M, Naslund E*, et al.* Downregulation of electron transport chain genes in visceral adipose tissue in type 2 diabetes independent of obesity and possibly involving tumor necrosis factor-alpha. Diabetes. 2006;55: 1792-1799.
10. de Boer VC, van Schothorst EM, Dihal AA, van der Woude H, Arts IC, Rietjens IM*, et al.* Chronic quercetin exposure affects fatty acid catabolism in rat lung. Cell Mol Life Sci. 2006;63: 2847-2858.
11. de Meijer VE, Le HD, Meisel JA, Sharif MR, Pan A, Nose V*, et al.* Dietary fat intake promotes the development of hepatic steatosis independently from excess caloric consumption in a murine model. Metabolism. 2010;59: 1092-1105.
12. Dhahbi JM, Mote PL, Wingo J, Rowley BC, Cao SX, Walford RL*, et al.* Caloric restriction alters the feeding response of key metabolic enzyme genes. Mech Ageing Dev. 2001;122: 1033-1048.
13. Friedewald WT, Levy RI, Fredrickson DS Estimation of the concentration of low-density lipoprotein cholesterol in plasma, without use of the preparative ultracentrifuge. Clin Chem. 1972;18: 499-502.
14. Hancock CR, Han DH, Higashida K, Kim SH, Holloszy JO Does calorie restriction induce mitochondrial biogenesis? A reevaluation. FASEB J. 2010;(in press):
15. Higami Y, Pugh TD, Page GP, Allison DB, Prolla TA, Weindruch R Adipose tissue energy metabolism: altered gene expression profile of mice subjected to long-term caloric restriction. FASEB J. 2004;18: 415-417.
16. Hochberg Y, Benjamini Y More powerful procedures for multiple significance testing. Stat Med. 1990;9: 811-818.
17. Houthoofd K, Braeckman BP, Lenaerts I, Brys K, De Vreese A, Van Eygen S*, et al.* No reduction of metabolic rate in food restricted Caenorhabditis elegans. Exp Gerontol. 2002;37: 1359-1369.
18. Hulbert AJ, Clancy DJ, Mair W, Braeckman BP, Gems D, Partridge L Metabolic rate is not reduced by dietary-restriction or by lowered insulin/IGF-1 signalling and is not correlated with individual lifespan in Drosophila melanogaster. Exp Gerontol. 2004;39: 1137-1143.
19. Jager S, Bucci C, Tanida I, Ueno T, Kominami E, Saftig P*, et al.* Role for Rab7 in maturation of late autophagic vacuoles. J Cell Sci. 2004;117: 4837-4848.
20. Jung CH, Ro SH, Cao J, Otto NM, Kim DH mTOR regulation of autophagy. FEBS Lett. 2010;584: 1287-1295.

21. Kalupahana NS, Voy BH, Saxton AM, Moustaid-Moussa N Energy-Restricted High-Fat Diets Only Partially Improve Markers of Systemic and Adipose Tissue Inflammation. Obesity (Silver Spring). 2010;
22. Kanki T, Klionsky DJ The molecular mechanism of mitochondria autophagy in yeast. Mol Microbiol. 2010;75: 795-800.
23. Keijer J, van Schothorst EM Adipose tissue failure and mitochondria as a possible target for improvement by bioactive food components. Curr Opin Lipidol. 2008;19: 4-10.
24. Kelly DP, Scarpulla RC Transcriptional regulatory circuits controlling mitochondrial biogenesis and function. Genes Dev. 2004;18: 357-368.
25. Kenyon CJ The genetics of ageing. Nature. 2010;464: 504-512.
26. Kopelman PG Obesity as a medical problem. Nature. 2000;404: 635-643.
27. Lagouge M, Argmann C, Gerhart-Hines Z, Meziane H, Lerin C, Daussin F*, et al.* Resveratrol improves mitochondrial function and protects against metabolic disease by activating SIRT1 and PGC-1alpha. Cell. 2006;127: 1109-1122.
28. Lambert AJ, Wang B, Yardley J, Edwards J, Merry BJ The effect of aging and caloric restriction on mitochondrial protein density and oxygen consumption. Exp Gerontol. 2004;39: 289-295.
29. Lara-Castro C, Newcomer BR, Rowell J, Wallace P, Shaughnessy SM, Munoz AJ*, et al.* Effects of short-term very low-calorie diet on intramyocellular lipid and insulin sensitivity in nondiabetic and type 2 diabetic subjects. Metabolism. 2008;57: 1-8.
30. Ledikwe JH, Blanck HM, Kettel Khan L, Serdula MK, Seymour JD, Tohill BC*, et al.* Dietary energy density is associated with energy intake and weight status in US adults. Am J Clin Nutr. 2006;83: 1362-1368.
31. Lee CK, Allison DB, Brand J, Weindruch R, Prolla TA Transcriptional profiles associated with aging and middle age-onset caloric restriction in mouse hearts. Proc Natl Acad Sci U S A. 2002;99: 14988-14993.
32. Lee CK, Klopp RG, Weindruch R, Prolla TA Gene expression profile of aging and its retardation by caloric restriction. Science. 1999;285: 1390-1393.
33. Leonard AE, Pereira SL, Sprecher H, Huang YS Elongation of long-chain fatty acids. Prog Lipid Res. 2004;43: 36-54.
34. Li B, Shin J, Lee K Interferon-stimulated gene ISG12b1 inhibits adipogenic differentiation and mitochondrial biogenesis in 3T3-L1 cells. Endocrinology. 2009;150: 1217-1224.
35. Liang G, Yang J, Horton JD, Hammer RE, Goldstein JL, Brown MS Diminished hepatic response to fasting/refeeding and liver X receptor agonists in mice with selective deficiency of sterol regulatory element-binding protein-1c. J Biol Chem. 2002;277: 9520-9528.
36. Lin J, Yang R, Tarr PT, Wu PH, Handschin C, Li S*, et al.* Hyperlipidemic effects of dietary saturated fats mediated through PGC-1beta coactivation of SREBP. Cell. 2005;120: 261-273.
37. Linford NJ, Beyer RP, Gollahon K, Krajcik RA, Malloy VL, Demas V*, et al.* Transcriptional response to aging and caloric restriction in heart and adipose tissue. Aging Cell. 2007;6: 673-688.
38. Matsuzaka T, Shimano H, Yahagi N, Yoshikawa T, Amemiya-Kudo M, Hasty AH*, et al.* Cloning and characterization of a mammalian fatty acyl-CoA elongase as a lipogenic enzyme regulated by SREBPs. J Lipid Res. 2002;43: 911-920.
39. Nadler ST, Stoehr JP, Schueler KL, Tanimoto G, Yandell BS, Attie AD The expression of adipogenic genes is decreased in obesity and diabetes mellitus. Proc Natl Acad Sci U S A. 2000;97: 11371-11376.
40. Narendra D, Tanaka A, Suen DF, Youle RJ Parkin is recruited selectively to impaired mitochondria and promotes their autophagy. J Cell Biol. 2008;183: 795-803.
41. Oberkofler H, Fukushima N, Esterbauer H, Krempler F, Patsch W Sterol regulatory element binding proteins: relationship of adipose tissue gene expression with obesity in humans. Biochim Biophys Acta. 2002;1575: 75-81.
42. Ogden CL, Carroll MD, Curtin LR, Lamb MM, Flegal KM Prevalence of high body mass index in US children and adolescents, 2007-2008. JAMA. 2010;303: 242-249.
43. Park KS, Wiederkehr A, Kirkpatrick C, Mattenberger Y, Martinou JC, Marchetti P*, et al.* Selective actions of mitochondrial fission/fusion genes on metabolism-secretion coupling in insulin-releasing cells. J Biol Chem. 2008;283: 33347-33356.
44. Park SK, Prolla TA Lessons learned from gene expression profile studies of aging and caloric restriction. Ageing Res Rev. 2005;4: 55-65.

45. Pellis L, Franssen-van Hal NL, Burema J, Keijer J The intraclass correlation coefficient applied for evaluation of data correction, labeling methods, and rectal biopsy sampling in DNA microarray experiments. Physiol Genomics. 2003;16: 99-106.
46. Peters SJ, Harris RA, Wu P, Pehleman TL, Heigenhauser GJ, Spriet LL Human skeletal muscle PDH kinase activity and isoform expression during a 3-day high-fat/low-carbohydrate diet. Am J Physiol Endocrinol Metab. 2001;281: E1151-1158.
47. Petro AE, Cotter J, Cooper DA, Peters JC, Surwit SJ, Surwit RS Fat, carbohydrate, and calories in the development of diabetes and obesity in the C57BL/6J mouse. Metabolism. 2004;53: 454-457.
48. Prentice AM, Jebb SA Fast foods, energy density and obesity: a possible mechanistic link. Obes Rev. 2003;4: 187-194.
49. Reimer RA, Maurer AD, Lau DC, Auer RN Long-term dietary restriction influences plasma ghrelin and GOAT mRNA level in rats. Physiol Behav. 2010;99: 605-610.
50. Rezzi S, Martin FP, Shanmuganayagam D, Colman RJ, Nicholson JK, Weindruch R Metabolic shifts due to long-term caloric restriction revealed in nonhuman primates. Exp Gerontol. 2009;44: 356-362.
51. Riegelhaupt JJ, Waase MP, Garbarino J, Cruz DE, Breslow JL Targeted disruption of steroidogenic acute regulatory protein D4 leads to modest weight reduction and minor alterations in lipid metabolism. J Lipid Res. 2010;51: 1134-1143.
52. Rodriguez-Agudo D, Ren S, Wong E, Marques D, Redford K, Gil G*, et al.* Intracellular cholesterol transporter StarD4 binds free cholesterol and increases cholesteryl ester formation. J Lipid Res. 2008;49: 1409-1419.
53. Scarpulla RC Transcriptional paradigms in mammalian mitochondrial biogenesis and function. Physiol Rev. 2008;88: 611-638.
54. Semple RK, Crowley VC, Sewter CP, Laudes M, Christodoulides C, Considine RV*, et al.* Expression of the thermogenic nuclear hormone receptor coactivator PGC-1alpha is reduced in the adipose tissue of morbidly obese subjects. Int J Obes Relat Metab Disord. 2004;28: 176-179.
55. Sobel BE, Frye R, Detre KM Burgeoning dilemmas in the management of diabetes and cardiovascular disease: rationale for the Bypass Angioplasty Revascularization Investigation 2 Diabetes (BARI 2D) Trial. Circulation. 2003;107: 636-642.
56. Soukas A, Cohen P, Socci ND, Friedman JM Leptin-specific patterns of gene expression in white adipose tissue. Genes Dev. 2000;14: 963-980.
57. Strable MS, Ntambi JM Genetic control of de novo lipogenesis: role in diet-induced obesity. Crit Rev Biochem Mol Biol. 2010;45: 199-214.
58. Trayhurn P, Beattie JH Physiological role of adipose tissue: white adipose tissue as an endocrine and secretory organ. Proc Nutr Soc. 2001;60: 329-339.
59. van Helden YG, Heil SG, van Schooten FJ, Kramer E, Hessel S, Amengual J*, et al.* Knockout of the Bcmo1 gene results in an inflammatory response in female lung, which is suppressed by dietary beta-carotene. Cell Mol Life Sci. 2010;67: 2039-2056.
60. van Schothorst EM, Bunschoten A, Schrauwen P, Mensink RP, Keijer J Effects of a high-fat, low- versus high-glycemic index diet: retardation of insulin resistance involves adipose tissue modulation. FASEB J. 2009;23: 1092-1101.
61. van Schothorst EM, Flachs P, Franssen-van Hal NL, Kuda O, Bunschoten A, Molthoff J*, et al.* Induction of lipid oxidation by polyunsaturated fatty acids of marine origin in small intestine of mice fed a high-fat diet. BMC Genomics. 2009;10: 110.
62. Van Schothorst EM, Franssen-van Hal N, Schaap MM, Pennings J, Hoebee B, Keijer J Adipose gene expression patterns of weight gain suggest counteracting steroid hormone synthesis. Obes Res. 2005;13: 1031-1041.
63. van Schothorst EM, Keijer J, Pennings JL, Opperhuizen A, van den Brom CE, Kohl T*, et al.* Adipose gene expression response of lean and obese mice to short-term dietary restriction. Obesity (Silver Spring). 2006;14: 974-979.
64. van Schothorst EM, Pagmantidis V, de Boer VC, Hesketh J, Keijer J Assessment of reducing RNA input for Agilent oligo microarrays. Anal Biochem. 2007;363: 315-317.
65. Weindruch R, Naylor PH, Goldstein AL, Walford RL Influences of aging and dietary restriction on serum thymosin alpha 1 levels in mice. J Gerontol. 1988;43: B40-42.
66. Wettenhall JM, Smyth GK limmaGUI: a graphical user interface for linear modeling of microarray data. Bioinformatics. 2004;20: 3705-3706.
67. WHO/Europe July 2010. European HFA Database;

68. Yoon Y, Galloway CA, Jhun BS, Yu T Mitochondrial Dynamics in Diabetes. Antioxid Redox Signal. 2010;
69. Zhang J, Ney PA Role of BNIP3 and NIX in cell death, autophagy, and mitophagy. Cell Death Differ. 2009;16: 939-946.

Chapter 3

Assessment of metabolic flexibility of old and adult mice using three non-invasive, indirect calorimetry-based treatments.

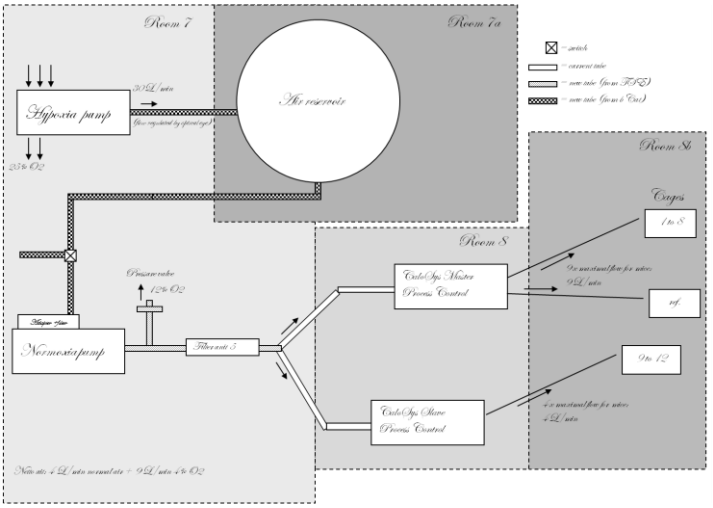

Loes P.M. Duivenvoorde, Evert M. van Schothorst, Hans Swarts, and Jaap Keijer

Published in: Journal of Gerontology, Series A: Biological Sciences (2015) 70, 282-293

Abstract

Indirect calorimetry (InCa) can potentially be used to non-invasively assess metabolic and age-related flexibility. To assess the use of InCa for this purpose, we tested the sensitivity and response stability over time of three InCa-based treatments in old versus adult mice. Diurnal patterns of respiratory exchange ratio were followed for 24 hours under standard conditions (Treatment 1), but the results were not stable between test periods. As a challenge, fasted mice received glucose to test switch-effectiveness from fat to glucose oxidation (Treatment 2). No differences between groups were observed, although old mice showed higher adiposity and lower white adipose tissue mitochondrial density, indicative of age-impaired metabolic health. Lastly, adaptation to a challenge of oxygen restriction (OxR, 14.5 % O_2) was assessed as a novel approach (Treatment 3). This treatment stably detected significant differences: old mice did not maintain reduced oxygen consumption under OxR during both test periods, while adult mice did. Further biochemical and gene expression analyses showed that OxR affected glucose and lactate homeostasis in liver and WAT of adult mice, supporting the observed differences in oxygen consumption.

In conclusion, InCa analysis of the response to OxR in mice is a sensitive and reproducible treatment to non-invasively measure age-impaired metabolic health.

Introduction

Health can be defined as the ability to adequately respond to physiological stress – that is, to be flexible and display homeostatic robustness (20). Metabolic flexibility is the capacity of an organism to adequately respond to changes in the environment, such as changes in nutritional input, energetic demand, or environmental changes like oxygen limitation. Metabolic flexibility can, therefore, be used as a measure for health.

A major disadvantage of many methods that assess health status is necessity of invasive procedures, which induce stress and modify physiological status. Blood sampling and injection have a pronounced effect on both blood glucose levels and body temperature in mice (25). Even simple routine procedures, such as lifting by the tail and restraining by hand, can have a significant influence on stress markers, such as plasma corticosterone levels, heart rate, and body temperature (38). Therefore, stress does not only affect whole body metabolism, but also increases variability of experimental data and reduces the quality and reproducibility of data obtained. Non-invasive techniques might overcome these drawbacks.

Indirect calorimetry (InCa) is commonly used as a non-invasive method to assess metabolism without disrupting an animal's normal behavior. In InCa the levels of O_2 consumption and CO_2 production are measured and used to calculate whole body energy expenditure (EE) and respiratory exchange ratio (RER), which reflects substrate use (23).

Deviations from the normal diurnal pattern of RER and EE can indicate health problems. In humans, for example, the absence of a clear day and night rhythm relates to an increased risk of Type 2 diabetes and cardiovascular diseases (3, 39). In mice, deviations from the normal circadian rhythm relate to decreased longevity (35), and increased body weight (1, 46). Alternatively, feeding a high-fat diet disturbs the expression of regulatory genes of the diurnal clock (4).

Next to the assessment of diurnal patterns under standard, free-feeding conditions, InCa also facilitates the incorporation of challenge tests. Challenge tests have major advantages above static physiological measurements, because they also assess the ability to adequately respond thus enlarging the effects of an experimental procedure (55). Indeed, nutritional (28) and environmental challenges (32) within InCa have been used efficiently to sensitively test metabolic health.

To conclude, analysis of metabolic health by InCa is promising and has numerous potential applications. The objective of this study was, therefore, to further establish InCa as a way to measure age-impaired metabolic health in mice and to identify the most sensitive and reproducible treatment. We compared three treatments and validated their reproducibility over time in two groups of apparently healthy male C57BL/6J mice that differed in age (adult vs. old). Treatment 1 was used to assess the natural diurnal pattern of RER. Treatments 2 and 3 were used to assess the response to a nutritional and environmental challenge. With treatment 2, we assessed metabolic

switch-flexibility of fasted mice in response to glucose consumption. With treatment 3, we used a novel approach to measure metabolic flexibility; mice were challenged by exposure to low oxygen conditions (oxygen restriction, OxR, 14.5 % O2) and their adaptive response was tested. The level of 14.5% oxygen is comparable to the situation at high altitude (around 10,000 ft.) and in certain airplanes, or the situation in obesity related disorders such as obstructive sleep apnea (18). The mild restriction in oxygen availability, therefore, resembles a condition that we can encounter in normal daily life. Moreover, pilot studies showed that this oxygen reduction is enough to apply a certain pressure on mouse physiology and to alter metabolism. Each treatment was tested twice with at least 10 weeks in between to examine the reproducibility of the treatment.

Materials and methods

Animals and experimental manipulations

The Animal Welfare Committee of Wageningen University, Wageningen, The Netherlands approved the experimental protocols (males: DEC2009061, females: DEC2011014). Eighteen male C57BL/6JOlaHsd mice (Harlan Laboratories, Horst, The Netherlands) were individually housed and maintained under environmentally controlled conditions (21 ± 1 ºC, 12 h/12 h light–dark cycle, 45% ± 10% humidity) with *ad libitum* access to feed and water. Mice received a pelletized diet (2016 Teklad Global 16% Protein Rodent Diet, Harlan) with 22% energy from protein, 12% energy from fat, and 66% energy from carbohydrates from weaning until the end of the study to exclude possible nutritional interference (34). Mice arrived at 8 weeks of age, at two different time-points - mice for the ‘old’ group arrived 62 weeks before the mice of the ‘adult’ group. After the mice for the ‘adult’ group arrived, all mice were housed in the same room and could adapt for two weeks. At the start of the study (t=0), the adult mice (n=12) were 10 weeks of age and the old mice (n=6) were 72 weeks of age. Bodyweight was determined weekly. Feed intake was determined weekly between week -2 and week 5, between week 8 and 11, and in the last week of the study by weighing the amount of feed in each cage at the start and at the end of the week. InCa treatment 1 and 2 were applied in weeks 0 and 13. Treatment 3 was applied in weeks 4 and 15. Mice were sacrificed in week 18. All analyses were done for 12 adult mice and 6 old mice, except where indicated. Treatment 3 was also applied to 6 adult (13 weeks) and 6 old (75 weeks) female C57BL/6JRcc mice.

At the end of the study, all mice received two grams of feed at the start of the dark phase and were sacrificed in random order 19 to 21 hours afterwards. Half of the adult mice were exposed to OxR for six hours prior to section, whereas the other 6 adult mice remained under ambient conditions. At the time point of sacrifice, mice were anesthetized by inhalation of 5% isoflurane with either 14.5% oxygen (OxR groups) or ambient air (ambient group) as a carrier. Blood was sampled after decapitation and

collected in Mini collect serum tubes (Greiner Bio-one, Longwood, USA), and centrifuged for 10 min at 3000 g and 4 °C to obtain serum. Serum samples were aliquoted and stored at –80 °C. After blood collection, gonadal white adipose tissue (WAT) and liver tissue were dissected, weighted, and snap frozen in liquid nitrogen and stored at –80 °C.

Indirect calorimetry (normal and low oxygen conditions)

The PhenoMaster Indirect Calorimetry System (TSE Systems, Bad Homburg, Germany) is equipped for simultaneous measurements of a reference cage and 12 individual mice in type II macrolon cages, using a constant flow rate of 0.40 L/min and a sample flow rate of 0.38 L/min, as published (27). The system was supplemented with a *Workhorse* hypoxia pump (b-Cat B.V., Tiel, the Netherlands) that stably decreases air oxygen concentration to 14.5%. When inflow air was switched from ambient air to OxR, or vice versa, 30 minutes were needed before measurements were stable (see suppl. fig. 1 for an example of the measurements with empty cages). Air samples are analyzed with a high-speed Siemens Ultramat/Oxymat 6 O_2 / CO_2 analyzer (TSE) that can sensitively and accurately measure O_2 in a range between 0% and 100% and CO_2 in a range between 0% and 1.5%. Here, the measuring range for O_2 was set between 0.0% and 21.5% and for CO_2 between 0.0% and 1.0%. The analyzer was calibrated with two gas mixtures: one with 0.000% O_2 and 1.007% CO_2, and the second with 20.949% O_2 and 0.000% CO_2 (Linde Gas, Schiedam, Netherlands). For all InCa measurements, mice remained in their home cage, with cage lids being replaced by airtight PhenoMaster cage lids. Mice were adapted in the Phenomaster system for at least 24h before the start of each measurement (see below). Rates of oxygen consumption (VO_2, ml/h) and carbon dioxide production (VCO_2, ml/h) were calculated by TSE software, using the reference cage as measurement of (adjusted) oxygen and carbon dioxide inflow, and used to calculate the respiratory exchange ratio (RER = VCO_2/VO_2) and energy expenditure (EE= (3.941*VO2+1.106*VCO2)/1000 in kcal/h). Physical activity is measured in the indirect calorimetry system with a frame containing 8 infrared beams at the long side (X-frame) of the animal cage and 6 infrared beams at the short side (Y-frame) of the cage. Physical activity was recorded for 8 animals simultaneously and expressed as total beam breaks (both X and Y) per minute.

Diurnal pattern of RER (Treatment 1).

Feed and water were provided *ad libitum*. InCa parameters and feed intake were measured for 24 hr. Mean RER values were calculated over 24 hours and distinctly over the light and dark phase.

Response to glucose administration (Treatment 2).

Mice received a restricted amount of feed (2 gram per animal) at the start of the dark phase (18.00h). After the start of the following light phase, in a fasted state, all animals received a single glucose pellet (2g / kg BW). The time point when all glucose was consumed (within 1 to 3 minutes) was taken as time point t=0. Mice were followed for

120 minutes afterwards and the RERs of individual animals were used to calculate the incremental area under the curve.

Response to OxR challenge (Treatment 3).

Mice received 2 gram of feed at the start of the dark phase. After start of the light phase, the oxygen level was decreased from ambient (20.8%) to 14.5% (OxR). After 30 minutes, the oxygen level stabilized and measurements were recorded for six hours under OxR. Next, the oxygen level was normalized to ambient within 30 minutes and measurements were again recorded for another 2 hours under ambient conditions. The experiment was divided in blocks of 100 minutes: 100 minutes before OxR exposure; 0-100 min, 100-200 min, and 200-300 minutes during OxR exposure; and 100 minutes after OxR. Blocks were compared within each animal group.

Analysis of serum and tissue parameters

Liver (40-60 mg per sample) and WAT (80-120 mg per sample) were homogenized in liquid nitrogen and dissolved in 1 ml TRIS-HCl buffer (50 mM, pH 7.4) with an automated Pellet Mixer (VWR International B.V., Amsterdam, the Netherlands). The tissue homogenates were centrifuged at 12,000 g at 4^0C for 5 minutes and supernatants were transferred to new precooled tubes and kept on ice. Total protein concentration was determined with the RC DC protein assay (Biorad), using Bovine Serum Albumin Fraction V dilutions (Roche Diagnostics GmbH, Mannheim, Germany) as standard. The tissue homogenates were subsequently stored at -80 ^{0}C until determination of lactate and citrate synthase activity levels.

Lactate levels in serum, WAT, and liver were determined using the Lactate Assay Kit II (Biovision, Mountain View, USA). Preparation of the samples was carried out according to the manufacturer's protocol. Serum, liver, and WAT samples were 30x, 4x, and 2x diluted in assay buffer, respectively. Lactate concentrations were calculated based on the linear regression curve of a serial diluted lactate standard (provided by the kit). The lactate concentration in homogenized WAT and liver was corrected for the amount of total protein in each sample.

Glucose levels in blood were determined with a *Freestyle* blood glucose system (Abbott Diabetes Care, Hoofddorp, the Netherlands) according to the manufacturer's instructions.

Tissue homogenates were diluted to 1 mg/ml protein for liver and 0.15 mg/ml for WAT to measure the citrate synthase activity level with the Citrate Synthase Assay Kit (Sigma Aldrich) according to the manufacturer's instructions (although for WAT, 16 µL of sample was used; and for liver and WAT, absorbance was measured for 60 minutes). Activity levels were calculated from the linear slope (15^{th} to 60^{th} minute) of the absorbance curves.

Hepatic glycogen was detected with iodine. Liver samples were grinded in liquid nitrogen and homogenized in 1 µl of 7% perchloric acid per mg tissue. Samples were centrifuged for 15 minutes at 4^0C and 1000 g and the resulting supernatant was left for

1.5 hours at -80^{0}C after which 1 ml (per 300 µl $HClO_4$) petroleum ether was added. Subsequent vortexing resulted into a separation into two layers of which the lower phase was used for further analysis: 10 µl sample was incubated for 10 minutes in a 96-wells plate with 260 µl reagent containing 0.89M calcium chloride, 1.32mM iodine, and 11.4 mM potassium iodide. Absorption was measured at 460 nm. Glycogen concentrations were calculated based on the linear regression curve of a serial diluted glycogen standard.

The ratio of mitochondrial DNA to nuclear DNA in WAT was determined by qRT-PCR as described previously (19) with the following modification: total DNA was extracted from homogenized eWAT by digestion with Proteinase K in a lysis buffer (50 mM Tris-HCL, pH 7.5, 0.5% SDS and 12.5 mM EDTA, pH 8.0). After overnight incubation at 56°C, Proteinase K was inactivated by a 10-minutes incubation at 70°C. Samples were then incubated with 40 µg/ml RNAse A (Sigma-Aldrich) for 1h at 37°C. After centrifugation, the aqueous phase was mixed and extracted with an equal amount of phenol-chloroform-isoamylacohol and twice with chloroform. DNA was precipitated by 96% ethanol and sodium acetate (3M, pH 5.2). DNA was washed with 750 µl of cold 70% ethanol, air-dried and re-suspended in 10 µl of RNAse DNAse free water. DNA concentration was adjusted to 65 ng/µl with RNAse DNAse free water.

RNA isolations and cDNA synthesis from liver and WAT were performed as described (57). qRT-PCR was performed as previously described (56). Ribosomal protein S15 (*Rps15*) and endoplasmic reticulum chaperone SIL1 homolog (*Sil1*) were used as reference genes. The primer sequences and PCR annealing temperatures for each gene are provided in table 1. Analyses of gene expression, and glucose, glycogen, protein and lactate levels were only performed in adult mice.

Table 1 Primer sequences and PCR annealing temperatures used for qRT-PCR.

Gene	Forward primer 5' – 3'	Reverse primer 5' – 3'	PCR temp.
Hk1	ATCTGTATGCCATGCGGCTCTCT	TGAAATCCCCCTTTTCTGAGCCGT	60.0ºC
Hk2	GACCAGAGCATCCTCCTCAAGTG	CTTCATAGCCACAAGTCATCATAGTCC	58.0ºC
Ldha	CACGCTGCTTCTCCTCGCCAGT	GGCACAAGCCATGCCAACAGCAC	62.0ºC
Pdk1	TGAAGCAGTTCCTGGACTTCGGGTC	TGTCGGGGAGGAGGCTGATTTCT	62.0ºC
Pklr	TGGCGGACACCTTCCTGGAACA	TCTGCATGGTACTCATGGGAGCCA	60.0ºC
*Rps15**	CGGAGATGGTGGGTAGCATGG	ACGGGTTTGTAGGTGATGGAGAAC	62.0ºC
*Sil1**	GGCCGCCTTTTCCAGCAATC	CGGGGAGAGGCTGGTTTGTG	62.0ºC
Slc16a1	GGCCACCACTTTTAGGCCGC	AGTCGATAGTTGATGCCCATGCCA	62.0ºC

Hk1, hexokinase 1; *Hk2*, hexokinase 2; *Ldha*, lactate dehydrogenase A; *Pdk1*, pyruvate dehydrogenase kinase 1; *Pklr*, pyruvate kinase; *Rps15,* ribosomal protein S15; *Sil1,* endoplasmic reticulum chaperone SIL1 homolog; *Slc16a1*, solute carrier family 16 (lactate importer). Genes denoted with an asterisk were used as reference genes for normalization.

Statistical analyses

Data are expressed as mean ± SEM; statistical analyses were performed using GraphPad Prism version 5.03 (Graphpad, San Diego, USA). P-values < 0.05 were considered statistically significant and denoted as follows: p<0.05 (*), p<0.01 (**), and p<0.001 (***). *Pdk1* and *Pklr* expression levels in WAT were not normally distributed

and were log-transformed. Measurements at single time points between 2 independent groups were analyzed by independent Student's *t*-tests. To compare the different periods before, during and after OxR within each group, blocks of 100 minutes were analyzed by one-way repeated measures ANOVA and subsequent Bonferroni Posthoc analysis. Oxygen consumption during OxR was also analyzed with ANCOVA using SPSS Statistics for Windows, version 19 (IBM Corp., Armonk, USA), in which body weight was used as confounding factor.

Results

Old and adult mice differ in body weight, body composition, and mitochondrial density in WAT.

To assess health status of adult and old mice, differences in BW, body composition, and mitochondrial density in liver and WAT were analyzed. Decreased WAT mitochondrial density is associated with impaired metabolic health (e.g. (10)). Mean BW of old mice was significantly greater during the complete course of the study compared with adult mice (fig. 1A, solid lines).

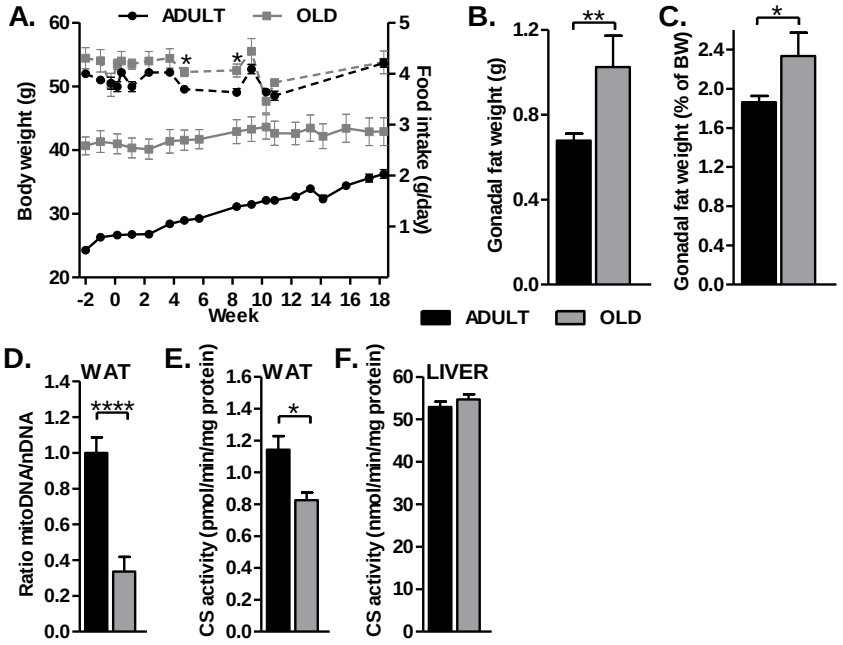

Figure 1 Body weight, feed intake, adiposity, and mitochondrial density in WAT and liver of ADULT and OLD mice. Adult mice (n=12, 10 weeks old at start of the experiment) and old mice (n=6, 72 weeks at start of the experiment) were individually housed and received *ad libitum* chow diet. In week 18, at the start of the dark phase, mice received a restricted amount (2 gr.) of feed, and tissues were harvested in the following light phase. Individual body weight (solid lines) and feed intake (dashed lines) (A) were followed during the complete period of study. Gonadal fat pad weight is analyzed as absolute values (B) and relatively to the animal's body weight (C). Mitochondrial density in WAT was determined by the ratio of mitochondrial DNA over nuclear DNA (D) and by citrate synthase activity levels (E). Citrate synthase activity levels were also determined in liver (F).

The absolute (fig. 1B) and relative (fig. 1C) gonadal fat pad weights at the end of the study were significantly larger in old mice. Overall, feed intake was not significantly different between groups; only in weeks 5 and 8 old mice consumed more feed compared with adult mice (fig. 1A, dashed lines). Old mice had a significant lower ratio of mitochondrial DNA to nuclear DNA in WAT than adult mice, which indicates a decrease in mitochondrial density (fig. 1D). This is supported by a significantly lower citrate synthase (CS) activity level in WAT of old mice, which is also considered a marker for tissue mitochondrial density (fig. 1E). In contrast, hepatic CS activity level was not significantly different between both groups of mice (fig. 1F).

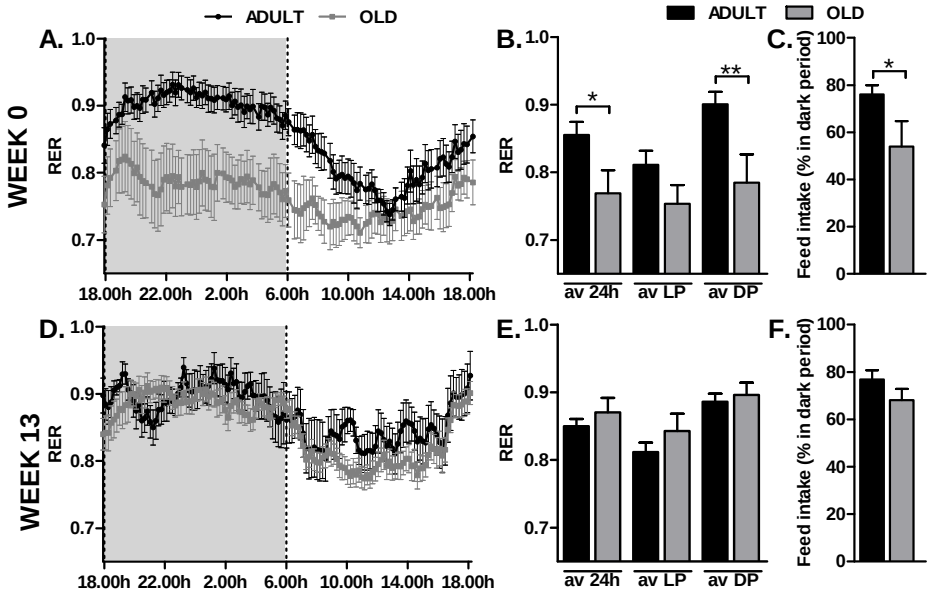

Figure 2 TREATMENT 1 - Mean RER and feed intake of ADULT and OLD mice under free-feeding conditions. RERs of adult (n=12; 10 weeks old in week 0) and old (n=6; 72 weeks old in week 0) mice were recorded for 24 hours after a 24h adaptation in the indirect calorimetry system in week 0 (A) and week 13 (D), during which they had *ad libitum* access to feed and water. For both measurements, mean RER was calculated over the complete 24 hours, as well as over the complete light and dark phase (B=week 0, and E=week 13). Feed intake was measured continuously during the calorimetric recordings and is presented as the % of feed intake in the dark phase (C=week 0, and F= week 13).

Old mice showed an impaired diurnal pattern of RER and food intake in week 0, although these differences disappeared in week 13

In week 0, adult and old mice displayed a different diurnal RER pattern (fig. 2A); the mean RER of old mice was significantly lower during the complete 24 hours and during the dark phase, compared with the mean RER of adult mice in both time frames (fig. 2B). Consistently, old mice consumed a smaller percentage of their feed during the dark phase versus adult mice (fig. 2C). In week 13, however, the difference between both groups had disappeared (fig. 2D), and both old and adult mice consumed a similar

percentage of feed during the dark phase (fig. 2F) and did not differ in mean values of RER (fig. 2E). During calorimetric measurements, adult mice consumed 3.52±0.29 (wk. 0) and 2.74±0.15 (wk. 13) gram over 24 hours, whereas old mice consumed 2.85±0.42 (wk. 0) and 3.53±0.38 (wk. 13) gram over 24 hours.

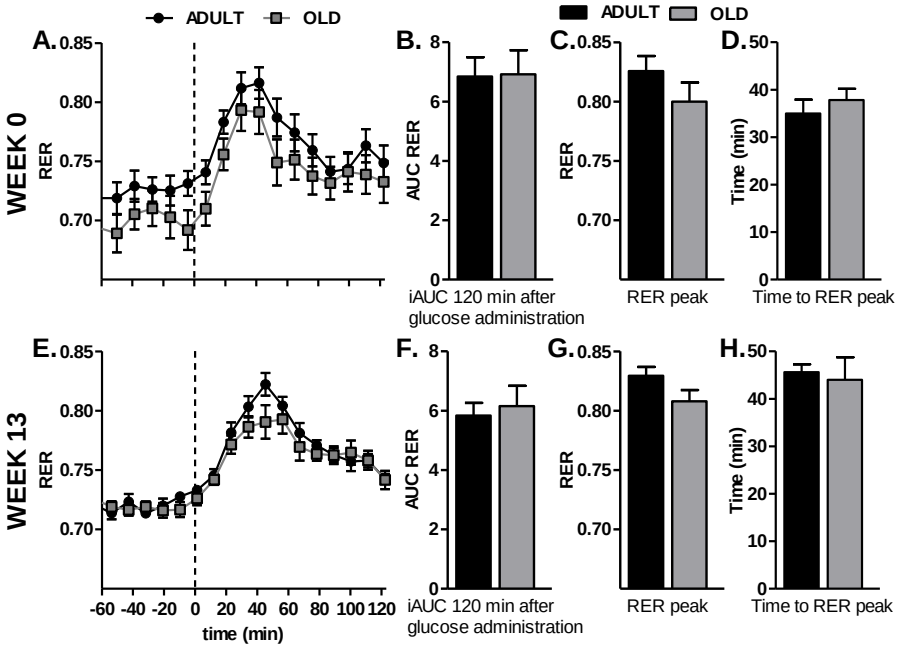

Figure 3 TREATMENT 2 - Respiratory response to a glucose bolus in fasted ADULT and OLD mice. Adult (n=12, 10 weeks old in week 0) and old (n=6, 72 weeks old in week 0) mice were fasted in the indirect calorimetry system (restricted feed (2 gr.) at the start of the dark phase) and received a glucose pellet (2 gr/kg BW) after start of the following light phase. RER was recorded for 2 hours after voluntary consumption of the glucose pellet in week 0 (A) and week 13 (E). T=0 represents the time point when the glucose pellet was fully consumed (within 1-3 minutes after provision). RER after glucose consumption was analyzed as the incremental area under the curve (iAUC) (B=week 0, and F= week 13), as the highest individual RER peak after glucose consumption (C=week 0, and G= week 13), and as the time needed to reach the RER peak (D=week 0, and H= week 13).

Physical activity follows the same pattern as the RER; in week 0, old mice lack a clear day- and night rhythm, whereas this was present in adult mice (suppl. fig. 3A). In week 13, old and adult mice do not differ in their activity pattern (suppl. fig. 3B). It should be noted that the activity measurements in week 0 were partially hampered by the available nesting material in the animal cages. This resulted in an overall underestimation of activity. We solved this for the remaining measurements by slightly reducing the available nesting material to a level that it did not interfere with beam break measures. Old mice have a higher energy expenditure than adult mice in both measurements (suppl. fig 4A+B).

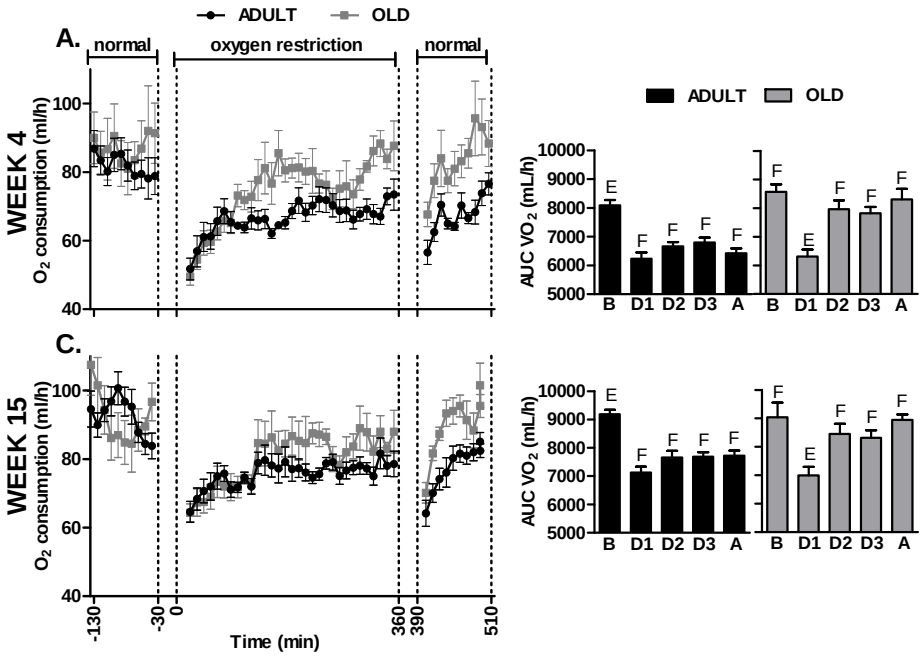

Figure 4 TREATMENT 3 - Respiratory response to oxygen restriction in fasted ADULT and OLD mice. Adult (n=12, 14 weeks old in week 4) and old (n=6, 76 weeks old in week 4) mice were fasted in the indirect calorimetry system (restricted feed (2 gr.) at the start of the dark phase) and were exposed to oxygen restriction after the start of the following light phase. Oxygen consumption was recorded for 2 hours before, 6 hours during, and 2 hours after exposure to oxygen restriction in week 4 (A) and week 15 (C). Oxygen consumption was analyzed within each animal group as the total area under the curve (AUC) in blocks of 100 minutes: 100 minutes before exposure; 0 to 100 min, 100 to 200 min, and 200 to 300 minutes during exposure; and 100 minutes after exposure (B=week 4, and D= week 15). Bars with different letters are statistically different.

Adult and old mice do not differ significantly in the response to glucose consumption

For treatment 2 and 3, mice were fasted by providing them with a restricted amount of food (2gr) at the start of the dark phase. Mice generally eat the restricted amount of food during the first part of the dark phase. With this method we ascertain that all mice are in fasting state before the start of the light phase, and we can control timing and quantity of feed intake before mice are challenged with glucose or OxR. Both adult and old mice, indeed, showed a mean RER between 0.69 and 0.72 at least one hour before glucose consumption, which indicates fasting. After glucose consumption, mean RER increased to approximately 0.83 and decreased after approximately 45 minutes (fig. 3A and 3E). The response to glucose administration was analyzed by the incremental area under the curve (iAUC) of individual RER curves over 120 minutes after glucose consumption. The mean iAUC was not significantly different (fig. 3B and 3F) indicating a similar glucose tolerance. Furthermore, adult and old mice showed similar RER peak

values and a similar time needed to reach the RER peak in both week 0 (fig. 3C and 3D) and week 13 (fig. 3G and 3H).

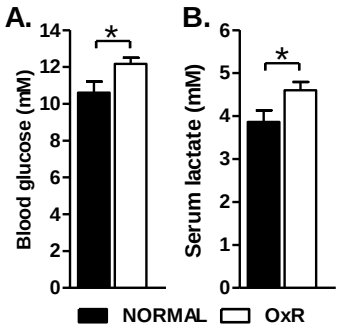

Figure 5 Serum lactate and blood glucose levels of adult mice that were either exposed to OxR or NORMAL air. Adult mice (28 weeks old) were fasted (restricted feed (2 gr.) at the start of the dark phase) and placed in normal (n=6) or oxygen restriction (n=6) conditions for 6 hours prior to blood collection. Blood glucose levels were determined directly after the exposure to oxygen restriction (B). Whole blood was then used to separate serum, in which lactate levels were determined (A).

In week 0, old mice are, on average, more active before and after glucose consumption than aged mice; whereas both groups do not differ in physical activity in week 13 (suppl. fig. 3C+D). In week 0, adult mice have higher EE levels before and after glucose consumption compared with old mice, whereas the opposite pattern was observed in week 13 (suppl. fig 4E+F).

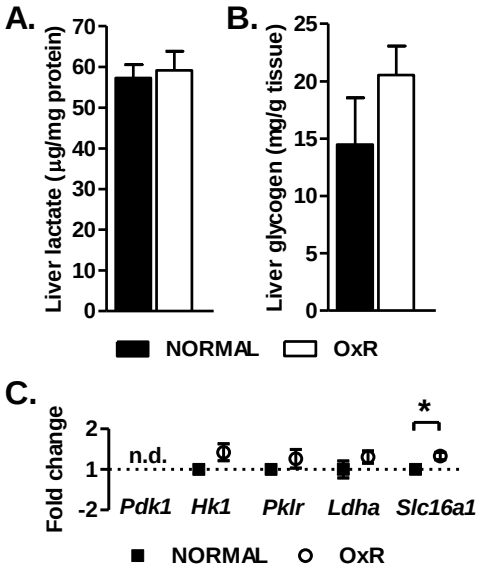

Figure 6 Parameters of lactate and glucose metabolism in liver tissue of adult mice that were either exposed to OxR or NORMAL air. Mice (28 weeks old) were fasted (restricted feed (2 gr.) at the start of the dark phase) and placed in normal (n=6) or oxygen restriction (n=6) conditions for 6 hours prior to tissue harvest. Liver tissue was homogenized to determine lactate (A) and glycogen (B) levels. Total mRNA was isolated to measure the expression of genes involved in glucose and lactate metabolism (C), which is expressed as the fold change of mice that were exposed to oxygen restriction over mice that remained under normal conditions. Hepatic *Pdk1* expression was below detection level. n.d., not determined; *Pdk1*, pyruvate dehydrogenase kinase 1; *Hk1*, hexokinase 1; *Hk2*, hexokinase 2; *Pklr*, pyruvate kinase; *Ldha*, lactate dehydrogenase A; *Slc16a1*, solute carrier family 16 (lactate importer).

Exposure to OxR only decreases oxygen consumption in adult mice

Because old adult mice differ in body weight we decided to only analyze oxygen consumption before, during and after OxR within each animal group. OxR significantly decreased oxygen consumption in both adult and old mice during the first 100 minutes of exposure (fig. 4). In adult mice, the drop in oxygen consumption continued during the complete period of OxR, even after returning back to normoxia. In old mice, on the

contrary, the decrease in oxygen consumption disappeared after the first 100 minutes of OxR (fig. 4). Similar patterns were observed in week 15, supporting the reproducibility of the treatment. RER values remained stable and within the physiological range during the exposure (suppl. fig. 2A+B). Although OxR decreases physical activity in both groups of mice, old and adult mice do not differ in physical activity (suppl. fig. 3E+F). The levels of EE follow the same pattern as the level of oxygen consumption during and after exposure to OxR (suppl. fig 4E+F).

To analyze differences in oxygen consumption during OxR between old and adult mice we used ANCOVA to correct for the difference in body weight (2, 52). ANCOVA showed that, when corrected for body weight, old and adult mice do not differ in average oxygen consumption during OxR (wk4: p=0.53 and wk15: p=0.84). Body weight on itself also did not account for the difference between old an adult mice (wk4: p=0.08 and wk15: p=0.20). VO2 during OxR rather depends on the combination of both age and body weight. Furthermore, we analyzed body weight and oxygen consumption during OxR within each group with linear regression. We did not find a correlation between body weight and oxygen consumption during OxR in neither of the groups (Week 4: p=0.22, R^2=0.14 for adult mice and p=0.11, R^2=0.52 for old mice; Week 15: p=0.99, R^2<0.00 for adult mice and p=0.17, R^2=0.42 for old mice). The OxR challenge was also applied to female mice and, as in males, we observed sustained decreased oxygen consumption in adult, but not in old mice (data not shown).

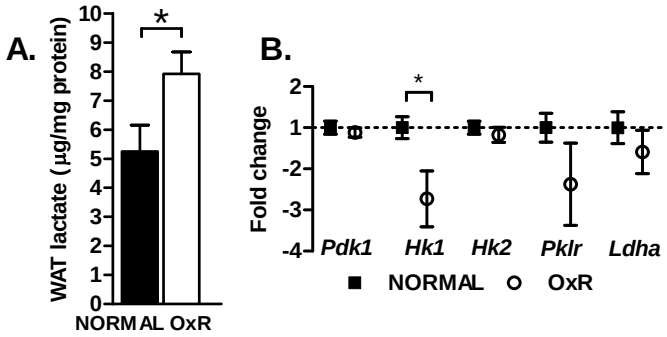

Figure 7 Parameters of lactate and glucose metabolism in WAT of adult mice that were either exposed to OxR or NORMAL air. Mice (28 weeks old) were fasted (restricted feed (2 gr.) during the dark phase) and placed in normal (n=6) or oxygen restriction (n=6) conditions for 6 hours prior to tissue harvest. WAT was homogenized to determine lactate levels (A). Total mRNA was isolated to measure the expression of genes involved in glucose and lactate metabolism (B), which is expressed as the fold change of mice that were exposed to oxygen restriction over mice that remained under normal conditions. *Pdk1*, pyruvate dehydrogenase kinase 1; *Hk1*, hexokinase 1; *Hk2*, hexokinase 2; *Pklr*, pyruvate kinase; *Ldha*, lactate dehydrogenase A

OxR altered glucose and lactate metabolism

The physiological mechanisms involved in the adaptation in oxygen consumption were further analyzed in the adult mice. Blood glucose and serum and WAT lactate levels

were significantly increased by OxR (fig. 5A+B and fig 7A). Hepatic lactate concentrations, however, were not significantly altered by OxR (fig. 6A), suggesting an increase in the lactate clearance rate in liver by gluconeogenesis. To investigate this in more detail, hepatic glycogen levels and expression levels of genes involved in glucose and lactate metabolism were studied in WAT and liver tissue of adult mice that were either exposed to OxR or normal air. Hepatic glycogen levels were unaltered by the exposure to OxR (fig. 6B). OxR significantly decreased the expression of hexokinase 1 in WAT (fig. 7B) and significantly increased the expression of the lactate importer *Slc16a1* (*Mct1*) in liver tissue (fig. 6C), which suggests an increase in gluconeogenesis in liver tissue. The other genes that were measured in liver and WAT were not significantly different between groups (fig. 6C and 7B). Hepatic *Pdk1* mRNA was below detection level in both groups of mice.

Discussion

Three different InCa-based treatments to measure age-dependent metabolic health were compared and examined for stability over time. The OxR challenge appeared to be most stable and sensitive to identify differences between adult and old mice. The observed changes in oxygen consumption were supported by gene expression and biochemical analysis in adult mice.

Old mice show a decrease in metabolic health

Aging affects metabolic health and correlates with an increase in bodyweight and risk factors for cardiovascular diseases and type 2 diabetes (15). Old mice indeed had a higher body weight and adiposity compared with adult mice and showed decreased mitochondrial density in WAT. In support, the expression of nuclear-encoded mitochondrial genes involved in oxidative phosphorylation, lipid metabolism and biosynthesis was previously shown to decrease with age in mice WAT (30). Furthermore, obese as well as insulin resistant rodents and humans show decreased WAT mitochondrial density (7, 10, 12, 19, 26, 29, 41, 49, 51), which suggests that the old mice display decreased adipose tissue health and associated decreased metabolic health. Next to WAT, the liver plays an important role in the maintenance of metabolic homeostasis. The mitochondrial density in liver tissue was, however, not affected by the aging process. The liver might be less susceptible to changes in mitochondrial density, as was previously seen in a dietary intervention with resveratrol (33).

The diurnal pattern of RER can indicate metabolic health but depends on feeding behavior

The mammalian circadian rhythm is affected by both aging (14) and obesity (37). Therefore, we expected to find differences in the pattern of RER between old and adult mice that would remain over time. Old versus adult mice indeed showed a disturbed

pattern of RER in week 0; they lacked a clear day- and night-rhythm and their mean RER was lower during the dark phase, compared with adult mice. These differences in RER are probably due to a difference in feeding pattern between both groups. Old mice consumed significantly less feed during the dark phase. The observed difference in the diurnal pattern of RER between adult and old mice is consistent with the disturbed pattern of EE and physical activity levels of old mice in week 0 and is expected to be a reliable observation. The measurements in week 0 showed that the old mice have a disturbed diurnal pattern, which is a common characteristic of aging (59).

In week 13, surprisingly, the pattern of RER appeared to be normalized to the values of adult mice. The change in the pattern of RER between weeks 0 and 13 is reflected by a change in feeding behavior of the old mice. Old mice had, in fact, increased feed intake in the dark phase to a similar level as adult mice, which suggests that the old mice have adapted their behavior to that of adult mice. Behavioral adaptation of old to adult mice might have been facilitated by sensory contact between mice. Although mice were individually housed, the transparent cages with a wire bar lid enable mice to communicate by smell, hearing and sight (54). Cages of both age groups were placed mixed and in random order on the same shelf. Sensory contact with an unfamiliar male mouse can cause dramatic changes in physiology and behavior, such as changes in heart rate, body temperature, and physical activity (45), which might explain the behavioral changes in old mice during the course of the study. The change in behavior that we observed in the old mice during the course of the study might be comparable to the behavioral changes that are seen in intergenerational programs in humans, in which generations are brought together in, for example, day care activities to support both young and old. Elderly people, who had the opportunity to engage in joined activities with children on a daily base, reported to feel “energized and vitalized by interactions with children” (58).

Our results show that care should be taken to draw conclusions on the health status of mice solely based on InCa measurements under free-feeding conditions. In particular factors that influence feeding behavior, such as the influence of sensory contact between mice.

Old and adult mice show similar responses to glucose administration

We expected that old mice would be less glucose tolerant, causing a delayed and blunted response in RER, as was shown recently for old mice using a standard glucose tolerance test (47). Moreover, it was shown that re-feeding in the InCa system leads to different responses in RER between mice with a different health status (28), indicating the value of the InCa system to distinguish between dietary groups based on the response to nutrient intake. We, however, observed no differences between old and adult mice in either of the two test periods, which indicates similar glucose tolerance.

The absence of differences in the response to glucose consumption may, in the first place, be due to the C57BL/6JOlaHsd strain that we used. This strain is known to have

an improved glucose tolerance compared with other BL/6J strains (24). Alternatively, a different method of glucose administration or a higher dose of glucose might have revealed differences in the RER response. Here, mice received pelleted glucose to avoid disturbances in respiratory exchange caused by opening of the calorimetric cage, or by stress of handling, injection, or oral gavage. Flachs, *et al.* (22), however, showed that a large dose of dissolved glucose does result in differences in RER between two dietary groups. Although, the increase in RER is comparable in both studies, we cannot exclude that a standard caloric load, which was based on a regular oral glucose tolerance test, is insufficient to pick up differences in glucose uptake and oxidation with the InCa system. Also we cannot exclude that the absence of a difference in RER response in our study is due to the use of liquid versus pelleted glucose, since the latter speeds up gastric emptying, which could increase the response in RER. Finally, it is possible that glucose is partly converted to glycogen, which is not reflected in changes in RER. Old and adult mice might differ in the degree of the conversion. It seems, however, unlikely that this difference will complete mask a difference in (RER) response. For future research it will be interesting to directly link InCa measurements for glucose tolerance to conventional oral glucose tolerance tests.

Adult versus old mice consume less oxygen during and after exposure to OxR

Oxygen restriction (14.5% O_2) in the InCa system is a novel approach to investigate parameters of metabolic health in mice and is based on the assumption that flexibility of cellular oxygen utilization depends on metabolic health status (6). Adequate oxygen delivery is essential for cell survival and normal metabolic function. When oxygen is restricted, metabolic adaptations are needed to assure sufficient ATP production and prevent development of oxidative stress.

In vitro studies have shown that extreme OxR increases glycolytic ATP (and lactate) production and reduces mitochondrial fatty acid oxidation (48), causing a decrease in cellular oxygen consumption (44). Next to an increase in glycolysis, hypoxia stimulates gluconeogenesis in hepatocytes (9) to clear lactate from the blood. The majority of *in vivo* studies confirm the results of *in vitro* studies. Long term exposure to OxR causes an increase in the expression of genes involved in angiogenesis and glycolysis, and a decrease in the expression of hepatic genes involved in lipid metabolism in mice (5, 17), and an increase in glucose transport (50) and hexokinase activity (13) in rat heart. On whole body level, OxR decreases oxygen consumption and energy expenditure in both rodents and humans (40, 42, 43), which reflects the decrease in mitochondrial activity that is seen in *in vitro* studies.

Our results show that OxR indeed decreased oxygen consumption during, but also after the exposure in adult mice, whereas old mice only sustained this lower level during the first 100 minutes of exposure. This was also seen when we repeated the measurements in week 15, showing treatment reproducibility.

The reduction in oxygen consumption can partly be explained by the reduction in physical activity that was seen during OxR. The unit 'beam breaks/ minute' that was used to describe physical activity represents the sum of total beam breaks in x-axis and y-axis in the horizontal plane. Infrared beam interruptions may, however, miss out on the more subtle types of activity (21), making them less suitable to calculate activity-induced EE (AEE) in relation to total energy expenditure (TEE). Since we cannot accurately calculate AEE, we used an alternative approach that estimates AEE by comparing TEE with (resting metabolic rate) RMR (AEE = TEE - RMR). If we use our available data from treatment 1, we see that AEE contributes to 17.7 % of TEE. Based on published data and modeling, it was calculated that AEE contributes to roughly 13.5% of TEE (53). The reduction in EE during OxR is 31.8% compared to TEE. Based on both calculations of AEE it seems unlikely that the reduction in EE and VO_2 during OxR only depends on a reduction in AEE. We rather think that old and adult mice differ in the response to OxR because of a difference in metabolic adaptation.

To further analyze metabolic adaptation to OxR in adult mice we analyzed circulating lactate levels, which were found to be significantly increased by the exposure to OxR. The increase in serum lactate suggests an overall increase in anaerobic glycolysis leading to lactate production. An increase in ATP production by glycolysis might partly explain the decrease in oxygen consumption during OxR. The liver showed only a slight (non-significant) increase in glycolytic enzymes, which suggests that other tissues might be involved in production of lactate. OxR, indeed, increased lactate levels in WAT, supporting the metabolic changes seen in hypoxia exposed cells (36) or reprogrammed cancer cells (31). However, no major changes in gene expression were found in this tissue. Hexokinase 1 was down-regulated, whereas the expression of hexokinase 2, pyruvate kinase and lactate dehydrogenase were unaltered by OxR. Apparently, the mild 6 hr. OxR did not result in major differences in gene expression levels *in vivo*. The increase in WAT lactate levels might be due to changes in glycolytic enzymes at protein level. Alternatively, the degree of fasting that was induced preceding and during OxR might in part overrule or delay metabolic switching.

Hepatic lactate levels were not altered by OxR, which suggests that the liver is involved in lactate clearance - that is, uptake of lactate from the bloodstream and subsequent conversion to glucose, which can be released to provide glucose to other tissues. Indeed, we observed upregulation of the hepatic lactate importer (*Slc16a*1) supporting increased hypoxia-mediated hepatic gluconeogenesis (9) and an increase in blood glucose levels. Furthermore, we did not find a decrease in glycogen levels between both groups, which indicates that the increase in blood glucose levels is not caused by hepatic glycogenolysis but rather suggests increased hepatic gluconeogenesis from lactate. The resulting glucose is expected to be partly secreted into the blood stream and partly stored as glycogen, causing the increase in blood glucose levels and the slight, although non-significant, increase in hepatic glycogen levels in mice that were

exposed to OxR. Blood glucose levels were under both conditions slightly higher than expected; this is most likely due to the use of isoflurane prior to decapitation (11, 16).
The continuation of decreased oxygen consumption of adult mice after their return to normoxia supports functional down-regulation of metabolism. The decrease in oxygen consumption after the exposure to OxR - when the oxygen level is restored to normal values - is accompanied with a slight increase in RER in this time period (suppl. fig. 2). RER possibly increases because the overload of blood glucose (that was induced by OxR) is cleared from the blood and stored, as the mice are still in a fasted state. For future research it might be interesting to focus on the molecular background of the recovery to normal metabolism after exposure to OxR. It is tempting to speculate that autophagy has a role in the functional metabolic adaptation to OxR and, thereby, facilitates the lowering of oxygen demand. Autophagy can provide cells with 'emergency' substrates and is induced by hypoxia and impaired in aging (8).

A challenge concept is more valuable to test metabolic health with InCa

In our study, implementation of a challenge (glucose and OxR) produced more reliable and stable results between measurements, compared with measurements under free-feeding conditions (RER diurnal pattern). Similar drawbacks of InCa under free-feeding conditions were previously described by Even and Nadkarni (21), who concluded that feed intake should be totally controlled and activity precisely measured.
The exposure to OxR appeared to be more sensitive to identify differences between old and adult mice, compared with the administration of glucose. Our results were confirmed in female mice and could be further strengthened by validation in other models. OxR combined with InCa measurements is a promising novel concept to non-invasively assess physiological health status.

Acknowledgements

We thank all members of Human and Animal Physiology for helpful contributions, especially Inge van der Stelt, Femke Hoevenaars, Elise Hoek- van den Hil, and Davina Derous. We thank Dr. Jan Kopecky (ASCR, Prague) for the constructive discussions.
This work was supported by the European Union's Seventh Framework Program FP7 2007-2013 under grant agreement no. 244995 (BIOCLAIMS Project).

References

1. Arble DM, Bass J, Laposky AD, Vitaterna MH, Turek FW Circadian timing of food intake contributes to weight gain. Obesity (Silver Spring). 2009;17: 2100-2102.
2. Arch JR, Hislop D, Wang SJ, Speakman JR Some mathematical and technical issues in the measurement and interpretation of open-circuit indirect calorimetry in small animals. Int J Obes (Lond). 2006;30: 1322-1331.
3. Ayas NT, White DP, Manson JE, Stampfer MJ, Speizer FE, Malhotra A*, et al.* A prospective study of sleep duration and coronary heart disease in women. Arch Intern Med. 2003;163: 205-209.
4. Barnea M, Madar Z, Froy O High-fat diet delays and fasting advances the circadian expression of adiponectin signaling components in mouse liver. Endocrinology. 2009;150: 161-168.
5. Baze MM, Schlauch K, Hayes JP Gene expression of the liver in response to chronic hypoxia. Physiol Genomics. 2010;41: 275-288.
6. Burtscher M Exercise limitations by the oxygen delivery and utilization systems in aging and disease: coordinated adaptation and deadaptation of the lung-heart muscle axis - a mini-review. Gerontology. 2013;59: 289-296.
7. Chattopadhyay M, Guhathakurta I, Behera P, Ranjan KR, Khanna M, Mukhopadhyay S*, et al.* Mitochondrial bioenergetics is not impaired in nonobese subjects with type 2 diabetes mellitus. Metabolism. 2011;60: 1702-1710.
8. Choi AM, Ryter SW, Levine B Autophagy in human health and disease. N Engl J Med. 2013;368: 1845-1846.
9. Choi JH, Park MJ, Kim KW, Choi YH, Park SH, An WG*, et al.* Molecular mechanism of hypoxia-mediated hepatic gluconeogenesis by transcriptional regulation. FEBS Lett. 2005;579: 2795-2801.
10. Choo HJ, Kim JH, Kwon OB, Lee CS, Mun JY, Han SS*, et al.* Mitochondria are impaired in the adipocytes of type 2 diabetic mice. Diabetologia. 2006;49: 784-791.
11. Constantinides C, Mean R, Janssen BJ Effects of isoflurane anesthesia on the cardiovascular function of the C57BL/6 mouse. ILAR J. 2011;52: e21-31.
12. Dahlman I, Forsgren M, Sjogren A, Nordstrom EA, Kaaman M, Naslund E*, et al.* Downregulation of electron transport chain genes in visceral adipose tissue in type 2 diabetes independent of obesity and possibly involving tumor necrosis factor-alpha. Diabetes. 2006;55: 1792-1799.
13. Daneshrad Z, Garcia-Riera MP, Verdys M, Rossi A Differential responses to chronic hypoxia and dietary restriction of aerobic capacity and enzyme levels in the rat myocardium. Mol Cell Biochem. 2000;210: 159-166.
14. Davidson AJ, Yamazaki S, Arble DM, Menaker M, Block GD Resetting of central and peripheral circadian oscillators in aged rats. Neurobiol Aging. 2008;29: 471-477.
15. Davidson MB The effect of aging on carbohydrate metabolism: a review of the English literature and a practical approach to the diagnosis of diabetes mellitus in the elderly. Metabolism. 1979;28: 688-705.
16. Desaulniers D, Yagminas A, Chu I, Nakai J Effects of anesthetics and terminal procedures on biochemical and hormonal measurements in polychlorinated biphenyl treated rats. Int J Toxicol. 2011;30: 334-347.
17. Dolt KS, Karar J, Mishra MK, Salim J, Kumar R, Grover SK*, et al.* Transcriptional downregulation of sterol metabolism genes in murine liver exposed to acute hypobaric hypoxia. Biochem Biophys Res Commun. 2007;354: 148-153.
18. Drager LF, Li J, Reinke C, Bevans-Fonti S, Jun JC, Polotsky VY Intermittent hypoxia exacerbates metabolic effects of diet-induced obesity. Obesity (Silver Spring). 2011;19: 2167-2174.
19. Duivenvoorde LP, van Schothorst EM, Bunschoten A, Keijer J Dietary restriction of mice on a high-fat diet induces substrate efficiency and improves metabolic health. J Mol Endocrinol. 2011;47: 81-97.
20. *Editorial* What is health? The ability to adapt. Lancet. 2009;373: 781.
21. Even PC, Nadkarni NA Indirect calorimetry in laboratory mice and rats: principles, practical considerations, interpretation and perspectives. Am J Physiol Regul Integr Comp Physiol. 2012;303: R459-476.

22. Flachs P, Ruhl R, Hensler M, Janovska P, Zouhar P, Kus V*, et al.* Synergistic induction of lipid catabolism and anti-inflammatory lipids in white fat of dietary obese mice in response to calorie restriction and n-3 fatty acids. Diabetologia. 2011;54: 2626-2638.
23. Frankenfield DC On heat, respiration, and calorimetry. Nutrition. 2010;26: 939-950.
24. Freeman H, Shimomura K, Cox RD, Ashcroft FM Nicotinamide nucleotide transhydrogenase: a link between insulin secretion, glucose metabolism and oxidative stress. Biochem Soc Trans. 2006;34: 806-810.
25. Gerdin AK, Igosheva N, Roberson LA, Ismail O, Karp N, Sanderson M*, et al.* Experimental and husbandry procedures as potential modifiers of the results of phenotyping tests. Physiol Behav. 2012;106: 602-611.
26. Heilbronn LK, Gan SK, Turner N, Campbell LV, Chisholm DJ Markers of mitochondrial biogenesis and metabolism are lower in overweight and obese insulin-resistant subjects. J Clin Endocrinol Metab. 2007;92: 1467-1473.
27. Hoevenaars FP, Keijer J, Swarts HJ, Snaas-Alders S, Bekkenkamp-Grovenstein M, van Schothorst EM Effects of dietary history on energy metabolism and physiological parameters in C57BL/6J mice. Exp Physiol. 2013;98: 1053-1062.
28. Horakova O, Medrikova D, van Schothorst EM, Bunschoten A, Flachs P, Kus V*, et al.* Preservation of metabolic flexibility in skeletal muscle by a combined use of n-3 PUFA and rosiglitazone in dietary obese mice. PLoS One. 2012;7: e43764.
29. Kaaman M, Sparks LM, van Harmelen V, Smith SR, Sjolin E, Dahlman I*, et al.* Strong association between mitochondrial DNA copy number and lipogenesis in human white adipose tissue. Diabetologia. 2007;50: 2526-2533.
30. Katic M, Kennedy AR, Leykin I, Norris A, McGettrick A, Gesta S*, et al.* Mitochondrial gene expression and increased oxidative metabolism: role in increased lifespan of fat-specific insulin receptor knock-out mice. Aging Cell. 2007;6: 827-839.
31. Keijer J, van Dartel D Reprogrammed metabolism of cancer cells as a potential therapeutic target. Curr Pharmac Des. 2013;(Ahead of print):
32. Klaus S, Rudolph B, Dohrmann C, Wehr R Expression of uncoupling protein 1 in skeletal muscle decreases muscle energy efficiency and affects thermoregulation and substrate oxidation. Physiol Genomics. 2005;21: 193-200.
33. Lagouge M, Argmann C, Gerhart-Hines Z, Meziane H, Lerin C, Daussin F*, et al.* Resveratrol improves mitochondrial function and protects against metabolic disease by activating SIRT1 and PGC-1alpha. Cell. 2006;127: 1109-1122.
34. Le Couteur DG, Wilder SM, de Cabo R, Simpson SJ The Evolution of Research on Ageing and Nutrition. J Gerontol A Biol Sci Med Sci. 2013;
35. Libert S, Bonkowski MS, Pointer K, Pletcher SD, Guarente L Deviation of innate circadian period from 24 h reduces longevity in mice. Aging Cell. 2012;11: 794-800.
36. Malthankar-Phatak GH, Patel AB, Xia Y, Hong S, Chowdhury GM, Behar KL*, et al.* Effects of continuous hypoxia on energy metabolism in cultured cerebro-cortical neurons. Brain Res. 2008;1229: 147-154.
37. Mantele S, Otway DT, Middleton B, Bretschneider S, Wright J, Robertson MD*, et al.* Daily rhythms of plasma melatonin, but not plasma leptin or leptin mRNA, vary between lean, obese and type 2 diabetic men. PLoS One. 2012;7: e37123.
38. Meijer MK, Spruijt BM, van Zutphen LF, Baumans V Effect of restraint and injection methods on heart rate and body temperature in mice. Lab Anim. 2006;40: 382-391.
39. Meisinger C, Heier M, Loewel H, Study MKAC Sleep disturbance as a predictor of type 2 diabetes mellitus in men and women from the general population. Diabetologia. 2005;48: 235-241.
40. Mimura Y, Furuya K Mechanisms of adaptation to hypoxia in energy metabolism in rats. J Am Coll Surg. 1995;181: 437-443.
41. Mootha VK, Lindgren CM, Eriksson KF, Subramanian A, Sihag S, Lehar J*, et al.* PGC-1alpha-responsive genes involved in oxidative phosphorylation are coordinately downregulated in human diabetes. Nat Genet. 2003;34: 267-273.
42. Mortola JP, Matsuoka T, Saiki C, Naso L Metabolism and ventilation in hypoxic rats: effect of body mass. Respir Physiol. 1994;97: 225-234.
43. Oltmanns KM, Gehring H, Rudolf S, Schultes B, Schweiger U, Born J*, et al.* Persistent suppression of resting energy expenditure after acute hypoxia. Metabolism. 2006;55: 669-675.

44. Papandreou I, Cairns RA, Fontana L, Lim AL, Denko NC HIF-1 mediates adaptation to hypoxia by actively downregulating mitochondrial oxygen consumption. Cell Metab. 2006;3: 187-197.
45. Rettich A, Kasermann HP, Pelczar P, Burki K, Arras M The physiological and behavioral impact of sensory contact among unfamiliar adult mice in the laboratory. J Appl Anim Welf Sci. 2006;9: 277-288.
46. Salgado-Delgado R, Angeles-Castellanos M, Saderi N, Buijs RM, Escobar C Food intake during the normal activity phase prevents obesity and circadian desynchrony in a rat model of night work. Endocrinology. 2010;151: 1019-1029.
47. Santulli G, Lombardi A, Sorriento D, Anastasio A, Del Giudice C, Formisano P*, et al.* Age-related impairment in insulin release: the essential role of beta(2)-adrenergic receptor. Diabetes. 2012;61: 692-701.
48. Semenza GL Targeting HIF-1 for cancer therapy. Nat Rev Cancer. 2003;3: 721-732.
49. Semple RK, Crowley VC, Sewter CP, Laudes M, Christodoulides C, Considine RV*, et al.* Expression of the thermogenic nuclear hormone receptor coactivator PGC-1alpha is reduced in the adipose tissue of morbidly obese subjects. Int J Obes Relat Metab Disord. 2004;28: 176-179.
50. Sivitz WI, Lund DD, Yorek B, Grover-McKay M, Schmid PG Pretranslational regulation of two cardiac glucose transporters in rats exposed to hypobaric hypoxia. Am J Physiol. 1992;263: E562-569.
51. Sutherland LN, Capozzi LC, Turchinsky NJ, Bell RC, Wright DC Time course of high-fat diet-induced reductions in adipose tissue mitochondrial proteins: potential mechanisms and the relationship to glucose intolerance. Am J Physiol Endocrinol Metab. 2008;295: E1076-1083.
52. Tschop MH, Speakman JR, Arch JRS, Auwerx J, Bruning JC, Chan L*, et al.* A guide to analysis of mouse energy metabolism. Nature Methods. 2012;9: 57-63.
53. Van Klinken JB, van den Berg SA, Havekes LM, Willems Van Dijk K Estimation of activity related energy expenditure and resting metabolic rate in freely moving mice from indirect calorimetry data. PLoS One. 2012;7: e36162.
54. Van Loo PL, Van Zutphen LF, Baumans V Male management: Coping with aggression problems in male laboratory mice. Lab Anim. 2003;37: 300-313.
55. van Ommen B, Keijer J, Heil SG, Kaput J Challenging homeostasis to define biomarkers for nutrition related health. Mol Nutr Food Res. 2009;53: 795-804.
56. van Schothorst EM, Flachs P, Franssen-van Hal NL, Kuda O, Bunschoten A, Molthoff J*, et al.* Induction of lipid oxidation by polyunsaturated fatty acids of marine origin in small intestine of mice fed a high-fat diet. BMC Genomics. 2009;10: 110.
57. Van Schothorst EM, Franssen-van Hal N, Schaap MM, Pennings J, Hoebee B, Keijer J Adipose gene expression patterns of weight gain suggest counteracting steroid hormone synthesis. Obes Res. 2005;13: 1031-1041.
58. Weintraub APC, Killian TS Intergenerational programming: Older persons' perceptions of its impact. Journal of Applied Gerontology. 2007;26: 370-384.
59. Wyse CA, Coogan AN Impact of aging on diurnal expression patterns of CLOCK and BMAL1 in the mouse brain. Brain Res. 2010;1337: 21-31.

Supplemental figures

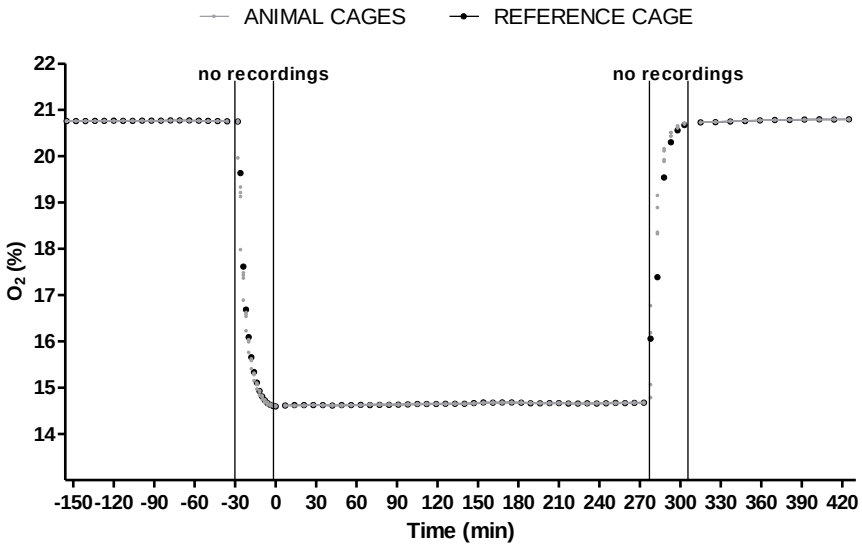

Supplemental figure 1 Measurements under normoxic and hypoxic conditions in empty cages of the indirect calorimetry system. In our indirect calorimetry system the air composition in the animal cages (in grey, each cage individually plotted) is compared to the air composition of an empty reference cage (in black). The delta O2 and CO2 are used to calculate O_2 consumption and CO_2 production by the software. In this example all ANIMAL CAGES were empty in order to check the stability of air composition in individual cages and the comparability of the animal cages with the REFERENCE CAGE. This clearly shows stability during hypoxic conditions, similar to normoxic conditions.

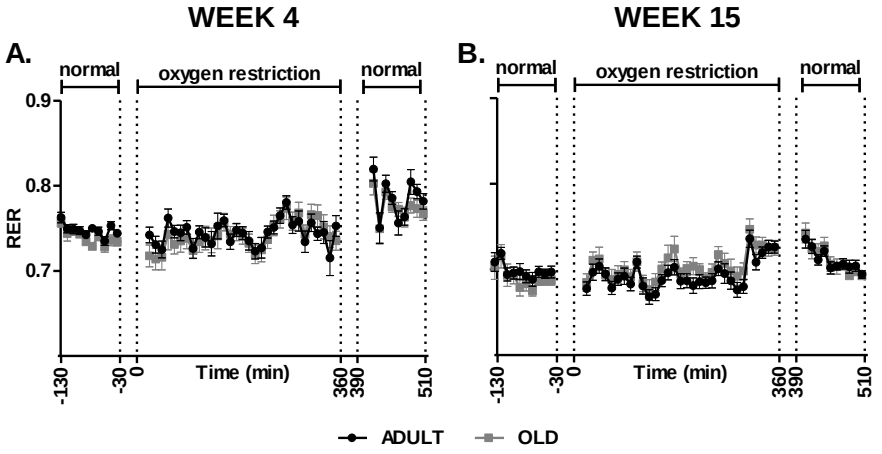

Supplemental figure 2 Average RER before, during and after the exposure to OxR (treatment 3) of ADULT and OLD mice in WEEK 4 and WEEK 15. Adult (n=12, 14 weeks old in week 4) and old (n=6, 76 weeks old in week 4) mice were fasted in the indirect calorimetry system by providing them with a restricted amount (2 gr.) of feed at the start of the dark phase and were exposed to oxygen restriction after the start of the following light phase. RER was recorded for 2 hours before, 6 hours during, and 2 hours after exposure to oxygen restriction in week 4 (A) and week 15 (B).

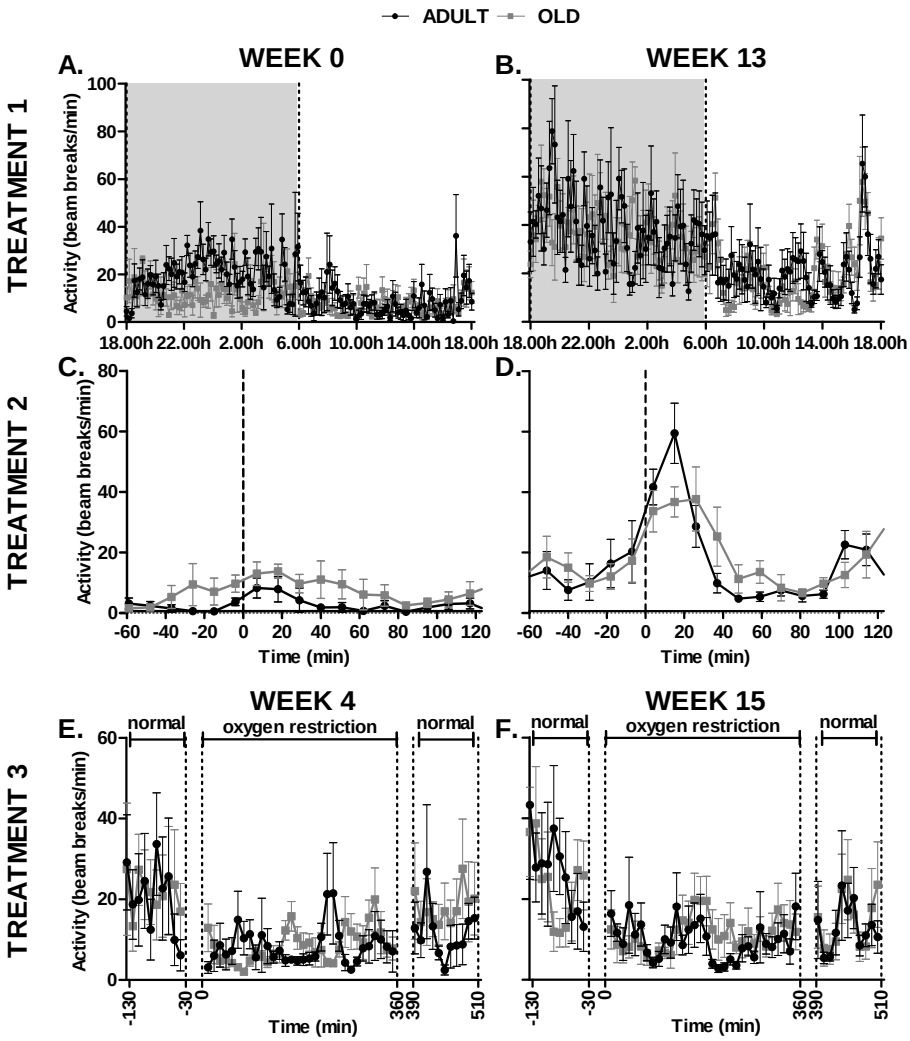

Supplemental figure 3 Average activity of ADULT and OLD mice during TREATMENT 1, 2 and 3. For treatment 1 and 2, activity of adult (n=8; 10 weeks old in week 0) and old (n=6; 72 weeks old in week 0) mice was recorded in the indirect calorimetry system for, respectively, 24 and 3 hours after the 24h adaptation in week 0 (A+C) and week 13 (B+D). For treatment 1, mice had *ad libitum* access to feed and water. For treatment 2, mice were fasted (restricted feed (2 gr.) at the start of the dark phase) and received a glucose pellet (2 gr/kg BW) after start of the following light phase. T=0 represents the time point when the glucose pellet was fully consumed (within 1-3 minutes after provision). For Treatment 3, adult (n=8, 14 weeks old in week 4) and old (n=6, 76 weeks old in week 4) mice were fasted in the indirect calorimetry system (restricted feed (2 gr.) at the start of the dark phase) and were exposed to oxygen restriction after the start of the following light phase. Activity was recorded for 2 hours before, 6 hours during, and 2 hours after exposure to oxygen restriction in week 4 (E) and week 15 (F).

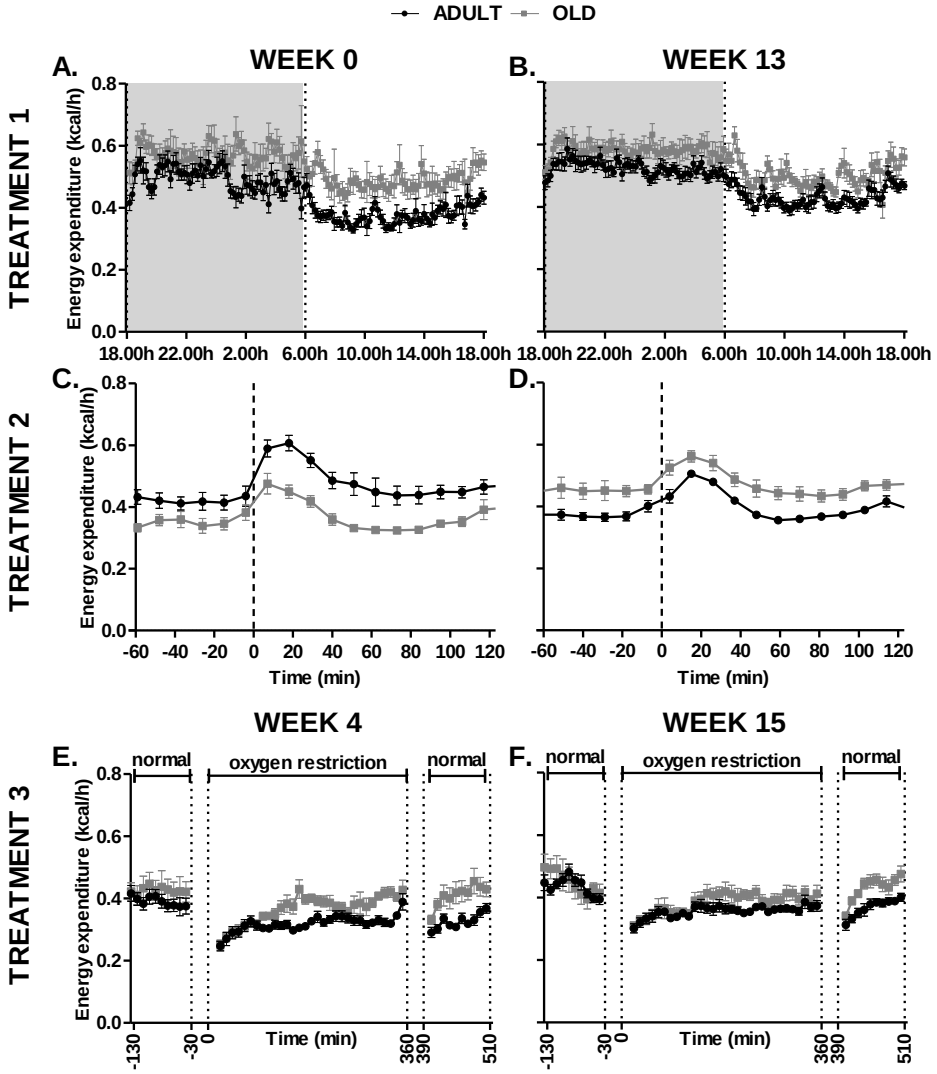

Supplemental figure 4 Average energy expenditure of ADULT and OLD mice during TREATMENT 1, 2 and 3. For Treatment 1 and 2, energy expenditure of adult (n=12; 10 weeks old in week 0) and old (n=6; 72 weeks old in week 0) mice was recorded for, respectively, 24 and 3 hours after a 24h adaptation in the indirect calorimetry system in week 0 (A+C) and week 13 (B+D). For Treatment 1, mice had *ad libitum* access to feed and water. For Treatment 2, mice were fasted (restricted feed (2 gr.) at the start of the dark phase) and received a glucose pellet (2 gr/kg BW) after start of the following light phase. T=0 represents the time point when the glucose pellet was fully consumed (within 1-3 minutes after provision). For Treatment 3, adult (n=12, 14 weeks old in week 4) and old (n=6, 76 weeks old in week 4) mice were fasted in the indirect calorimetry system (restricted feed (2 gr.) at the start of the dark phase) and were exposed to oxygen restriction after the start of the following light phase. Energy expenditure was recorded for 2 hours before, 6 hours during, and 2 hours after exposure to oxygen restriction in week 4 (E) and week 15 (F).

Chapter 4

Oxygen restriction as challenge test reveals early high-fat diet-induced changes in glucose and lipid metabolism.

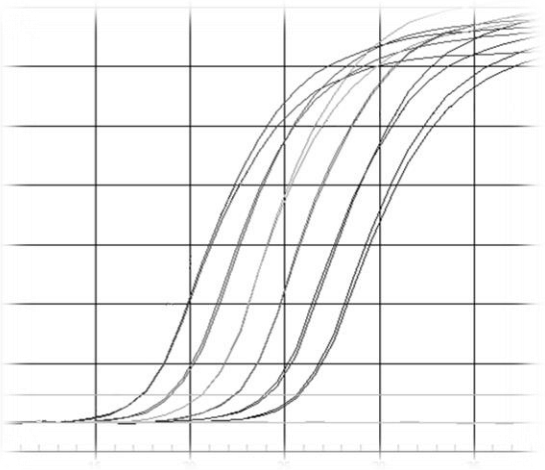

Loes P.M. Duivenvoorde, Evert M. van Schothorst, Davina Derous, Inge van der Stelt, Jinit Masania, Naila Rabbani, Paul J. Thornalley and Jaap Keijer

Published in: Pflügers Archiv – European Journal of Physiology (2014)
doi:10.1007/s00424-014-1553-8

Abstract

Challenge tests stress homeostasis and may reveal deviations in health that remain masked under unchallenged conditions. Ideally, challenge tests are non-invasive and applicable in an early phase of an animal experiment. Oxygen restriction (OxR; based on ambient, mild normobaric hypoxia) is a non-invasive challenge test that measures the flexibility to adapt metabolism. Metabolic inflexibility is one of the hallmarks of the metabolic syndrome.

To test whether OxR can be used to reveal early diet-induced health effects, we exposed mice to a low-fat (LF) or high-fat (HF) diet for only five days. The response to OxR was assessed by calorimetric measurements, followed by analysis of gene expression in liver and epididymal white adipose tissue (eWAT), and serum markers – for e.g. protein glycation and oxidation.

Although HF feeding increased body weight, HF and LF mice did not differ in indirect calorimetric values under normoxic conditions and in a fasting state. Exposure to OxR, however, increased oxygen consumption and lipid oxidation in HF mice vs. LF mice. Furthermore, OxR induced gluconeogenesis and an antioxidant response in liver of HF mice, whereas it induced *de novo* lipogenesis and an antioxidant response in eWAT of LF mice; indicating that HF and LF mice differed in their adaptation to OxR. OxR also increased serum markers of protein glycation and oxidation in HF mice, whereas these changes were absent in LF mice.

Cumulatively, OxR is a promising new method to test food products on potential beneficial effects for human health.

Introduction

Challenge tests, such as the oral glucose tolerance test, are an important tool to reveal early diet-induced health effects (55). Early dietary effects are typically masked by homeostasis under normal conditions. By challenging homeostasis, however, subtle changes in health status can be revealed. The response to fasting and refeeding, for example, shows subtle changes in carbohydrate use between mice fed different high-fat diets or between mice that differ in adiponectin expression, whereas normal indirect calorimetric measurements do not differentiate between these groups (2, 22). Metabolic challenge tests are preferably non-invasive and determine the flexibility to switch between different metabolic substrates in an early phase of a nutritional intervention. Early detection of changes in metabolic flexibility can shorten animal studies and reduces age-related variation between animals. More importantly, early diet-induced changes can be predictive for diet-induced changes at the long-term. Consumption of a high-fat diet, for example, induces changes in gene expression in mice white adipose tissue (WAT) after 5 days that are sustained until 12 weeks of feeding (57).

Oxygen restriction (OxR) was recently described as a new challenge test to reveal differences in metabolic health between adult and old mice (14). The challenge with OxR that was used in this study was based on mild ambient, normobaric hypoxia and was performed in the indirect calorimetry (InCa) system. OxR affects whole body metabolism (33, 40), and it is hypothesised that only animals that exhibit metabolic flexibility can adapt in an adequate way. Metabolic flexibility is, for this purpose, defined as the capacity to adequately respond to the environment, being either altered nutritional input, energetic demand, or environmental changes like oxygen limitation. The flexibility to adapt to OxR can be assessed at whole body level from respiratory output and at tissue and circulation level from the expression of different molecular markers.

Metabolic adaptations to OxR are extensively described. It is widely accepted that OxR induces a switch from oxidative to (anaerobic) glycolytic ATP production (32, 48) to reduce oxygen consumption and prevent the formation of reactive oxygen species. Local hypoxia in adipose tissue that occurs in obesity can, indeed, lead to chronic and low-grade inflammation when oxygen supply does not match oxygen demand (58, 59). Furthermore, OxR decreases insulin sensitivity (44) and increases lipolysis (60) in adipocytes. Previously, we showed that OxR reduces oxygen consumption and increases blood glucose and lactate levels in adult mice. Serum lactate levels of adult mice exposed to OxR were almost 20% higher than serum lactate levels of adult mice that remained under normoxic conditions, which indicates an increase in glucose utilization through the glycolytic pathway. The changes in oxygen consumption were, however, absent in old mice suggesting a reduction in metabolic flexibility (14). The use of OxR as a challenge test to investigate the effect of food components on (mouse)

health status is promising because of its non-invasive nature and the similarities with obesity-related-disorders, such as sleep apnoea (12).

InCa measurements can be used to investigate energy expenditure (EE) and respiratory energy ratio (RER) under normal, free-feeding conditions, but also to investigate the response to a nutritional or environmental challenge, such as fasting and re-feeding (22) or changes in housing temperature (11). RER and EE in mice during free-feeding conditions directly correlate to the composition of the diet consumed (20). Compared to mice fed a standard diet, mice that consume a high-fat diet generally have a low diurnal RER and a high EE because of the increase in fat oxidation (e.g. 34). The consumption of a high-fat diet can, furthermore, increase diet induced thermogenesis by brown adipose tissue (3). Basal metabolic rate – that is, when mice are fasted and housed under thermoneutral conditions – is, however, not influenced by consumption of a high-fat diet (17). Here, we tested whether OxR in the InCa system can be used in an early phase of an animal study to identify differences between dietary groups, which are not observed under a normoxic conditions.

For this study, we therefore measured the response to OxR of mice that were either fed a semi-purified, standardized LF or HF diet for five days. The HF diet that was used in this study is known to increase weight gain, insulin resistance and circulating leptin levels, and decrease circulating adiponectin levels in C57BL/6J mice after several weeks of *ad libitum* feeding (20, 57). We expected that the mice on the LF and the HF diets would not differ in indirect calorimetric values under normoxic conditions. OxR is, on the other hand, expected to reveal differences in indirect calorimetric values of HF and LF mice. The adaptation to OxR was further investigated by analysis of gene expression patterns in liver and WAT and by assessment of serum markers of protein glycation and oxidation.

Materials and methods

Animals and experimental manipulations

Forty-eight male C57BL/6JOlaHsd mice were used for this study (Harlan Laboratories, Horst, The Netherlands). The experimental protocol was approved by the Animal Welfare Committee of Wageningen University, Wageningen, The Netherlands (DEC2012035). Mice arrived at 10 weeks of age and were individually housed and maintained under environmentally controlled conditions (20 - 22.5 ºC, 12 h/12 h light–dark cycle, 40 - 55% humidity) and had *ad libitum* access to feed and water. The study consisted of a three week adaptation phase and a 5 day experimental phase – a schematic overview of the study can be found in supplemental figure 1. During the adaptation phase, mice received the purified low-fat BIOCLAIMS standard diet, which contains 10% energy from fat (for a detailed description of the diet, see (21)). For the experimental phase mice were stratified by body weight and allocated to the HF or LF group. The experimental phase lasted for five days, during which mice were housed in

the indirect calorimetry system. The HF diet had the same ingredients as the LF diet, but carbohydrate - wheat starch - was partly replaced by fat (70% sunflower oil, 18% coconut oil, and 12% flaxseed oil) to 40% energy from fat (21). Feed intake and body weights were monitored on a weekly basis during the adaptation phase, and after the 5 days of either LF or HF feeding. In the InCa system, feed intake was recorded real-time during the 5 experimental days. At the end of the experimental phase, 12 mice of each group were exposed to OxR (LFo and HFo) in the indirect calorimetry system (see below), while the remaining 12 mice of each group remained under normoxic conditions (LFn and HFn). LFo and HFo mice were killed directly after the exposure to OxR; LFn and HFn mice were killed at the same time point.

Indirect calorimetry (normal and oxygen restriction conditions)

Indirect calorimetry was measured with a PhenoMaster System (TSE Systems, Bad Homburg, Germany) equipped for simultaneous measurements of oxygen consumption and carbon dioxide production of 12 individual mice as published (20). The system is supplemented with a *Workhorse* hypoxia pump (b-Cat B.V., Tiel, the Netherlands), which filters oxygen out of normal room air and stably decreases the oxygen concentration from 20.9% to 12%, as published (14). For all calorimetric measurements, mice remained in their home cage, while the cage lids were replaced by air tight PhenoMaster cage lids, which guarantee a stable air flow through the animal cage and enables air sampling for calorimetric measurements every 13 minutes during the measurements under normal conditions and every 11 minutes during the measurements under OxR. Rates of oxygen consumption (VO_2, ml/h) and carbon dioxide production (VCO_2, ml/h) were calculated and used by the TSE software to calculate the respiratory exchange ratio ($RER=VCO_2/VO_2$). The percentage of energy derived from glucose and fat oxidation was calculated from average RER values during OxR of individual LF and HF fed mice (39).

Measurements under normoxic conditions

Mice were adapted in the Phenomaster system for at least 24h before the start of the measurements. After those 24h, both groups of mice (LF and HF) received a fresh batch of feed after which the actual measurements started. O_2 consumption, CO_2 production and feed intake were measured for the following 5 days. The average VO_2, RER and physical activity were calculated for each mouse individually over the 2^{nd}, 3^{rd}, 4^{th} and 5^{th} day of HF or LF feeding. Data obtained during day 1 were discarded since the introduction of a fresh batch of feed generally causes a slight over-consumption in mice.

Measurements under oxygen restriction

After the five days of HF or LF feeding, mice remained in the indirect calorimetry system for the measurements under OxR or normal conditions – a detailed scheme of

the exposure can be found in supplemental figure 1. At the start of the dark phase, all feed was removed and mice received a restricted amount of feed - 1.8 gram for the LF diet and 1.5 gram for the HF diet - to ensure identical caloric intake. The restricted amount of feed is generally consumed within 6 hours after start of the dark phase, which means that all mice are in a fasted state (RER<0.8) at least one hour before the start of the light phase. The two hours preceding exposure to OxR were used to analyse VO_2, RER, and physical activity during fasting and normoxic conditions. One hour after the start of the light phase (when mice were still in a fasted state) the oxygen level was decreased from 20.9% to 12% within 30 minutes as described previously (14). After 30 minutes, oxygen level is stabilized and measurements were recorded for six hours under OxR.

Tissue and blood collection (at time of section)

Mice were decapitated directly after the exposure to the OxR (LFo and HFo) or normal air (LFn and HFn). Blood was collected in Mini collect serum tubes (Greiner Bio-one, Longwood, USA), and centrifuged for 10 minutes at 3000 g and 4°C to obtain serum. Serum samples were aliquoted and stored at -80°C. Glucose concentration was measured in whole blood with a *Freestyle* blood glucose system (Abbott Diabetes Care, Hoofddorp, the Netherlands) according to the manufacturer's instructions. After blood collection, gonadal WAT and liver tissue were dissected and snap frozen in liquid nitrogen and stored at –80 °C. The right epididymal fat depot was weighted directly after dissection and was used as an indicator of whole body adiposity.

Serum glycation and oxidation markers

Serum glycation and oxidation markers were analysed by stable isotopic dilution analysis liquid chromatography with tandem mass spectrometric detection (LC-MS/MS), as described (51), recently revised for additional analytes (43). Analytes determined were: early glycation adduct Nε-fructosyl-lysine (FL); advanced glycation endproducts (AGEs) - Nε-(carboxymethyl)lysine (CML), Nε-(1-carboxyethyl)lysine (CEL) and methylglyoxal-derived hydroimidazolone (MG-H1); oxidation markers - N-formylkynurenine (NFK), dityrosine (DT) and protein carbonyl glutamic γ-semialdehyde (GSA); protein nitration marker 3-nitrotyrosine (3-NT); and related amino acids, lys, arg, tyr and trp. Glycation, oxidation and nitration adducts of serum protein were determined after exhaustive enzymatic hydrolysis by incubation with pepsin, pronase E and finally aminopeptidase with prolidase under argon. Antioxidant and pH conditions in pre-analytical processing prevented artifactual formation or loss of analytes. Serum (25 µl) was diluted to 500 µl with water and washed by 4 cycles of 10-fold concentration and dilution in water over a 10 kDa cut-off microspin filter at 4 ^{0}C. The final washed protein concentrate (50 µl) was delipidated by extraction with water-saturated ether and assayed for protein concentration by the Bradford method. An aliquot of protein (100 µg) was digested for analysis. Analytes were detected by electrospray positive

ionisation multiple reaction monitoring LC-MS/MS and quantified by stable isotopic dilution analysis. Serum protein content of glycation, oxidation and nitration adducts is reported as mmol/mol related to amino acid.

RNA isolation, cDNA synthesis and Quantitative real-time reverse transcription-polymerase chain reaction (qRT-PCR)

RNA isolation from WAT was performed as described previously (56). Briefly, WAT was homogenized in liquid nitrogen using a cooled mortar and pestle. Total RNA was isolated using TRIzol reagent, chloroform, and isoamyl alcohol (PCI) (Invitrogen, Breda, The Netherlands) followed by purification with RNeasy columns (Qiagen, Venlo, The Netherlands) using the instructions of the manufacturer. RNA concentration and purity were measured using the Nanodrop (IsoGen Life Science, Maarsen, The Netherlands). RNA quality was additionally checked on the Experion automated electrophoresis system (Bio-Rad, Veenendaal, The Netherlands) using Experion StdSense chips (Bio-Rad).

RNA isolation from liver was performed with RNeasy columns (Qiagen) according to the manufacturer's protocol.

qRT-PCR was performed as previously described (56). Data were normalized against the geometrical mean of the reference genes ribosomal protein S15 (*Rps15*), and beta-2 microglobulin (*B2m*), which were confirmed for their stable gene expression levels (geNorm, Ghent University Hospital, Ghent, Belgium). Primers were designed using NCBI Primer-Blast (NCBI Website). The primer sequences and PCR annealing temperatures for each gene are summarized in supplemental table 1.

Statistical analyses

Data are expressed as mean ± SEM. Statistical analyses were performed using GraphPad Prism version 5.04 (Graphpad, San Diego, USA) and SPSS Statistics for Windows, version 19 (IBM Corp., Armonk, USA). Data were checked for normality using the D'Agostino and Pearson omnibus normality test. Test results that were not normally distributed were log-transformed. Measurements at single time points between 2 independent groups (body and WAT weight, average values of time course data: RER, VO_2 and physical activity, feed intake, serum glycation and oxidation markers and qRT-PCR results) were analysed by independent Students' *t*-tests.

Time course data (RER, VO_2, and physical activity during OxR) were analysed with 2-way-ANOVA and Bonferoni Posthoc analysis (factor 1=diet, factor 2=time).

VO_2 during OxR was also analysed with ANCOVA, in which body weight was used as confounding factor. The correlation between oxygen consumption and body weight was further analysed with linear regression.

Results

5 days high-fat feeding increased body weight and did not alter eWAT weight nor fasting blood glucose levels

The consumption of the HF diet increased energy intake in HF mice compared to LF mice, which led to a significant increase in body weight in HF mice (phenotypical data are presented in table 1). Epididymal WAT (eWAT) weight and fasting blood glucose levels were unaltered by the period of HF feeding. Since calorimetric analyses are only based on mice that were exposed to OxR, phenotypical data were also compared between these subgroups of mice (LFo and HFo). LFo and HFo mice did not differ in body weight or eWAT weight.

Table 1 Phenotypical data of mice fed semisynthetic LF or HF diet over a period of 5 days

	LF (n=24)	**HF (n=24)**
Initial body weight (g)	25.54 ± 0.20	25.62 ± 0.20
Final body weight (g)	27.66 ± 0.32	28.62 ± 0.31 *
Total body weight gain (g)	2.15 ± 0.19	2.99 ± 0.23 **
eWAT weight (g)	0.29 ± 0.07	0.30 ± 0.07
eWAT weight (%/BW)	1.03 ± 0.04	1.04 ± 0.04
Energy intake (kcal/day)	13.97 ± 0.30	15.62 ± 0.35 ***
Fasting glucose (mM)	6.43 ± 0.20	6.86 ± 0.27
	LFo (n=12)	**HFo (n=12)**
Initial body weight (g)	25.54 ± 0.18	25.56 ± 0.20
Final body weight (g)	27.28 ± 0.54	28.53 ± 0.36
Total body weight gain (g)	1.74 ± 0.24	2.96 ± 0.35
eWAT weight (g)	0.28 ± 0.02	0.30 ± 0.02
eWAT weight (%/BW)	1.00 ± 0.06	1.04 ± 0.05

Data are expressed as mean ± SEM for the full group of animals (top) and subset of mice exposed to OxR (bottom). eWAT weight resembles the weight of the right epididymal fat depot. Asterisks denote significant differences from control (LF) values.

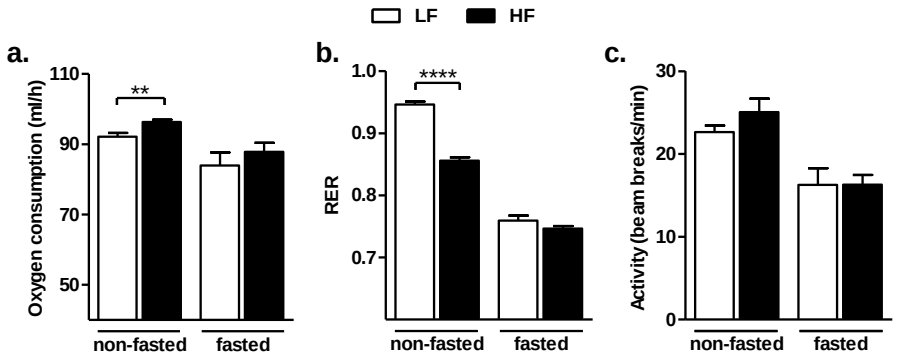

Figure 1 Oxygen consumption, RER and physical activity under normoxic conditions of LF and HF mice. Oxygen consumption (a), RER (b) and physical activity (c) under normal, free-feeding conditions were averaged over the last 4 days of the 5 days of high- or low-fat feeding. The 2 hours before the exposure to OxR - when mice were in a fasted state - were used to analyse VO_2, RER and physical activity under normal, although fasted, conditions.

Fasting under normal conditions eliminated differences in RER and VO_2 between HF and LF mice

VO_2 and RER during *ad libitum* conditions were significantly different between HF and LF mice (fig. 1a+b); HF feeding increased VO_2 (92.1 ml/h in LF vs. 96.3 ml/h in HF) and decreased RER (0.946 in LF vs. 0.856 in HF), which indicates increased fat oxidation. When mice were in a fasted state - prior to the exposure to OxR - differences in VO_2 and RER between HF and LF fed mice disappeared (fig. 1a+b). The absence of differences of VO_2, RER and physical activity enabled us to distinguish the effect of OxR on each of these measurements and to establish whether dietary background influences the response to OxR. LF and HF mice did not differ in physical activity, neither when fasted nor in non-fasted state (fig. 1c).

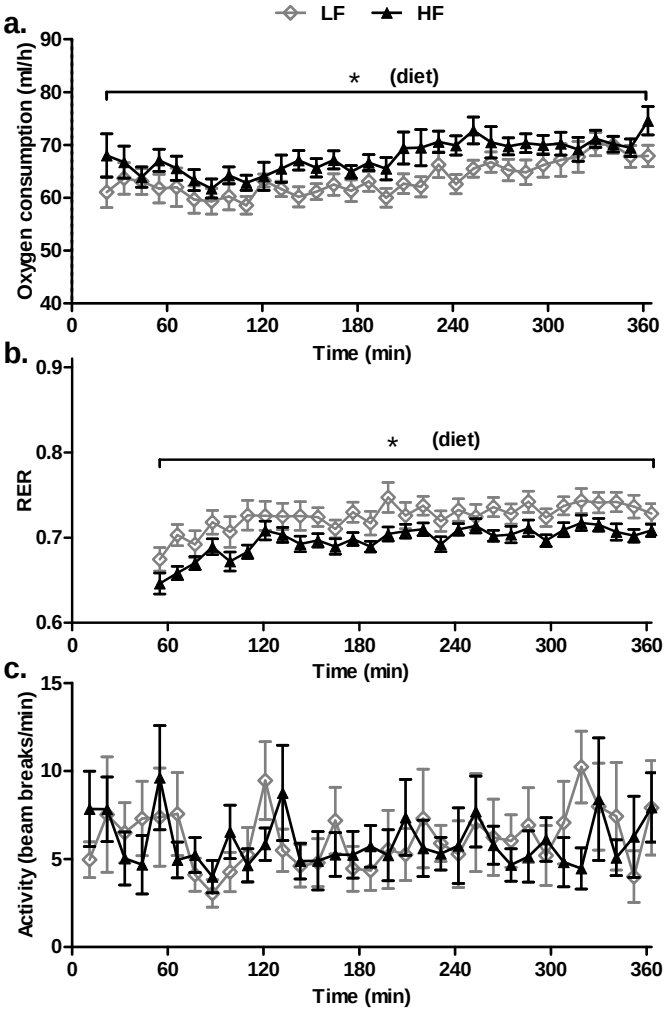

Figure 2 Oxygen consumption, RER and physical activity during OxR of LF and HF fed mice. Oxygen consumption (a), RER (b) and physical activity (c) during 6 hours of OxR after 5 days of low- or high-fat feeding. Mice were fasted prior to the exposure to OxR.

Exposure to OxR revealed differences between fasted HF and LF mice

HF mice showed a significantly higher oxygen consumption during OxR compared with LF mice (fig. 2a), whereas their RER was significantly reduced (fig. 2b). LF and HF mice did not differ in physical activity during the exposure to OxR (fig. 2c). Levels of VO_2, RER, and physical activity were significantly reduced by OxR compared to levels under normoxic fasted conditions for both dietary groups (suppl. table 2).

HF mice had a significantly lower glucose oxidation rate during OxR, which is accompanied by a significant higher rate of fat oxidation (fig. 3a). OxR increased blood glucose levels, although no differences were found between HF and LF mice (fig. 3b).

Since oxygen consumption and energy expenditure during indirect calorimetry are more complicated to interpret when animals differ in body weight (5, 6, 53), we also analysed average oxygen consumption of LF and HF mice in relation to body weight. Oxygen consumption significantly correlated to body weight during both normoxic conditions (fig. 4a) and during OxR (fig. 4b). Although the subgroups of LF and HF mice that were exposed to OxR did not differ significantly in body weight, the difference in average oxygen consumption during OxR between LF and HF mice disappeared when correcting for body weight with ANCOVA (fig. 4c). To further understand the effect of body weight on oxygen consumption during OxR ($VO_{2,OxR}$) we also analysed its correlation with oxygen consumption during normoxic conditions ($VO_{2,norm}$). The relation between $VO_{2,OxR}$ and $VO_{2,norm}$ shows to what extend the physiological status - including body weight - can predict oxygen consumption during OxR. In other words, in this analysis not only body weight is taken into account but all other factors that influence the level of oxygen consumption. Interestingly, in LF mice $VO_{2,OxR}$ strongly correlates with $VO_{2,norm}$ (fig. 4d). In HF mice $VO_{2,OxR}$ does not correlate with $VO_{2,norm}$, which suggests that other factors, apart from body weight, play a role in the adaptation to OxR.

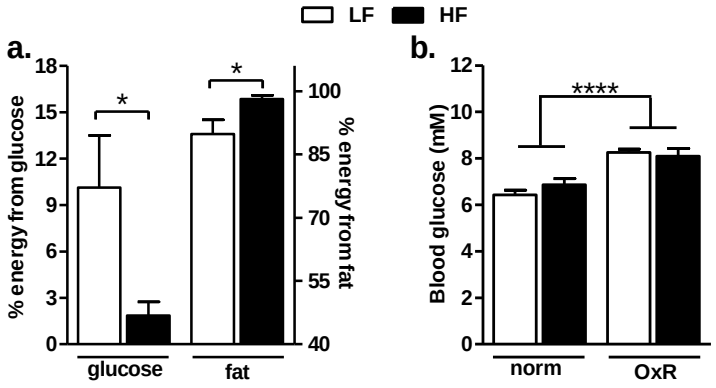

Figure 3 Energy from glucose and fat oxidation and blood glucose levels of LF and HF mice during and after OxR. The percentage of energy derived from glucose (a, left axis) or fat oxidation (a, right axis) were derived from average RER values during OxR of individual LF and HF fed mice. Blood glucose levels (b) were measured directly after the exposure to OxR.

OxR increased protein oxidation and glycation adducts in serum of HF mice

Serum proteins can be oxidized or glycated by reactions with free radicals and saccharides, respectively. Changes in the level of protein oxidation and glycation adducts in serum can either result from changes in the level of total body oxidative and glycation damage or changes in clearance of the adducts from the circulation by protein turn-over or renal clearance (52). Since LF and HF mice differed in glucose oxidation rate and oxygen consumption during OxR, we investigated serum levels of several markers for protein oxidation and glycation (fig. 5). Dityrosine and 3-nitrotyrosine residues of serum protein were significantly increased upon OxR in HF mice but unchanged by exposure to OxR in LF mice. AGE adduct, MG-H1 and CML, residue contents of serum protein tended towards increase by OxR in HF mice but failed to reach statistical significance (p=0.054 and p=0.074, resp.), whereas their levels remained unaltered by OxR in LF mice. Glycation and oxidation adduct residue contents of serum protein were not changed by LF or HF feeding under normoxic conditions whereas the protein nitration adduct, 3-nitrotyrosine, residue content of serum protein was decreased in HF mice compared with LF mice.

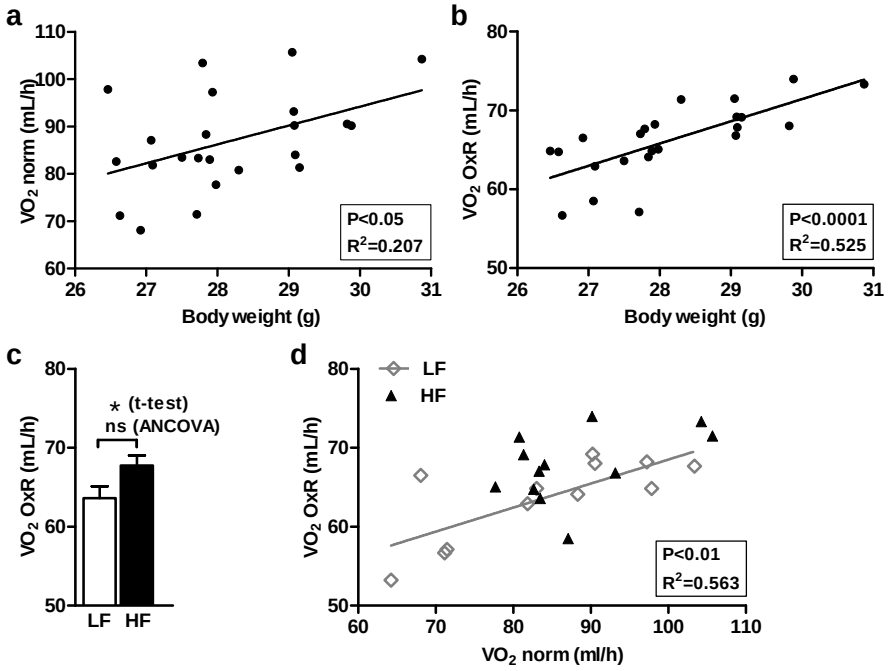

Figure 4 Oxygen consumption of LF and HF mice during OxR and correction for body weight. Oxygen consumption levels during normoxia (VO_2,norm; a) and OxR (VO_2,OxR; b) positively correlated with body weight. HF mice have a significantly higher oxygen consumption level during the 6 hours of OxR, but not when corrected for body weight (c). Oxygen consumption levels during OxR (VO_2,OxR) were positively correlated with oxygen consumption levels during normoxia (VO_2,OxR) in LF mice, but not in HF mice (d).

OxR induced an antioxidant response, gluconeogenesis, and *de novo* lipogenesis in liver of HF mice

Altered oxygen levels can affect redox balance and glucose and lipid metabolism. We therefore investigated hepatic transcript levels encoding proteins involved in the response to oxidative stress and the formation of cytosolic NADPH and transcripts involved in glucose and lipid metabolism in LF and HF mice that were either exposed to OxR or remained under normoxic conditions. An integrated schematic overview of the function of each gene of interest is shown for the response to oxidative stress (fig. 6a), and gluconeogenesis and *de novo* lipogenesis (DNL; fig. 6b).

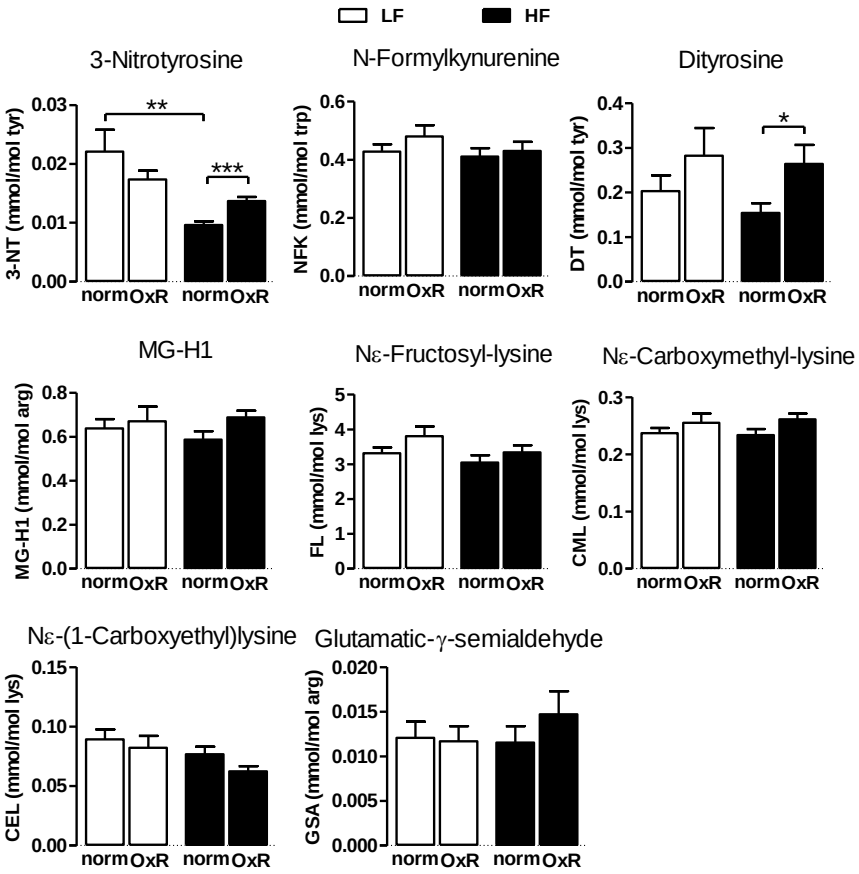

Figure 5 Serum markers for protein glycation and oxidation of LF and HF mice after OxR. Different markers for protein glycation and oxidation were analysed in serum of LF and HF mice that were sacrificed immediately after the exposure to OxR.

In HF mice, all key enzymes involved in gluconeogenesis were significantly upregulated by the exposure to OxR; except for solute carrier family 2 (*Slc2a2*), which expression was unaltered by OxR, and phosphoenolpyruvate carboxykinase 1 *(Pck1)*, which

expression was only marginally (p=0.056) increased in HF mice (fig. 7c). Opposite to the increase in gluconeogenesis in HF mice, the expression of pyruvate kinase (*Pklr*) was also elevated by OxR, suggesting an increase in glycolysis. Furthermore, OxR induced an increase in the expression of superoxide dismutase 2 (*Sod2*) and uncoupling protein 2 (*Ucp2*), which are involved in the response to oxidative stress in HF mice. OxR also induced DNL, as shown by the increased expression of acetyl-Coenzyme A carboxylase alpha (*Acaca*) and fatty acid synthase (*Fasn*).

In LF mice, gene expression data does not indicate changes in gluconeogenesis (fig. 7b). Only *Pklr* and solute carrier family 16 (*Slc16a1*) mRNA levels were found to be elevated by OxR, which suggest an increase in glycolysis and an increase in lactate import. The increase in the expression of stearoyl-Coenzyme A desaturase 1 (*Scd1*) suggests that OxR increased the formation of unsaturated fatty acids in LF mice. None of the genes involved in the response to oxidative stress were altered by OxR in LF mice.

Under normoxic conditions, none of these genes were differentially expressed between LF and HF mice, except for malic enzyme *(Me1*) and *Scd1*, which both had a lower expression level in HF mice compared with LF mice (fig. 7a). Relative expression levels of all genes, which is the expression level corrected by the expression level of both reference genes, can be found in supplemental figure 2a.

OxR induces an antioxidant response and alters mitochondrial activity and *de novo* lipogenesis in WAT of LF mice

WAT is, next to the liver, also expected to play an important role in the adaptation to OxR. In LF mice, the response to oxidative stress was significantly upregulated by OxR in WAT (*Sod2* and *Ucp2;* fig. 8b). Vascular endothelial growth factor A (*Vegfa*), which is a direct target of the hypoxia inducible factor 1 (*Hif1a),* was also significantly upregulated by OxR. OxR also had a strong effect on genes involved in DNL in LF mice: all 5 genes involved in DNL were found to be upregulated by OxR, of which all but one (*Scd1)* were significantly increased. Furthermore, OxR seemed to have altered mitochondrial activity in WAT of LF mice; the expression of citrate synthase (*Cs*), which is an important component of the citric acid cycle, was elevated, and the expression of pyruvate dehydrogenase kinase 1 (*Pdk1*), which phosphorylates and inhibits the pyruvate dehydrogenase complex and thus reduces the formation of acetyl-coA from pyruvate, was elevated. In HF mice no changes in gene expression levels in WAT were found (fig. 8c).

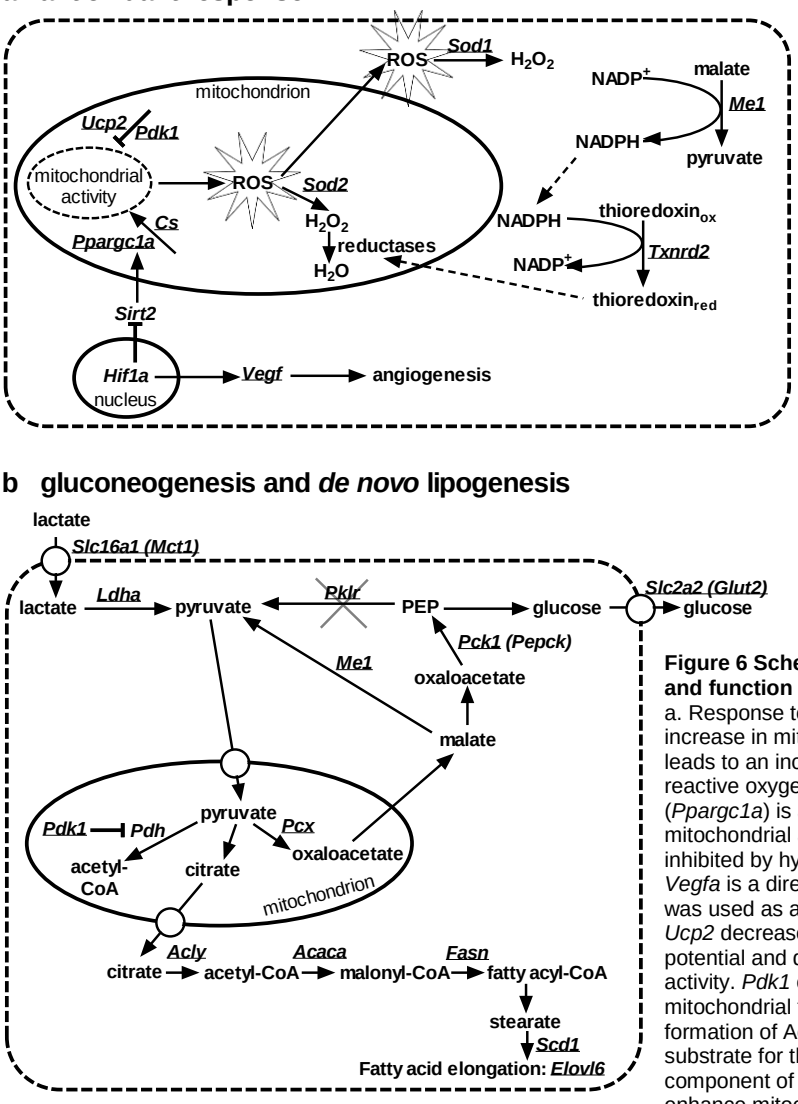

Figure 6 Schematic overview of the role and function of each gene of interest.
a. Response to oxidative stress. An increase in mitochondrial activity generally leads to an increase in the formation of reactive oxygen species (ROS). *Pgc1a* (*Ppargc1a*) is a key regulator of mitochondrial activity and density and is inhibited by hypoxia inducible factor (*Hif1a*). *Vegfa* is a direct target gene of *Hif1a* and was used as a marker for *Hif1a* availability. *Ucp2* decreases mitochondrial membrane potential and decreases mitochondrial activity. *Pdk1* can also decrease mitochondrial function by limiting the formation of Acetyl-CoA, the major substrate for the TCA cycle. *Cs* is a major component of the TCA cycle and can enhance mitochondrial activity.

Figure 6 continued
Sod1 (cytosolic) and *Sod2* (mitochondrial) work as antioxidants by converting O^{2-} to H_2O_2. NADPH is formed during the conversion of malate to pyruvate, which is catalysed by *Me1*. *Txnrd2* maintains thioredoxin in a reduced state. NADPH plays an important role in antioxidant defence by serving as the main electron donor for reductases, such as thioredoxin that is involved in the conversion of H_2O_2 to H_2O.
b. Gluconeogenesis and *de novo* lipogenesis (DNL). Gluconeogenesis occurs during fasting or when circulating lactate levels are elevated and only takes places in the liver. During gluconeogenesis, lactate is taken up from circulation by *Slc16a1 (MCT1)*. Lactate is converted to pyruvate by *Ldha*. Pyruvate is transported into the mitochondrion and converted to oxaloacetate by *Pcx*. The conversion of pyruvate to acetyl-coA (by *Pdh*) is blocked by *Pdk1*. Oxaloacetate is converted to PEP by *Pck1* (cytosolic) or *Pck2* (mitochondrial). In the cytoplasm, PEP is converted into glucose and glucose can be transported out of hepatocytes by *Slc2a2*. The expression of *Pklr*, which converts PEP back to pyruvate, is blocked. Malate can also be converted back to pyruvate by *Me1*. DNL is the synthesis of fatty acids from non-lipid precursors and can occur in both liver and adipose tissue. For DNL, citrate is transported out of the mitochondrion and converted into acetyl-CoA by *Acly.* Acetyl-CoA can then be converted to long chain (unsaturated) fatty acids by subsequently *Acaca, Fasn, Scd1,* and *Elovl6*. Genes that are underlined were measured in this study.

To further understand the changes in lipid and mitochondrial activity in LF mice, we studied the expression of *Pnpla2* and *Cpt1*, two key enzymes in lipolysis and beta oxidation. Neither of the two genes was found to be regulated by OxR in LF and HF mice. Under normoxic conditions, the expression levels of *Ucp2*, *Vegfa*, *Txrnd2* and *Cpt1a* were higher in HF mice compared with LF mice (fig. 8a). Relative expression levels of all genes can be found in supplemental figure 2b.

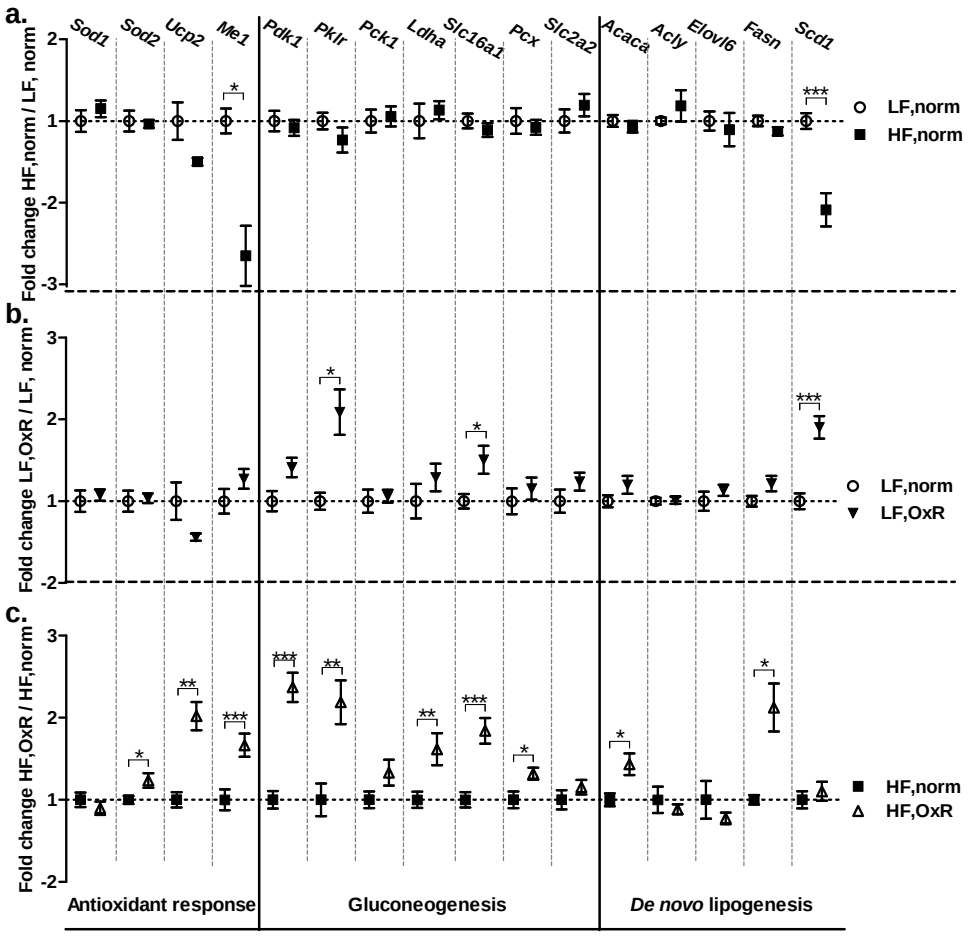

Figure 7 Gene expression in liver tissue of LF and HF mice that were either exposed to OxR or remained under normoxic conditions. Total mRNA was isolated to measure the expression of genes involved in antioxidant response, gluconeogenesis and *de novo* lipogenesis in liver tissue of LF and HF mice. Gene expression is calculated as the fold change of HF mice under normoxic conditions over LF mice under normoxic conditions (a); and of LF (b) and HF (c) mice that were exposed to oxygen restriction over the LF and HF mice that remained under normoxic conditions. *Sod1,* superoxide dismutase 1; *Sod2,* superoxide dismutase 2; *Ucp2,* uncoupling protein 2; *Me1*, malic enzyme; *Pdk1*, pyruvate dehydrogenase kinase 1; *Pklr*, pyruvate kinase; *Pck1* phosphoenolpyruvate carboxykinase 1 *(Pepck)*; *Ldha*, lactate dehydrogenase A; *Slc16a1*, solute carrier family 16 (*Mct1*); *Pcx*, pyruvate carboxylase; *Slc2a2,* solute carrier family 2 (facilitated glucose transporter; Glut2); *Acaca*, acetyl-Coenzyme A carboxylase alpha; *Acly*, ATP citrate lyase; *Elovl6*, ELOVL family member 6, elongation of long chain fatty acids; *Fasn*, fatty acid synthase; *Scd1*, stearoyl-Coenzyme A desaturase 1.

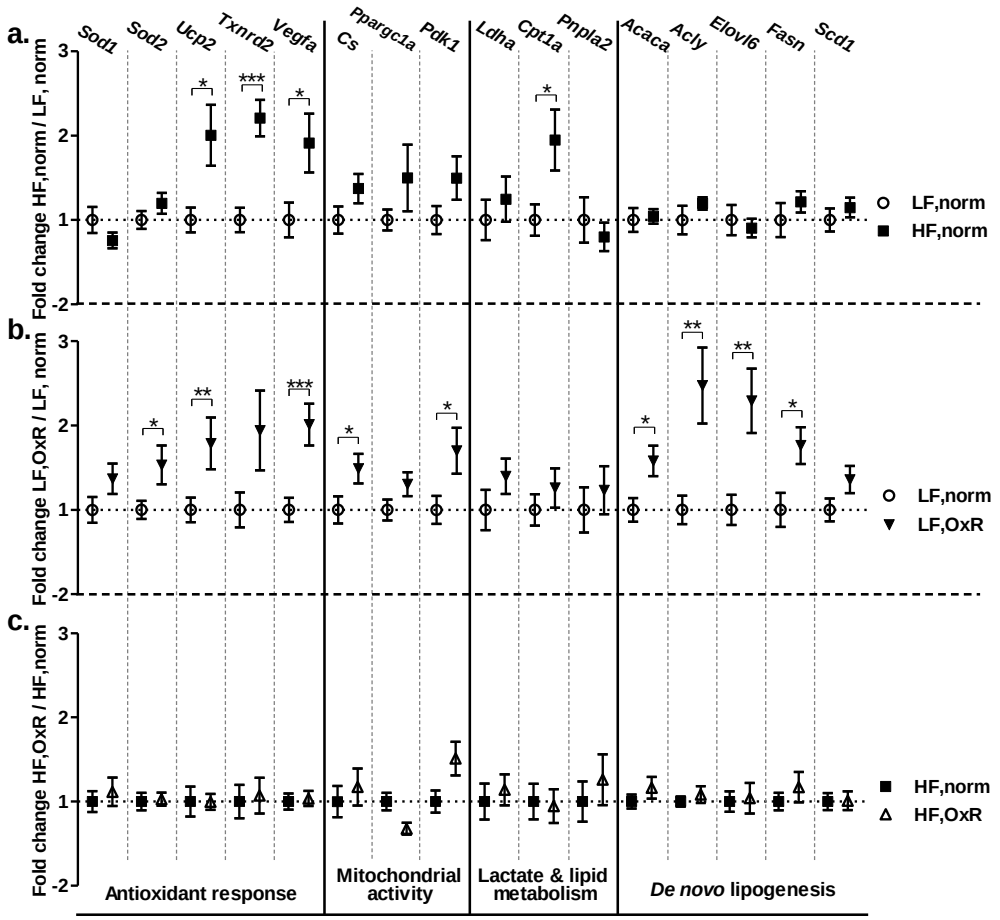

Figure 8 Gene expression in WAT of LF and HF mice that were either exposed to OxR or remained under normoxic conditions. Total mRNA was isolated to measure the expression of genes involved in antioxidant response, mitochondrial activity, lactate and lipid metabolism and *de novo* lipogenesis in eWAT of LF and HF mice. Gene expression is calculated as the fold change of HF mice under normoxic conditions over LF mice under normoxic conditions (a); and of LF (b) and HF (c) mice that were exposed to oxygen restriction over the LF and HF mice that remained under normoxic conditions. *Sod1,* superoxide dismutase 1; *Sod2,* superoxide dismutase 2; *Ucp2,* uncoupling protein 2; *Txnrd2,* thioredoxin reductase 2; *Vegfa*, vascular endothelial growth factor A; *Cs*, citrate synthase; *Ppargrc1a* peroxisome proliferative activated receptor gamma coactivator 1 alpha (*Pgc1a*); *Pdk1*, pyruvate dehydrogenase kinase 1; *Ldha*, lactate dehydrogenase A; *Cpt1a,* carnitine palmitoyltransferase 1a; *Pnpla2*, patatin-like phospholipase domain containing 2; *Acaca*, acetyl-Coenzyme A carboxylase alpha; *Acly*, ATP citrate lyase; *Elovl6*, ELOVL family member 6, elongation of long chain fatty acids; *Fasn*, fatty acid synthase; *Scd1*, stearoyl-Coenzyme A desaturase 1.

Discussion

5 days high-fat feeding increased body weight

HF versus LF mice had a higher energy intake and, as a result, a higher body weight after five days of feeding. The increase in body weight that was seen in our study is

predictive for the detrimental effects of long-term high-fat feeding (57). The absence of significant differences in blood glucose levels and adipose tissue weight makes it possible to compare the effect of OxR between both dietary backgrounds.

Feeding a high-fat diet increased oxygen consumption and decreased RER; although no differences were present when mice were in a fasted state

Whole body oxygen consumption depends on various factors, such as physical activity and body weight, but also metabolic rate and diet composition (20, 24). LF and HF mice did not differ in physical activity and HF mice had a higher caloric intake compared with LF mice. Diet composition can, specifically, determine the level of diet-induced thermogenesis (DIT). DIT depends on the activity of brown adipose tissue and its responsiveness to adrenergic stimulation and can be measured by the increase in norepinephrine-induced oxygen consumption (3). High-fat feeding is known to increase DIT, and therefore, oxygen consumption in mice (17). Diurnal RER, on the other hand, highly depends on the food quotient (FQ) of the diet. The FQ of the LF diet was 0.93 and the FQ of the HF diet was 0.85 (calculations based on Livesey et al. (29)). Therefore, and as expected, HF mice had a higher oxygen consumption and a lower RER, compared with LF mice during free-feeding conditions. When fasted, however, the effect of dietary history is diminished and HF and LF mice did not differ in RER and oxygen consumption. This result is consistent with a human study (8), which also showed that fasting RER correlates with insulin resistance, but was not significantly different between subjects with different habitual dietary intakes. The absence of an effect of dietary background on fasting RER and oxygen consumption values facilitates comparison of the response to OxR between both groups.

LF and HF mice differed in their adaption to OxR

The level of OxR mimics mild ambient hypoxia that occurs at moderate-high altitude (± 4000 m.), in certain airplanes, and on a systemic level, during obstructive sleep apnoea (12, 36). The exposure to OxR had a strong effect on whole body metabolism: it significantly decreased physical activity and oxygen consumption in both HF and LF mice. The decrease in physical activity is likely partly responsible for the reduction in oxygen consumption during OxR. A metabolic switch from mitochondrial oxidative to glycolytic ATP production may also contribute to the decreased oxygen consumption, as has been shown before (14, 35). A switch to glycolytic ATP production also explains the increase in blood glucose levels that were induced by OxR in both groups of mice. OxR is known to increase blood glucose and insulin levels (12, 38, 45), which is presumably caused by the conversion of lactate to glucose in liver tissue (10) or by - or in combination with - a reduction in insulin and glucose sensitivity that is frequently observed after exposure to OxR (30, 37, 45).

Although both groups of mice showed clear changes in blood glucose levels, oxygen consumption, RER and physical activity before and during OxR; also clear differences

existed in the adaptation to OxR. LF and HF mice did, on the other hand, not differ in physical activity during OxR; differences in indirect calorimetric values are, therefore, likely to be caused by differences in metabolic adaptation.
HF mice had, in fact, lower RERs during OxR, which directly relates to a decrease in the level of whole body glucose oxidation in HF mice compared with LF mice. The switch from fatty acid oxidation to glucose oxidation is expected to be favourable during periods of low oxygen availability because glucose oxidation utilizes less oxygen compared to fat oxidation (23). HF mice, indeed, consumed more oxygen during OxR compared with LF mice, whereas no significant differences were present between both groups prior to the exposure. Although, it should be noted that - when taking the heat equivalents of oxygen of both carbohydrate and fat into account (29) - a switch from 100% fat oxidation to 100% carbohydrate oxidation results in a decrease of approximately 7% in oxygen consumption, which means that the switch from lipid to glucose oxidation during OxR that was seen in LF mice, only accounts for a small proportion to the decrease in whole body oxygen consumption. Larger differences in oxygen consumption could be achieved by an increase in anaerobic glycolysis, by increased metabolic efficiency and/or by induction of autophagy dependent metabolism. The latter has been shown to contribute to adaptation to hypoxia in rodents (18) and humans (31). These changes will not necessarily affect RER, but can be visualized using oxygen consumption.
The differences in indirect calorimetry during OxR between HF and LF mice may indicate a decrease in metabolic flexibility in HF mice. *Ex vivo* studies, indeed, showed that the flexibility to switch from fat to glucose oxidation reflects the donor's metabolic characteristics, such as the percentage of body fat and serum free fatty acid levels (54). Five days of high-fat feeding might be sufficient to elicit differences in metabolic status that can be revealed by a challenge with OxR.

OxR induced an increase in several markers for protein glycation and oxidation in serum of HF mice

Oxygen restriction can result in increased glycolytic flux, as well as increased oxidative stress. An increased glycolytic flux may be due to a switch from fat to glucose oxidation and by a switch from oxidative ATP production to anaerobic ATP production (50). Although, ATP production via anaerobic glycolysis is only effective if lactate clearance does not match lactate production. Increased oxidative stress may be caused by an increased production of reactive oxygen species (ROS). Indeed, ambient hypoxia can lead to the production of mitochondrial ROS, with the level of ROS production depending on basal metabolism and the degree and duration of hypoxia (50). Hypoxia also leads to increased flux through anaerobic glycolysis with increased formation of methylglyoxal and related AGE formation – although this may be countered by hypoxia-induced increased expression of the protective enzyme, glyoxalase 1 (49). ROS are

thought to contribute to increased serum markers of oxidative damage and reactive dicarbonyl metabolites, such as glyoxal and methylglyoxal, and increased serum markers of AGEs (52). To assess possible effects of the level of OxR, that was imposed here, on glycolytic flux and oxidative stress, we examined protein adducts as serum markers of glycation and oxidative stress. The consumption of a HF diet on itself did not lead to differences in the serum markers of interest, except for 3-nitrotyrosine – one of the serum markers for oxidative stress and nitric oxide availability (42). Serum protein 3-NT residue content was decreased in HF mice compared with LF mice under normoxic conditions. This likely relates to decreased nitric oxide bioavailability (15). Serum protein 3-nitrotyrosine and dityrosine residue content were significantly increased upon OxR under HF diet conditions, but not under LF diet conditions. This suggests hypoxia mediated mitochondrial ROS production due to limited oxygen availability. The increase in 3-nitrotyrosine and dityrosine in HF mice may be explained by the higher oxygen consumption during OxR, which will result in a higher apparent hypoxia in HF mice compared with LF mice. Alternatively, this may be explained by a relative larger switch to glycolytic metabolism. Taken together, our data suggest that OxR increases oxidative stress in particular under HF conditions.

OxR induced gluconeogenesis, *de novo* lipogenesis, and an antioxidant response in liver tissue of HF mice

Exposure to a similar level of ambient normobaric hypoxia leads to an almost three-fold reduction in oxygen saturation in mouse liver tissue (45). OxR may, therefore, result in an increase in glycolytic flux and peripheral lactate production and clearance by the liver (10). OxR can, furthermore, induce an increase in oxidative stress at tissue level, which leads to an increase in the expression of genes involved in oxidative stress. Finally, OxR might also induce hepatic *de novo* lipogenesis (DNL). Hepatic DNL is increased in obesity (16) and decreased during caloric restriction (47), and is therefore considered as a relevant marker for metabolic health. Long-term exposure to OxR increases the expression of genes involved in DNL (4) and therefore resembles the effects seen in obesity. The combination of short-term HF feeding and exposure to OxR that we used in this study might, consequently, have a synergistic effect on DNL gene expression.

Before we discuss the changes in gene expression level that are induced by OxR in LF and HF mice, we will first focus on the changes in gene expression induced by HF feeding on itself – under normoxic conditions. Five days of HF feeding appeared to have a minor effect on the genes that were analysed in this study, with only two genes being significantly regulated. The decreased expression of Malic enzyme (*Me1*) suggests a lower conversion of cytoplasmic malate to pyruvate in HF mice as part of fatty acid synthesis from glycolytic intermediates, which is expected because of the lower amount of carbohydrates and higher amount of lipids in the HF diet. The

decrease in stearoyl-Coenzyme A desaturase 1 (*Scd1*) is likely due to the large amount of unsaturated fatty acids in the HF diet.

The hepatic response to OxR in LF mice seems quite straight forward. Both pyruvate kinase (*Pklr*), which is involved in the last step of the glycolytic pathway and is stimulated by shortage of ATP; and lactate dehydrogenase (*Ldha*), which converts pyruvate to lactate during anaerobic glycolysis, were upregulated by OxR. The increase in hepatic glycolysis in LF mice might contribute to the decrease in oxygen consumption that was observed during OxR. LF mice do not show changes in the genes involved in hepatic gluconeogenesis, suggesting that lactate levels are below threshold values. From the 5 DNL genes that were analysed, only *Scd1* was significantly induced by OxR in LF mice. Furthermore, none of the genes that respond to oxidative stress were altered, suggesting that oxygen supply in liver tissue matched the oxygen demand.

The hepatic response to OxR in HF mice, on the other hand, appeared to be more complicated. HF mice showed a strong and consistent upregulation of genes involved in gluconeogenesis, suggesting that the liver is stimulated to clear lactate from the blood. Next to the increase in gluconeogenesis, we also see an increase in the expression of *Pklr*, suggesting that glycolysis is also upregulated. Upregulation of both gluconeogenesis and glycolysis would lead to an apparent, energy-costly pyruvate-malate-phosphoenolpyruvate (PEP) cycling (also see figure 6a). Under normal conditions, insulin stimulates *Pklr* , but inhibits simultaneously pyruvate carboxylase (*Pcx*) and PEP carboxykinase (*Pck*) but this regulation seems to be disturbed during OxR in HF mice. Another possibility could be that the pyruvate-malate-PEP cycling is interrupted by the direct conversion of malate to pyruvate by cytoplasmic malic enzyme (*Me1*), which leads to cytosolic NADPH production. NADPH plays an important role in antioxidant defence by serving as the main electron donor for reductases, such as thioredoxin that is involved in the conversion of ROS to water (1). In support of this, intermittent hypoxia was also shown to induce the expression of hepatic *Me1* in obese mice (28).

OxR, indeed, induced a strong antioxidant gene expression response in liver tissue of HF mice, suggesting that oxygen availability did not match oxygen demand in these mice. This is supported by the increase in serum markers for oxidative stress specifically in HF mice. It is possible that oxygen demand in HF mice is increased by an insufficient reduction of fatty acid beta oxidation. Indeed, HF mice showed a higher whole body lipid oxidation rate compared with LF mice. Fatty acid beta oxidation is possibly higher in HF mice to ensure sufficient ATP production for gluconeogenesis. Finally, HF mice also showed an increase in hepatic DNL, based on the increase in the expression of acetyl-Coenzyme A carboxylase alpha (*Acaca)* and fatty acid synthase (*Fasn*). Hepatic DNL is associated with obesity and promotes lipotoxicity, insulin resistance and non-alcoholic fatty liver disease (41).

OxR induces an antioxidant response and DNL in WAT of LF mice

WAT can rapidly expand during periods of high caloric intake. When tissue expansion exceeds vascularization, parts of the tissue will become hypoxic, which is suggested to lead to inflammation and the formation of ROS (46). Tissue hypoxia can be counteracted by transcriptional activation via *Hif1a*, leading to an increase in the antioxidant response and vascularization. Ambient OxR might induce similar responses in WAT to prevent hypoxia at tissue level. Hypertrophic WAT is expected to be the first tissue to experience problems in oxygen supply and availability during low oxygen conditions. Although LF and HF mice did not differ in epididymal WAT tissue mass, both groups differed in the expression of genes involved in the response to oxidative stress during OxR. In HF mice, no changes were found in the expression of any of the genes of interest. In LF mice, however, we found a consistent upregulation of genes involved in the response to oxidative stress. Controversially, we also found an upregulation in the expression of citrate synthase, which plays an important role in the citric acid cycle and is expected to increase mitochondrial activity. OxR did, however, not alter the expression of *Pnpla2* and *Cpt1a*, which suggests that the difference in antioxidant response by OxR between HF and LF mice is not caused by a difference in WAT lipolysis or fatty acid beta oxidation. It should be noted that three of the genes involved in the response to oxidative stress - *Vegfa*, *Ucp2* and *Txnrd2* - were already upregulated in HF mice compared to LF mice under normoxic conditions, which indicates that HF mice were already involved in WAT adaptation prior to the exposure to OxR. Physiological adaptation of WAT during high-fat feeding facilitates fat storage without decreasing the oxygenation of the cells. The exposure to OxR was possibly not severe enough to overcome or further strengthen the preconditioning by high-fat feeding; the increase in gene expression caused by high-fat feeding might prevent mice to further increase gene expression during OxR. It was, indeed, recently shown that high-fat feeding in mice increased metabolic health parameters such as plasma leptin and the expression of tumour necrosis factor (*Tnf*) in WAT; exposure to ambient hypoxia did, however, increase leptin and *Tnf* in lean mice but not in obese mice (45). Furthermore, it was recently shown that mice with a larger potential for WAT remodelling had, when exposed to ambient hypoxia, a larger degree of tissue hypoxia and higher expression of angiogenesis-related genes in WAT (26). These findings result from genetic differences of the two mouse strains used. Diet might, however, also influence the potential for WAT remodelling.

Next to the increase in genes involved in oxidative stress, OxR also induced a consistent increase in DNL in WAT of LF mice. An increase in DNL in adipose tissue is associated with a healthy phenotype in mice, eg. during caloric restriction (13), whereas a decrease in WAT DNL is associated with obesity and type 2 diabetes (16). Induction of DNL by OxR may increase WAT palmitoleate production (7), which might serve to

improve insulin sensitivity in response to the increase in blood glucose levels that was observed during OxR.

OxR is a promising challenge test to investigate early diet-induced changes in metabolism.

In this study we show that, after only 5 days of HF or LF feeding, mice differ in their adaptation to OxR. The adaptation in HF mice is possibly less effective because of the higher level of oxygen consumption that was observed and the increase in protein glycation and oxidation adducts in serum. The apparent difference in the adaptation to OxR between HF and LF mice is emphasised by the changes in genes expression that were induced by OxR. OxR, in fact, induced an almost reverse pattern of gene expression in LF versus HF mice: while the majority of hepatic genes was upregulated by OxR in HF mice, these genes remained unaffected in LF mice. In contrast, the majority of genes that were upregulated by OxR in eWAT of LF mice, remained unaffected in HF mice. Next to the metabolic changes that were induced by OxR in mice, OxR is also known to affect human metabolism. Similar levels of OxR lead, for example, to significant changes in oxygen saturation and CO_2 production in humans (9, 19). Although conflicting results were shown for the effect of hypoxia on blood glucose levels in humans (27, 37); acute hypoxia does alter glucose utilization in humans (25, 37). OxR as a challenge test might be suitable to be included in future dietary studies for early, sensitive detection of changes in metabolic health in animal models but might also be considered to be used in human studies.

Acknowledgements

This work was supported by the European Union's Seventh Framework Program FP7 2007-2013 under grant agreement no. 244995 (BIOCLAIMS Project).

Furthermore, we would like to thank all members of Human and Animal Physiology for their helpful contributions, especially Hans Swarts, Dylan Eikelenboom and Esther Steenbergh for their help during the animal experiment and the analysis of gene expression.

References

1. Aon MA, Stanley BA, Sivakumaran V, Kembro JM, O'Rourke B, Paolocci N*, et al.* Glutathione/thioredoxin systems modulate mitochondrial H2O2 emission: an experimental-computational study. J Gen Physiol. 2012;139: 479-491.
2. Asterholm IW, Scherer PE Enhanced Metabolic Flexibility Associated with Elevated Adiponectin Levels. American Journal of Pathology. 2010;176: 1364-1376.
3. Bartelt A, Heeren J The holy grail of metabolic disease: brown adipose tissue. Curr Opin Lipidol. 2012;23: 190-195.
4. Baze MM, Schlauch K, Hayes JP Gene expression of the liver in response to chronic hypoxia. Physiol Genomics. 2010;
5. Butler AA, Kozak LP A recurring problem with the analysis of energy expenditure in genetic models expressing lean and obese phenotypes. Diabetes. 2010;59: 323-329.
6. Cannon B, Nedergaard J Nonshivering thermogenesis and its adequate measurement in metabolic studies. J Exp Biol. 2011;214: 242-253.
7. Cao H, Gerhold K, Mayers JR, Wiest MM, Watkins SM, Hotamisligil GS Identification of a lipokine, a lipid hormone linking adipose tissue to systemic metabolism. Cell. 2008;134: 933-944.
8. Carstens MT, Goedecke JH, Dugas L, Evans J, Kroff J, Levitt NS*, et al.* Fasting substrate oxidation in relation to habitual dietary fat intake and insulin resistance in non-diabetic women: a case for metabolic flexibility? Nutr Metab (Lond). 2013;10: 8.
9. Charlot K, Pichon A, Richalet JP, Chapelot D Effects of a high-carbohydrate versus high-protein meal on acute responses to hypoxia at rest and exercise. Eur J Appl Physiol. 2013;113: 691-702.
10. Choi JH, Park MJ, Kim KW, Choi YH, Park SH, An WG*, et al.* Molecular mechanism of hypoxia-mediated hepatic gluconeogenesis by transcriptional regulation. FEBS Lett. 2005;579: 2795-2801.
11. David JM, Chatziioannou AF, Taschereau R, Wang H, Stout DB The hidden cost of housing practices: using noninvasive imaging to quantify the metabolic demands of chronic cold stress of laboratory mice. Comp Med. 2013;63: 386-391.
12. Drager LF, Li J, Reinke C, Bevans-Fonti S, Jun JC, Polotsky VY Intermittent hypoxia exacerbates metabolic effects of diet-induced obesity. Obesity (Silver Spring). 2011;19: 2167-2174.
13. Duivenvoorde LP, van Schothorst EM, Bunschoten A, Keijer J Dietary restriction of mice on a high-fat diet induces substrate efficiency and improves metabolic health. J Mol Endocrinol. 2011;47: 81-97.
14. Duivenvoorde LPM, van Schothorst EM, Swarts HJ, Keijer J Assessment of metabolic flexibility of old and adult mice using three non-invasive, indirect calorimetry-based treatments. J Gerontol A Biol Sci Med Sci 2014;
15. Eccleston HB, Andringa KK, Betancourt AM, King AL, Mantena SK, Swain TM*, et al.* Chronic exposure to a high-fat diet induces hepatic steatosis, impairs nitric oxide bioavailability, and modifies the mitochondrial proteome in mice. Antioxid Redox Signal. 2011;15: 447-459.
16. Eissing L, Scherer T, Todter K, Knippschild U, Greve JW, Buurman WA*, et al.* De novo lipogenesis in human fat and liver is linked to ChREBP-beta and metabolic health. Nat Commun. 2013;4: 1528.
17. Feldmann HM, Golozoubova V, Cannon B, Nedergaard J UCP1 Ablation Induces Obesity and Abolishes Diet-induced Thermogenesis in Mice Exempt from Thermal Stress by Living at Thermoneutrality. Cell Metab. 2009;9: 203-209.
18. Gamboa JL, Andrade FH Mitochondrial content and distribution changes specific to mouse diaphragm after chronic normobaric hypoxia. Am J Physiol Regul Integr Comp Physiol. 2010;298: R575-583.
19. Golja P, Flander P, Klemenc M, Maver J, Princi T Carbohydrate ingestion improves oxygen delivery in acute hypoxia. High Alt Med Biol. 2008;9: 53-62.
20. Hoevenaars FP, Keijer J, Swarts HJ, Snaas-Alders S, Bekkenkamp-Grovenstein M, van Schothorst EM Effects of dietary history on energy metabolism and physiological parameters in C57BL/6J mice. Exp Physiol. 2013;98: 1053-1062.

21. Hoevenaars FP, van Schothorst EM, Horakova O, Voigt A, Rossmeisl M, Pico C*, et al.* BIOCLAIMS standard diet (BIOsd): a reference diet for nutritional physiology. Genes Nutr. 2012;7: 399-404.
22. Horakova O, Medrikova D, van Schothorst EM, Bunschoten A, Flachs P, Kus V*, et al.* Preservation of metabolic flexibility in skeletal muscle by a combined use of n-3 PUFA and rosiglitazone in dietary obese mice. PLoS One. 2012;7: e43764.
23. Hutter JF, Schweickhardt C, Piper HM, Spieckermann PG Inhibition of fatty acid oxidation and decrease of oxygen consumption of working rat heart by 4-bromocrotonic acid. J Mol Cell Cardiol. 1984;16: 105-108.
24. Jequier E, Acheson K, Schutz Y Assessment of energy expenditure and fuel utilization in man. Annu Rev Nutr. 1987;7: 187-208.
25. Kelly KR, Williamson DL, Fealy CE, Kriz DA, Krishnan RK, Huang H*, et al.* Acute altitude-induced hypoxia suppresses plasma glucose and leptin in healthy humans. Metabolism. 2010;59: 200-205.
26. Kim DH, Gutierrez-Aguilar R, Kim HJ, Woods SC, Seeley RJ Increased adipose tissue hypoxia and capacity for angiogenesis and inflammation in young diet-sensitive C57 mice compared with diet-resistant FVB mice. Int J Obes (Lond). 2013;37: 853-860.
27. Larsen JJ, Hansen JM, Olsen NV, Galbo H, Dela F The effect of altitude hypoxia on glucose homeostasis in men. J Physiol. 1997;504 (Pt 1): 241-249.
28. Li J, Grigoryev DN, Ye SQ, Thorne L, Schwartz AR, Smith PL*, et al.* Chronic intermittent hypoxia upregulates genes of lipid biosynthesis in obese mice. J Appl Physiol (1985). 2005;99: 1643-1648.
29. Livesey G, Elia M Estimation of energy expenditure, net carbohydrate utilization, and net fat oxidation and synthesis by indirect calorimetry: evaluation of errors with special reference to the detailed composition of fuels. Am J Clin Nutr. 1988;47: 608-628.
30. Louis M, Punjabi NM Effects of acute intermittent hypoxia on glucose metabolism in awake healthy volunteers. J Appl Physiol (1985). 2009;106: 1538-1544.
31. Masschelein E, Van Thienen R, D'Hulst G, Hespel P, Thomis M, Deldicque L Acute environmental hypoxia induces LC3 lipidation in a genotype-dependent manner. FASEB J. 2014;28: 1022-1034.
32. Mazzatti D, Lim FL, O'Hara A, Wood IS, Trayhurn P A microarray analysis of the hypoxia-induced modulation of gene expression in human adipocytes. Arch Physiol Biochem. 2012;118: 112-120.
33. Mimura Y, Furuya K Mechanisms of adaptation to hypoxia in energy metabolism in rats. J Am Coll Surg. 1995;181: 437-443.
34. Montgomery MK, Hallahan NL, Brown SH, Liu M, Mitchell TW, Cooney GJ*, et al.* Mouse strain-dependent variation in obesity and glucose homeostasis in response to high-fat feeding. Diabetologia. 2013;56: 1129-1139.
35. Mortola JP, Rezzonico R, Lanthier C Ventilation and oxygen consumption during acute hypoxia in newborn mammals: a comparative analysis. Respir Physiol. 1989;78: 31-43.
36. Nieto FJ, Young TB, Lind BK, Shahar E, Samet JM, Redline S*, et al.* Association of sleep-disordered breathing, sleep apnea, and hypertension in a large community-based study. Sleep Heart Health Study. JAMA. 2000;283: 1829-1836.
37. Oltmanns KM, Gehring H, Rudolf S, Schultes B, Rook S, Schweiger U*, et al.* Hypoxia causes glucose intolerance in humans. Am J Respir Crit Care Med. 2004;169: 1231-1237.
38. Ostreicher I, Meissner U, Plank C, Allabauer I, Castrop H, Rascher W*, et al.* Altered leptin secretion in hyperinsulinemic mice under hypoxic conditions. Regul Pept. 2009;153: 25-29.
39. Peronnet F, Massicotte D Table of nonprotein respiratory quotient: an update. Can J Sport Sci. 1991;16: 23-29.
40. Pison CM, Chauvin C, Perrault H, Schwebel C, Lafond JL, Boujet C*, et al.* In vivo hypoxic exposure impairs metabolic adaptations to a 48 hour fast in rats. Eur Respir J. 1998;12: 658-665.
41. Postic C, Girard J Contribution of de novo fatty acid synthesis to hepatic steatosis and insulin resistance: lessons from genetically engineered mice. J Clin Invest. 2008;118: 829-838.
42. Rabbani N, Chittari MV, Bodmer CW, Zehnder D, Ceriello A, Thornalley PJ Increased glycation and oxidative damage to apolipoprotein B100 of LDL cholesterol in patients with type 2 diabetes and effect of metformin. Diabetes. 2010;59: 1038-1045.
43. Rabbani N, Shaheen F, Anwar A, Masania J, Thornalley PJ Assay of methylglyoxal-derived protein and nucleotide AGEs. Biochemical Society Transactions. 2014;in press:

44. Regazzetti C, Peraldi P, Gremeaux T, Najem-Lendom R, Ben-Sahra I, Cormont M*, et al.* Hypoxia decreases insulin signaling pathways in adipocytes. Diabetes. 2009;58: 95-103.
45. Reinke C, Bevans-Fonti S, Drager LF, Shin MK, Polotsky VY Effects of different acute hypoxic regimens on tissue oxygen profiles and metabolic outcomes. J Appl Physiol. 2011;111: 881-890.
46. Rupnick MA, Panigrahy D, Zhang CY, Dallabrida SM, Lowell BB, Langer R*, et al.* Adipose tissue mass can be regulated through the vasculature. Proc Natl Acad Sci U S A. 2002;99: 10730-10735.
47. Saito K, Ohta Y, Sami M, Kanda T, Kato H Effect of mild restriction of food intake on gene expression profile in the liver of young rats: reference data for in vivo nutrigenomics study. Br J Nutr. 2010;104: 941-950.
48. Semenza GL, Roth PH, Fang HM, Wang GL Transcriptional regulation of genes encoding glycolytic enzymes by hypoxia-inducible factor 1. J Biol Chem. 1994;269: 23757-23763.
49. Takeuchi M, Kimura S, Kuroda J, Ashihara E, Kawatani M, Osada H*, et al.* Glyoxalase-I is a novel target against Bcr-Abl+ leukemic cells acquiring stem-like characteristics in a hypoxic environment. Cell Death Differ. 2010;17: 1211-1220.
50. Taylor CT Mitochondria and cellular oxygen sensing in the HIF pathway. Biochem J. 2008;409: 19-26.
51. Thornalley PJ, Battah S, Ahmed N, Karachalias N, Agalou S, Babaei-Jadidi R*, et al.* Quantitative screening of advanced glycation endproducts in cellular and extracellular proteins by tandem mass spectrometry. Biochem J. 2003;375: 581-592.
52. Thornalley PJ, Rabbani N Detection of oxidized and glycated proteins in clinical samples using mass spectrometry - A user's perspective. Biochim Biophys Acta. 2014;1840: 818-829.
53. Tschop MH, Speakman JR, Arch JR, Auwerx J, Bruning JC, Chan L*, et al.* A guide to analysis of mouse energy metabolism. Nature Methods. 2012;9: 57-63.
54. Ukropcova B, McNeil M, Sereda O, de Jonge L, Xie H, Bray GA*, et al.* Dynamic changes in fat oxidation in human primary myocytes mirror metabolic characteristics of the donor. J Clin Invest. 2005;115: 1934-1941.
55. van Ommen B, Keijer J, Heil SG, Kaput J Challenging homeostasis to define biomarkers for nutrition related health. Mol Nutr Food Res. 2009;53: 795-804.
56. Van Schothorst EM, Franssen-van Hal N, Schaap MM, Pennings J, Hoebee B, Keijer J Adipose gene expression patterns of weight gain suggest counteracting steroid hormone synthesis. Obesity Research. 2005;13: 1031-1041.
57. Voigt A, Agnew K, van Schothorst EM, Keijer J, Klaus S Short-term, high fat feeding-induced changes in white adipose tissue gene expression are highly predictive for long-term changes. Mol Nutr Food Res. 2013;57: 1423-1434.
58. Weisberg SP, McCann D, Desai M, Rosenbaum M, Leibel RL, Ferrante AW Obesity is associated with macrophage accumulation in adipose tissue. Journal of Clinical Investigation. 2003;112: 1796-1808.
59. Xu HY, Barnes GT, Yang Q, Tan Q, Yang DS, Chou CJ*, et al.* Chronic inflammation in fat plays a crucial role in the development of obesity-related insulin resistance. Journal of Clinical Investigation. 2003;112: 1821-1830.
60. Yin J, Gao Z, He Q, Zhou D, Guo Z, Ye J Role of hypoxia in obesity-induced disorders of glucose and lipid metabolism in adipose tissue. Am J Physiol Endocrinol Metab. 2009;296: E333-342.

Supplemental figures and tables

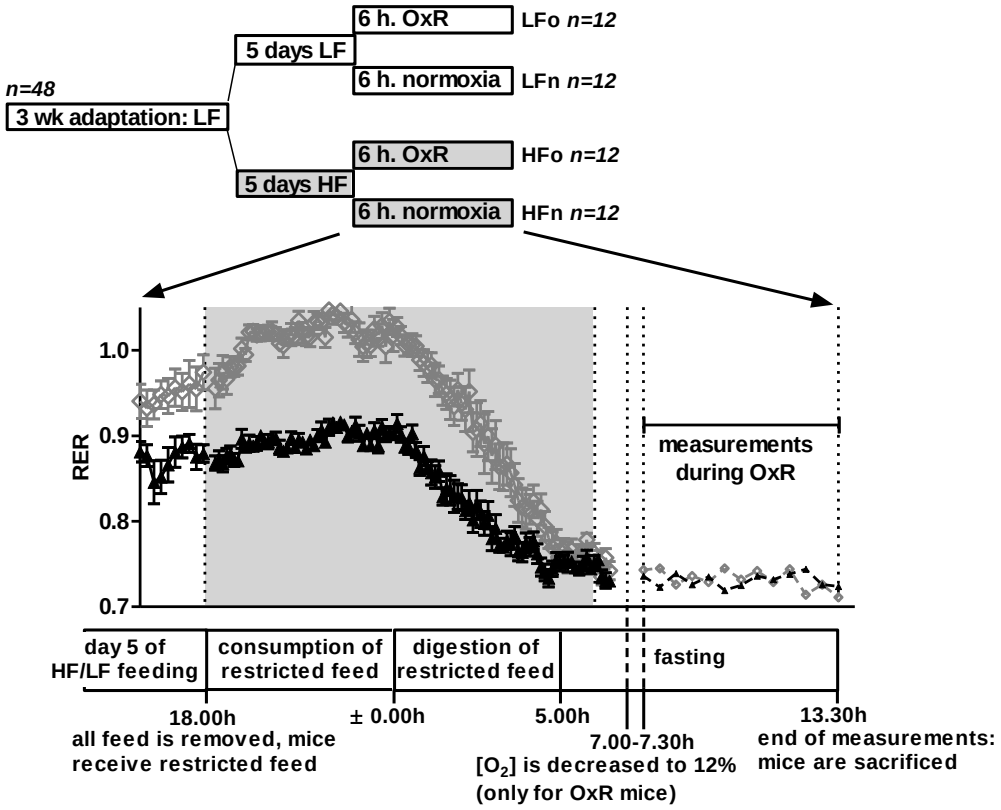

Supplemental figure 1 Schematic overview of the study design and exposure to OxR. The complete study lasted for three weeks. 48 male mice arrived at 10 weeks of age. After three weeks on the low-fat diet, mice were stratified and individually housed in the indirect calorimetry system. Mice could adapt to the InCa system for 24h after which 24 mice received a fresh batch of LF diet and 24 mice switched to the high-fat diet. After 5 days of HF- or LF feeding, mice were exposed to OxR or remained under normal air conditions for 6 hours. Mice were fasted by providing them a restricted amount of feed at the start of the dark phase (18.00h) preceding the OxR or normoxic challenge. The restricted amount of feed is generally consumed within 6 hours (around 0.00h). Around 5.00h, all mice were in a fasted state (RER<0.8). For the LFo and HFo mice, oxygen is decreased from 20.9% to 12% from 7.00h to 7.30h. LFn and HFn mice remained under normoxic conditions. Indirect calorimetry values during OxR or normoxia were then recorded from 7.30h to 13.30h, after which mice were immediately sacrificed.

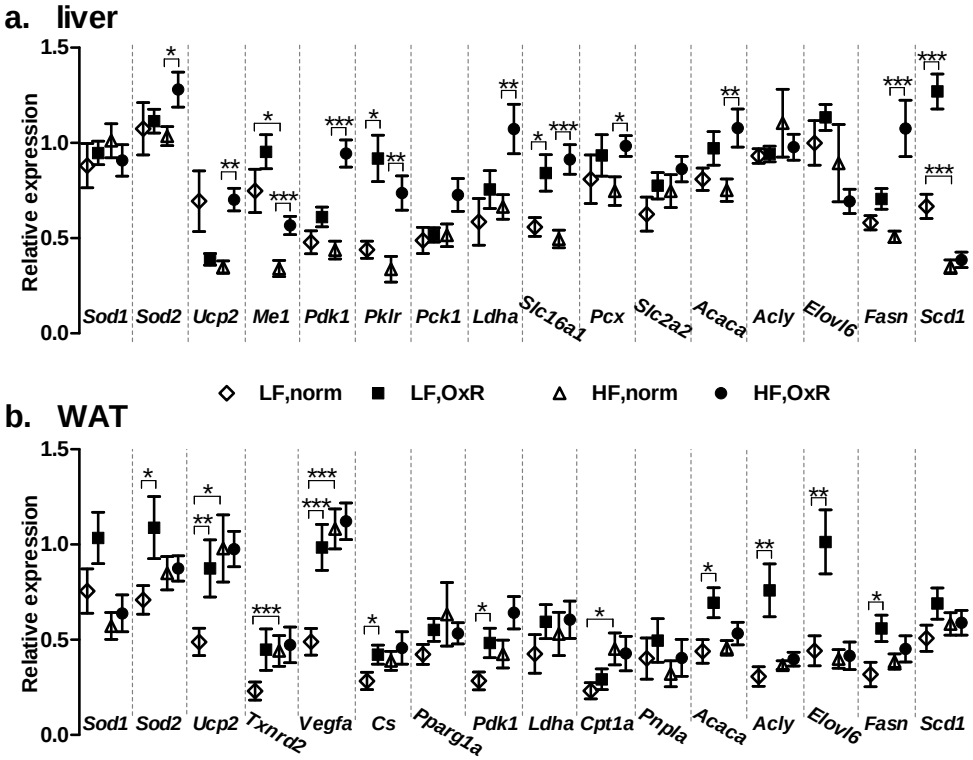

Supplemental figure 2 Relative gene expression in liver tissue and WAT of LF and HF mice that were either exposed to OxR or normoxic air. Gene expression in liver (a) and WAT (b) was calculated relatively to the geometric mean of the reference genes.
Sod1, superoxide dismutase 1; *Sod2,* superoxide dismutase 2; *Ucp2,* uncoupling protein 2; *Slc2a2,* solute carrier family 2 (facilitated glucose transporter; Glut2); *Pdk1*, pyruvate dehydrogenase kinase 1; *Pklr*, pyruvate kinase; *Pck1* phosphoenolpyruvate carboxykinase 1 *(Pepck)*; *Ldha*, lactate dehydrogenase A; *Slc16a1*, solute carrier family 16 (*Mct1*); *Pcx*, pyruvate carboxylase; *Me1*, malic enzyme; *Txnrd2,* thioredoxin reductase 2; *Vegfa*, vascular endothelial growth factor A; *Ppargrc1a* peroxisome proliferative activated receptor gamma coactivator 1 alpha (*Pgc1a*); *Cs*, citrate synthase; *Cpt1a,* carnitine palmitoyltransferase 1a; *Pnpla2*, patatin-like phospholipase domain containing 2; *Acaca*, acetyl-Coenzyme A carboxylase alpha; *Acly*, ATP citrate lyase; *Elovl6*, ELOVL family member 6, elongation of long chain fatty acids; *Fasn*, fatty acid synthase; *Scd1*, stearoyl-Coenzyme A desaturase 1.

Supplemental table 1 Primer sequences and PCR annealing temperatures for qRT-PCR

Gene	Forward primer 5' – 3'	Reverse primer 5' – 3'	PCR temp.
Acaca	GTTGAAGGCACAGTGAAGGCTTAC	ATGGCGACTTCTGGGTTGGC	58.0ºC
Acly	TGGGCTTCATTGGGCACTACC	TGGGCTTCATTGGGCACTACC	62.0ºC
*B2m**	CCCCACTGAGACTGATACATACGC	AGAAACTGGATTTGTAATTAAGCAGGTTC	60.0ºC
Cpt1a	CTGAGACAGACTCACACCGC	GTGGAGCCTACGGTTGTTCT	58.0ºC
Cs	ACAGTGAAAGCAACTTCGCC	GTCAATGGCTCCGATACTGC	58.0ºC
Elovl6	GGCACTAAGACCGCAAGGCA	GCTACGTGTTCTCTGCGCCT	62.0ºC
Fasn	AGTTAGAGCAGGACAAGCCCAAG	TTCAGTGAGGCGTAGTAGACAGTG	58.0ºC
Ldha	CACGCTGCTTCTCCTCGCCAGT	GGCACAAGCCATGCCAACAGCAC	62.0ºC
Me1	GAGGTCATATCTCAGCAAGTGTCAG	AATCAGGTAGGATCTGGTCATAATTAGTG	56.0ºC
Pck1	ACTGTTGGCTGGCTCTCACTG	TCTCAAAGTCCTCTTCCGACATCC	58.0ºC
Pcx	AGGGCGGAGCTAACATCTAC	GGCTTCATCAGCTTTCTGCC	60.0ºC
Pdk1	TGAAGCAGTTCCTGGACTTCGGGTC	TGTCGGGGAGGAGGCTGATTTCT	62.0ºC
Pklr	TGGCGGACACCTTCCTGGAACA	TCTGCATGGTACTCATGGGAGCCA	60.0ºC
Pnpla2	CCAGTTCAACCTTCGCAATCTCTAC	GCATGTTGGAAAGGGTGGTCATC	58.0ºC
Ppargc1a	CCCTGCCATTGTTAAGACC	TGCTGCTGTTCCTGTTTTC	60.0ºC
*Rps15**	CGGAGATGGTGGGTAGCATGG	ACGGGTTTGTAGGTGATGGAGAAC	62.0ºC
Scd1	TCATGGTCCTGCTGCACTTGG	CTGTGGCTCCAGAGGCGATG	58.0ºC
Slc2a2	TTGTCATCGCCCTCTGCTTCC	GTGGTTCCTCCTGGTCGGTTC	58.0ºC
Slc16a1	GGCCACCACTTTTAGGCCGC	AGTCGATAGTTGATGCCCATGCCA	62.0ºC
Sod1	TCGGCTTCTCGTCTTGCTCTC	GTTCACCGCTTGCCTTCTGC	60.0ºC
Sod2	TTCTGGACAAACCTGAGCCCTAAG	GCAGCAATCTGTAAGCGACCTTG	60.0ºC
Txnrd2	TGGCTGACTATGTGGAACCT	ACTTGACTTTCCTGTCCTGC	62.5ºC
Ucp2	AGTTCCGCCCTCGGTGTCGT	TTGTGTCCGGACCGCAGGAGA	58.0ºC
Vegfa	AAGCCAGCACATAGGAGAGATGAG	TCTTTGGTCTGCATTCACATCTGC	60.0ºC

Genes denoted with an asterisk were used as reference genes for normalization.

Supplemental table 2 Average oxygen consumption, RER and physical activity levels of LF and HF mice during OxR and normoxic conditions in the indirect calorimetry system

	normoxic	OxR
VO_2 LF	83.9 ± 3.71	63.6 ± 1.50 ***
RER LF	0.76 ± 0.01	0.73 ± 0.01 *
Physical activity LF	16.28 ± 2.00	6.17 ± 1.03 ***
VO_2 HF	87.8 ± 2.61	67.7 ± 1.29 ***
RER HF	0.75 ± 0.00	0.70 ± 0.01 ***
Physical activity HF	16.31 ± 1.14	5.96 ± 0.70 ***

Data are expressed as mean ± SEM, n=12 mice per group. Asterisks denote significant differences from control (normoxic) values. All measurements were performed during fasting conditions.

Chapter 5

A difference in fatty acid composition of isocaloric high-fat diets alters metabolic flexibility in male C57BL/6JOlaHsd mice.

Loes P.M. Duivenvoorde, Evert M. van Schothorst, Hans M. Swarts, Ondrej Kuda, Esther Steenbergh, Sander Termeulen, Jan Kopecky, and Jaap Keijer

Revision submitted to PLOS ONE.

Abstract

Poly-unsaturated fatty acids (PUFAs) are considered to be healthier than saturated fatty acids (SFAs), but others postulate that especially the ratio of omega-6 to omega-3 PUFAs (n6/n3 ratio) determines health. Health can be determined with biomarkers, but functional health status is likely better reflected by challenge tests that assess metabolic flexibility. The aim of this study was to determine the effect of high-fat diets with different fatty acid compositions, but similar n6/n3 ratio, on metabolic flexibility. Therefore, adult male mice received isocaloric high-fat diets with either predominantly PUFAs (HFpu diet) or predominantly SFAs (HFs diet) but similar n6/n3 ratio for six months, during and after which several biomarkers for health were measured. Metabolic flexibility was assessed by the response to an oral glucose tolerance test, fasting and re-feeding test and oxygen restriction test (OxR; normobaric hypoxia). The latter two are non-invasive, indirect calorimetry-based tests that measure the adaptive capacity of the body as a whole. We found that the HFs diet increased mean adipocyte size and ectopic lipid storage in liver and muscle, but did not cause differences in body weight, total adiposity, adipose tissue health, serum adipokines, whole body energy balance, or circadian rhythm. HFs mice were, furthermore, less flexible in their response to both fasting- re-feeding and OxR, while glucose tolerance was indistinguishable.

To conclude, the HFs versus the HFpu diet increased ectopic fat storage and mean adipocyte size and reduced metabolic flexibility in male mice. This study underscores the physiological relevance of indirect calorimetry-based challenge tests.

Introduction

Excessive dietary fat intake is positively associated with weight gain and the development of metabolic diseases (4), such as insulin resistance, cardiovascular diseases, and type 2 diabetes. Metabolic diseases are often associated with a decrease in metabolic flexibility. Metabolic flexibility can be considered as the ability to switch between carbohydrate oxidation and fat oxidation (61) and is e.g. apparent in type 2 diabetics, who fail to adequately switch to glucose oxidation upon glucose consumption. Metabolic flexibility can, however, also be seen in a broader sense, in which it is defined as the capability to maintain homeostasis during a nutritional or environmental challenge (70). Such a challenge can consist of administration of a single nutrient, such as glucose (2, 27) or lipid (64), or a combination of nutrients like in a meal test (20, 36). Alternatively, it can consist of exposure to an environmental challenge, such as oxygen restriction (OxR), in which a major determinant for aerobic fuel oxidation – oxygen – is limited (15, 16). An adequate response to the challenge, ultimately, requires substrate switching, which is impaired when metabolic flexibility declines. Metabolic inflexibility arises from deficiencies in the handling of incoming and circulating nutrients by one or several of the organs that play a major role in metabolism, such as the liver, skeletal muscle, adipose tissue, brain and pancreas (62). Detection of metabolic inflexibility would, thus, benefit from a multiple level approach, in which different organs or metabolic systems are challenged.

Next to the amount of dietary fat, the composition and type of fat affect the development of metabolic disease and metabolic inflexibility. Saturated fatty acids (SFAs) increase fasting insulin levels, weight gain, circulating leptin levels, liver triacylglycerols, mean adipocyte size and adipose tissue inflammation, and decrease adiponectin levels, compared to poly-unsaturated fatty acids (PUFAs) (5, 10, 19, 21, 40, 43, 44, 66). Furthermore, the proportion of fatty acids to each other seems to determine health effects (21). Among the SFAs, for example, medium chain SFAs protect against the detrimental effects of long chain SFAs in both humans and rodents (60, 73); and among the PUFAs, omega-3 PUFAs (n-3 PUFAs) were shown to be more beneficial for rodent health status than omega-6 PUFAs (n-6 PUFAs) (23, 51, 65) that appear to have pro-inflammatory properties (72). It has, indeed, been suggested that especially the ratio of n-6 PUFAs to n-3 PUFAs (n6/n3 ratio) determines the pathogenesis of metabolic diseases, rather than the absolute amounts of n-3 PUFAs and n-6 PUFAs (59). The influence of the fatty acid composition of the diet on metabolic flexibility, however, remains largely unknown. In this study we, therefore, investigate the effect of two isocaloric high-fat (HF) diets that differ in fatty acid composition on metabolic health and metabolic flexibility in mice. The first diet (HFpu diet) is a standardized HF diet that is used in several previous studies (15, 33, 35, 71) and mainly contains PUFAs in the fat fraction. The second diet (HFs diet) is identical to the HFpu diet, except for the fat fraction, which mainly contained saturated fatty acids from

palm oil. Palm oil is the dominant fat constituent of most experimental rodent HF diets and is increasingly prevalent in human food products. Although the HFpu diet contains much more PUFAs, the ratio of n-6 FAs to n-3 FAs was kept similar between both diets. Metabolic flexibility was measured with one invasive challenge test: the oral glucose tolerance test (OGTT), which monitors the homeostatic blood glucose clearance in response to a glucose challenge; and two non-invasive challenge tests that were monitored with indirect calorimetry instead of blood sampling. Indirect calorimetry-based challenge tests are suitable to asses metabolic flexibility because indirect calorimetry directly displays the extent and time course of substrate switching. For this study we used a nutritional challenge: a fasting and re-feeding challenge, and an environmental challenge with mild reduction in the availability of oxygen (OxR: $[O_2]$ = 12% vs 21 % in normoxia). Using food as a challenge will target a wider range of processes than during an OGTT and, therefore, provides a broader reflection of metabolic sensitivity. OxR forces the use of metabolic pathways that facilitate adaptation to decreased oxygen availability and thus directly targets flexibility. Body weight, adiposity, liver and adipose tissue health, and circulating hormone and adipokine levels were also monitored during the course of the experiment to evaluate metabolic health status.

Materials and methods

Animals and experimental manipulations

Thirty male C57BL/6JOlaHsd mice were used for this study (Harlan Laboratories, Horst, The Netherlands). The experimental protocol was approved by the Animal Welfare Committee of Wageningen University, Wageningen, The Netherlands (DEC2012088). Mice arrived at 10 weeks of age and were individually housed and maintained under environmentally controlled conditions (21 ± 1ºC, 12 h/12 h light–dark cycle, 50 ± 10% humidity) and had *ad libitum* access to feed and water. The study consisted of a three week adaptation phase and an experimental phase of 27 weeks (wk1 - wk27). During the adaptation phase, mice received the purified low-fat BIOCLAIMS standard diet, which contains 10% energy from fat (35). For the experimental phase, mice were stratified by body weight and allocated to the HFpu or HFs group. Both high-fat diets contained 40% energy from fat, but differed in the composition of the fat component. The control diet is the BIOCLAIMS purified standardized HF diet (HFpu diet), with 70% (w/w) sunflower oil, 18% coconut oil and 12% flax seed oil (71). The HFs diet contains 98.1% palm oil and 1.9% flax seed oil (for a detailed description of both diets, see table 1). The HFs diet thus contained more saturated and long chain fatty acids, and less medium chain and n-3 fatty acids than the HFpu diet. The HFs contained the minimal requirements for n-3 fatty acids (50) and the ratio of n6/n3 fatty acids was kept similar between both diets. Body weight, body composition - by using an EchoMRI™ Whole Body Composition Analyser (EchoMRI™,

Houston, USA) - and feed intake were monitored on a weekly basis. Mice received a fresh batch of feed at the start of each week and feed intake was determined from week 5 onwards by weighing the amount of feed at the start and at the end of each week. Three mice of each dietary group were sacrificed after 5 days of HF-feeding to analyse liver steatosis at the start of the experiment. The remaining 12 mice per dietary group continued until the end of the experiment; although, 1 mouse of the HFpu group died before the end of the experiment for reasons unrelated to the dietary intervention and was excluded from all analyses.

Table 1 Diet composition of HFpu and HFs

Ingredients (g kg-1)	HFpu	HFs
Casein	267	267
Wheat starch	172.5	172.5
Maltodextrin	100	100
Glucose	50	50
Sucrose	100	100
Coconut oil	37.8	0
Sunflower oil	147	0
Flaxseed	25.2	4
Palm oil	0	206
Cholesterol	97 mg	97 mg
Cellulose	50	50
Mineral mixture	35	35
Vitamin mixture	10	10
Choline bitartrate	2.5	2.5
L-Cysteine	3	3
Energy (kJ g-1)	19.7	19.7
Energy (% of total energy content)		
Carbohydrate	36.8	36.8
Fat	40.2	40.2
Protein	23.0	23.0
Fatty acid profile (g kg-1)		
Caprylic acid (C8:0)	2.8	0
Capric acid (C10:0)	2.3	0
Lauric acid (C12:0)	16.9	0.2
Myristic acid (C14:0)	6.4	2.1
Palmitic acid (C16:0)	13.1	89.8
Stearic acid (C18:0)	8.5	9.0
Oleic acid (C18:1 n-9)	35.5	76.1
Linoleic acid (C18:2 n-6)	100.9	19.3
α-Linolenic acid (C18:3 n-3)	13.5	2.5
Fatty acid profile (% of total energy content)		
Saturated fatty acids	9.6	19.4
Medium chain fatty acids (C6:0 –C12:0)	4.2	0
Long chain fatty acids (C14:0- C18:0)	5.4	19.3
Mono-unsaturated fatty acids	6.8	14.6
Poly-unsaturated fatty acids	21.9	4.2
Omega 3 fatty acids	2.6	0.5
Omega 6 fatty acids	19.3	3.7
Ratio n-6/n-3 fatty acids	7.5	7.6

The macronutrient content of the HFs diet was matched to the macronutrient content of the HFpu diet, which is a standardized high-fat diet that we also used in previous studies (35). Diets only differ in the amount and type of dietary oil that was added to obtain two isocaloric diets with 40 energy % from fat. The fatty acid profile of the used dietary oils was derived from the USDA National Nutrient Database for Standard Reference (68).

Indirect calorimetry was performed in weeks 5 and 20. OGTTs were performed in week 22; the response to fasting and re-feeding and the response to OxR was measured in week 25. Mice were sacrificed in week 27 by decapitation to prevent effects of anaesthesia on metabolic parameters (9, 11), after which blood was collected in Mini collect serum tubes (Greiner Bio-one, Longwood, USA), and centrifuged for 10 minutes at 3000 g and 4°C to obtain serum. Serum samples were aliquoted and stored at -80°C. Glucose concentration was measured in whole blood with a Freestyle blood glucose system (Abbott Diabetes Care, Hoofddorp, the Netherlands) according to the manufacturer's instructions. After blood collection, liver tissue, the left epididymal WAT (eWAT) depot and the acromion trapezius muscle, which is situated between the shoulder blades and underneath the brown adipose depot, were dissected and snap frozen in liquid nitrogen and stored at –80 °C. The right eWAT depot was weighted and stored in Dulbecco's Phosphate Buffered Saline (PBS; Gibco, Paisley, UK) with 3.7% formaldehyde (Merck KGaA Darmstadt, Germany) (pH=7.40) at 4^0C.

WAT and liver histology and mitochondrial density

The caudal part (one third of the complete tissue) of the right eWAT depot was fixed in PBS with 3.7% formaldehyde (pH=7.40) at 4^0C for 24 hours with moderate shaking, and then washed in PBS for 2 hours with moderate shaking and stored in PBS with 0.1% sodium azide for several days at 4^0C until further use. Fixed tissues were embedded in paraffin and sectioned at 5 µm. Adipocyte size and the amount of crown-like structures (CLS) in eWAT were determined as published (6) with adaptations as described (32, 33) in 8 mice per dietary group (randomly selected) and used as an indication of adipose tissue health (55). Briefly, macrophages were stained with a monoclonal anti-MAC2 antibody (diluted 1:5000, overnight incubation at 4 °C; Cedarlane Laboratories Limited, Burlington, Canada). Next, sections were rinsed in PBS and incubated for 60 min at room temperature with a secondary goat anti-rat biotinylated antibody (diluted 1:200; Vector laboratories, Burlingame, CA, USA), rinsed again with PBS, and incubated for 60 min at room temperatures with Vectastain Elite ABC reagent (dilution 1:1000; Vector laboratories). After rinsing with PBS, the sections were incubated for 2 minutes at room temperature with 3,3′-diaminobenzidine solution (dilution 1:200; Vector laboratories). To determine adipocyte size, sections were stained with haematoxylin QS (Vector laboratories). To determine adipocyte size, we used sections from three distant layers of the adipose depot (with 150 µm in between layers). Within each layer, approximately 5 pictures were taken with a Zeiss Axioscope 2 microscope equipped with an axioCamMRc 5 digital camera (Zeiss Inc., Jena, Germany). All adipocytes in each picture were manually encircled with the Axiovision software (Carl Zeiss, version 4.8) to determine the surface area of at least 400 adipocytes per mouse. The number of CLS was scored manually per 1000 adipocytes per mouse in the similar distant areas as the sections that were used to determine adipocyte size. All analyses were performed blinded to dietary background.

Mitochondrial density in eWAT was determined as indicator of WAT health. The ratio of mitochondrial DNA to nuclear DNA was measured with reverse transcription quantitative real-time PCR (RT-qPCR) as published (42) and with modifications as described (16). Briefly, total DNA was extracted from homogenized eWAT by digestion with Proteinase K (Sigma-Aldrich) in a lysis buffer (50 mM Tris-HCL, pH 7.5, 0.5% SDS and 12.5 mM EDTA, pH 8.0) and RNAse A (Sigma-Aldrich). Samples were then centrifuged, after which the aqueous phase was mixed and extracted with phenol-chloroform-isoamylacohol and twice with chloroform. DNA was precipitated by 96% ethanol and sodium acetate (3M, pH 5.2), washed with cold 70% ethanol, air-dried and re-suspended in 10 µl of RNAse DNAse free water. Quality and quantity of DNA in each sample was analysed with the Nanodrop (IsoGen Life Science, Maarssen, The Netherlands) and each sample was diluted to the same DNA concentration of 100 ng µL-1.

Serum and tissue analyses

Serum insulin, leptin and adiponectin levels were determined with the Bio-Plex Pro Mouse Diabetes Assay (Bio-Rad, Veenendaal, The Netherlands) according to the instructions of the manufacturer with the Bio-Plex 200 system (Bio-Rad) and used as indicators of adipose tissue health. Serum aspartate transaminase and alanine transaminase levels were determined with the AST and ALT enzymatic assay kit (Bioo Scientific Corporation, Austin, USA) according to the instructions of the manufacturer. Triacylglycerol levels were determined with the Triglycerides Liquicolor Kit (Human, Wiesbaden, Germany) according to the instructions of the manufacturer and as published (30). Approximately 20 mg of liver or muscle tissue was grinded to a powder in liquid nitrogen. Grinded tissue was dissolved in homogenisation buffer (10 mM TRIS-HCl, 2mM EDTA, 250 mM sucrose, pH 7.5) to a concentration of 40 mg tissue/ ml buffer. Tissue homogenates were homogenized with an automated pellet mixer (VWR, Boxmeer, The Netherlands) for at least one minute and by pulling the homogenate through a 25 gauge needle at least three times until all tissue was fully dissolved.

Oral glucose tolerance test (OGTT)

On the day of the OGTT, food was removed 1.5 hour after start of the light phase. Mice remained without food for the following 5 hours, after which blood glucose was measured via a tail cut with the Freestyle blood glucose system (Abott Diabetes Care) and 2 g glucose /kg bodyweight was given by oral gavage. Fifteen, 30, 60, 90, and 120 min following glucose administration, glucose concentration was determined using the Freestyle blood glucose system. Glucose tolerance was analysed with individual time course data of blood glucose levels and the individual incremental area under the curve (iAUC).

Indirect calorimetry

Oxygen consumption and carbon dioxide production were measured with an open indirect calorimetry system (TSE Systems, Bad Homburg, Germany) that is equipped for simultaneous measurements of 12 individual mice, as published (34). Mice could adapt to the indirect calorimetry system for 24 hours, after which the actual measurement started and O_2 consumption and CO_2 production were recorded every thirteen minutes. Energy expenditure (EE), respiratory exchange ratio (RER) and physical activity were determined as described previously (16).

To measure the response to fasting and re-feeding, mice received 1.5 gram of their own feed at the start of the dark phase (18.00h) in the indirect calorimetry system. All feed was consumed within the first 6 hours of the dark phase, after which RER starts to decline. Between 6.00h and 14.00h of the following light phase mice are in a fasted state (RER<0.75). At 14.00h, mice regained *ad libitum* access to the HFpu diet (HFpu mice) or HFs diet (HFs mice). RER values of each mouse were averaged during the period of fasting (from 23.00h to 6.00h), during the period when mice are fasted (from 6.00h to 14.00h) and during the period of re-feeding (from 14.00h to 22.00h). The maximal RER-value during re-feeding was calculated as the average of the three highest consecutive RER values representing a time span of 26 minutes during the complete period of re-feeding and was used for comparison with the food quotient of both diets. Food quotients were calculated with the heat equivalents of CO_2 of each component of the diet (3). Heat equivalents of the individual dietary oils were derived from Livesey and Elia (45). The percentage of energy from glucose oxidation was derived from average RER values of individual mice with the table of Peronnet (52).

Indirect calorimetry during OxR was performed as described (15, 16). For the exposure to OxR we used the same fasting regime as during the response to fasting and re-feeding (mice received 1.5 gram of feed at the start of the dark phase). One hour after start of the following light phase, oxygen concentration in each animal cage was decreased to 12% and O_2 consumption and CO_2 production were recorded every thirteen minutes for the following 6 hours. The day previous to the exposure to OxR, mice were kept in the indirect calorimetry system under the same (fasting) conditions and during the same time period of the day but under normoxic conditions, which means that in the analysis to the response to OxR, mice served as their own control. Blood glucose was measured directly after the exposure to OxR or normal air via a tail cut and with the Freestyle blood glucose system.

Statistics

Data are expressed as mean ± SEM. All analyses are based on the data of the 11 HFpu mice and 12 HFs mice; except for the analysis of adipocyte size and WAT CLS, which is based on 8 mice per group. Statistical analyses were performed using GraphPad Prism version 5.04 (Graphpad, San Diego, USA). Data were checked for normality using the D'Agostino and Pearson omnibus normality test. Test results that

were not normally distributed were log-transformed or analysed with a non-parametric test (feed intake in the indirect calorimetry system wk20). Measurements at single time points between 2 independent groups were analysed by independent Students' *t*-tests (all data in Table 2 and Figure 2, the iAUC of the OGTT and the RER peak during re-feeding).

Comparisons between two groups that were repeated over time (all data in Table 3, Figure 1 and Figure 5, glucose levels during the OGTT, RER during fasting and re-feeding) were analysed with two-way repeated measures ANOVA (factor 1=diet, factor 2=time) and Bonferroni post-hoc analysis. P-values smaller than 0.05 were considered to be statistically significant.

Results

The HFs diet mainly affected mean adipocyte size in eWAT and ectopic lipid storage in liver and skeletal muscle

After 27 weeks of feeding mice with isocaloric HF diets differing only in fatty acid composition, we detected no differences in BW, adiposity (fig. 1), cumulative feed intake, WAT mitochondrial density, serum glucose, insulin, leptin, or adiponectin levels (table 2) between HFpu and HFs mice. Of note, both groups of mice had relatively high fasting insulin levels that are well above levels that are usually seen in high-fat fed male C57BL/6J mice (around 0.11 nmol L-1 after 18 weeks of feeding (49)).

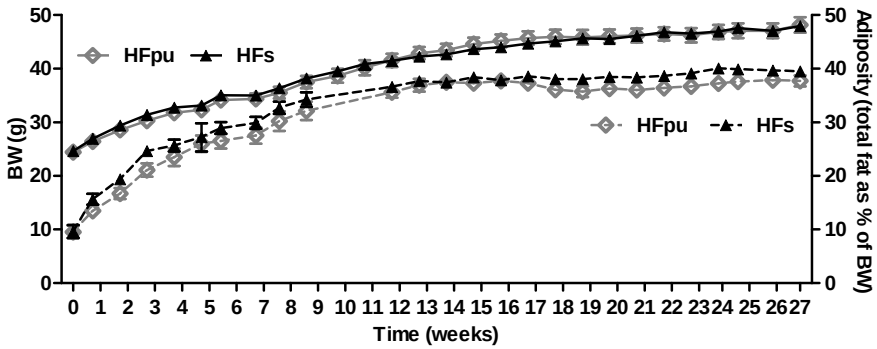

Figure 1 Body weight and total adiposity during 27 weeks of HF feeding. Body weight (solid lines) and total adiposity (dotted lines) were determined on a weekly basis during the 27 weeks of HFpu and HFs feeding. Total adiposity is expressed as the percentage of total body fat over body weight.

Adipocytes in eWAT were significantly larger in HFs mice compared to HFpu mice (fig. 2A and B), whereas no difference in the number of crown-like structures in eWAT was observed (fig. 2C). Moreover, the mice that consumed the HFs diet had significantly higher triacylglycerol levels in liver and muscle (table 2), which indicates increased ectopic lipid storage. Consistently, serum aspartate transaminase and alanine

transaminase levels, markers for liver damage, were both significantly increased in HFs mice compared with HFpu mice (table 2). To obtain an impression of the extent of liver steatosis in week 27 compared to the situation at the start of the intervention, hepatic lipids were stained with Oil-red-O after either 5 days or 27 weeks of high-fat feeding in a limited number of mice per group (suppl. fig. 1). Both the number and size of hepatic lipid droplets strongly increased over time.

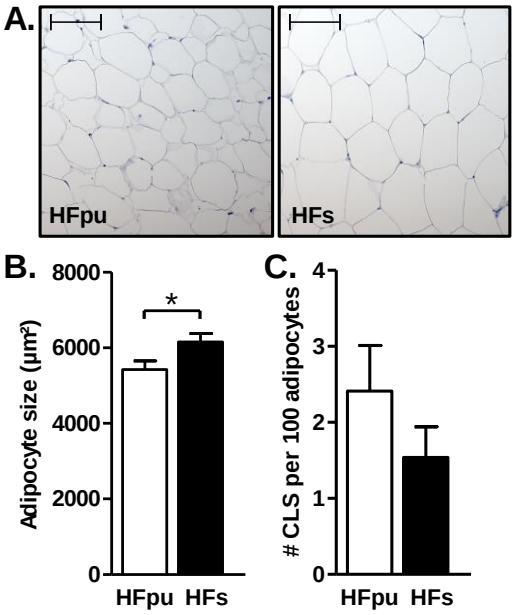

Figure 2 Mean adipocyte size and prevalence of crown-like structures in eWAT after 27 weeks of HF feeding. Representative images (A) of the haematoxylin stainings that were used to determine the average adipocyte surface area (B) in eWAT of HFpu and HFs mice. The bar in each picture represents a distance of 100 µm. The number of CLS (C) was determined with a MAC-2 macrophage staining in eWAT. * P< 0.05 HFs mice vs. HFpu mice.

Substrate oxidation and energy expenditure under non-challenged conditions do not explain the increase in adipocyte size and ectopic lipid storage

Energy expenditure, physical activity and the respiratory exchange ratio under non-challenged conditions were measured with indirect calorimetry in week 5 and week 20 of HF feeding (table 3). We also analysed diurnal (or circadian) rhythm, since it is known that a disturbance in circadian rhythm relates to metabolic dysfunction (57). To ensure accurate measurement of EE, RER and physical activity, we also analysed 24h feed and water intake in the indirect calorimetry system and compared that with the feed intake in the home cage in the same week and also between dietary groups. A drop in feed intake might indicate stress and disturbs the measurement of diurnal RER. EE and physical activity can also be affected by stress. Diurnal feed and water intake in the indirect calorimetry system were not significantly different between both dietary groups (table 3).

Table 2 Phenotypical data of mice fed the HFpu or HFs diet for 27 weeks

	HFpu	HFs	p-value
Cumulative feed intake (kg)	0.350 ± 0.007	0.339 ± 0.005	n.s.
Serum insulin (nmol L-1)	2.36 ± 0.17	1.92 ± 0.20	n.s.
Serum glucose (mmol L-1)	6.90 ± 0.19	7.16 ± 0.15	n.s.
Serum leptin (nmol L-1)	6.13 ± 0.71	5.67 ± 0.94	n.s.
Serum adiponectin (mg L-1)	15.5 ± 1.10	18.9 ± 1.35	n.s.
Serum triacylglycerols (g L-1)	6.02 ± 0.29	6.69 ± 0.57	n.s.
WAT mitochondrial density (ratio to HFpu)	1.00 ± 0.09	0.87 ± 0.07	n.s.
eWAT weight (g)	0.795 ± 0.067	0.866 ± 0.036	n.s
Liver triacylglycerol (mg g-1 liver)	52.7 ± 3.30	66.1 ± 3.02	0.007
Muscle triacylglycerols (mg g-1 muscle)	17.9 ± 1.61	22.9 ± 1.67	0.045
Serum aspartate transaminase activity (µmol s-1 L-1)	0.69 ± 0.06	1.07 ± 0.12	0.009
Serum alanine transaminase activity (µmol s-1 L-1)	0.83 ± 0.06	1.51 ± 0.16	<0.001

Data are expressed as mean ± SEM (n=11 for HFpu and n=12 for HFs). All parameters were measured after 27 weeks of HFpu or HFs feeding and when mice were in a fasted state. The cumulative feed intake is calculated from the total feed intake between week 4 and week 27. eWAT weight represents the weight of the right epididymal WAT depot only. n.s. non-significant.

Feed intake in the indirect calorimetry system was, furthermore, not significantly different from feed intake in the home cage. Feed intake in the home cage was 2.98 ± 0.05 for HFpu and 2.88 ± 0.05 for HFs in week 5 and 3.39 ± 0.08 for HFpu and 3.28 ± 0.05 for HFs in week 20. HFpu mice had significantly higher physical activity levels compared with HFs mice. The increase in physical activity did, however, not result in a significant increase in energy expenditure. HFpu and HFs mice neither differed in diurnal RER in week 5 nor in week 20. Physical activity was significantly higher in week 5 compared to week 20, whereas energy expenditure was higher in week 20 compared to week 5.

Table 3 Indirect calorimetry measurements of HFpu and HFs mice in week 5 and week 20

	Week 5		**Week 20**		
	HFpu	**HFs**	**HFpu**	**HFs**	**sign.**
Respiratory exchange ratio	0.832 ± 0.008	0.812 ± 0.011	0.836 ± 0.007	0.829 ± 0.008	n.s.
Energy expenditure (J s-1)	0.583 ± 0.008	0.575 ± 0.009	0.684 ± 0.018	0.678 ± 0.013	§§§§
Activity (total beam breaks (x1000))	36.4 ± 2.94	26.5 ± 2.03	25.8 ± 2.89	19.7 ± 1.37	§§§, ŦŦ
% of activity in the DP	70.0 ± 3.46	67.1 ± 1.57	64.9 ± 3.57	66.5 ± 1.44	n.s.
Feed intake (g)	2.77 ± 0.10	2.61 ± 0.24	3.14 ± 0.13	2.95 ± 0.22	n.s.
% of FI in the DP	70.4 ± 2.12	66.1 ± 5.74	63.8 ± 3.30	68.5 ± 2.94	n.s.
Water intake (ml)	1.74 ± 0.16	1.45 ± 0.20	2.25 ± 0.21	1.84 ± 0.14	§§

Data are expressed as mean ± SEM (n=11 for HFpu and n=12 for HFs). Indirect calorimetry measurements during normal, free-feeding conditions were performed after 5 and after 20 weeks of feeding the HFpu or HFs diet. Data were recorded and averaged over 24 hours. Feed intake (FI) and physical activity are also expressed as the percentage in the dark phase (DP) to give insight into the diurnal pattern. § indicates a significant effect of time (§§ P<0.01, §§§ P<0.001 and §§§§ P<0.0001). Ŧ indicates a significant effect of the diet (ŦŦ P<0.01). n.s. non-significant.

Finally, we analysed the diurnal pattern with the percentage of physical activity and the percentage of feed intake in the dark phase. Both HFpu and HFs mice were more active and consumed more feed during the dark phase in both measurements (p<0.0001 for all 4 comparisons) as expected for nocturnal animals. HFpu and HFs

mice did not differ in the percentage of physical activity or the percentage of feed intake in the dark phase, which shows that they have similar diurnal patterns.

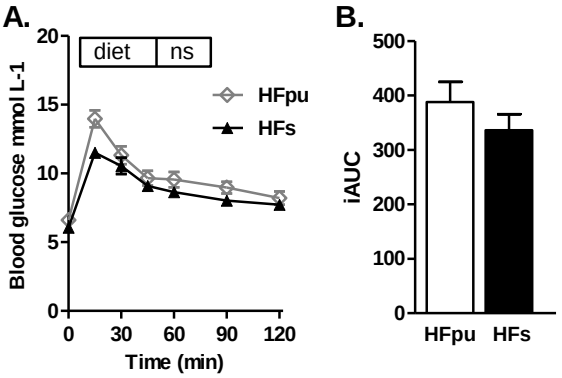

Figure 3 Oral glucose tolerance test after 22 weeks of HF feeding. HFpu and HFs mice were fasted for 5 hours at the start of the light phase, after which mice received glucose via oral gavage and blood glucose levels were monitored for the 2 hours afterwards (A), and expressed as iAUC (B).

Assessment of metabolic flexibility

One of the major aims of this study was to investigate functional implications of changes in health status by assessing metabolic flexibility. The first test that we used was a standardized OGTT. The two isocaloric HF diets showed a comparable glucose tolerance after 22 weeks of feeding (Figures 3A and B).

Metabolic flexibility was also assessed with a fasting and re-feeding test. HFpu and HFs mice had low RER values when fasted, which indicates preferential whole body fat oxidation. During re-feeding, RER increased, which indicates a combination of both fat and carbohydrate oxidation on whole body level (fig. 4A). HFpu and HFs mice did not differ in mean RER during fasting (from 23.00h to 6.00h) or when they were in a fasted state (from 6.00h to 14.00h). During re-feeding (from 14.00h to 22.00h), however, HFpu mice showed a significantly larger increase in RER compared to HFs mice. Furthermore, the average RER over the complete period of re-feeding (fig. 4B) and maximal RER-value during re-feeding (fig. 4C) of HFpu mice matched the food quotient of the HFpu diet, which indicated that HFpu mice effectively alter their metabolism to use the nutrients that are available in the diet. In contrast, HFs mice did not increase RER levels above 0.815, which is significantly lower to the levels that were obtained in HFpu mice and is remarkably lower than the food quotient of the HFs diet. The reduction in the response to re-feeding in HFs mice indicates a reduction in metabolic flexibility. During re-feeding, mice had *ad libitum* access to feed, during which HFpu and HFs mice consumed a similar amount of feed (fig. 4C).

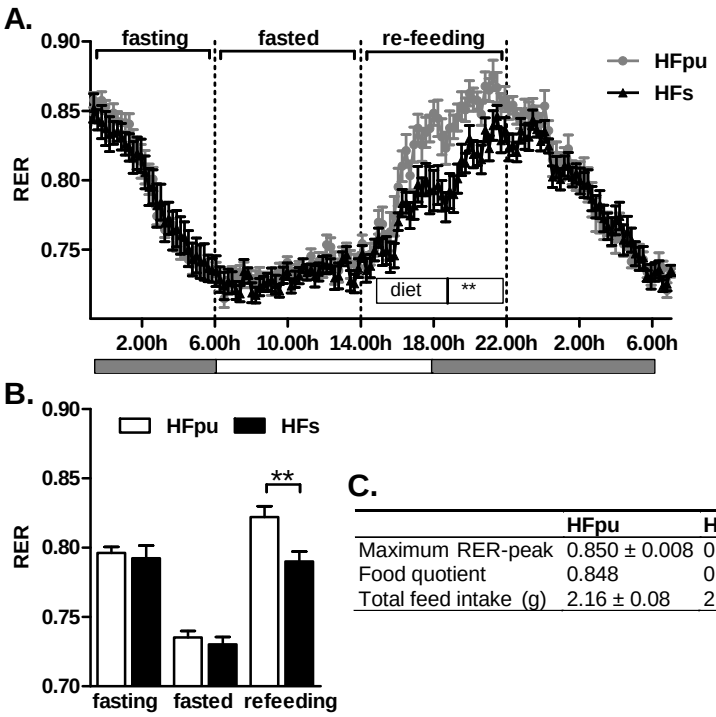

C.

	HFpu	HFs
Maximum RER-peak	0.850 ± 0.008	0.815 ± 0.009 **
Food quotient	0.848	0.844
Total feed intake (g)	2.16 ± 0.08	2.02 ± 0.13

Figure 4 RER during the fasting and re-feeding challenge after 25 weeks of HF feeding. HFpu and HFs mice were fasted and regained *ad libitum* access to their feed at 14.00h while RER was monitored continuously (A, the grey bar below the figure indicates the dark phase). RER values of individual mice were averaged when mice were fasting (from 23.00h to 6.00h), when mice were in a fasted state (from 6.00h to 14.00h) and during re-feeding (from 14.00h to 22.00h) (B). The table (C) summarises the maximal RER-value during re-feeding based on three consecutive measures, the food quotients of the diets, and the feed intake during the 8 hours of re-feeding. ** P< 0.01 HFs mice vs. HFpu mice.

Finally, metabolic flexibility was assessed using an exposure to OxR. HFpu and HFs mice did not differ in RER under normoxic conditions (fig. 5A). Exposure to OxR increased RER in HFpu mice compared to HFs mice (fig. 5B and C), which translates to an increase in the percentage of energy from full glucose oxidation (fig. 5D). An increase in glucose oxidation is considered advantageous during OxR since the oxidation of one mole of glucose requires less oxygen compared to the oxidation of one mole of fat. Furthermore, an increase in glucose oxidation can prevent the increase in blood glucose levels that is often seen during OxR (15). HFs mice seemed less flexible, based on the absence of a response to the reduction in oxygen availability. The analysis of blood glucose levels before and after exposure to OxR revealed a (statistical) interaction between the diet (HFpu and HFs) and oxygen level (OxR and normoxia) because HFpu and HFs responded differently to the exposure. Bonferroni post-hoc analysis revealed that HFs mice had higher blood glucose levels during OxR compared to HFpu mice (fig. 5E).

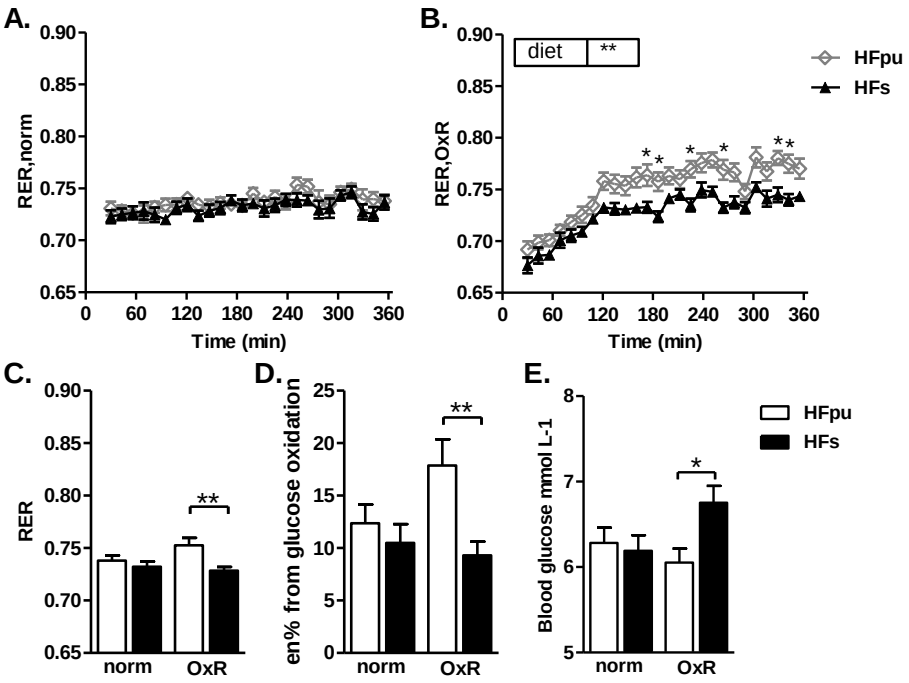

Figure 5 RER during the OxR challenge after 25 weeks of HF feeding. HFpu and HFs mice were fasted and exposed to normal air (A; 20.8% O_2) or to oxygen restriction (B; 12.0% O_2) for 6 hours. Asterisks (in B) indicate the individual time points at which the 2-way ANOVA post-hoc analysis revealed significant differences between HFpu and HFs mice. RER values of individual mice were averaged during the 6 hours in normal or hypoxic air (C) and used to estimate the percentage of energy from glucose oxidation (D). Blood glucose was measured directly after the exposure to OxR or normal air (E). * P<0.05 and ** P< 0.01 HFs mice vs. HFpu mice.

Discussion

We examined the effects of two isocaloric high-fat diets differing in fatty acid composition, but similar n6/n3 ratio, on metabolic flexibility and on different markers of metabolic health in adult male mice. The HFpu diet contained predominantly PUFAs, while the HFs diet mainly contained SFAs, supposedly being unhealthier. Unexpectedly, most biomarkers, including body weight, adiposity, WAT health, serum glucose, insulin and adipokine levels, and glucose tolerance did not differ between the two dietary groups. HFs mice, however, had bigger adipocytes, higher triacylglycerol levels in liver and skeletal muscle, higher serum alanine transaminase and aspartate transaminase levels, and a reduced physical activity level. Despite these relatively small phenotypical changes, HFs mice were less flexible in the response to the fasting and re-feeding challenge and the OxR challenge, which indicates a reduction in metabolic flexibility.

The ratio of n-6 to n-3 PUFAs might account for the small phenotypical differences between HFpu and HFs mice

The HFpu and HFs diets primarily differ in the amount of long chain SFAs (5.4% in HFpu vs. 19.3% in HFs) and PUFAs (21.9% in HFpu vs. 4.2% in HFs). Excessive consumption of saturated fat leads to WAT expansion, WAT inflammation and inhibition of glucose and fat oxidation (reviewed by 40). Long chain SFAs (C14-C18), compared to medium chain SFAs (C6-C12), further increase weight gain and fat-mass gain (21, 48). n-3 PUFAs, on the other hand, reduce weight gain (24), protect against cardiovascular diseases (12) and reduce inflammatory proteins (38). These effects seem to contrast our results. However, differences in weight gain, WAT inflammation, or adiposity are not always reported in studies in which the amount of SFAs is increased compared to other (unsaturated) fatty acids (19, 21, 43, 65). Moreover, studies in which the amount of n-3 PUFAs is increased compared to other (saturated or n-6) FAs do not always show improvements in body weight, liver lipids or inflammatory cytokines (1, 7, 25, 77). One explanation for the absence of major differences in the studied markers for metabolic health between HFpu and HFs mice may be that both diets have a similar n6/n3 PUFA ratio. It has been proposed that health effects of HF diets primarily depend on this ratio (59). A ten-fold increase in the n6/n3 ratio in isocaloric high-fat diets with similar SFA content, for example, increased hepatic lipid storage, even though feed intake was significantly higher in the low n6/n3 group (54). It was also shown that a 4-fold increase in the amount of SFAs did not increase body weight, WAT inflammation or adipocyte size when the n6/n3 ratio was kept equal between diets (21). However, there are also studies that show that the n6/n3 ratio does not influence body weight (76) or lipid peroxidation in liver (14), and it was suggested that the absolute mass of essential fatty acids, rather than the n6/n3 ratio, determines long-term health effects of a diet (75). Our study however, shows that body weight gain and WAT health are equally affected as long as the dietary n6/n3 ratio is kept similar.

The HFs diet and HFpu diet differently affect lipid storage in WAT, muscle and liver

After 27 weeks of high-fat feeding, HFs mice had bigger adipocytes and more ectopic lipid storage in muscle and liver than HFpu mice, which suggests that the type of dietary fat affects the allocation of fat storage. Adipocyte hypertrophy is known to indicate a reduced capacity to initiate hyperplasia (29). A certain reduction in the formation of new adipocytes increases fat storage in existing adipocytes, leading to further adipocyte enlargement. Large adipocytes are less sensitive to insulin than smaller adipocytes (reviewed by 28) and adipocyte size is positively associated with insulin resistance and Type 2 diabetes in both humans and rodents (56, 74). The failure to recruit new adipocytes does not only increase adipocyte hypertrophy but also increases ectopic fat storage (29). Ectopic fat deposition, or steatosis, can lead to cell dysfunction and cell death (69) and is strongly associated with insulin resistance (46).

n-3 PUFAs are known to prevent both adipocyte hypertrophy and obesity-related adipose remodelling (37), which might explain the increase in adipocyte size, and possibly related ectopic lipid storage, in HFs vs. HFpu mice. The increase in ectopic lipid accumulation in HFs mice might, on the other hand, also result from increased lipid uptake, increased fatty acid synthesis, or reduced fat oxidation in liver and muscle tissue (58), which are also affected by dietary fat composition (18, 43, 47). The dietary fatty acid composition, thus, seems to alter the allocation of fat storage, even though total adiposity remains equal between both groups. The increase in ectopic lipid storage is expected to lead to differences in metabolic health and metabolic flexibility.

The changes in the response to fasting and re-feeding and oxygen restriction in HFs mice indicate impairment of carbohydrate metabolism

Despite the significant changes in adipocyte size and ectopic lipid storage, HFs and HFpu mice did not differ in in their response to the OGTT. The stress response that is induced by oral gavage or blood sampling (63, 67) may potentially have masked any differences in the response. It is, however, more likely that HFs and HFpu mice simply had a similar glucose tolerance, because both diets provide a similar glycaemic load. Next to the OGTT, metabolic flexibility was analysed with two non-invasive tests in the indirect calorimetry system. Under unchallenged conditions, HFpu and HFs mice did not differ in mean diurnal RER; furthermore, diurnal RER values matched the food quotient of the diet consumed, which means that under free-feeding conditions, macronutrient oxidation matches macronutrient availability. Fasting RER values were also similar between HFs and HFpu mice, indicating that mice do not differ in the flexibility to switch to the mobilization and oxidation of stored lipids (26). When mice were, however, challenged to switch from a fasting to a fed state, it became apparent that HFs mice made less efficient use of the carbohydrates in the diet. Also during the challenge with OxR, HFpu mice reached higher RER values than HFs mice, which indicates a higher level of glucose oxidation. The increase in RER during OxR was also observed in low-fat versus high-fat fed mice (15) and was accompanied by a reduction in oxygen consumption in low-fat versus high-fat fed mice. A metabolic switch from fat to glucose oxidation can lead to a small reduction in oxygen consumption (45), which is considered favourable during low-oxygen conditions. Mice that are less flexible, e.g. because of HF-feeding, proved to be less effective in this adaptation (15), which was also seen here in HFs versus HFpu mice. Both indirect calorimetry-based challenge tests, thus, show that HFs mice have a reduced capacity to increase glucose oxidation. The mechanistic background behind this reduction in metabolic flexibility needs further investigation. The type of dietary fat does, unlike the amount of fat (8), not affect intestinal absorption of carbohydrates (53); the difference in diet composition, therefore, does not account for the difference in substrate oxidation after re-feeding. HFs mice might, however, be less flexible because of a reduced mitochondrial capacity to oxidize carbohydrates. Chronic HF feeding is known to disturb β-oxidation, leading to increased

accumulation of β-oxidative intermediates and reduced glucose oxidation: a condition that is referred to as 'mitochondrial overload' (41). Saturated fatty acids are oxidized more slowly than unsaturated fatty acids (10, 39), but it is as yet unclear whether the changes in the rate of oxidation also increase incomplete FA oxidation. Alternatively, HFs mice might be more prone to use glucose for hepatic *de novo* lipogenesis (DNL) instead of using it for mitochondrial oxidation. Hepatic DNL is positively associated with obesity and other metabolic disorders (17), where it increases ectopic lipid storage (13). Furthermore, hepatic DNL was observed as a response to OxR in mice in high-fat fed mice (15).

Conclusions

A diet high in SFAs versus a diet high in PUFAs, but similar n6/n3 ratio, did not affect many parameters of metabolic health in male mice, but led to an increase in mean adipocyte size in eWAT, ectopic lipid accumulation in liver and skeletal muscle, and to liver damage. Both indirect calorimetry-based challenge tests showed that HFs mice were less flexible in the switch from fat to carbohydrate use, which indicates a reduction in metabolic flexibility.

Acknowledgements

The research leading to these results has received funding from the European Union's Seventh Framework Programme FP7 2007-2013 under grant agreement no. 244995 (BIOCLAIMS Project). We would like to thank all members of Human and Animal Physiology for their helpful contributions, especially Inge van der Stelt, Dylan Eikelenboom, Wuhua Ren and Dimitra Mastorakou for their help during the animal experiment and molecular and histological analyses.

References

1. Barcelli UO, Beach DC, Pollak VE The influence of n-6 and n-3 fatty acids on kidney phospholipid composition and on eicosanoid production in aging rats. Lipids. 1988;23: 309-312.
2. Berthiaume N, Zinker BA Metabolic responses in a model of insulin resistance: comparison between oral glucose and meal tolerance tests. Metabolism. 2002;51: 595-598.
3. Black AE, Prentice AM, Coward WA Use of food quotients to predict respiratory quotients for the doubly-labelled water method of measuring energy expenditure. Hum Nutr Clin Nutr. 1986;40: 381-391.
4. Bray GA, Popkin BM Dietary fat intake does affect obesity! Am J Clin Nutr. 1998;68: 1157-1173.
5. Buettner R, Parhofer KG, Woenckhaus M, Wrede CE, Kunz-Schughart LA, Scholmerich J*, et al.* Defining high-fat-diet rat models: metabolic and molecular effects of different fat types. J Mol Endocrinol. 2006;36: 485-501.
6. Cinti S, Mitchell G, Barbatelli G, Murano I, Ceresi E, Faloia E*, et al.* Adipocyte death defines macrophage localization and function in adipose tissue of obese mice and humans. J Lipid Res. 2005;46: 2347-2355.
7. Cintra DE, Costa AV, Peluzio Mdo C, Matta SL, Silva MT, Costa NM Lipid profile of rats fed high-fat diets based on flaxseed, peanut, trout, or chicken skin. Nutrition. 2006;22: 197-205.
8. Collier G, O'Dea K The effect of coingestion of fat on the glucose, insulin, and gastric inhibitory polypeptide responses to carbohydrate and protein. Am J Clin Nutr. 1983;37: 941-944.
9. Constantinides C, Mean R, Janssen BJ Effects of isoflurane anesthesia on the cardiovascular function of the C57BL/6 mouse. ILAR J. 2011;52: e21-31.
10. DeLany JP, Windhauser MM, Champagne CM, Bray GA Differential oxidation of individual dietary fatty acids in humans. Am J Clin Nutr. 2000;72: 905-911.
11. Desaulniers D, Yagminas A, Chu I, Nakai J Effects of anesthetics and terminal procedures on biochemical and hormonal measurements in polychlorinated biphenyl treated rats. Int J Toxicol. 2011;30: 334-347.
12. Djousse L, Pankow JS, Eckfeldt JH, Folsom AR, Hopkins PN, Province MA*, et al.* Relation between dietary linolenic acid and coronary artery disease in the National Heart, Lung, and Blood Institute Family Heart Study. Am J Clin Nutr. 2001;74: 612-619.
13. Donnelly KL, Smith CI, Schwarzenberg SJ, Jessurun J, Boldt MD, Parks EJ Sources of fatty acids stored in liver and secreted via lipoproteins in patients with nonalcoholic fatty liver disease. J Clin Invest. 2005;115: 1343-1351.
14. Du C, Sato A, Watanabe S, Wu CZ, Ikemoto A, Ando K*, et al.* Cholesterol synthesis in mice is suppressed but lipofuscin formation is not affected by long-term feeding of n-3 fatty acid-enriched oils compared with lard and n-6 fatty acid-enriched oils. Biol Pharm Bull. 2003;26: 766-770.
15. Duivenvoorde LP, van Schothorst EM, Derous D, van der Stelt I, Masania J, Rabbani N*, et al.* Oxygen restriction as challenge test reveals early high-fat-diet-induced changes in glucose and lipid metabolism. Pflugers Arch. 2014. doi: 10.1007/s00424-014-1553-8.
16. Duivenvoorde LP, van Schothorst EM, Swarts HJ, Keijer J Assessment of Metabolic Flexibility of Old and Adult Mice Using Three Noninvasive, Indirect Calorimetry-Based Treatments. . J Gerontol A Biol Sci Med Sci. 2014;DOI: 10.1093/gerona/glu1027.
17. Eissing L, Scherer T, Todter K, Knippschild U, Greve JW, Buurman WA*, et al.* De novo lipogenesis in human fat and liver is linked to ChREBP-beta and metabolic health. Nat Commun. 2013;4: 1528.
18. El-Badry AM, Graf R, Clavien PA Omega 3 - Omega 6: What is right for the liver? J Hepatol. 2007;47: 718-725.
19. El Akoum S, Lamontagne V, Cloutier I, Tanguay JF Nature of fatty acids in high fat diets differentially delineates obesity-linked metabolic syndrome components in male and female C57BL/6J mice. Diabetol Metab Syndr. 2011;3: 34.
20. Ellenbroek D, Kressler J, Cowan RE, Burns PA, Mendez AJ, Nash MS Effects of prandial challenge on triglyceridemia, glycemia, and pro-inflammatory activity in persons with chronic paraplegia. J Spinal Cord Med. 2014. doi: 10.1179/2045772314Y.0000000199.
21. Enos RT, Davis JM, Velazquez KT, McClellan JL, Day SD, Carnevale KA*, et al.* Influence of dietary saturated fat content on adiposity, macrophage behavior, inflammation, and metabolism: composition matters. J Lipid Res. 2013;54: 152-163.

22. Fiorini RN, Kirtz J, Periyasamy B, Evans Z, Haines JK, Cheng G*, et al.* Development of an unbiased method for the estimation of liver steatosis. Clin Transplant. 2004;18: 700-706.
23. Flachs P, Rossmeisl M, Kopecky J The effect of n-3 fatty acids on glucose homeostasis and insulin sensitivity. Physiol Res. 2014;63 Suppl 1: S93-S118.
24. Flachs P, Ruhl R, Hensler M, Janovska P, Zouhar P, Kus V*, et al.* Synergistic induction of lipid catabolism and anti-inflammatory lipids in white fat of dietary obese mice in response to calorie restriction and n-3 fatty acids. Diabetologia. 2011;54: 2626-2638.
25. Gaiva MH, Couto RC, Oyama LM, Couto GE, Silveira VL, Ribeiro EB*, et al.* Diets rich in polyunsaturated fatty acids: effect on hepatic metabolism in rats. Nutrition. 2003;19: 144-149.
26. Galgani JE, Moro C, Ravussin E Metabolic flexibility and insulin resistance. Am J Physiol Endocrinol Metab. 2008;295: E1009-1017.
27. Gerich JE, Mitrakou A, Kelley D, Mandarino L, Nurjhan N, Reilly J*, et al.* Contribution of impaired muscle glucose clearance to reduced postabsorptive systemic glucose clearance in NIDDM. Diabetes. 1990;39: 211-216.
28. Guilherme A, Virbasius JV, Puri V, Czech MP Adipocyte dysfunctions linking obesity to insulin resistance and type 2 diabetes. Nat Rev Mol Cell Biol. 2008;9: 367-377.
29. Heilbronn L, Smith SR, Ravussin E Failure of fat cell proliferation, mitochondrial function and fat oxidation results in ectopic fat storage, insulin resistance and type II diabetes mellitus. Int J Obes Relat Metab Disord. 2004;28 Suppl 4: S12-21.
30. Hoek-van den Hil EF, Beekmann K, Keijer J, Hollman PC, Rietjens IM, van Schothorst EM Interference of flavonoids with enzymatic assays for the determination of free fatty acid and triglyceride levels. Anal Bioanal Chem. 2012;402: 1389-1392.
31. Hoek-van den Hil EF, Keijer J, Bunschoten A, Vervoort JJ, Stankova B, Bekkenkamp M*, et al.* Quercetin induces hepatic lipid omega-oxidation and lowers serum lipid levels in mice. PLoS One. 2013;8: e51588.
32. Hoevenaars FP, Bekkenkamp-Grovenstein M, Janssen RJ, Heil SG, Bunschoten A, Hoek-van den Hil EF*, et al.* Thermoneutrality results in prominent diet-induced body weight differences in C57BL/6J mice, not paralleled by diet-induced metabolic differences. Mol Nutr Food Res. 2014;58: 799-807.
33. Hoevenaars FP, Keijer J, Herreman L, Palm I, Hegeman MA, Swarts HJ*, et al.* Adipose tissue metabolism and inflammation are differently affected by weight loss in obese mice due to either a high-fat diet restriction or change to a low-fat diet. Genes Nutr. 2014;9: 391.
34. Hoevenaars FP, Keijer J, Swarts HJ, Snaas-Alders S, Bekkenkamp-Grovenstein M, van Schothorst EM Effects of dietary history on energy metabolism and physiological parameters in C57BL/6J mice. Exp Physiol. 2013;98: 1053-1062.
35. Hoevenaars FP, van Schothorst EM, Horakova O, Voigt A, Rossmeisl M, Pico C*, et al.* BIOCLAIMS standard diet (BIOsd): a reference diet for nutritional physiology. Genes Nutr. 2012;7: 399-404.
36. Horakova O, Medrikova D, van Schothorst EM, Bunschoten A, Flachs P, Kus V*, et al.* Preservation of metabolic flexibility in skeletal muscle by a combined use of n-3 PUFA and rosiglitazone in dietary obese mice. PLoS One. 2012;7: e43764.
37. Huber J, Loffler M, Bilban M, Reimers M, Kadl A, Todoric J*, et al.* Prevention of high-fat diet-induced adipose tissue remodeling in obese diabetic mice by n-3 polyunsaturated fatty acids. Int J Obes (Lond). 2007;31: 1004-1013.
38. James MJ, Gibson RA, Cleland LG Dietary polyunsaturated fatty acids and inflammatory mediator production. Am J Clin Nutr. 2000;71: 343S-348S.
39. Jones PJ, Pencharz PB, Clandinin MT Whole body oxidation of dietary fatty acids: implications for energy utilization. Am J Clin Nutr. 1985;42: 769-777.
40. Kennedy A, Martinez K, Chuang CC, LaPoint K, McIntosh M Saturated fatty acid-mediated inflammation and insulin resistance in adipose tissue: mechanisms of action and implications. J Nutr. 2009;139: 1-4.
41. Koves TR, Ussher JR, Noland RC, Slentz D, Mosedale M, Ilkayeva O*, et al.* Mitochondrial overload and incomplete fatty acid oxidation contribute to skeletal muscle insulin resistance. Cell Metab. 2008;7: 45-56.
42. Lagouge M, Argmann C, Gerhart-Hines Z, Meziane H, Lerin C, Daussin F*, et al.* Resveratrol improves mitochondrial function and protects against metabolic disease by activating SIRT1 and PGC-1alpha. Cell. 2006;127: 1109-1122.

43. Lee JS, Pinnamaneni SK, Eo SJ, Cho IH, Pyo JH, Kim CK, *et al.* Saturated, but not n-6 polyunsaturated, fatty acids induce insulin resistance: role of intramuscular accumulation of lipid metabolites. J Appl Physiol (1985). 2006;100: 1467-1474.
44. Lee JY, Zhao L, Hwang DH Modulation of pattern recognition receptor-mediated inflammation and risk of chronic diseases by dietary fatty acids. Nutr Rev. 2010;68: 38-61.
45. Livesey G, Elia M Estimation of energy expenditure, net carbohydrate utilization, and net fat oxidation and synthesis by indirect calorimetry: evaluation of errors with special reference to the detailed composition of fuels. Am J Clin Nutr. 1988;47: 608-628.
46. Monetti M, Levin MC, Watt MJ, Sajan MP, Marmor S, Hubbard BK, *et al.* Dissociation of hepatic steatosis and insulin resistance in mice overexpressing DGAT in the liver. Cell Metab. 2007;6: 69-78.
47. Montell E, Turini M, Marotta M, Roberts M, Noe V, Ciudad CJ, *et al.* DAG accumulation from saturated fatty acids desensitizes insulin stimulation of glucose uptake in muscle cells. Am J Physiol Endocrinol Metab. 2001;280: E229-237.
48. Nagao K, Yanagita T Medium-chain fatty acids: functional lipids for the prevention and treatment of the metabolic syndrome. Pharmacol Res. 2010;61: 208-212.
49. Naggert J, Svenson KL, Smith RV, Paigen B, Peters LL Diet effects on bone mineral density and content, body composition, and plasma glucose, leptin, and insulin levels in 43 inbred strains of mice on a high-fat atherogenic diet. MPD:Naggert1. Mouse Phenome Database web site, The Jackson Laboratory, Bar Harbor, Maine USA. http://phenome.jax.org [Cited 23 Jan, 2015].
50. NationalResearchCouncil. Nutrient Requirements of Laboratory Animals Fourth Revised Edition, 1995 Washington, DC: The National Academies Press; 1995.
51. Nuernberg K, Breier BH, Jayasinghe SN, Bergmann H, Thompson N, Nuernberg G, *et al.* Metabolic responses to high-fat diets rich in n-3 or n-6 long-chain polyunsaturated fatty acids in mice selected for either high body weight or leanness explain different health outcomes. Nutr Metab (Lond). 2011;8: 56.
52. Peronnet F, Massicotte D Table of nonprotein respiratory quotient: an update. Can J Sport Sci. 1991;16: 23-29.
53. Radulescu A, Hassan Y, Gannon MC, Nuttall FQ The degree of saturation of fatty acids in dietary fats does not affect the metabolic response to ingested carbohydrate. J Am Coll Nutr. 2009;28: 286-295.
54. Riediger ND, Othman R, Fitz E, Pierce GN, Suh M, Moghadasian MH Low n-6:n-3 fatty acid ratio, with fish- or flaxseed oil, in a high fat diet improves plasma lipids and beneficially alters tissue fatty acid composition in mice. Eur J Nutr. 2008;47: 153-160.
55. Salans LB, Knittle JL, Hirsch J The role of adipose cell size and adipose tissue insulin sensitivity in the carbohydrate intolerance of human obesity. J Clin Invest. 1968;47: 153-165.
56. Schneider BS, Faust IM, Hemmes R, Hirsch J Effects of altered adipose tissue morphology on plasma insulin levels in the rat. Am J Physiol. 1981;240: E358-362.
57. Sherman H, Genzer Y, Cohen R, Chapnik N, Madar Z, Froy O Timed high-fat diet resets circadian metabolism and prevents obesity. FASEB J. 2012;26: 3493-3502.
58. Shulman GI Cellular mechanisms of insulin resistance. J Clin Invest. 2000;106: 171-176.
59. Simopoulos AP The importance of the omega-6/omega-3 fatty acid ratio in cardiovascular disease and other chronic diseases. Exp Biol Med (Maywood). 2008;233: 674-688.
60. St-Onge MP, Ross R, Parsons WD, Jones PJ Medium-chain triglycerides increase energy expenditure and decrease adiposity in overweight men. Obesity Research. 2003;11: 395-402.
61. Storlien L, Oakes ND, Kelley DE Metabolic flexibility. Proceedings of the Nutrition Society. 2004;63: 363-368.
62. Storlien L, Oakes ND, Kelley DE Metabolic flexibility. Proc Nutr Soc. 2004;63: 363-368.
63. Tabata H, Kitamura T, Nagamatsu N Comparison of effects of restraint, cage transportation, anaesthesia and repeated bleeding on plasma glucose levels between mice and rats. Lab Anim. 1998;32: 143-148.
64. Tiret L, Gerdes C, Murphy MJ, Dallongeville J, Nicaud V, O'Reilly DS, *et al.* Postprandial response to a fat tolerance test in young adults with a paternal history of premature coronary heart disease - the EARS II study (European Atherosclerosis Research Study). Eur J Clin Invest. 2000;30: 578-585.
65. Todoric J, Loffler M, Huber J, Bilban M, Reimers M, Kadl A, *et al.* Adipose tissue inflammation induced by high-fat diet in obese diabetic mice is prevented by n-3 polyunsaturated fatty acids. Diabetologia. 2006;49: 2109-2119.

66. Tsukumo DM, Carvalho-Filho MA, Carvalheira JB, Prada PO, Hirabara SM, Schenka AA*, et al.* Loss-of-function mutation in Toll-like receptor 4 prevents diet-induced obesity and insulin resistance. Diabetes. 2007;56: 1986-1998.
67. Tuli JS, Smith JA, Morton DB Corticosterone, adrenal and spleen weight in mice after tail bleeding, and its effect on nearby animals. Lab Anim. 1995;29: 90-95.
68. U.S. Department of Agriculture ARS USDA National Nutrient Database for Standard Reference. 2013;Release 26: Nutrient Data Laboratory Home Page, http://www.ars.usda.gov/ba/bhnrc/ndl
69. Unger RH, Orci L Diseases of liporegulation: new perspective on obesity and related disorders. FASEB J. 2001;15: 312-321.
70. van Ommen B, Keijer J, Heil SG, Kaput J Challenging homeostasis to define biomarkers for nutrition related health. Mol Nutr Food Res. 2009;53: 795-804.
71. Voigt A, Agnew K, van Schothorst EM, Keijer J, Klaus S Short-term, high fat feeding-induced changes in white adipose tissue gene expression are highly predictive for long-term changes. Mol Nutr Food Res. 2013;57: 1423-1434.
72. Wang S, Wu D, Matthan NR, Lamon-Fava S, Lecker JL, Lichtenstein AH Reduction in dietary omega-6 polyunsaturated fatty acids: eicosapentaenoic acid plus docosahexaenoic acid ratio minimizes atherosclerotic lesion formation and inflammatory response in the LDL receptor nuII mouse. Atherosclerosis. 2009;204: 147-155.
73. Wein S, Wolffram S, Schrezenmeir J, Gasperikova D, Klimes I, Sebokova E Medium-chain fatty acids ameliorate insulin resistance caused by high-fat diets in rats. Diabetes Metab Res Rev. 2009;25: 185-194.
74. Weyer C, Foley JE, Bogardus C, Tataranni PA, Pratley RE Enlarged subcutaneous abdominal adipocyte size, but not obesity itself, predicts type II diabetes independent of insulin resistance. Diabetologia. 2000;43: 1498-1506.
75. Wijendran V, Hayes KC Dietary n-6 and n-3 fatty acid balance and cardiovascular health. Annu Rev Nutr. 2004;24: 597-615.
76. Yamashita T, Oda E, Sano T, Ijiru Y, Giddings JC, Yamamoto J Varying the ratio of dietary n-6/n-3 polyunsaturated fatty acid alters the tendency to thrombosis and progress of atherosclerosis in apoE-/- LDLR-/- double knockout mouse. Thromb Res. 2005;116: 393-401.
77. Yin H, Liu W, Goleniewska K, Porter NA, Morrow JD, Peebles RS, Jr. Dietary supplementation of omega-3 fatty acid-containing fish oil suppresses F2-isoprostanes but enhances inflammatory cytokine response in a mouse model of ovalbumin-induced allergic lung inflammation. Free Radic Biol Med. 2009;47: 622-628.

Supplemental figure

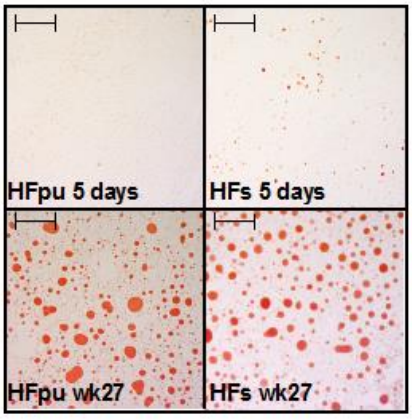

Supplemental figure 1 Hepatic lipid droplets after 5 days and 27 weeks of HF feeding. Representative images of the Oil-red-O stainings in liver after 5 days and 27 weeks of HFpu or HFs feeding. Pictures were used to visualise the extent of hepatic steatosis at the end of the study. The bar in each picture represents a distance of 100 µm.

Methodology:
Liver tissue was immediately frozen after dissection, after which part of the left lobe was removed and sectioned at 7 µm with a cryostat (Leica Microsystems, Nussloch GmbH, Germany). Sections were made in four equally distant (distance: 56 µm) parts of the left lobe to achieve representative sections. Sections were, then, left at room temperature for 30 minutes and were fixed in 3.7% buffered formalin and stained with Oil-red-O (Sigma-Aldrich, St Louis, MO, USA) as published (22) and with modifications as described (31). Oil-red-O stainings were performed for 3 mice per group (randomly selected).

Chapter 6

Metabolic adaptation of white adipose tissue to acute short-term oxygen restriction in mice

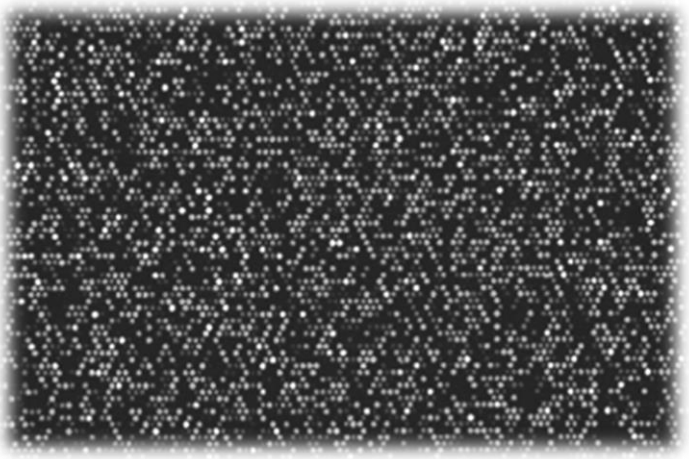

Loes P.M. Duivenvoorde, Evert M. van Schothorst, Ondrej Kuda, Martina Cerna, Inge van der Stelt, Elise Hoek-van den Hil, Dimitra Mastorakou, Jan Kopecky and Jaap Keijer

Submitted for publication.

Abstract

Oxygen availability can be limited during expansion of white adipose tissue (WAT) in obesity. Little is known on the adaptation of WAT to mild oxygen restriction (OxR). Therefore, we studied metabolic adaptation to acute OxR in fasted, diet-induced moderately obese mice that were exposed to mild hypoxic (12% O_2) or normoxic (20.9% O_2) conditions for 6 hours.

Adaptation to OxR was assessed by determination of amino acid and (acyl)carnitine levels in serum and in WAT, and by whole genome gene expression analysis of WAT. Adaptation was also assessed during OxR with indirect calorimetry.

We found that OxR reduced mitochondrial oxidation at whole-body level, as shown by a reduction in whole-body oxygen consumption and an increase in serum long-chain acylcarnitine levels. WAT did not seem to contribute to this serum profile since only short-chain acylcarnitines were increased in WAT and gene expression analysis indicated an increase in mitochondrial oxidation, based on coordinate down-regulation of *Sirt4*, *Gpam* and *Chchd3/Minos3*. In addition, OxR did not induce oxidative stress in WAT, but increased molecular pathways involved in cell growth and proliferation. OxR increased levels of the amino acids tyrosine, lysine, and ornithine in serum, and of leucine/isoleucine in WAT.

This study shows that OxR limits oxidative phosphorylation at whole-body level, but in WAT compensatory mechanisms seem to operate. The down-regulation of the mitochondria-related genes *Sirt4*, *Gpam,* and *Chchd3* may be considered as a biomarker profile for WAT mitochondrial reprogramming in response to acute exposure to limited oxygen availability.

Introduction

Oxygen restriction (OxR) was recently introduced as a challenge test to investigate metabolic flexibility in mice (11, 12) and is based on short-term exposure to ambient hypoxia. OxR reduces whole-body oxygen consumption and increases serum glucose and lactate levels in rodents (11, 12, 31). *In vitro* studies consistently show that, when cells are exposed to hypoxic air, the level of anaerobic glycolysis increases (reviewed by 41), leading to increased lactate formation and reduced cellular oxygen consumption (34). The metabolic response to mild ambient hypoxia ($[O_2]$=12%) *in vivo*, as applied in the OxR challenge, however, depends on the metabolic flexibility of the body as a whole. Each organ reacts in a specific way that matches the oxygen demand, functional capacity and metabolic function of the organ. The liver, for example, decreases sterol metabolism to spare oxygen and increases gluconeogenesis to clear lactate from circulation (4, 9, 11). The heart responds to chronic hypoxia by increasing cardiac hypertrophy and stroke volume (13). Not much is known about the adaptation of white adipose tissue (WAT) to OxR, even though WAT plays a major role in the maintenance of metabolic health and is known to be the primary organ that is sensitive to tissue hypoxia in obesity (35). Knowledge on the metabolic response of WAT to short term OxR will contribute to understanding its role in metabolic flexibility and in the interpretation of WAT focused metabolic flexibility assessment. The only study that, to our knowledge, investigated the effect of OxR on energy metabolism in WAT *in vivo* used a chronic exposure to OxR in lean mice (45), assessing long term metabolic adaptation, rather than a short term exposure as applied here, where the primary response is assessed. Also, the effect of short-term OxR on mitochondrial function in WAT *in vivo* remains largely unknown, whereas these organelles are expected to be essential for metabolic adaptation to OxR considering their role in energy production and their reliance on oxygen availability. *In vitro* studies, indeed, show that mitochondrial function is inhibited during acute hypoxic exposure, leading to a reduction in oxygen consumption and to cell death (34). Furthermore, it was shown that acute hypoxia *in vivo*, as for example seen in perinatal hypoxia, causes an increase in circulating acylcarnitines, whereas free carnitine (or L-carnitine) levels decrease (2, 3, 42). Free carnitines are essential cofactors for mitochondrial transport and mitochondrial fatty acid (FA) oxidation, whereas acylcarnitines are intermediates of FA oxidation. High plasma levels of acylcarnitines indicate incomplete FA oxidation (24, 25, 32), which indicates that OxR also affects mitochondrial function *in vivo*.

Here, we determined the effect of acute, normobaric OxR on whole body energy metabolism and aimed to elucidate the role of WAT in the response to OxR. In this study, we used moderately obese mice that were fed a semi-purified high-fat diet that mainly contains unsaturated fatty acids to induce WAT expansion without increased WAT inflammation (43). The metabolic response to OxR at whole body level was assessed by determination of oxygen consumption and respiratory exchange ratio

(RER) using indirect calorimetry (InCa) and by determination of blood glucose and serum adiponectin levels. Liquid chromatography–mass spectrometry was used to analyse free carnitine, acylcarnitines and amino acids levels in both serum and WAT. Finally, we employed whole-genome gene expression analysis of WAT and measured tissue lactate levels and aconitase functionality.

Materials and methods

Animals and experimental manipulations

The experimental protocol for animal handling was approved by the Animal Welfare Committee of Wageningen University, Wageningen, The Netherlands (DEC2012088). Twenty-four male C57BL/6JOlaHsd mice were used for this study (Harlan Laboratories, Horst, The Netherlands). Mice arrived at 10 weeks of age and were individually housed and maintained under environmentally controlled conditions (21 ± 1ºC, 12 h/12 h light–dark cycle, 50 ± 10% humidity) and had *ad libitum* access to feed and water. During the first three weeks of the study, mice could adapt to the new environment and received the purified low-fat BIOCLAIMS standard diet, which contains 10% energy from fat (19). Thereafter, mice received the purified BIOCLAIMS high-fat diet, which contains 40% energy from fat (11, 48) for the remaining 6 weeks of the study. Body weight and body composition - by using an EchoMRI Whole Body Composition Analyser (EchoMRI, Houston, FL, USA) - were monitored on a weekly basis. At the end of the study, mice were randomly allocated to the oxygen restriction (OxR mice) or the normoxia (Norm mice) treatment (12 mice per group). Mice were directly sacrificed after the exposure to OxR or normoxic air by decapitation to prevent effects of anaesthesia on metabolic parameters (5, 8), after which blood was collected in Mini collect serum tubes (Greiner Bio-one, Longwood, FL, USA). Glucose concentration was measured in whole blood with a Freestyle blood glucose system (Abbott Diabetes Care, Hoofddorp, the Netherlands) according to the manufacturer's instructions. After blood collection, the left epididymal WAT (eWAT) depot was dissected, snap frozen in liquid nitrogen and stored at –80 °C. Serum tubes were centrifuged for 10 minutes at 3000 g and 4°C to obtain serum, which was aliquoted and stored at -80°C.

Indirect calorimetry during OxR or normal air

Indirect calorimetry (TSE Systems, Bad Homburg, Germany) during oxygen restriction was performed as described (11, 12). In short, mice could adapt to the InCa system for 24 hours, all feed was removed at start of the dark phase and mice received a restricted amount of feed (1.5 gram) to ensure a fasting state at the start of the following light phase. One hour after start of the light phase, oxygen concentration in each animal cage was decreased from 20.9% to 12% (for OxR mice) and VO_2 and VCO_2 were recorded every thirteen minutes for the following 6 hours. Norm mice were treated in the same manner, but remained under normoxic conditions.

Serum and tissue analyses

Serum adiponectin levels were determined with the Bio-Plex Pro Mouse Diabetes Assay (Bio-Rad, Veenendaal, The Netherlands), according to the instructions of the manufacturer, with the Bio-Plex 200 system (Bio-Rad). Serum and WAT acylcarnitine and amino acid levels were determined with ultra high performance liquid chromatography–mass spectrometry (UltiMate3000 RSLC, Thermo Scientific, Sunnyvale, CA, USA; QTRAP 5500, AB-Sciex, Framingham, MA, USA) according to a published method (36). Acylcarnitines and amino acids were separated with a HILIC Kinetex column, 50x2.1 mm, 1.7 µm (Phenomenex Inc., Ca, USA) at 25°C using gradient elution: eluent A, 90/10 (v/v) acetonitrile/buffer; eluent B, 90/10 (v/v) water/buffer; ammonium formate (20 mM, pH 4.0) as the buffer. Elution began with 100% eluent B at a flow rate of 0.5 mL/min, decreased to 25% A in 8.5 minutes, returned to 100% D in 0.5 min and stayed at 100% D for 0.5 minutes. The total run time was 9.5 min. Metabolites were identified by multiple reaction monitoring. Serum and WAT samples were treated with methanol and 0.1% formic acid and an internal standard with labeled amino acids and acylcarnitines (Chromsystems Instruments and Chemicals GmbH, Gräfelfing, Germany) was added to each sample. The concentration of individual metabolites was calculated with the peak area of the metabolite of interest and the peak area of the corresponding internal standard. The amino acids leucine and isoleucine are detected together within one peak.

The aconitase activity level is a marker for oxidative stress (14), and was measured as described (40). Briefly, WAT samples were ground in liquid nitrogen and homogenized in Tris-HCl (50 mM, pH 7.4) buffer with a digital ultrasonic sonifier (Branson Ultrasonic Corporation, Danbury, CT, USA). WAT citrate synthase activity and lactate levels were measured with the Citrate Synthase Assay Kit (Sigma Aldrich) and Lactate Assay Kit II (Biovision, Mountain View, USA), respectively, according to the manufacturer's instructions and as published (12). To assure similar sample input for the aconitase, lactate, and citrate synthase assays, samples were diluted to the same total protein concentration, as determined with the RC DC protein assay (Biorad) using Bovine Serum Albumin Fraction V dilutions (Roche Diagnostics GmbH, Mannheim, Germany) as standard.

RNA isolation and micro array hybridization

Total RNA was isolated from eWAT using TRIzol reagent, chloroform, and isoamyl alcohol (PCI) (Invitrogen, Breda, The Netherlands) as described (46) followed by purification with RNeasy columns (Qiagen, Venlo, The Netherlands) using the instructions of the manufacturer. RNA concentration and purity were measured using the Nanodrop (IsoGen Life Science, Maarssen,The Netherlands) and the Experion automated electrophoresis system (Bio-Rad). For global transcriptome analysis, 8 × 60 K Agilent whole-mouse genome microarrays (G4852A, Agilent Technologies Inc.,

Santa Clara, CA, USA) were used according to the manufacturer's protocol with a few modifications as described previously (17). All arrays are deposited in GEO under number GSE64238. Two arrays from the OxR group were, based on their aberrant MA plots, excluded for further analysis. In total, 33,845 of the 59,305 probes on the array had a fluorescent signal twice above the background signal and were statistically analysed.

Statistics

Data are expressed as mean ± SEM. All analyses are based on the data of 12 Norm mice and 12 OxR mice; except for the measurement of physical activity, which is based on 8 random selected mice per experimental group. Gene expression data is based on 12 Norm mice and 10 OxR mice. Statistical analyses were performed using GraphPad Prism version 5.04 (Graphpad, San Diego, CA, USA). Statistical analyses of gene expression data were performed using GeneMaths XT version 2.12 (Applied Maths, Inc. Austin, TX, USA). Data were checked for normality using the D'Agostino and Pearson omnibus normality test. All data that were normally distributed were analysed by independent Students' *t*-tests. Test results that were not normally distributed were analysed with a Mann-Whitney test (the case for free carnitine, C5, C5-1 and C5DC acylcarnitines in WAT). P-values smaller than 0.05 were considered to be statistically significant.

Results

Effects of OxR on whole body level

Mice from the OxR and Norm group did not significantly differ in body weight or body composition prior to the exposure (Norm mice: BW 33.2 ± 1.11 g, total fat mass 9.35 ± 0.83 g, lean mass 22.34 ± 0.36 g; OxR mice: BW 34.2 ± 0.80 g, total fat mass 10.40 ± 0.54 g, lean mass 22.42 ± 0.24 g). The response to OxR was continuously monitored during the exposure to OxR or normoxic air with the InCa system. Average oxygen consumption (fig. 1A) and energy expenditure (fig. 1B) were significantly lower during the six hour exposure to OxR indicating an immediate reduction in metabolic rate. Average RER (fig. 1C), representing substrate usage, was marginally decreased by OxR, whereas no statistical significant differences were seen in physical activity (fig. 1D).

Blood glucose (fig. 2A) and serum adiponectin levels (fig. 2B), and serum free carnitine, acylcarnitine, and amino acid levels (table 1) were measured directly after the exposure to OxR or normoxic air. Blood glucose levels significantly increased by the exposure to OxR, whereas adiponectin levels remained unaffected. In serum, 18 of the 53 metabolites that could be detected were significantly altered by OxR (for the complete list of measured metabolites in serum, see supplemental table 1). OxR decreased levels of free carnitine, did not alter any of the short-chain acylcarnitines (C4-C8), but

stably increased the level of several medium-chain (C10-C14) and long-chain (C16-C20) acylcarnitines in serum. OxR also increased the serum level of the amino acids tyrosine, lysine, and ornithine.

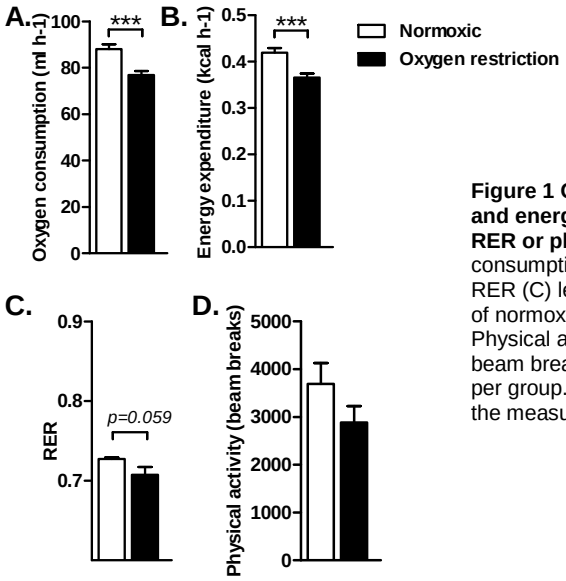

Figure 1 OxR decreases oxygen consumption and energy expenditure but does not alter RER or physical activity. Whole body oxygen consumption (A), energy expenditure (B), and RER (C) levels were averaged over the 6 hours of normoxia or OxR in 12 mice per group. Physical activity (D) was determined as total beam break during OxR or normoxia in 8 mice per group. Mice remained in a fasted state during the measurements. ***P < 0.001

Effects of OxR in WAT

The effect of OxR on energy metabolism in WAT was, at first, studied by the determination of lactate and aconitase activity levels in WAT. The presence of lactate indicates increased anaerobic metabolism; WAT lactate levels were not altered by the exposure to OxR (fig. 2C). Decreased aconitase activity levels indicate increased oxidative stress (18). We also measured citrate synthase activity in WAT, as a marker for mitochondrial density. Changes in the level of mitochondrial density would interfere with the measurement of aconitase activity. We found that OxR did not alter mitochondrial density, as assessed by citrate synthase activity (fig. 2D), or ROS production, as assessed by aconitase activity (fig. 2E).

Second, we measured the influence of OxR on (acyl)carnitine and amino acid levels in WAT (table 1). We found that 7 of the 59 metabolites that could be detected were significantly altered by OxR (for the complete list of measured metabolites in WAT, see supplemental table 1). OxR increased free carnitine levels, did not alter any of the long- or medium-chain acylcarnitines, but increased the levels of several short-chain acylcarnitines. OxR also increased the level of the amino acids leucine and isoleucine.

We also studied the influence of OxR on WAT whole genome gene expression, to gain insight into the molecular background of the observed changes in WAT metabolism. We found that 82 micro-array probes were significantly regulated ($p<0.01$) by OxR. These 82 probes correspond to 78 unique genes that were categorised by function

(table 2). Forty-five of those genes had a known function (additional information of the genes with a known function can be found in supplemental table 2). The majority of those 45 genes is involved in cell growth and survival and most genes are regulated in the direction to stimulate cell proliferation and inhibit apoptosis.

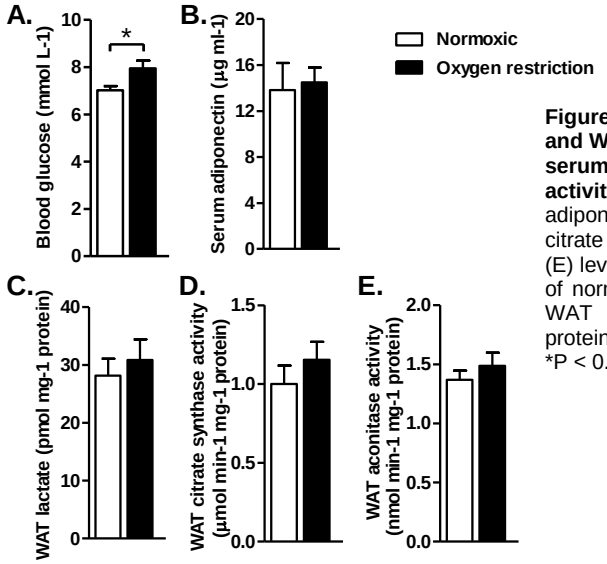

Figure 2 OxR increases blood glucose and WAT lactate levels but does not alter serum adiponectin or WAT aconitase activity. Blood glucose levels (A), serum adiponectin (B), WAT lactate (C) and WAT citrate synthase (D) and aconitase activity (E) levels were determined after the 6 hours of normoxia or OxR in 12 mice per group. WAT measurements were corrected for protein content of the tissue homogenate. *P < 0.05

The second class of regulated genes contains genes involved in transcription and translation, a process that is closely related to cell growth and survival. Consistently, most genes in the second class are regulated in the direction to stimulate transcription and translation. Zooming in on genes annotated to mitochondria, three genes were identified: Sirtuin 4 (*Sirt4*), glycerol-3-phosphate acyltransferase, mitochondrial (*Gpam*) and coiled-coil-helix-coiled-coil-helix domain containing 3 (*Chchd3/ Minos).*These genes play an important role in the regulation of fatty acid oxidation and mitochondrial structure and were all significantly down regulated by OxR. Since the metabolite analysis revealed an effect of OxR on acyl carnitines and amino acids, expression of genes encoding proteins with central functions in their metabolism were analysed (table 3). However, none of these genes were significantly regulated by OxR.

Finally, we also focussed on genes involved in the response to oxidative damage, which might increase when energy demand does not match oxygen availability. We found no changes in genes involved in antioxidant response (such as superoxide dismutase 1 or 2 or catalase) or genes involved in autophagy (such as general transcription factor 2 (P62) or microtubule-associated protein 1 (LC3)). We found no clear changes in genes involved in ER stress, such as activating transcription factor 6 or protein phosphatase 1 r15a , except for Der1-like domain family 3 (*Derl3*). *Derl3* is involved in the degradation of misfolded glycoproteins and was significantly down regulated by OxR (table 2).

Table 1 Overview of significantly regulated amino acids, acylcarnitines and free carnitine in serum and WAT

Metabolite Name		Fold change	p-value	Fold change	p-value
		SERUM		WAT	
Free carnitine					
C0	free carnitine	-1.26	**0.003**	1.50	**0.012**
Short-chain acylcarnitines					
C3	propionylcarnitine	1.01	0.918	2.25	**0.039**
C4DC	methylmalonylcarnitine	-	-	1.45	**0.045**
C5	methylbutyrylcarnitine	1.04	0.586	2.60	**0.004**
C5-1	methylcrotonylcarnitine	1.24	0.311	15.59	**0.003**
C5DC	glutarylcarnitine	-	-	2.90	**0.004**
Medium-chain acylcarnitines					
C10	decanoylcarnitine	1.36	**0.003**	-1.73	0.197
C10-1	decenoylcarnitine	1.34	**0.008**	-1.11	0.598
C12-1	dodecenoylcarnitine	2.40	**<0.001**	-1.70	0.184
Long-chain acylcarnitines					
C16	palmitoylcarnitine	1.39	**<0.001**	1.13	0.579
C16-1	palmitoleylcarnitine	1.55	**<0.001**	-1.46	0.315
C16-2	hexadecadienoylcarnitine	1.41	**<0.001**	-1.82	0.143
C16DC	dicarboxypalmitoylcarnitine	1.26	**0.003**	1.31	0.087
C18-1	oleylcarnitine	1.35	**<0.001**	-1.07	0.797
C18-1OH	3-hydroxyoleoylcarnitine	1.27	**0.047**	-1.06	0.860
C18-2	linoleylcarnitine	1.47	**<0.001**	-1.25	0.427
C18-2OH	3-hydroxylinoleoylcarnitine	1.76	**0.014**	-1.07	0.821
C18-3	linolenoylcarnitine	1.41	**0.003**	-1.29	0.444
C20-3	eicosatrienoylcarnitine	1.52	**0.002**	-1.07	0.879
C20-4	eicosatetraenoylcarnitine	1.29	**0.023**	-1.10	0.786
Amino acids					
leu + ile	leucine + isoleucine	1.15	0.223	2.06	**0.029**
lys	lysine	1.39	**0.003**	-	-
orn	ornithine	2.54	**0.002**	1.47	0.732
tyr	tyrosine	1.26	**0.036**	1.43	0.18

Data are expressed as the fold change of the level in OxR mice compared with the level in Norm mice. n=12 mice per group.

Table 2 Functional categorization of all 78 genes that were significantly regulated ($p<0.01$) after 6 hours of OxR in WAT

Function	# of genes	Gene symbol (and fold change)
Cell growth & survival	11	*Fam107a* (1.4), *Dusp9* (1.3), *Haus7* (1.2), *Nt5c2* (1.2), *Hbegf* (1.3), *Prdm4* (1.2), *Traf4* (-1.2), *Tchp* (-1.1), *Cdip1* (-1.2), *Rabgap* (-1.2), *Tubgcp4* (-1.2)
Transcription & translation	6	*Med24* (1.2), *Tnks2* (1.2), *Zfp319* (1.2), *Hsf2* (-1.3), *Zfp523* (-1.2), *Hoxb3* (-1.2)
Neuronal plasticity & transport	5	*Synpo* (1.3), *Stau2* (1.3), *Samd14* (1.3), *Kifc2* (-1.2), *Homer1* (-1.2)
Immune response	4	*Retnlg* (1.6), *Gpr65* (1.2), *Podxl2* (1.2), *Trim59* (1.3)
Active and passive transmembrane transport	4	*Clca1* (1.4), *Sec63* (1.2), *Atp2b4* (-1.3), *Vamp1* (-1.2)
Redox homeostasis	3	*Mt1* (1.4), *Hspb7* (1.3), *Pdia5* (1.2)
Mitochondrial function	3	*Gpam* (-1.3), *Chchd3* (-1.2), *Sirt4* (-1.2)
Signal transduction	3	*Ms4a4a* (1.3), *Adrbk2* (-1.2), *Pigc* (-1.2)
Blood pressure & angiogenesis	2	*Ren2* (1.8), *Apold1* (1.3)
Diverse functions	3	*Lhfp* (1.2; lipoma formation), *Derl3* (-1.3; degradation of misfolded ER proteins); *Olfr1466* (-1.2; olfactory receptor)
Unknown function	34	

Fold changes (OxR to Norm) are shown in parentheses behind each gene symbol. Additional information about the significantly regulated genes can be found in supplemental table 2.

Discussion

OxR reduces mitochondrial oxidation at whole body level

OxR significantly decreased oxygen consumption and increased blood glucose levels, which is consistent with previous studies using the OxR challenge (11, 12). The increase in blood glucose levels probably indicates an increase in hepatic gluconeogenesis (4, 11). The decrease in oxygen consumption indicates a decrease in mitochondrial oxidative phosphorylation at whole-body level. A reduction in oxygen consumption can be achieved by a switch from aerobic (mitochondrial) to anaerobic glycolytic ATP production; however, also the small, although non-significant, decrease in physical activity might contribute to the reduction in oxygen consumption. Hypothermia is also known to play a role in the reduction of oxygen consumption in mice during hypoxia (15); however, body temperature was not assessed in our study.

OxR, furthermore, increased serum levels of the amino acids lysine, ornithine and tyrosine. Elevations in circulating amino acid levels are strongly related to obesity (33), where it is expected to impair skeletal muscle glucose uptake and increase hepatic gluconeogenesis (26, 27). Interestingly, also during OxR, hepatic gluconeogenesis (4, 11) and circulating glucose levels are increased. In contrast to the studies that focus on amino acid levels in obesity, in our study amino acid levels changed independently from dietary intake. The increase in amino acids that is seen in both obesity and OxR might, therefore, be seen as a regulator of glucose homeostasis, rather than solely a consequence of dietary intake.

Table 3 Regulation of genes involved in carnitine and amino acid metabolism after 6 hours of OxR in WAT

Gene symbol	Gene name	Fold change	p-value	Function
Bcat1	branched chain aminotransferase 1	1.21	0.11	catabolism of BCAA, cytosolic
Bcat2	branched chain aminotransferase 2	-1.10	0.68	catabolism of BCAA, mitochondrial
Bckdha	branched chain ketoacid dehydrogenase E1, α	-1.09	0.74	inactivation of the branched-chain alpha-ketoacid dehydrogenase complex: the key regulatory enzyme of the valine, leucine and isoleucine catabolic pathways
Bckdhb	branched chain ketoacid dehydrogenase E1, β	-1.19	0.56	
Bckdk	branched chain ketoacid dehydrogenase kinase	-1.03	0.85	
Dbt	dihydrolipoamide branched chain transacylase E2	-1.00	1.00	component of branched-chain alpha-keto acid dehydrogenase complex
Dld	dihydrolipoamide dehydrogenase	1.04	0.85	carnitine transport out of the cell
Slc16a9	solute carrier family 16, member 9	1.08	0.28	cellular carnitine import and export
Slc22a5	solute carrier family 22, member 5	-1.05	0.42	carnitine transport into the cell
Slc22a16	solute carrier family 22, member 16	nd		transport of acylcarnitines across the mitochondrial inner membrane
Slc25a20	solute carrier family 25, member 20	-1.05	0.61	catabolism of leucine, isoleucine, and valine

Changes in gene expression are shown as the fold change of the level in OxR mice (n=10) compared to the level in Norm mice (n=12). n.d., not detected

Next to the changes in serum amino acid levels, OxR increased serum long-chain acylcarnitines, which confirms that mitochondrial oxidative phosphorylation is reduced during OxR. Elevated levels of long-chain acylcarnitines indicate incomplete FA oxidation (24, 25, 32) and are, in combination with a reduction in free carnitines, strongly correlated to hypoxic exposure in both humans and rodents (1-3, 49). At tissue level, a decrease in free carnitine levels leads to a decrease in the transport of fatty acids into the mitochondria, which further limits mitochondrial fatty acid oxidation, especially in those tissues that cannot synthesize carnitines by itself, such as skeletal muscle or adipose tissue (47). Consistently, acute hypoxia was recently shown to reduce fatty acid oxidation at whole-body level in mice (22). It is, however, as yet unclear which tissues are mostly responsible for changes in circulating acylcarnitine levels. It was recently hypothesized that mostly the liver and skeletal muscle contribute to changes in plasma acylcarnitines, for example during fasting (49), whereas another study showed no relation between tissue and plasma acylcarnitines (39).

WAT does not contribute to the rise in serum acylcarnitine but rather seems to upregulate mitochondrial FA oxidation

When oxygen availability does not match oxygen demand, oxidative ATP production generally decreases while glycolytic ATP production increases (23). This metabolic switch did, however, not occur in WAT during the exposure to OxR. Lactate levels remained unaltered, indicating no change in anaerobe glycolysis, and in contrast to the increase in long-chain acylcarnitines in serum, in WAT only short-chain acylcarnitines were increased by OxR. The C3- and C5- acylcarnitines, which were found to be increased in WAT, are byproducts of branched-chain amino acid (BCAA) catabolism. Interestingly, the BCAAs leucine and isoleucine were also significantly increased in WAT, but no genes in BCAA metabolism were regulated. WAT plays an important role in BCAA metabolism. The rate of BCAA oxidation per mg of tissue is even higher in WAT than in skeletal muscle (16). In obese or diabetic individuals, BCAA catabolism in WAT is reduced (28), presumably because other macronutrients are abundantly available in the obese state. In healthy individuals, BCAA oxidation only occurs during prolonged fasting and serves as a last resort to prevent hypoglycaemia. Amino acids can, however, be used to fuel high-energy demanding processes, such as gluconeogenesis, even when other fuels are available (50). It is as yet unclear why OxR would increase BCAA catabolism in WAT. Mice are kept in a fasted state, which implies that the adipose tissue is activated to release energy in the form of fatty acids. BCAA catabolism might complement fat catabolism to support energetic demands of other tissues, which energy metabolism is affected by the restricted oxygen availability. Alternatively, the increase in BCAAs and BCAA derivatives that we found in WAT might be produced in other organs, such as the liver, and taken up by WAT to clear them from circulation. This would also explain why none of the genes involved in BCAA catabolism was found to be regulated in WAT.

Methylmalonylcarnitine (C4-DC), which was also increased in WAT by OxR, is a byproduct of the TCA cycle. Its upregulation by OxR in WAT suggests that OxR increases TCA cycle activity. We have more reasons to believe that mitochondrial function in WAT is increased during OxR. First, the absence of changes in the level of long-chain acylcarnitines indicates that fatty acid oxidation is not disturbed. Second, in contrast to long-chain acylcarnitines, accumulation of short- and medium-chain acylcarnitines does not disturb mitochondrial activity (38). Third, free carnitine levels were increased in WAT by OxR, which promotes FA uptake into the mitochondria. Moreover, chronic hypoxic exposure was previously shown to increase rather than decrease oxidative metabolism in mouse WAT (45). Finally, this view is supported by the analysis of whole genome gene expression.

Whole genome expression analysis confirms that WAT increases mitochondrial activity

OxR did not lead to major changes in WAT gene expression, but several key metabolic genes were altered, of which *Sirt4* is one of the best studied. SIRT4 plays an important role in the regulation of lipid metabolism and cell proliferation; it was recently shown to inhibit mitochondrial glutamine metabolism and fatty acid oxidation, and to promote anaplerosis, cell cycle arrest and lipid synthesis (21, 29). Furthermore, *Sirt4* expression was found to be induced by DNA damage *in vitro* (21), and reduced in mouse WAT by fasting (29) and during dietary restriction (10). All mice were fasted prior to the exposure to OxR or normoxia, which thus likely reduced *Sirt4* mRNA in WAT. OxR appeared to further downregulate *Sirt4* expression, which would lead to an even larger increase in FA oxidation. OxR consistently led to a small decrease in whole-body RER, although this was only marginally significant (p=0.059). Second, OxR decreased the expression of *Gpam*, encoding the mitochondrial enzyme GPAT1 that is involved in the initial and committing step of triglyceride and glycerolipid biosynthesis. Its downregulation, therefore, prevents that FAs are diverted away from oxidation. The regulation of *Sirt4* and *Gpam* suggests an increase in WAT FA oxidation and lipolysis, which is supported by others showing that acute hypoxia increases lipolysis in WAT (22).

Next to the regulation of lipolysis and FA oxidation, SIRT4 plays an important role in the regulation of cell growth and survival. SIRT4 was, in fact, found to be down-regulated in human cancer, contributing to increased cell proliferation and to increased energy production via glutamine catabolism (6). Interestingly, whole-genome analysis in WAT revealed a large number of genes involved in cell proliferation and transcription and translation, which are regulated in the direction to stimulate cell proliferation and prevent apoptosis.

Chchd3 is the third and final mitochondrial gene that was significantly regulated by OxR. CHCHD3,a mitochondrial inner membrane protein that faces toward the intermembrane space, is part of the mitochondrial inner membrane organizing system

(MINOS) and plays an important role in maintaining mitochondrial cristae morphology (7). Complete silencing of *Chchd3* causes fragmentation of the mitochondrial network and changes in the shape of mitochondrial cristae, leading to a reduced capacity to generate ATP (7). The 20% decrease in *Chchd3* expression that was observed in our study is obviously less dramatic than complete *Chchd3* depletion, but the down-regulation that occurred during OxR might have led to a decrease in cristae surface and/or a decrease in mitochondrial fusion. Reduction in cristae surface and reduction in fusion may both serve to decrease mitochondrial membrane potential, which decreases the formation of damaging reactive oxygen species and prevents cell damage (30). Of note, no clear changes were observed in genes involved in ER stress, autophagy or antioxidant response.

Thus, in contrast to our expectations, OxR seems to increase *in vivo* FA oxidation and cell proliferation. Furthermore, tissue lactate levels suggest that WAT does not switch from oxidative to glycolytic ATP production.

Conclusions

Mild normobaric oxygen restriction reduces metabolic rate and disturbs mitochondrial fatty acid oxidation at whole-body level. Both metabolite and gene expression analysis, however, show that WAT mitochondrial FA oxidation is not disturbed by OxR. WAT even seems to increase mitochondrial activity via the down-regulation of *Sirt4* and *Gpam*, and possibly via oxidation of acetyl-CoA generated from BCAA catabolism. Although it is yet unclear why WAT energy metabolism increased during OxR, it does not lead to an increase in oxidative stress markers, such as changes in the expression of genes involved in anti-oxidant response or reduction in aconitase activity. It can be postulated that WAT increases oxidative ATP production to compensate for the reduction in oxidative capacity at whole-body level. Previous research showed that OxR reduces oxygen saturation in WAT by almost three-fold (37). Healthy adipose tissue might be more flexible than expected, enabling the tissue to function normally under these circumstances and to prevent inflammation dysregulation of adipokine secretion that are seen in metabolic disease (20, 44).

The joint regulation of *Sirt4*, *Gpam,* and *Chchd3*, moreover, emerges as a biomarker profile for WAT mitochondrial reprogramming in response to acute exposure to limited oxygen availability.

Acknowledgements

The research leading to these results has received funding from the European Union's Seventh Framework Programme FP7 2007-2013 under grant agreement no. 244995 (BIOCLAIMS Project).

We thank all members of the Department of Human and Animal Physiology for their helpful contributions, especially Hans Swarts and Li Meng for their help during the animal experiment.

References

1. Bayes R, Campoy C, Goicoechea A, Peinado JM, Pedroso T, Baena RM*, et al.* Role of intrapartum hypoxia in carnitine nutritional status during the early neonatal period. Early Human Development. 2001;65: S103-S110.
2. Bruder ED, Raff H Cardiac and plasma lipid profiles in response to acute hypoxia in neonatal and young adult rats. Lipids Health Dis. 2010;9: 3.
3. Cam H, Yildirim B, Aydin A, Say A Carnitine levels in neonatal hypoxia. J Trop Pediatr. 2005;51: 106-108.
4. Choi JH, Park MJ, Kim KW, Choi YH, Park SH, An WG*, et al.* Molecular mechanism of hypoxia-mediated hepatic gluconeogenesis by transcriptional regulation. Febs Letters. 2005;579: 2795-2801.
5. Constantinides C, Mean R, Janssen BJ Effects of isoflurane anesthesia on the cardiovascular function of the C57BL/6 mouse. ILAR J. 2011;52: e21-31.
6. Csibi A, Fendt SM, Li CG, Poulogiannis G, Choo AY, Chapski DJ*, et al.* The mTORC1 Pathway Stimulates Glutamine Metabolism and Cell Proliferation by Repressing SIRT4. Cell. 2013;153: 840-854.
7. Darshi M, Mendiola VL, Mackey MR, Murphy AN, Koller A, Perkins GA*, et al.* ChChd3, an Inner Mitochondrial Membrane Protein, Is Essential for Maintaining Crista Integrity and Mitochondrial Function. Journal of Biological Chemistry. 2011;286: 2918-2932.
8. Desaulniers D, Yagminas A, Chu I, Nakai J Effects of anesthetics and terminal procedures on biochemical and hormonal measurements in polychlorinated biphenyl treated rats. Int J Toxicol. 2011;30: 334-347.
9. Dolt KS, Karar J, Mishra MK, Salim J, Kumar R, Grover SK*, et al.* Transcriptional downregulation of sterol metabolism genes in murine liver exposed to acute hypobaric hypoxia. Biochem Biophys Res Commun. 2007;354: 148-153.
10. Duivenvoorde LP, van Schothorst EM, Bunschoten A, Keijer J Dietary restriction of mice on a high-fat diet induces substrate efficiency and improves metabolic health. J Mol Endocrinol. 2011;47: 81-97.
11. Duivenvoorde LP, van Schothorst EM, Derous D, van der Stelt I, Masania J, Rabbani N*, et al.* Oxygen restriction as challenge test reveals early high-fat-diet-induced changes in glucose and lipid metabolism. Pflugers Arch. 2014;DOI: 10.1007/s00424-00014-01553-00428.
12. Duivenvoorde LP, van Schothorst EM, Swarts HJ, Keijer J Assessment of Metabolic Flexibility of Old and Adult Mice Using Three Noninvasive, Indirect Calorimetry-Based Treatments. . J Gerontol A Biol Sci Med Sci. 2014;DOI: 10.1093/gerona/glu1027.
13. Fan C, Iacobas DA, Zhou D, Chen Q, Lai JK, Gavrialov O*, et al.* Gene expression and phenotypic characterization of mouse heart after chronic constant or intermittent hypoxia. Physiol Genomics. 2005;22: 292-307.
14. Gardner PR Aconitase: Sensitive target and measure of superoxide. Superoxide Dismutase. 2002;349: 9-23.
15. Gautier H Interactions among metabolic rate, hypoxia, and control of breathing. J Appl Physiol (1985). 1996;81: 521-527.
16. Herman MA, She PX, Peroni OD, Lynch CJ, Kahn BB Adipose Tissue Branched Chain Amino Acid (BCAA) Metabolism Modulates Circulating BCAA Levels. Journal of Biological Chemistry. 2010;285: 11348-11356.
17. Hoek-van den Hil EF, van Schothorst EM, van der Stelt I, Swarts HJ, Venema D, Sailer M*, et al.* Quercetin decreases high-fat diet induced body weight gain and accumulation of hepatic and circulating lipids in mice. Genes Nutr. 2014;9: 418.
18. Hoevenaars FP, Bekkenkamp-Grovenstein M, Janssen RJ, Heil SG, Bunschoten A, Hoek-van den Hil EF*, et al.* Thermoneutrality results in prominent diet-induced body weight differences in C57BL/6J mice, not paralleled by diet-induced metabolic differences. Mol Nutr Food Res. 2014;58: 799-807.
19. Hoevenaars FP, van Schothorst EM, Horakova O, Voigt A, Rossmeisl M, Pico C*, et al.* BIOCLAIMS standard diet (BIOsd): a reference diet for nutritional physiology. Genes Nutr. 2012;7: 399-404.
20. Hosogai N, Fukuhara A, Oshima K, Miyata Y, Tanaka S, Segawa K*, et al.* Adipose tissue hypoxia in obesity and its impact on adipocytokine dysregulation. Diabetes. 2007;56: 901-911.

21. Jeong SM, Xiao CY, Finley LWS, Lahusen T, Souza AL, Pierce K*, et al.* SIRT4 Has Tumor-Suppressive Activity and Regulates the Cellular Metabolic Response to DNA Damage by Inhibiting Mitochondrial Glutamine Metabolism. Cancer Cell. 2013;23: 450-463.
22. Jun JC, Shin MK, Yao Q, Bevans-Fonti S, Poole J, Drager LF*, et al.* Acute hypoxia induces hypertriglyceridemia by decreasing plasma triglyceride clearance in mice. American Journal of Physiology-Endocrinology and Metabolism. 2012;303: E377-E388.
23. Kim JW, Tchernyshyov I, Semenza GL, Dang CV HIF-1-mediated expression of pyruvate dehydrogenase kinase: a metabolic switch required for cellular adaptation to hypoxia. Cell Metab. 2006;3: 177-185.
24. Koves TR, Li P, An J, Akimoto T, Slentz D, Ilkayeva O*, et al.* Peroxisome proliferator-activated receptor-gamma co-activator 1 alpha-mediated metabolic remodeling of skeletal myocytes mimics exercise training and reverses lipid-induced mitochondrial inefficiency. Journal of Biological Chemistry. 2005;280: 33588-33598.
25. Koves TR, Ussher JR, Noland RC, Slentz D, Mosedale M, Ilkayeva O*, et al.* Mitochondrial overload and incomplete fatty acid oxidation contribute to skeletal muscle insulin resistance. Cell Metab. 2008;7: 45-56.
26. Krebs M, Brehm A, Krssak M, Anderwald C, Bernroider E, Nowotny P*, et al.* Direct and indirect effects of amino acids on hepatic glucose metabolism in humans. Diabetologia. 2003;46: A202-A202.
27. Krebs M, Krssak M, Bernroider E, Anderwald C, Brehm A, Meyerspeer M*, et al.* Mechanism of amino acid-induced skeletal muscle insulin resistance in humans. Diabetes. 2002;51: 599-605.
28. Lackey DE, Lynch CJ, Olson KC, Mostaedi R, Ali M, Smith WH*, et al.* Regulation of adipose branched-chain amino acid catabolism enzyme expression and cross-adipose amino acid flux in human obesity. American Journal of Physiology-Endocrinology and Metabolism. 2013;304: E1175-E1187.
29. Laurent G, German NJ, Saha AK, de Boer VCJ, Davies M, Koves TR*, et al.* SIRT4 Coordinates the Balance between Lipid Synthesis and Catabolism by Repressing Malonyl CoA Decarboxylase. Molecular Cell. 2013;50: 686-698.
30. Liesa M, Palacin M, Zorzano A Mitochondrial dynamics in mammalian health and disease. Physiological Reviews. 2009;89: 799-845.
31. Mimura Y, Furuya K Mechanisms of Adaptation to Hypoxia in Energy-Metabolism in Rats. Journal of the American College of Surgeons. 1995;181: 437-443.
32. Muoio DM, Newgard CB Molecular and metabolic mechanisms of insulin resistance and beta-cell failure in type 2 diabetes. Nature Reviews Molecular Cell Biology. 2008;9: 193-205.
33. Newgard CB, An J, Bain JR, Muehlbauer MJ, Stevens RD, Lien LF*, et al.* A Branched-Chain Amino Acid-Related Metabolic Signature that Differentiates Obese and Lean Humans and Contributes to Insulin Resistance (vol 9, pg 311, 2009). Cell Metab. 2009;9: 565-566.
34. Papandreou I, Cairns RA, Fontana L, Lim AL, Denko NC HIF-1 mediates adaptation to hypoxia by actively downregulating mitochondrial oxygen consumption. Cell Metab. 2006;3: 187-197.
35. Pasarica M, Sereda OR, Redman LM, Albarado DC, Hymel DT, Roan LE*, et al.* Reduced Adipose Tissue Oxygenation in Human Obesity Evidence for Rarefaction, Macrophage Chemotaxis, and Inflammation Without an Angiogenic Response. Diabetes. 2009;58: 718-725.
36. Peng M, Liu L, Jiang M, Liang C, Zhao X, Cai Y*, et al.* Measurement of free carnitine and acylcarnitines in plasma by HILIC-ESI-MS/MS without derivatization. J Chromatogr B Analyt Technol Biomed Life Sci. 2013;932: 12-18.
37. Reinke C, Bevans-Fonti S, Drager LF, Shin MK, Polotsky VY Effects of different acute hypoxic regimens on tissue oxygen profiles and metabolic outcomes. J Appl Physiol (1985). 2011;111: 881-890.
38. Sauer SW, Okun JG, Hoffmann GF, Koelker S, Morath MA Impact of short- and medium-chain organic acids, acylcarnitines, and acyl-CoAs on mitochondrial energy metabolism. Biochimica Et Biophysica Acta-Bioenergetics. 2008;1777: 1276-1282.
39. Schooneman MG, Achterkamp N, Argmann CA, Soeters MR, Houten SM Plasma acylcarnitines inadequately reflect tissue acylcarnitine metabolism. Biochim Biophys Acta. 2014;1841: 987-994.
40. Schulz TJ, Thierbach R, Voigt A, Drewes G, Mietzner B, Steinberg P*, et al.* Induction of oxidative metabolism by mitochondrial frataxin inhibits cancer growth - Otto Warburg revisited. Journal of Biological Chemistry. 2006;281: 977-981.

41. Semenza GL Targeting HIF-1 for cancer therapy. Nature Reviews Cancer. 2003;3: 721-732.
42. Solberg R, Enot D, Deigner HP, Koal T, Scholl-Burgi S, Saugstad OD*, et al.* Metabolomic analyses of plasma reveals new insights into asphyxia and resuscitation in pigs. PLoS One. 2010;5: e9606.
43. Todoric J, Loffler M, Huber J, Bilban M, Reimers M, Kadl A*, et al.* Adipose tissue inflammation induced by high-fat diet in obese diabetic mice is prevented by n-3 polyunsaturated fatty acids. Diabetologia. 2006;49: 2109-2119.
44. Trayhurn P, Wood IS Adipokines: inflammation and the pleiotropic role of white adipose tissue. Br J Nutr. 2004;92: 347-355.
45. van den Borst B, Schols AMWJ, de Theije C, Boots AW, Kohler SE, Goossens GH*, et al.* Characterization of the inflammatory and metabolic profile of adipose tissue in a mouse model of chronic hypoxia. J Appl Physiol (1985). 2013;114: 1619-1628.
46. Van Schothorst EM, Franssen-van Hal N, Schaap MM, Pennings J, Hoebee B, Keijer J Adipose gene expression patterns of weight gain suggest counteracting steroid hormone synthesis. Obes Res. 2005;13: 1031-1041.
47. Vaz FM, Wanders RJA Carnitine biosynthesis in mammals. Biochemical Journal. 2002;361: 417-429.
48. Voigt A, Agnew K, van Schothorst EM, Keijer J, Klaus S Short-term, high fat feeding-induced changes in white adipose tissue gene expression are highly predictive for long-term changes. Mol Nutr Food Res. 2013;57: 1423-1434.
49. Wang YP, Wei JY, Yang JJ, Gao WN, Wu JQ, Guo CJ Riboflavin Supplementation Improves Energy Metabolism in Mice Exposed to Acute Hypoxia. Physiological Research. 2014;63: 341-350.
50. Williamson JR, Walajtysrode E, Coll KE Effects of Branched-Chain Alpha-Ketoacids on the Metabolism of Isolated Rat-Liver Cells .1. Regulation of Branched-Chain Alpha-Ketoacid Metabolism. Journal of Biological Chemistry. 1979;254: 1511-1520.

Supplemental tables

Supplemental table 1 Serum and WAT levels of amino acids, acylcarnitines and free carnitine in mice that were exposed to OxR or remained under normoxic conditions

	SERUM				WAT			
Metabolite	Conc. Norm	Conc. OxR	FC OxR/ norm	p-value	Conc. Norm	Conc. OxR	FC OxR/ norm	p-value
	Amino acids (µM)				**Amino acids (pM mg-1 WAT)**			
Ala	140.1	150.4	1.07	0.44	154.0	204.0	1.33	0.14
Cit	29.5	26.1	-1.13	0.89	10.1	9.6	0.95	0.83
Glu	23.5	40.8	1.74	0.07	451.6	477.0	1.06	0.87
Gly	11.9	21.3	1.79	0.21	71.0	55.1	0.78	0.66
HydroxyPro	0.4	0.4	-1.11	0.33	*nd*	*nd*	-	-
Leu+Ileu	104.5	119.8	1.15	0.22	17.9	36.9	2.06	**0.03**
Lys	1.0	1.4	1.39	**0.00**	*nd*	*nd*	-	-
Orn	35.9	91.1	2.54	**0.00**	14.3	21.1	1.47	0.73
Phe	1.1	1.3	1.16	0.08	17.3	27.6	1.60	0.07
Pro	37.7	43.4	1.15	0.10	19.7	27.4	1.39	0.18
Ser	99.8	113.1	1.13	0.29	83.8	118.3	1.41	0.13
Thr	108.8	106.7	-1.02	0.81	54.1	54.2	1.00	1.00
Trp	16.3	16.3	1.00	0.96	45.9	51.0	1.11	0.58
Tyr	42.1	53.2	1.26	**0.04**	17.9	25.5	1.43	0.18
Val	44.1	45.0	1.02	0.79	13.8	14.8	1.07	0.81
	Free carnitine (µM)				**Free carnitine (pM mg-1 WAT)**			
C0	9.9	7.8	-1.26	**0.00**	42.7	64.3	1.50	**0.01**
	Short-chain acylcarnitines (nM)				**Short-chain acylcarnitines (pM g-1 WAT)**			
C2	8767.5	8713.0	-1.01	0.94	15170.8	17824.5	1.17	0.34
C3	102.8	103.5	1.01	0.92	330.4	743.8	2.25	**0.04**
C3DC	*nd*	*nd*	-	-	2.8	3.0	1.06	0.76
C4	132.1	138.2	1.05	0.52	394.4	708.7	1.80	0.06
C4OH	*nd*	*nd*	-	-	342.0	423.6	1.24	0.31
C4DC	*nd*	*nd*	-	-	1125.0	1633.4	1.45	**0.04**
C5	23.0	24.0	1.04	0.59	89.5	232.9	2.60	**0.02**
C5-1	3.4	4.2	1.24	0.31	0.1	1.4	15.59	**0.01**
C5DC	*nd*	*nd*	-	-	14.7	42.6	2.90	**0.02**
C6	29.0	33.5	1.15	0.10	102.2	108.1	1.06	0.80
C6-1	*nd*	*nd*	-	-	15.2	12.6	0.83	0.41
C6DC	5.1	5.4	1.07	0.67	*nd*	*nd*	-	-
C7DC	nd	nd	-	-	65.8	70.1	1.06	0.80
C7OH	1.3	1.0	-1.32	0.22	*nd*	*nd*	-	-
C8	8.6	9.4	1.09	0.49	49.4	45.8	0.93	0.68
C8-1	18.2	18.8	1.03	0.61	52.0	48.6	-1.40	0.93
	Medium-chain acylcarnitines (nM)				**Medium-chain acylcarnitines (pM g-1 WAT)**			
C10	6.7	9.2	1.36	**0.00**	19.3	11.1	0.58	0.20
C10-1	11.9	16.0	1.34	**0.01**	14.5	13.1	0.90	0.60
C10-2	2.4	2.8	1.17	0.37	3.8	3.7	0.98	0.92
C12	11.9	13.3	1.12	0.40	144.7	109.6	0.76	0.37
C12-1	2.1	4.9	2.40	**0.00**	18.8	11.1	0.59	0.18
C12DC	*nd*	*nd*	-	-	7.0	5.8	0.82	0.53
C14	2125.4	2166.1	1.02	0.91	284.2	243.7	0.86	0.61
C14-1	2172.5	2372.5	1.09	0.65	85.0	49.6	0.58	0.19
C14-2	565.3	777.7	1.38	0.08	11.7	6.2	0.53	0.14
C14OH	60.3	84.1	1.39	0.33	78.2	74.4	0.95	0.87
C14-1OH	*nd*	*nd*	-	-	101.5	72.0	0.71	0.30
C14-2OH	*nd*	*nd*	-	-	27.0	18.8	0.70	0.26

Supplemental table 1 continued from page 139

Metabolite	SERUM Conc. Norm	SERUM Conc. OxR	SERUM FC OxR/ norm	SERUM p-value	WAT Conc. Norm	WAT Conc. OxR	WAT FC OxR/ norm	WAT p-value
	Long-chain acylcarnitines (nM)				**Long-chain acylcarnitines (pM g-1 WAT)**			
C16	143.6	200.0	1.39	**0.00**	841.9	954.1	1.13	0.58
C16-1	39.9	61.7	1.55	**0.00**	213.7	146.7	0.69	0.31
C16-2	12.5	17.6	1.41	**0.00**	43.3	23.8	0.55	0.14
C16OH	7.8	9.7	1.25	0.13	142.1	146.7	1.03	0.92
C16-1OH	2.6	3.1	1.18	0.41	158.6	121.2	0.76	0.43
C16-2OH	*nd*	*nd*	-	-	42.1	37.3	0.89	0.67
C16DC	83.8	105.5	1.26	**0.00**	45.5	59.7	1.31	0.09
C18	57.4	64.2	1.12	0.10	154.1	195.1	1.27	0.31
C18-1	254.5	343.1	1.35	**0.00**	562.6	526.8	0.94	0.80
C18-2	141.7	207.6	1.47	**0.00**	258.0	206.6	0.80	0.43
C18-3	14.3	20.1	1.41	**0.00**	26.9	20.8	0.77	0.44
C18OH	9.1	10.5	1.16	0.07	21.7	25.6	1.18	0.56
C18-1OH	13.4	17.0	1.27	**0.05**	209.5	198.0	0.94	0.86
C18-2OH	4.0	7.0	1.75	**0.01**	81.3	75.9	0.93	0.82
C20	5.5	6.6	1.21	0.10	9.8	13.0	1.32	0.21
C20-1	7.4	9.1	1.23	0.08	19.2	21.6	1.12	0.65
C20-2	5.7	5.7	1.00	1.00	13.8	13.7	1.00	1.00
C20-3	3.6	5.5	1.52	**0.00**	5.0	4.7	0.94	0.88
C20-4	12.0	15.4	1.29	**0.02**	20.2	18.4	0.91	0.79

Data are shown as the mean per group (n=12) and as the fold change (FC) of OxR mice over Norm mice. *nd,* not detected

Supplemental table 2 Overview of genes that were significantly regulated by the exposure to OxR (p<0.01) in WAT

Gene symbol	Gene name	Fold change	p-value
Apold1	apolipoprotein L domain containing 1	1.31	0.003
Clca1	chloride channel calcium activated 1	1.38	0.004
Dusp9	dual specificity phosphatase 9	1.30	0.008
Fam107a	family with sequence similarity 107, member A	1.38	0.010
Gpr65	G-protein coupled receptor 65	1.17	0.003
Gpr65	G-protein coupled receptor 65	1.19	0.010
Haus7	HAUS augmin-like complex, subunit 7	1.23	0.007
Hbegf	heparin-binding EGF-like growth factor	1.31	0.006
Hspb7	heat shock protein family, member 7 (cardiovascular)	1.27	0.006
Lhfp	lipoma HMGIC fusion partner	1.21	0.005
Med24	mediator complex subunit 24	1.21	0.006
Ms4a4a	membrane-spanning 4-domains, subfamily A, member 4A	1.31	0.004
Mt1	metallothionein 1	1.40	0.004
Nt5c2	5'-nucleotidase, cytosolic II	1.18	0.006
Pdia5	protein disulfide isomerase associated 5	1.16	0.005
Podxl2	podocalyxin-like 2	1.24	0.007
Prdm4	PR domain containing 4	1.20	0.010
Ren2	renin 2 tandem duplication of Ren1	1.84	0.006
Retnlg	resistin like gamma	1.62	0.007
Samd14	sterile alpha motif domain containing 14	1.28	0.010
Sec63	SEC63-like (S. cerevisiae)	1.19	0.004
Stau2	staufen (RNA binding protein) homolog 2 (Drosophila)	1.29	0.004
Synpo	synaptopodin	1.29	0.002
Tnks2	tankyrase, TRF1-interacting ankyrin-related ADP-ribose polymerase 2	1.16	0.008
Trim59	tripartite motif-containing 59	1.30	0.004
Zfp319	zinc finger protein 319	1.19	0.001

Supplemental table 2 continued from page 140

Gene symbol	Gene name	Fold change	p-value
Adrbk2	adrenergic receptor kinase, beta 2	-1.18	0.006
Atp2b4	AATPase, Ca++ transporting, plasma membrane 4	-1.26	0.001
Cdip1	5730403B10Rik|cell death inducing Trp53 target 1	-1.19	0.008
Chchd3	coiled-coil-helix-coiled-coil-helix domain containing 3	-1.21	0.000
Derl3	Der1-like domain family, member 3	-1.27	0.004
Gpam	glycerol-3-phosphate acyltransferase, mitochondrial	-1.29	0.004
Homer1	homer homolog 1 (Drosophila)	-1.16	0.001
Hoxb3	homeobox B3	-1.20	0.004
Hsf2	heat shock factor 2	-1.25	0.002
Kifc2	kinesin family member C2	-1.24	0.001
Olfr1466	olfactory receptor 1466	-1.18	0.006
Pigc	phosphatidylinositol glycan anchor biosynthesis, class C	-1.15	0.005
Rabgap1	RAB GTPase activating protein 1	-1.19	0.009
Sirt4	sirtuin 4	-1.21	0.002
Tchp	trichoplein, keratin filament binding	-1.13	0.010
Traf4	TNF receptor associated factor 4	-1.24	0.008
Tubgcp4	tubulin, gamma complex associated protein 4	-1.20	0.009
Vamp1	vesicle-associated membrane protein 1	-1.20	0.006
Zfp523	zinc finger protein 523	-1.18	0.004

Genes are divided into genes that were significantly upregulated by the exposure to OxR or significantly downregulated and within each category shown in alphabetic order. Fold changes are calculated with the level of gene expression in OxR mice (n=10) compared to the level in Norm mice (n=12). Only genes with a known function are shown.

Chapter 7

General discussion

The aim of this thesis was to assess metabolic health using transcriptome analysis and non-invasive challenge tests. In this thesis I focussed on transcriptome analysis in white adipose tissue (WAT) as a method to monitor multiple processes on organ level, and on the development and validation of non-invasive, indirect calorimetry (InCa) based challenge tests as a method to monitor the adaptive capacity, or flexibility, of the body as a whole. Both approaches are expected to contribute to research that aims to understand how dietary interventions can either improve or reduce metabolic health. In this chapter, the different methods that were used will be discussed on their relevance and applicability in nutrition-related research and recommendations for further research will be provided.

Delineation of metabolic health and metabolic flexibility

The terms ‘metabolic health’ and ‘metabolic flexibility’ are frequently used in nutrition-related research. The exact definition of both terms is, however, complex and challenging to interpret given the diversity of studies in which they are employed. Therefore, to start this general discussion I will first further define both terms in the context of this thesis, which may help to interpret the results that were obtained.

In a broad sense, metabolic health implies a physical state in which life-sustaining chemical transformations within the body are adequately regulated to ensure growth, reproduction, and cell survival. More specifically, metabolic health implies a state that enables the body to handle discontinuous nutrient supply during and in between meals by storing nutrients at times of surplus and releasing nutrients at times of need. The mechanism of energy metabolism has arisen in early evolution to meet to the requirements of free-living animals in nutrient-scarce environments (63). In modern human society, food is seldom scarce and therefore it should be noted that, for the Western civilization, metabolic health also implies that nutrients are oxidized rather than stored, or that food intake is limited, when nutrient stores are sufficiently filled. There are great differences in how individuals adapt their metabolism to caloric overload; some store most of this energy as fat, while others dissipate much of it through altered energy expenditure, including adaptive thermogenesis (55). A maladaptive response to caloric overload may lead to prolonged exposure to circulating nutrients or excessive WAT expansion: two conditions that are often associated with impaired metabolic health. Excessive WAT expansion, however, does not always lead to reduced metabolic health (33). As shown in **chapter 5**, mice can become overweight, but still exhibit normal glucose tolerance and adipose tissue health. Also in **chapter 3**, we showed that old, obese mice respond similarly to an InCa-based glucose tolerance test, compared to adult mice with a lower body weight. Also in humans, obesity can occur separately from changes in markers for metabolic disease (41), which indicates the relevance of suitable methods to assess metabolic health status. Metabolic flexibility can, in this context, be used as a relevant quantification of metabolic health. Metabolic flexibility was originally defined as the ability to switch from fat oxidation to glucose

oxidation (44, 45), where it was applied to study substrate preferences of the insulin resistant muscle. Later on, it became apparent that metabolic flexibility can be applied to a broader range of substrates and was, hence, defined as the capacity to adapt fuel oxidation to fuel availability (22), which is also the definition that was used in this thesis. The InCa-based challenge tests that are described in this thesis all rely on the observation that under normal (non-starved) conditions – when protein stores are not depleted – mitochondrial substrate selection primarily depends on the availability of glucose, fatty acids and oxygen. Oxygen is the terminal electron acceptor of oxidative phosphorylation, while glucose and fat are the primary carbon sources that, via the TCA cycle and β-oxidation, feed oxidative phosphorylation. Therefore, these substrates can be seen as the core requirements for mitochondrial fuel oxidation. Restriction or rather (re)supplementation of either of these substrates requires mitochondrial substrate switching or changes in the level of total mitochondrial activity.

The role of adipose tissue in maintenance of metabolic health: a transcriptomic approach

In most chapters of this thesis, WAT was the major organ of interest. WAT is, indeed, crucial for maintenance of metabolic health. Next to its function in storage and release of fatty acids, WAT is now established as a major endocrine organ that regulates physiological function of several metabolic organs. WAT can represent 10 to 70% of total bodyweight, and therefore, it is not surprising that changes in WAT function can substantially modulate whole-body energy homeostasis. In this thesis, WAT function was analysed with whole-genome microarrays in two conditions that were expected to require WAT adaptation: dietary restriction (**chapter 2**) and exposure to ambient oxygen restriction (OxR) (**chapter 6**). Transcriptome analysis in **chapter 6** was complemented with another 'omics' approach -metabolomics - to evaluate the effect of OxR on serum amino acid and (acyl)carnitine levels. Molecular adaptation to OxR was also studied with reverse transcription quantitative real-time polymerase chain reaction (RT-qPCR) in **chapter 4**. Dietary restriction appeared to have a large influence on WAT gene expression, whereas OxR appeared to elicit only minor changes in WAT gene expression. Below I will further discuss these findings and elaborate on the role of WAT in the improvement of metabolic health during dietary restriction. I will also examine the effect of diet on the response to OxR.

WAT function during dietary restriction

During dietary restriction, mice receive a limited amount of feed on a fixed time point per day. The restricted amount of feed is generally consumed within a few hours, which means that each day, mice are in a fed state for approximately one half of the day and remain in a fasted state for the remaining part of the day. This fixed pattern of fasting and re-feeding is significantly different from what we observe in *ad libitum* fed mice. Mice that have unlimited access to a high-fat diet never display a period of absolute fat

oxidation and the diurnal fluctuation of the respiratory exchange ratio (RER) is levelled off (see Figure 1).

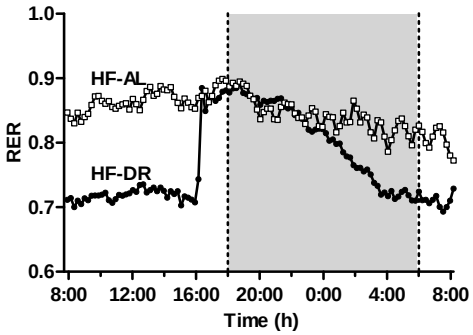

Figure 1 Diurnal pattern of RER of dietary restricted and *ad libitum* fed mice. Mice that are dietary restricted (HF-DR) have a fixed diurnal pattern for feeding and fasting, which can be visualised with the fluctuation of RER. *Ad libitum* fed mice (HF-AL), on the other hand, lack a clear pattern of fasting and feeding and remain in a fed state for the entire day. (data from (34))

The ability of WAT to store energy during feeding and release energy during fasting, or FA flux (Figure 2), is crucial for mouse survival during dietary restriction. A stable FA flux in WAT implies that during each re-feeding period enough energy is stored to meet the energetic demands of the subsequent fasting period in order to prevent further weight loss. Interestingly, in **chapter 2** we show that body weight stabilized after 5 weeks of dietary restriction, indicating that at that time point the WAT FA flux is stabilised and that mice have come to a state where energy intake and storage sustain total diurnal energy expenditure. In this stable phase, mice were considered metabolically healthy, as determined by their increased glucose tolerance and serum adiponectin levels and decreased serum leptin, glucose, and insulin levels, compared to the *ad libitum* fed mice.

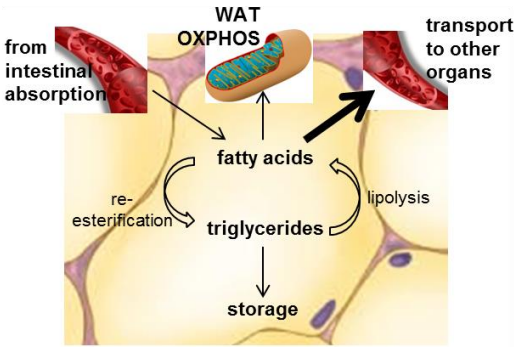

Figure 2 Fatty acid flux in adipose tissue. Fatty acids are derived from the bloodstream and can be stored in the form of triglycerides. During fasting, triglycerides are converted back to fatty acids by lipolysis. Most fatty acids that are released during fasting are released into the bloodstream to be oxidised by other organs. A small proportion of the fatty acids is oxidised in the adipocyte itself.

The beneficial health effects of dietary restriction can, in the first place, be attributed to the limitation of feed intake, leading to a reduction of adipose mass and ectopic fat storage (4, 90). A decrease in adiposity is associated with improved insulin sensitivity (1, 23) and reduced levels of circulating markers for inflammation (17) and oxidative stress (88).

Next to the reduction in total adiposity, the occurrence of timed feeding that results from the fixed FA flux of DR-mice seems to play an important role in health improvement.

The effect of timed feeding on whole-body metabolism was already shown in 1989 in an experiment in which rats received a meal on a fixed time point each day. As expected, feed consumption increased circulating insulin levels; insulin levels, however, also increased during the fixed time period on the day when no meal was provided, suggesting that metabolism can be programmed (35). Later, the effect of timed feeding was substantiated with the recognition of clock genes that function as an endogenous circadian clock and are found in the brain but also in peripheral tissues, such as the liver, intestine, and adipose tissue (2, 21). Timed feeding did not only lead to circadian oscillation in response to the feeding schedule, but also improved the metabolic health of mice fed a high-fat diet, even though absolute caloric intake did not differ from mice that had *ad libitum* access to the high-fat diet (81). These observations suggest that metabolism becomes more efficient in handling of dietary fat when the body expects and is prepared to deal with the diet-induced increase in circulating lipid levels, which prevents lipotoxicity and insulin resistance and improves metabolic health.

Notably, a novelty of the study described in **chapter 2** is that mice were restricted on a high-fat diet, while in most studies restriction is based on a low-fat diet (e.g. 31, 54, 71). HF-DR mice eat less calories compared to HF-AL mice, but still consume twice as much fat compared to mice fed a standard low-fat diet (Figure 3). In contrast to mice that received the HF-diet on an *ad libitum* basis, HF-DR mice seem better equipped to deal with the high amount of fat in the diet and manage to maintain metabolic health. Transcriptome analysis confirmed the drastic metabolic reprogramming of HF-DR mice. Although mice were sacrificed in a fasted state, we observed a strong upregulation of genes involved in lipid metabolism and mitochondrial activity. We hence concluded that dietary restriction of a high-fat diet increases substrate efficiency; mice become more efficient in storage of circulating lipids, thereby preventing lipotoxicity and related ailments.

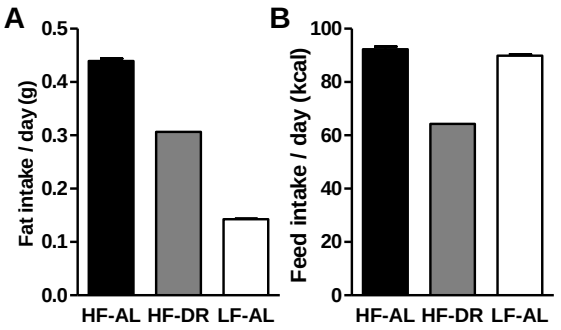

Figure 3 Energy and fat intake of dietary restricted and *ad libitum* fed mice. Diurnal fat (A) and energy (B) intake of mice that had *ad libitum* (HF-AL) or restricted (HF-DR) access to a high-fat diet (data from chapter 2), and of mice that had *ad libitum* access to a low-fat diet (LF-AL). (data derived from (34)). Data represent mean ± SEM (n=12) of 11 weeks of feeding feed intake of male C57BL/6JOlaHsd mice that were 24 weeks of age and after 11 weeks of feeding the dietary regime of interest.

Interestingly, we also found an increase in de-novo lipogenesis (DNL) in HF-DR mice, which is the synthesis of fatty acids from non-lipid precursors, such as glucose. An increase in DNL in WAT during dietary restriction on a high-fat diet might seem contradictory to their high dietary fat intake. DNL primarily leads to the formation of

palmitate. Palmitate can then be desaturated by stearoyl-CoA desaturase (*Scd1*), which was significantly upregulated in HF-DR mice, increasing the ratio of unsaturated fatty acids to saturated fatty acids. High ratios of unsaturated to saturated fat in adipose tissue are associated with improved insulin resistance (82), and a decrease in WAT DNL is, consistently, associated with obesity and type 2 diabetes (16).
Metabolic reprogramming, possibly due to oscillation of metabolic activity in response to timed feeding, increased substrate efficiency, and increased DNL, thus, contribute to healthy adipose tissue.

WAT function during oxygen restriction

The metabolic response to oxygen restriction depends on the interplay between several metabolic organs. Each organ reacts in a specific way to match its oxygen demand with its functional capacity and metabolic function. During the OxR challenge, mice were in a fasted state. During fasting, WAT is activated to release and oxidise fatty acids. Exposure to OxR might impede this function, leading to metabolic adaptation and related transcriptional changes. In **chapter 4**, molecular adaptation to OxR was studied by RT-qPCR in mice on two different diets: low-fat (LF) and a high-fat (HF) diet. In **chapter 6**, molecular and metabolic consequences of adaptation to OxR were studied on a single dietary background with whole genome micro-arrays for gene expression and metabolomics for amino acid and (acyl)carnitine levels in WAT. In **chapter 4**, we observed that HF-fed mice fail to initiate the transcriptional changes in WAT that were observed in LF-fed mice. LF mice showed an increase in the expression of genes involved in the antioxidant response, mitochondrial activity and DNL after the exposure to OxR, whereas this response was completely absent in WAT of HF-fed mice. Also in **chapter 3** we found that, in mice fed a low-fat diet, OxR increased the expression of hexokinase in WAT. Hexokinase performs the first step of glycolysis and is therefore seen as key regulator of glycolysis. We then hypothesised that the transcriptional response to OxR in HF-mice could remain masked by the transcriptional response to high-fat feeding: HF feeding as such (under normoxic conditions), indeed, led to functional adaptations to support adipose expansion.
We also hypothesised that the transcriptional response of WAT to OxR might be bigger after a longer period of HF-feeding: when WAT might be more adapted to the experimental diet and the WAT depot has expanded. Unexpectedly, whole genome analysis did not reveal a large effect of OxR on WAT gene expression after 6 weeks of HF-feeding (**chapter 6**). Only 78 genes were found to be significantly regulated by OxR, compared to the more than 8600 genes that were significantly regulated by dietary restriction (chapter 2). We did expect that OxR would induce an increase in anaerobic glycolysis or carbohydrate oxidation to spare oxygen consumption, leading to transcriptional downregulation of genes involved in mitochondrial activity or fatty acid oxidation and transcriptional upregulation of genes involved in glycolysis. OxR might also lead to transcriptional changes of genes involved in the antioxidant response to

prevent cell damage by oxidative stress, which might arise from the reduction in oxygen availability. Instead, we only identified three genes involved in mitochondrial structure and function: *Sirt4*, *Chchd3*, and *Gpam* that were all significantly downregulated. The downregulation of those genes indicates an increase in mitochondrial activity in WAT during OxR. Most of the other significantly regulated genes were involved in cell survival, proliferation, transcription and translation. The metabolite analysis revealed an increase in FA uptake in mitochondria, increased TCA activity, and increased protein catabolism by OxR. Thus, in contrast to our expectations, OxR did not lead to major changes in energy metabolism in WAT of mice fed a HF-diet. Moreover, the few changes that occurred seem to point towards an increase in mitochondrial FA oxidation, rather than the expected decrease.

I have three possible explanations for the absence of major changes in gene expression by OxR in WAT of HF-mice. At first, it might be that after 6 weeks of HF-feeding, gene expression is, like described in chapter 4, still masked by the adaptations required for WAT expansion. Adipose expansion is, in fact, at its maximum in the first weeks of HF feeding when total fat mass can increase by 1 to 2 grams per week. Adipocytes in eWAT, however, continue to grow even after week 6 (Figure 4), during which it is still considered beneficial to increase expression of genes involved in WAT remodelling and the antioxidant response. Similar pathways are involved in WAT expansion during HF feeding and adaptation to OxR, which can explain why we do not detect significant changes in gene expression in WAT after the exposure to OxR.

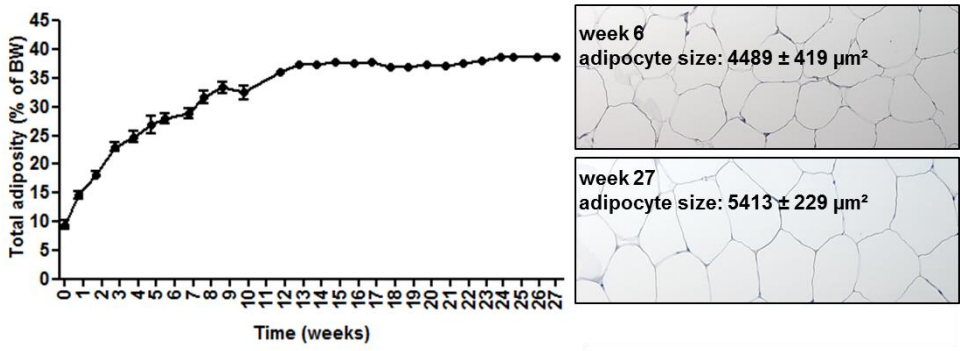

Figure 4 Adiposity and adipocyte size during high-fat feeding. Total adiposity mostly increases during the first weeks of HF-feeding and stabilises after approximately 14 weeks. Adipocytes continue to grow after week 6 and adipocytes are larger in week 27 compared to week 6 at borderline significance (p=0.055). Data represent the mean ± SEM, n=11 for adiposity and n=5 (week 6) and n=8 (week 27) for cell size. (data from chapter 5 (HFpu mice)).

Second, it might be that expanding adipocytes are less sensitive to cues that indicate limited oxygen availability, such as elevated glucose, insulin or lactate levels. The relation between adipocyte hypertrophy and insulin resistance and glucose intolerance is apparent (76, 91), but also lactate plays an important role in regulation of metabolism

in adipocytes (6), and the sensitivity to lactate is likewise reduced by high-fat feeding (89). WAT response to OxR might thus be blunted in HF-fed mice due to a reduced sensitivity to circulating cues that indicate WAT hypoxia, which is a direct hallmark of reduced metabolic flexibility.

Third, it may be that eWAT of HF-fed mice is already in a hypoxic condition due to the enlarged size of the eWAT depot, and that OxR does not further reduce oxygen availability in eWAT. eWAT expansion is, on the other hand, also known to reduce oxygen consumption in eWAT to prevent deficits in oxygen availability (28). This reduction in total eWAT activity that is already present prior to the exposure to OxR might circumvent major metabolic switching during OxR.

From these studies it can be extrapolated that the response of WAT to OxR depends on dietary background and/or the level of WAT expansion. The effect of OxR on whole genome gene expression in WAT of LF mice, however, still needs to be established.

Mitochondrial density in WAT and effect on metabolic health

Metabolic health is thought to depend on adequate mitochondrial function because of the association of metabolic disease with ROS formation (69) and the association between caloric intake and mitochondrial overload and associated mitochondrial dysfunction (51). Apart from the effect on mitochondrial function, we found that dietary restriction increased mitochondrial density in WAT (**chapter 2**). Dietary restriction was previously found to be positively related to changes in both the respiratory capacity of mitochondria and the cellular amount of mitochondria in different tissues (reviewed in 29). Next to dietary fat intake and ROS formation, mitochondrial density and function depend on endocrine factors (64), environmental temperature (80), and oxygen availability (57, 67).

In adipocytes, mitochondrial ATP production is required for e.g. cell maintenance, triglyceride synthesis and adipokine synthesis and secretion. Furthermore, next to their role in the regulation of adipocyte differentiation and apoptosis, WAT mitochondria can prevent fat accumulation by release or oxidation of fatty acids (reviewed in 52). Under normal conditions, WAT FA oxidation represents only around 1 to 3.5% of total WAT activity (20). WAT FA oxidation can, however, be increased by transcriptional activation of the electron transport chain, which has been shown to decrease total fat mass in rodents (94). Mitochondrial dysfunction in WAT is, on the other hand, associated with the pathogenesis of obesity and insulin resistance (10, 25, 43, 68). Interestingly, in **chapter 3** we found that WAT mitochondrial density was significantly reduced during aging, which further supports the idea that mitochondrial density in WAT can be used as a marker for healthy WAT functioning. Mitochondrial function and mitochondrial density are, in fact, closely related and positively regulated by the transcriptional peroxisome proliferator-activated receptor γ co-activator 1 (Pgc1α, mouse annotation: *Ppargc1a*) (93). Pgc1α expression decreases during the development of obesity and type 2 diabetes (14, 75, 79), which might explain the negative association of

mitochondrial density with body weight (38). Furthermore, it was found that high-fat feeding reduces mitochondrial density and Pgc1α expression in WAT (84). On the other hand, transgenic mice with enhanced Pgc1α expression in WAT have a higher mitochondrial density and are lean and insulin sensitive despite normal or increased caloric intake (42). Moreover, stimulation of Pgc1a signalling increases mitochondrial density in adipose tissue and decreases fat mass in rodents (40). Next to the decrease in mitochondrial density in WAT during the development of obesity by high-fat feeding, mitochondrial density and Pgc1α signalling was found to be decreased in adipocytes of insulin-resistant rodents and humans (13, 15, 30, 60). These studies, thus, support the notion that mitochondrial density in WAT might serve as functional marker for metabolic health. The mechanistic relation between mitochondrial density and metabolic health, however, still remains unclear (38), which offers opportunities for further research.

The value of InCa-based challenge tests

InCa-based challenge tests have major advantages over other challenge tests to measure metabolic flexibility. The most relevant advantage is that InCa-based challenge tests are non-invasive. Routine animal handling, injection, and oral gavage lead to significant elevations of heart rate, blood pressure, and glucocorticoid concentrations that persist for 30 to 60 minutes after the event (reviewed in 3). Procedures that are necessary for, for example, a standard oral glucose tolerance test significantly increase stress levels and might thereby influence the outcome of the test. Blood collection via the tail tip, for example, causes a three-fold increase in mouse corticosterone levels (87), and increases blood glucose levels with more than 40% (85). Simple handling of mice already doubles corticosterone levels in mice (77) and even moving of the cage increases blood glucose levels with 30% (85) (illustrated with a literature example in Figure 5). Invasive experiments, therefore, do not only affect wellbeing of laboratory animals but also increase data variability, which decreases the statistical power of the experiment.

Another advantage is that InCa measures the response of the 'whole metabolic system'. In the case of the fasting and re-feeding challenge this means: food digestion, nutrient absorption, transport and cellular uptake and, finally, nutrient oxidation or storage. This may better reflect overall metabolic health, since metabolic flexibility also depends on adequate functioning of the whole metabolic system. Furthermore, there is a higher chance to pick up differences in health status, because several components of metabolism are targeted.

In this thesis three InCa-based challenge tests were used: the OxR challenge (**chapters 3**, **4**, **5,** and **6**), which will be further discussed in the section below, the re-feeding challenge (**chapter 5**) and the glucose challenge (**chapter 3**).

The two nutrient-based tests were already described for their ability to analyse metabolic flexibility (e.g. 18, 36, 49) and were only used once in this thesis. The glucose challenge did not reveal differences between old and adult mice but it is

possible that the old and adult mice that were used in this study, indeed, had a similar glucose tolerance. Also in the study described in **chapter 5** we observed that the C57BL/6JOlaHsd mice, even after prolonged high-fat feeding, remained relatively tolerant to glucose and had fasting glucose levels within the normal range.
Notably, we observed that during the glucose challenge in **chapter 3**, mice only achieved maximal RER values around 0.80, which is much lower than the expected value of 1 to indicate glucose oxidation. Probably, the amount of glucose that was provided was too small to initiate complete nutrient switching. In our study, mice received 2 gram glucose per kg body weight. For an average mouse this means a pellet of around 70 mg. Mice that received a larger amount of glucose (225 mg per mouse), indeed reached higher RER values of around 0.90 (18). Consistently, supplying mice with an even smaller glucose load of 1gr/kg body weight hardly increased RER values (49). Supplying mice with a larger glucose load might have improved the functionality of the test.

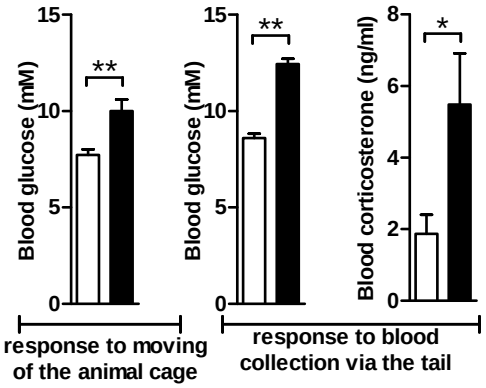

Figure 5 Circulating markers of stress response induced by mouse handling and the use of invasive methods. Moving of the animal cage and blood collection via the tail significantly elevate blood glucose in mice. Blood collection also increases corticosterone levels. Control mice were either not moved in their cage, or did not receive a tail cut. To study the effect of tail bleeding, mice were decapitated to collect blood samples. (data from (85) and (87)).

The re-feeding challenge did reveal differences in metabolic flexibility in the experiment described in **chapter 5**. The advantage of the re-feeding challenge is that the actual RER value that should be achieved after feeding can be deducted from the food quotient of the diet. When performing the re-feeding challenge on mice fed different experimental diets, it is important that all dietary groups are re-fed on a diet with similar macronutrient composition for correct interpretation of metabolic flexibility. Comparing mice re-fed e.g. a high- and low-fat diet is misleading because dietary fat delays gastric emptying and thereby delays mitochondrial substrate switching. Moreover, a diet with a high carbohydrate content will lead to a larger increase in RER than a diet with a low carbohydrate content. For the re-feeding challenge it is alos important to restrict feed intake to ensure that all mice have the same caloric intake, preferably within the same small time window.
Interestingly, in **chapter 5** we show that mice fed different isocaloric high-fat diets with similar food quotients do not differ in RER under normal conditions, but show a significantly different response to the re-feeding challenge. The re-feeding challenge is

an effective method because it 'synchronises' mice in a similar fasting and feeding pattern, which is very different from the *ad libitum* situation in which mice might be in different feeding states at any given time point (Figure 6).

The re-feeding challenge is, furthermore, effective because the switch from total fat oxidation during fasting to partial glucose oxidation during re-feeding requires the (transcriptional) activation and/or translation of the required enzymes for these conversions (e.g. pyruvate dehydrogenase). In the *ad libitum* situation, mice are never in an absolute fasted state and enzymes involved in both carbohydrate and fat oxidation might be continuously present and activated. In other words: during *ad libitum* feeding the capacity to switch between fat and carbohydrate oxidation is not targeted, masking relevant differences in metabolic flexibility.

Due to their non-invasive nature and the synchronization of mouse behaviour, the re-feeding and glucose challenge are promising methods for health assessment. Further optimization may be achieved by increasing the glucose load or by trying different experimental diets within one animal experiment. Also, mice could be sacrificed in challenged and non-challenged condition to further investigate the mechanistic background behind the observed differences in the flexibility to respond to the metabolic challenge.

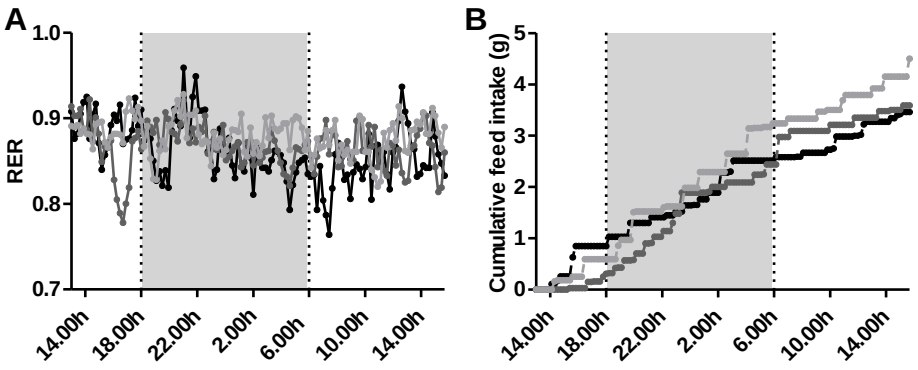

Figure 6 RER and feed intake during *ad libitum* high-fat feeding. Individual RER values (A) and cumulative feed intake (B) of three mice with *ad libitum* access to a high-fat diet (HFpu diet after 20 weeks of HF feeding). The continuous incline in feed intake shows that mice eat continuously throughout both the light and dark phase. The RER values confirm that mice do not achieve a fasting state. (data from chapter 5).

Introduction of OxR as a novel InCa-based challenge test

A major part of this thesis was dedicated to the development and validation of OxR as a challenge test to measure metabolic flexibility. Oxygen is essential for mitochondrial functioning and mitochondrial are responsible for 90% of whole body oxygen consumption (74). Exposure to oxygen restriction, therefore, requires metabolic and physiological adaptation to assure that ATP production matches ATP demand. The novelty of the OxR challenge is that, although metabolic switching is expected, mice

remain in a fasted state during the challenge, which implies that the response is independent of the diet and less affected by confounding factors, such as inter-individual differences in the timing and amount of feed intake or the efficiency of digestion. In setting up the OxR challenge test, we hypothesized that mice that differ in metabolic health would show a different response to OxR, which can be visualised by differences in oxygen consumption, respiratory exchange, circulating metabolite or hormone levels, or gene expression. Results that were obtained with the OxR challenge in this thesis are summarized in table 1 and will be discussed.

OxR and metabolic rate

Mammals are known to decrease metabolic rate when exposed to ambient oxygen restriction, which can be detected by a decrease in whole-body oxygen consumption (VO_2) (19, 32). The extent of the reduction depends on body size. Small animals generally have a high metabolic rate to compensate for passive heat loss due to their large surface area relatively to their inner mass (26). Since their metabolic rate is already high under resting conditions, small animals can achieve a larger reduction in metabolic rate during OxR compared to large animals (reviewed in 24). Consistently, the reduction in metabolic rate by OxR increases when ambient temperature was reduced prior to the exposure (73), which indicates that the drop in VO_2 depends on the discrepancy between room temperature and the thermoneutral zone of an animal. The reduction in metabolic rate can thus partly be achieved by a reduction in thermogenesis (61). A reduction in metabolic rate can, however, also be achieved by changes in mitochondrial substrate oxidation (67).

All studies described in this thesis confirm that OxR decreases VO_2 and thus energy expenditure (EE). The comparison of dietary groups between and within studies, indeed, reveals differences in the extent of the reduction. The reduction in VO_2 and EE is, for example, larger in young, lean mice (**chapter 4**), compared to old, obese mice **(chapter 3)** (24% in lean versus 9% in obese mice). However, before the extent of the drop in metabolic rate can be related to metabolic health status, it is important to evaluate whether mice already differed in resting metabolic rate prior to the exposure, as explained above.

Although conflictingly reported in literature (39, 86), lean mice might have a higher resting metabolic rate during normoxia compared to obese mice, enabling them to achieve a larger reduction in metabolic rate during OxR. However, such a difference was not observed in our studies. In **chapter 4** it was shown that, when under normoxic conditions and fasted and at rest, LF-fed and HF-fed mice do not differ in VO_2. During OxR, however, LF-mice had a lower VO_2 than HF-mice. This was also shown in **chapter 5**, in which mice fed a HF-diet with poly unsaturated fatty acids (HFpu) or a HF-diet with saturated fatty acids (HFs) did not differ in VO_2 in normal air when fasted and at rest, but VO_2 was significantly reduced in HFpu versus HFs mice during OxR (Figure 7). The differences in oxygen consumption during OxR, therefore, cannot be

attributed to differences in metabolic rate prior to the exposure and point towards a difference in the flexibility to adapt metabolism to low oxygen availability. Analysis of the response to OxR with InCa thus provides a useful strategy to analyse metabolic health in mice. To investigate whether the differences in the adaptation of oxygen consumption really reflect a difference in metabolic flexibility, it is necessary to focus on the physical and metabolic changes that underlie the reduction in metabolic rate.

OxR and physical activity

A reduction in physical activity might be one of the first mechanisms to reduce whole-body oxygen consumption, but it does not reflect metabolic health status. Therefore, all mice were tested during the light phase. During the light phase, mice are in a resting state, which decreases the influence of physical activity on the outcome of InCa measurements. Activity levels seem to decrease by OxR, but this was not consistently reported in our 4 studies. The inconsistencies between the studies are most likely due to differences in the choice for a control group. In chapter 3 and 4, we decided to use the first two hours prior to exposure to OxR to analyse physical activity under normoxic conditions. These two hours are, however, more close to the dark period, during which mice are more active.

In chapter 5 and 6 we decided to add an additional measurement under normoxic conditions on the day prior to the OxR exposure that completely resembles the measurement during hypoxic conditions in the procedure of fasting, duration of the measurement, and time period of the day. The comparison in chapter 5 and 6 can, thus, be considered as the most accurate estimation of the influence of OxR on physical activity, which implies that OxR does not affect physical activity levels in mice.

OxR and RER

During the exposure to OxR, mice are in a fasted state and, thus, primarily oxidize fat. A switch from 100% fat oxidation to 100% carbohydrate oxidation in a certain organ decreases oxygen consumption of the organ with approximately 7% (56) and can be visualized by an increase in RER. Whether this switch can be achieved depends on glycogen availability. As shown in table 1, the effect of OxR on RER levels seems inconsistent. This is probably due to the fact that, unlike in the normoxic situation, the RER during OxR shows a dynamic response. RER seems to decrease below normoxic levels at the start of the exposure, after which it inclines during the first 2 hours of exposure to reach a stable level for the final 4 hours. The RER during these last 4 hours is slightly higher than the RER under normoxic conditions. The initial decrease in RER at the start of the exposure might indicate gluconeogenesis (11), whereas the slight increase at the end might indicate a strategy to spare oxygen, as discussed above. This dynamic response is levelled out when RER is analysed as the average over the complete exposure. It is, therefore, advisable - in addition to the analysis of the complete curve - to separately analyse the stable (final) phase of the curve.

Table 1 Changes in respiratory exchange, physical activity and circulating hormone and metabolite levels during exposure to OxR

Measurable	Chapter #	Treatment group	Response
RER	3	adult	=
	3	old	=
	4	5 days LF	0.03 points ↓
	4	5 days HF	0.05 points ↓
	6	6 wks Hfpu	=
	6	6 wks HFs	=
	5	25 wks Hfpu	0.02 points ↑
	5	25 wks HFs	=
activity	3	adult	57.1% ↓
	3	old	60.4% ↓
	4	5 days LF	62.0% ↓
	4	5 days HF	63.4% ↓
	6	6 wks Hfpu	=
	6	6 wks HFs	=
	5	25 wks Hfpu	=
	5	25 wks HFs	=
oxygen consumption	3	adult	18.9% ↓
	3	old	14.4% ↓
	4	5 days LF	24.2% ↓
	4	5 days HF	22.9% ↓
	6	6 wks Hfpu	12.9% ↓
	6	6 wks HFs	12.5% ↓
	5	25 wks Hfpu	9.62% ↓
	5	25 wks HFs	8.66% ↓
energy expenditure	3	adult	18.2% ↓
	3	old	14.8% ↓
	4	5 days LF	27.3% ↓
	4	5 days HF	25.9% ↓
	6	6 wks Hfpu	12.7% ↓
	6	6 wks HFs	12.3% ↓
	5	25 wks Hfpu	8.05% ↓
	5	25 wks HFs	7.14% ↓
blood glucose	3	adult	15.1% ↑
	4	5 days LF	29.7% ↑
	4	5 days HF	17.4% ↑
	6	6 wks Hfpu	13.2% ↑
	6	6 wks HFs	12.9% ↑
	5	25 wks Hfpu	=
	5	25 wks HFs	9.06% ↑
serum lactate	3	adult	19.2% ↑
	4	5 days LF	=
	4	5 days HF	=
serum adiponectin	6	6 wks Hfpu	=
serum free carnitine	6	6 wks Hfpu	20.9% ↓
serum amino acids	6	6 wks Hfpu	Tyr: 26.4% ↑
serum short-chain acylcarnitines	6	6 wks Hfpu	=
serum medium-chain acylcarnitines	6	6 wks Hfpu	30-140% ↑
serum long-chain acylcarnitines	6	6 wks Hfpu	25-75% ↑

Overview of measurables that display the response to OxR at whole body level. The table summarises data from chapter 3, 4, 5, and 6. The response is displayed as the percentage increase (↑) or decrease (↓, highlighted cells) or no significant change (=) from the control (normoxia) group. The response in RER is displayed as the absolute reduction in RER.

It should, however, be noted that the increase in RER in the final phase embodies only a small change in RER (only a 0.03 RER difference), and thus reflects a minor switch in

nutrient oxidation at whole-body level or a larger switch in a single organ only. In conclusion, the small increase in RER contributes to the observed reduction in oxygen consumption, but cannot fully account for this reduction.

Another strategy to reduce oxygen consumption is to decrease mitochondrial oxidation by increasing ATP formation via anaerobic glycolysis, which can be regulated by the transcription factor hypoxia-inducible factor 1 alpha (Hif1α) (47). HIF1α protein is formed and degraded when sufficient oxygen is available. Hif1α degradation diminishes when oxygen availability decreases, leading to an increased level of the protein and transcriptional activation of its target genes to e.g. initiate (anaerobic) glycolytic ATP production (59, 78). A switch from fat oxidation to anaerobic glycolysis is a more effective way to reduce oxygen consumption. Anaerobic glycolysis, however, yields lactate, which may lead to acidosis, a condition that is harmful for normal metabolic functioning. Lactate can be cleared from circulation by hepatic gluconeogenesis. The conversion of lactate to glucose, however, requires ATP. Glycolytic metabolism is therefore only beneficial when ATP needed for lactate clearance does not exceeds the amount of ATP produced by glycolysis. A switch to anaerobic glycolytic ATP production in peripheral tissues can, however, not by visualised by a change in RER, therefore, we also analysed changes in several circulating metabolites.

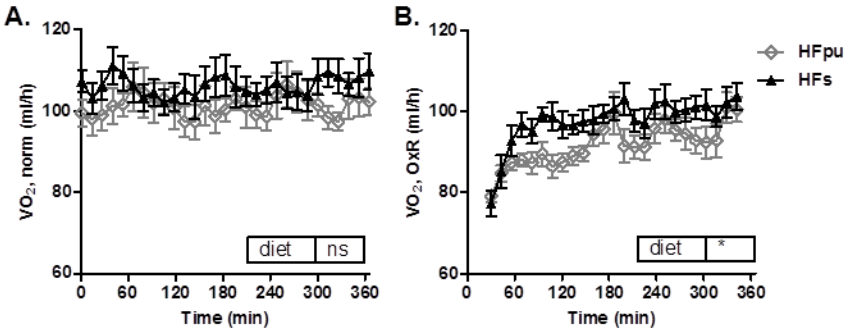

Figure 7 Oxygen consumption during normoxia and OxR. Mice fed the HFpu or HFs diet do not differ in resting oxygen consumption during normoxia (A), whereas HFs mice have a significantly higher oxygen consumption during OxR (B). Oxygen consumption was, in each condition, monitored during the same period in the light phase, when mice are at rest and fasted. (data from chapter 5)

OxR, glucose metabolism and acylcarnitines

To further investigate the effect of OxR on mitochondrial substrate use and glycolytic metabolism, we measured circulating levels of glucose, lactate and acylcarnitines. Acute OxR was previously shown to increase blood glucose and insulin levels in mice (66, 72). Blood glucose levels are expected to increase because of gluconeogenesis from lactate to glucose by the liver (12), but it is also proposed that hypoxia decreases insulin sensitivity (37, 70, 72) and thereby increases blood glucose and insulin levels.

Lactate release by e.g. adipocytes increases upon exposure to OxR as a consequence of anaerobic metabolism (92).
Blood levels of free carnitine and acylcarnitines are seen as a marker for hypoxia (5, 8, 83). Acylcarnitine levels increase when oxygen availability is limited and represent incomplete mitochondrial FA oxidation, whereas free carnitine levels decrease during OxR, leading to a decrease in mitochondrial uptake of fatty acids (50, 51, 62).
Our studies confirmed that OxR increases blood glucose levels. The largest increase in blood glucose levels was seen in the LF-fed mice in **chapter 4**, which suggests that the response in blood glucose might serve as a reliable marker for metabolic flexibility. Although the response in blood glucose levels seems to decline with increasing age and/or adiposity, mice fed a HF-diet with PUFAs (HFpu) did not increase blood glucose upon OxR, whereas mice fed a high fat diet with saturated fatty acids (HFs), that displayed a reduced metabolic flexibility, did (**chapter 5**). Based on these results, glucose levels after OxR are not recommended as a marker for metabolic flexibility when using OxR as a challenge test. Serum lactate levels were found to be increased by OxR in **chapter 3**, which confirms that a switch to glycolytic metabolism is used as a strategy to reduce VO_2. These results could, however, not be confirmed in **chapter 4**, where no significant differences were found between serum lactate levels of mice that were exposed to OxR and mice that remained in normal air. One explanation for this discrepancy might be that in chapter 3, mice were anaesthetized in hypoxic air before decapitation, whereas mice in chapter 4 were not anaesthetized prior to decapitation, which slightly prolonged the time spend in normoxic air before blood collection. Whether the very short exposure to normoxic air (around 15 to 30 seconds) prior to decapitation can revert increased lactate levels back to normal values remains to be studied.
Finally, we showed that OxR increases serum long acylcarnitines and decreases free carnitine, whereas it increased levels of short-chain acylcarnitines in WAT. The increase in circulating acylcarnitines indicates a decrease in mitochondrial FA oxidation at whole body level (50, 51, 62). The increase in short chain acylcarnitines in WAT, on the other hand, indicates increased protein catabolism. Autophagy and protein catabolism were previously shown to be induced by acute hypoxia in muscle (58), and may contribute to the reduction in oxygen consumption at whole body level. Tissue and serum levels of (acyl)carnitine levels in response to OxR were not yet compared between different dietary groups, but this is an interesting topic for further research that may reveal whether inhibition of mitochondrial FA oxidation is differently affected by OxR in mice with varying metabolic health states.

To summarize, OxR, which examines short term response to a limitation in oxygen availability, reduces whole body energy metabolism in mice. Next to the decrease in total (mitochondrial) energy expenditure, we found that OxR influenced mitochondrial fuel selection. The increase in serum lactate, glucose, and acylcarnitine levels, and the

slight increase in RER, indicate that OxR induces a switch from fatty acids to glucose oxidation and/ or an increase in anaerobic glycolytic metabolism. It is, as yet, unclear, which organ or organ system is responsible for the observed differences in glucose and fat metabolism. The whole genome expression analysis that was performed in **chapter 6** suggests that, in HF-fed mice, WAT plays only a minor role in whole-body adaptation to OxR.

Recommendations for further research

Based on the data described in this thesis, I would like to postulate that InCa-based challenge tests should become a standard procedure for the analysis of metabolic health. One important advantage is that InCa-based challenge tests are non-invasive, which decreases stress-related variation between animals. Moreover, the InCa-based challenge tests appeared to be more sensitive and integrative than the standard challenge tests, such as the oral glucose tolerance test.

Whole genome gene expression analysis proved to be a useful method to investigate the molecular background underlying changes in health status. Transcriptome analysis would, however, be more informative when combined with a challenge approach. Gene expression is often studied in a steady state: when mice are fasted. This steady state is expected to display animal physiology under normal conditions, but in principal it displays the animal that has switched to fatty acid oxidation. It would be an asset to nutrition-related research to compare whole-genome analysis between mice with different physiological states, depending on the focus of the study: e.g. fasted vs. fed or at thermoneutrality vs. room temperature (7). In the gene expression study described in **chapter 2**, for example, the inclusion of InCa and transcriptome analysis in WAT of HF-DR fed vs. HF-DR fasted and HF-AL fed vs. HF-AL fasted would have given us ultimate proof for the hypothesis that HF-DR mice have an improved ability to adequately respond to high dietary fat intake, including the underlying mechanisms.

Table 2 Contribution of different organs to basal metabolic rate in lean humans and rodents

	Organ weight (% of body weight)			**Metabolic rate (% of total)**		
Organ	Human ♂	Human ♀	Rat	Human ♂	Human ♀	Rat
Liver	2.6	2.4	5.0	21	21	20
Brain	2.0	2.1	1.5	20	21	3
Heart	0.5	0.4	0.5	9	8	3
Kidneys	0.4	0.5	0.9	8	9	7
Muscle	40.0	29.3	42.0	22	16	30
Adipose tissue	21.4	32.8	-	4	6	-
Other tissues	33.1	32.6	-	16	19	-
Total body weight	70 kg	58 kg	150 g			
Total EE (kcal/day)				1680	1340	-

Organ weight and metabolic rate of the reference male (♂), reference female (♀) and reference rat. Metabolic rate of adipose tissue was not supplied for the rat. (data from (48, 74))

It would also be interesting to use whole-genome analysis to verify whether high-fat feeding indeed blunts the transcriptional response in WAT during OxR compared to low-fat feeding, or to study the transcriptional response to OxR in other organs. WAT has, compared to other metabolic organs a low metabolic rate expressed per kg tissue and OxR might have more pronounced effects on organs that rely more on oxygen, such as skeletal muscle or the liver (also see table 2).

Finally, the non-invasiveness of InCa-based challenge tests qualifies them to be applied to study metabolic flexibility of humans. Humans might not achieve the large decrease in metabolic rate as was observed in mice (27), but it was previously shown that OxR significantly decreases blood oxygen saturation and CO_2 production (9, 27). Moreover, OxR increases blood glucose levels and alters glucose utilization in humans (46, 53, 65), which indicates that OxR also affects the metabolism of humans. The validation of OxR as a challenge test to measure metabolic health status in humans is a promising subject for further research.

References

1. Abate N, Garg A, Peshock RM, Stray-Gundersen J, Grundy SM Relationships of generalized and regional adiposity to insulin sensitivity in men. J Clin Invest. 1995;96: 88-98.
2. Ando H, Yanagihara H, Hayashi Y, Obi Y, Tsuruoka S, Takamura T*, et al.* Rhythmic messenger ribonucleic acid expression of clock genes and adipocytokines in mouse visceral adipose tissue. Endocrinology. 2005;146: 5631-5636.
3. Balcombe JP, Barnard ND, Sandusky C Laboratory routines cause animal stress. Contemp Top Lab Anim Sci. 2004;43: 42-51.
4. Bowman TA, Ramakrishnan SK, Kaw M, Lee SJ, Patel PR, Golla VK*, et al.* Caloric restriction reverses hepatic insulin resistance and steatosis in rats with low aerobic capacity. Endocrinology. 2010;151: 5157-5164.
5. Bruder ED, Raff H Cardiac and plasma lipid profiles in response to acute hypoxia in neonatal and young adult rats. Lipids Health Dis. 2010;9: 3.
6. Cai TQ, Ren N, Jin L, Cheng K, Kash S, Chen R*, et al.* Role of GPR81 in lactate-mediated reduction of adipose lipolysis. Biochem Biophys Res Commun. 2008;377: 987-991.
7. Caimari A, Oliver P, Keijer J, Palou A Peripheral blood mononuclear cells as a model to study the response of energy homeostasis-related genes to acute changes in feeding conditions. OMICS. 2010;14: 129-141.
8. Cam H, Yildirim B, Aydin A, Say A Carnitine levels in neonatal hypoxia. J Trop Pediatr. 2005;51: 106-108.
9. Charlot K, Pichon A, Richalet JP, Chapelot D Effects of a high-carbohydrate versus high-protein meal on acute responses to hypoxia at rest and exercise. Eur J Appl Physiol. 2013;113: 691-702.
10. Chattopadhyay M, GuhaThakurta I, Behera P, Ranjan KR, Khanna M, Mukhopadhyay S*, et al.* Mitochondrial bioenergetics is not impaired in nonobese subjects with type 2 diabetes mellitus. Metabolism-Clinical and Experimental. 2011;60: 1702-1710.
11. Chiolero R, Mavrocordatos P, Burnier P, Cayeux MC, Schindler C, Jequier E*, et al.* Effects of infused sodium acetate, sodium lactate, and sodium beta-hydroxybutyrate on energy expenditure and substrate oxidation rates in lean humans. Am J Clin Nutr. 1993;58: 608-613.
12. Choi JH, Park MJ, Kim KW, Choi YH, Park SH, An WG*, et al.* Molecular mechanism of hypoxia-mediated hepatic gluconeogenesis by transcriptional regulation. Febs Letters. 2005;579: 2795-2801.
13. Choo HJ, Kim JH, Kwon OB, Lee CS, Mun JY, Han SS*, et al.* Mitochondria are impaired in the adipocytes of type 2 diabetic mice. Diabetologia. 2006;49: 784-791.
14. Crunkhorn S, Dearie F, Mantzoros C, Gami H, da Silva WS, Espinoza D*, et al.* Peroxisome proliferator activator receptor gamma coactivator-1 expression is reduced in obesity - Potential pathogenic role of saturated fatty acids and p38 mitogen-activated protein kinase activation. Journal of Biological Chemistry. 2007;282: 15439-15450.
15. Dahlman I, Forsgren M, Sjogren A, Nordstrom EA, Kaaman M, Naslund E*, et al.* Downregulation of electron transport chain genes in visceral adipose tissue in type 2 diabetes independent of obesity and possibly involving tumor necrosis factor-alpha. Diabetes. 2006;55: 1792-1799.
16. Eissing L, Scherer T, Todter K, Knippschild U, Greve JW, Buurman WA*, et al.* De novo lipogenesis in human fat and liver is linked to ChREBP-beta and metabolic health. Nat Commun. 2013;4: 1528.
17. Festa A, D'Agostino R, Jr., Williams K, Karter AJ, Mayer-Davis EJ, Tracy RP*, et al.* The relation of body fat mass and distribution to markers of chronic inflammation. Int J Obes Relat Metab Disord. 2001;25: 1407-1415.
18. Flachs P, Ruhl R, Hensler M, Janovska P, Zouhar P, Kus V*, et al.* Synergistic induction of lipid catabolism and anti-inflammatory lipids in white fat of dietary obese mice in response to calorie restriction and n-3 fatty acids. Diabetologia. 2011;54: 2626-2638.
19. Frappell P, Lanthier C, Baudinette RV, Mortola JP Metabolism and ventilation in acute hypoxia: a comparative analysis in small mammalian species. Am J Physiol. 1992;262: R1040-1046.

20. Frayn KN, Langin D, Karpe F Fatty acid-induced mitochondrial uncoupling in adipocytes is not a promising target for treatment of insulin resistance unless adipocyte oxidative capacity is increased. Diabetologia. 2008;51: 394-397.
21. Froy O, Chapnik N Circadian oscillation of innate immunity components in mouse small intestine. Mol Immunol. 2007;44: 1954-1960.
22. Galgani JE, Moro C, Ravussin E Metabolic flexibility and insulin resistance. Am J Physiol Endocrinol Metab. 2008;295: E1009-1017.
23. Gastaldelli A, Cusi K, Pettiti M, Hardies J, Miyazaki Y, Berria R*, et al.* Relationship between hepatic/visceral fat and hepatic insulin resistance in nondiabetic and type 2 diabetic subjects. Gastroenterology. 2007;133: 496-506.
24. Gautier H Interactions among metabolic rate, hypoxia, and control of breathing. J Appl Physiol (1985). 1996;81: 521-527.
25. Gianotti TF, Sookoian S, Dieuzeide G, Garcia SI, Gemma C, Gonzalez CD*, et al.* A decreased mitochondrial DNA content is related to insulin resistance in adolescents. Obesity (Silver Spring). 2008;16: 1591-1595.
26. Gillooly JF, Brown JH, West GB, Savage VM, Charnov EL Effects of size and temperature on metabolic rate. Science. 2001;293: 2248-2251.
27. Golja P, Flander P, Klemenc M, Maver J, Princi T Carbohydrate ingestion improves oxygen delivery in acute hypoxia. High Alt Med Biol. 2008;9: 53-62.
28. Goossens GH, Bizzarri A, Venteclef N, Essers Y, Cleutjens JP, Konings E*, et al.* Increased adipose tissue oxygen tension in obese compared with lean men is accompanied by insulin resistance, impaired adipose tissue capillarization, and inflammation. Circulation. 2011;124: 67-76.
29. Gouspillou G, Hepple RT Facts and controversies in our understanding of how caloric restriction impacts the mitochondrion. Exp Gerontol. 2013;48: 1075-1084.
30. Heilbronn LK, Gan SK, Turner N, Campbell LV, Chisholm DJ Markers of mitochondrial biogenesis and metabolism are lower in overweight and obese insulin-resistant subjects. Journal of Clinical Endocrinology & Metabolism. 2007;92: 1467-1473.
31. Higami Y, Pugh TD, Page GP, Allison DB, Prolla TA, Weindruch R Adipose tissue energy metabolism: altered gene expression profile of mice subjected to long-term caloric restriction. FASEB J. 2004;18: 415-417.
32. Hill JR The Oxygen Consumption of New-Born and Adult Mammals - Its Dependence on the Oxygen Tension in the Inspired Air and on the Environmental Temperature. Journal of Physiology-London. 1959;149: 346-373.
33. Hoevenaars FP, Bekkenkamp-Grovenstein M, Janssen RJ, Heil SG, Bunschoten A, Hoek-van den Hil EF*, et al.* Thermoneutrality results in prominent diet-induced body weight differences in C57BL/6J mice, not paralleled by diet-induced metabolic differences. Mol Nutr Food Res. 2014;58: 799-807.
34. Hoevenaars FPM, Keijer J, Herreman L, Palm I, Hegeman MA, Swarts HJM*, et al.* Adipose tissue metabolism and inflammation are differently affected by weight loss in obese mice due to either a high-fat diet restriction or change to a low-fat diet. Genes and Nutrition. 2014;9:
35. Holmes LJ, Storlien LH, Smythe GA Hypothalamic monoamines associated with the cephalic phase insulin response. Am J Physiol. 1989;256: E236-241.
36. Horakova O, Medrikova D, van Schothorst EM, Bunschoten A, Flachs P, Kus V*, et al.* Preservation of metabolic flexibility in skeletal muscle by a combined use of n-3 PUFA and rosiglitazone in dietary obese mice. PLoS One. 2012;7: e43764.
37. Iiyori N, Alonso LC, Li J, Sanders MH, Garcia-Ocana A, O'Doherty RM*, et al.* Intermittent hypoxia causes insulin resistance in lean mice independent of autonomic activity. Am J Respir Crit Care Med. 2007;175: 851-857.
38. Kaaman M, Sparks LM, van Harmelen V, Smith SR, Sjolin E, Dahlman I*, et al.* Strong association between mitochondrial DNA copy number and lipogenesis in human white adipose tissue. Diabetologia. 2007;50: 2526-2533.
39. Kaiyala KJ, Morton GJ, Leroux BG, Ogimoto K, Wisse B, Schwartz MW Identification of body fat mass as a major determinant of metabolic rate in mice. Diabetes. 2010;59: 1657-1666.
40. Kakuma T, Wang ZW, Pan W, Unger RH, Zhou YT Role of leptin in peroxisome proliferator-activated receptor gamma coactivator-1 expression. Endocrinology. 2000;141: 4576-4582.
41. Karelis AD, Brochu M, Rabasa-Lhoret R Can we identify metabolically healthy but obese individuals (MHO)? Diabetes Metab. 2004;30: 569-572.

42. Katic M, Kennedy AR, Leykin I, Norris A, McGettrick A, Gesta S*, et al.* Mitochondrial gene expression and increased oxidative metabolism: role in increased lifespan of fat-specific insulin receptor knock-out mice. Aging Cell. 2007;6: 827-839.
43. Keller MP, Attie AD Physiological insights gained from gene expression analysis in obesity and diabetes. Annu Rev Nutr. 2010;30: 341-364.
44. Kelley DE, Mandarino LJ Fuel selection in human skeletal muscle in insulin resistance: a reexamination. Diabetes. 2000;49: 677-683.
45. Kelley DE, Mandarino LJ Hyperglycemia normalizes insulin-stimulated skeletal muscle glucose oxidation and storage in noninsulin-dependent diabetes mellitus. J Clin Invest. 1990;86: 1999-2007.
46. Kelly KR, Williamson DL, Fealy CE, Kriz DA, Krishnan RK, Huang H*, et al.* Acute altitude-induced hypoxia suppresses plasma glucose and leptin in healthy humans. Metabolism. 2010;59: 200-205.
47. Kim JW, Tchernyshyov I, Semenza GL, Dang CV HIF-1-mediated expression of pyruvate dehydrogenase kinase: a metabolic switch required for cellular adaptation to hypoxia. Cell Metab. 2006;3: 177-185.
48. Kinney JM. Energy metabolism: tissue determinants and cellular corollaries; 1992.
49. Korach-Andre M, Parini P, Larsson L, Arner A, Steffensen KR, Gustafsson JA Separate and overlapping metabolic functions of LXR alpha and LXR beta in C57Bl/6 female mice. American Journal of Physiology-Endocrinology and Metabolism. 2010;298: E167-E178.
50. Koves TR, Li P, An J, Akimoto T, Slentz D, Ilkayeva O*, et al.* Peroxisome proliferator-activated receptor-gamma co-activator 1 alpha-mediated metabolic remodeling of skeletal myocytes mimics exercise training and reverses lipid-induced mitochondrial inefficiency. Journal of Biological Chemistry. 2005;280: 33588-33598.
51. Koves TR, Ussher JR, Noland RC, Slentz D, Mosedale M, Ilkayeva O*, et al.* Mitochondrial overload and incomplete fatty acid oxidation contribute to skeletal muscle insulin resistance. Cell Metab. 2008;7: 45-56.
52. Kusminski CM, Scherer PE Mitochondrial dysfunction in white adipose tissue. Trends in Endocrinology and Metabolism. 2012;23: 435-443.
53. Larsen JJ, Hansen JM, Olsen NV, Galbo H, Dela F The effect of altitude hypoxia on glucose homeostasis in men. J Physiol. 1997;504 (Pt 1): 241-249.
54. Lee CK, Klopp RG, Weindruch R, Prolla TA Gene expression profile of aging and its retardation by caloric restriction. Science. 1999;285: 1390-1393.
55. Levine JA, Eberhardt NL, Jensen MD Role of nonexercise activity thermogenesis in resistance to fat gain in humans. Science. 1999;283: 212-214.
56. Livesey G, Elia M Estimation of energy expenditure, net carbohydrate utilization, and net fat oxidation and synthesis by indirect calorimetry: evaluation of errors with special reference to the detailed composition of fuels. Am J Clin Nutr. 1988;47: 608-628.
57. Magalhaes J, Ascensao A, Soares JM, Ferreira R, Neuparth MJ, Marques F*, et al.* Acute and severe hypobaric hypoxia increases oxidative stress and impairs mitochondrial function in mouse skeletal muscle. J Appl Physiol (1985). 2005;99: 1247-1253.
58. Masschelein E, Van Thienen R, D'Hulst G, Hespel P, Thomis M, Deldicque L Acute environmental hypoxia induces LC3 lipidation in a genotype-dependent manner. FASEB J. 2014;28: 1022-1034.
59. Mazzatti D, Lim FL, O'Hara A, Wood IS, Trayhurn P A microarray analysis of the hypoxia-induced modulation of gene expression in human adipocytes. Arch Physiol Biochem. 2012;118: 112-120.
60. Mootha VK, Lindgren CM, Eriksson KF, Subramanian A, Sihag S, Lehar J*, et al.* PGC-1 alpha-responsive genes involved in oxidative phosphorylation are coordinately downregulated in human diabetes. Nature Genetics. 2003;34: 267-273.
61. Mortola JP Implications of hypoxic hypometabolism during mammalian ontogenesis. Respir Physiol Neurobiol. 2004;141: 345-356.
62. Muoio DM, Newgard CB Molecular and metabolic mechanisms of insulin resistance and beta-cell failure in type 2 diabetes. Nature Reviews Molecular Cell Biology. 2008;9: 193-205.
63. Neel JV The "thrifty genotype" in 1998. Nutr Rev. 1999;57: S2-9.
64. Nelson BD Thyroid hormone regulation of mitochondrial function. Comments on the mechanism of signal transduction. Biochim Biophys Acta. 1990;1018: 275-277.

65. Oltmanns KM, Gehring H, Rudolf S, Schultes B, Rook S, Schweiger U*, et al.* Hypoxia causes glucose intolerance in humans. Am J Respir Crit Care Med. 2004;169: 1231-1237.
66. Ostreicher I, Meissner U, Plank C, Allabauer I, Castrop H, Rascher W*, et al.* Altered leptin secretion in hyperinsulinemic mice under hypoxic conditions. Regul Pept. 2009;153: 25-29.
67. Papandreou I, Cairns RA, Fontana L, Lim AL, Denko NC HIF-1 mediates adaptation to hypoxia by actively downregulating mitochondrial oxygen consumption. Cell Metab. 2006;3: 187-197.
68. Patti ME, Corvera S The role of mitochondria in the pathogenesis of type 2 diabetes. Endocr Rev. 2010;31: 364-395.
69. Raffaello A, Rizzuto R Mitochondrial longevity pathways. Biochim Biophys Acta. 2011;1813: 260-268.
70. Regazzetti C, Peraldi P, Gremeaux T, Najem-Lendom R, Ben-Sahra I, Cormont M*, et al.* Hypoxia decreases insulin signaling pathways in adipocytes. Diabetes. 2009;58: 95-103.
71. Reimer RA, Maurer AD, Lau DC, Auer RN Long-term dietary restriction influences plasma ghrelin and GOAT mRNA level in rats. Physiol Behav. 2010;99: 605-610.
72. Reinke C, Bevans-Fonti S, Drager LF, Shin MK, Polotsky VY Effects of different acute hypoxic regimens on tissue oxygen profiles and metabolic outcomes. J Appl Physiol (1985). 2011;111: 881-890.
73. Robinson KA, Haymes EM Metabolic effects of exposure to hypoxia plus cold at rest and during exercise in humans. J Appl Physiol (1985). 1990;68: 720-725.
74. Rolfe DF, Brown GC Cellular energy utilization and molecular origin of standard metabolic rate in mammals. Physiological Reviews. 1997;77: 731-758.
75. Rong JX, Qiu Y, Hansen MK, Zhu L, Zhang V, Xie M*, et al.* Adipose mitochondrial biogenesis is suppressed in db/db and high-fat diet-fed mice and improved by rosiglitazone. Diabetes. 2007;56: 1751-1760.
76. Schneider BS, Faust IM, Hemmes R, Hirsch J Effects of Altered Adipose-Tissue Morphology on Plasma-Insulin Levels in the Rat. American Journal of Physiology. 1981;240: E358-E362.
77. Seggie JA, Brown GM Stress response patterns of plasma corticosterone, prolactin, and growth hormone in the rat, following handling or exposure to novel environment. Can J Physiol Pharmacol. 1975;53: 629-637.
78. Semenza GL, Roth PH, Fang HM, Wang GL Transcriptional regulation of genes encoding glycolytic enzymes by hypoxia-inducible factor 1. Journal of Biological Chemistry. 1994;269: 23757-23763.
79. Semple RK, Crowley VC, Sewter CP, Laudes M, Christodoulides C, Considine RV*, et al.* Expression of the thermogenic nuclear hormone receptor coactivator PGC-1 alpha is reduced in the adipose tissue of morbidly obese subjects. International Journal of Obesity. 2004;28: 176-179.
80. Shabalina IG, Hoeks J, Kramarova TV, Schrauwen P, Cannon B, Nedergaard J Cold tolerance of UCP1-ablated mice: a skeletal muscle mitochondria switch toward lipid oxidation with marked UCP3 up-regulation not associated with increased basal, fatty acid- or ROS-induced uncoupling or enhanced GDP effects. Biochim Biophys Acta. 2010;1797: 968-980.
81. Sherman H, Genzer Y, Cohen R, Chapnik N, Madar Z, Froy O Timed high-fat diet resets circadian metabolism and prevents obesity. FASEB J. 2012;26: 3493-3502.
82. Sjogren P, Sierra-Johnson J, Gertow K, Rosell M, Vessby B, de Faire U*, et al.* Fatty acid desaturases in human adipose tissue: relationships between gene expression, desaturation indexes and insulin resistance. Diabetologia. 2008;51: 328-335.
83. Solberg R, Enot D, Deigner HP, Koal T, Scholl-Burgi S, Saugstad OD*, et al.* Metabolomic analyses of plasma reveals new insights into asphyxia and resuscitation in pigs. PLoS One. 2010;5: e9606.
84. Sutherland LN, Capozzi LC, Turchinsky NJ, Bell RC, Wright DC Time course of high-fat diet-induced reductions in adipose tissue mitochondrial proteins: potential mechanisms and the relationship to glucose intolerance. Am J Physiol Endocrinol Metab. 2008;295: E1076-1083.
85. Tabata H, Kitamura T, Nagamatsu N Comparison of effects of restraint, cage transportation, anaesthesia and repeated bleeding on plasma glucose levels between mice and rats. Lab Anim. 1998;32: 143-148.
86. Trayhurn P, James WP Thermoregulation and non-shivering thermogenesis in the genetically obese (ob/ob) mouse. Pflugers Arch. 1978;373: 189-193.
87. Tuli JS, Smith JA, Morton DB Corticosterone, adrenal and spleen weight in mice after tail bleeding, and its effect on nearby animals. Lab Anim. 1995;29: 90-95.

88. Urakawa H, Katsuki A, Sumida Y, Gabazza EC, Murashima S, Morioka K, *et al.* Oxidative stress is associated with adiposity and insulin resistance in men. J Clin Endocrinol Metab. 2003;88: 4673-4676.
89. Wanders D, Graff EC, Judd RL Effects of high fat diet on GPR109A and GPR81 gene expression. Biochem Biophys Res Commun. 2012;425: 278-283.
90. Weindruch R The retardation of aging by caloric restriction: studies in rodents and primates. Toxicol Pathol. 1996;24: 742-745.
91. Weyer C, Foley JE, Bogardus C, Tataranni PA, Pratley RE Enlarged subcutaneous abdominal adipocyte size, but not obesity itself, predicts Type II diabetes independent of insulin resistance. Diabetologia. 2000;43: 1498-1506.
92. Wood IS, Stezhka T, Trayhurn P Modulation of adipokine production, glucose uptake and lactate release in human adipocytes by small changes in oxygen tension. Pflugers Arch. 2011;462: 469-477.
93. Wu Z, Puigserver P, Andersson U, Zhang C, Adelmant G, Mootha V, *et al.* Mechanisms controlling mitochondrial biogenesis and respiration through the thermogenic coactivator PGC-1. Cell. 1999;98: 115-124.
94. Zhou YT, Wang ZW, Higa M, Newgard CB, Unger RH Reversing adipocyte differentiation: implications for treatment of obesity. Proc Natl Acad Sci U S A. 1999;96: 2391-2395.

Appendices

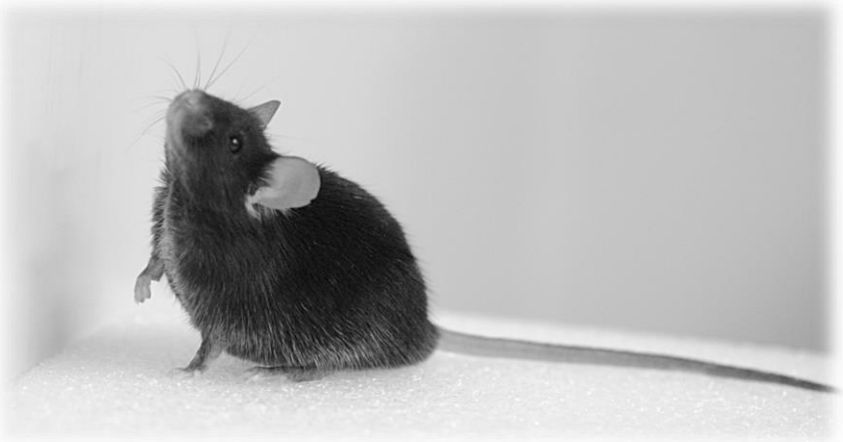

Summary of main findings

Maintenance of metabolic health not only ensures that energy is made available in times of need and stored in times of excess, but also prevents resistance to nutritional cues, ectopic lipid accumulation and dysfunction of metabolic organs. The proportion of humans that is at risk for reduced metabolic health increases worldwide due to the current epidemic of obesity and the increase in both mean and maximum life span. Better understanding of the various factors that influence metabolic health may offer opportunities to fight this threat to human health. This thesis aims to assess metabolic health using transcriptome analysis and non-invasive challenge tests. Special focus is on the development and validation of InCa-based non-invasive challenge tests. In most chapters of this thesis white adipose tissue (WAT) formed the major organ of interest because of its key role in whole-body energy homeostasis. WAT function was, among others, studied with whole-genome gene expression analysis, which, compared to single parameter analysis, extends the scale and depth of understanding biological processes.
Metabolic health was also quantified as metabolic flexibility, with the use of non-invasive, indirect calorimetry (InCa) based challenge tests. One of the InCa based challenge tests described in this thesis, the oxygen restriction (OxR) challenge, is a novel approach to investigate metabolic flexibility in mice. In each study, OxR was applied acute ($[O_2]$ reduction within 30 minutes) and for a short period of 6 hours in fasted mice. The other two InCa-based challenge tests: fasting and re-feeding and fasting and glucose consumption are nutrient-based and were described previously, although in different formats and settings.

In **chapter 2** we demonstrate that dietary restriction on a high-fat diet (HF-DR) improves metabolic health of mice compared with mice receiving the same diet on an *ad libitum* basis (HF-AL). Already after five weeks of restriction, the serum levels of cholesterol and leptin were significantly decreased in HF-DR mice, whereas their glucose tolerance and serum adiponectin levels were increased. The body weight and measured serum parameters remained stable in the following 7 weeks of restriction, implying metabolic adaptation. To understand the molecular events associated with this adaptation, we analysed gene expression in WAT with whole genome microarrays. HF-DR strongly influenced gene expression in WAT; in total, 8643 genes were differentially expressed between both groups of mice, with a major role for genes involved in lipid metabolism and mitochondrial functioning. DR also increases mitochondrial density in WAT. These results show that WAT, indeed, has an important role in the improvement of metabolic health of dietary restricted mice and suggest that the development of substrate efficiency plays an important role in the observed changes in health status. Finally, mitochondrial density might be used as a marker for WAT health status.

Chapter 3 shows how indirect calorimetry can be used to noninvasively assess metabolic and age-related flexibility in mice. In this study, we tested the sensitivity and response stability over time of three InCa-based treatments in old versus adult mice. For the first treatment, diurnal patterns of respiratory exchange ratio were followed for 24 hours under standard conditions. For the second and third treatment, which were both based on a challenge approach, mice were fasted and either received a glucose bolus to test switch-effectiveness from fat to glucose oxidation (Treatment 2), or were exposed to oxygen restriction (OxR, Treatment 3) in the InCa system, which was introduced as a novel approach to asses metabolic flexibility. Opposite to the mice that were dietary restricted (chapter 2), aging appeared to increase adiposity and decrease WAT mitochondrial density, which further suggests that WAT mitochondrial density might be used as a marker for WAT health. We observed that the test results of the first treatment were not stable between test periods, possibly because of behavioural differences within the group of old mice between both measurements. For the second treatment, no differences between groups were observed. With Treatment 3, however, stable significant differences could be detected: old mice did not maintain reduced oxygen consumption under OxR during both measurements, whereas adult mice did. Further biochemical and gene expression analyses showed that OxR affected glucose and lactate homeostasis in liver and WAT of adult mice, supporting the observed differences in oxygen consumption. This was the first study to show that InCa analysis of the response to OxR is a sensitive and reproducible treatment to noninvasively measure age-impaired metabolic health in mice. Evaluation of metabolic health under non-challenged conditions may be confounded by behavioural-induced variation between animals

The study described in **chapter 4** followed up on the promising results that were obtained with the OxR challenge in chapter 3. In this study we tested whether OxR can also be used to reveal diet-induced health effects in an early stage. Early detection of diet-induced health effects might shorten animal experiments and reduce costs and age-related variation. Timely identification may increase options for reversal. Mice were exposed to a low-fat (LF) or high-fat (HF) diet for only 5 days, after which they were exposed to OxR or remained under normoxic conditions. The response to OxR was assessed by calorimetric measurements, followed by analysis of gene expression in liver and WAT. A novelty described in this chapter was the analysis of serum markers for protein glycation and oxidation, to detect differences in the response to OxR between LF and HF mice. Although HF feeding increased body weight, HF and LF mice did not differ in indirect calorimetric values under normoxic conditions and in a fasting state. Exposure to OxR however, increased oxygen consumption and lipid oxidation in HF mice versus LF mice. Furthermore, OxR induced gluconeogenesis and an antioxidant response in the liver of HF mice, whereas it induced de novo lipogenesis and an antioxidant response in eWAT of LF mice, indicating that HF and LF mice

differed in their adaptation to OxR. OxR also increased serum markers of protein glycation and oxidation in HF mice, whereas these changes were absent in LF mice. From this study we concluded that OxR is a promising new method to test food products on potential beneficial effects for metabolic health.

The study described in **chapter 5** aimed to assess differences in metabolic health of mice on iso-caloric diets differing in fatty acid composition using the OxR challenge. We also implemented a fasting and re-feeding challenge. One diet, the HFpu diet, predominantly contained poly-unsaturated fatty acids (PUFAs), which are considered to be healthier than saturated fatty acids (SFAs) that mainly made up the fat component of the second diet, the HFs diet. Since health effects of fatty acids also depend on the ratio of dietary omega-6 to omega-3 PUFAs (n6/n3 ratio), this ratio was kept similar between both diets. Mice received the isocaloric high-fat diets for six months, during and after which several biomarkers for health were measured. We found that HFpu and HFs diets only induce minor differences in static health markers: HFpu and HFs mice did not differ in body weight, total adiposity, adipose tissue health, serum adipokines, whole body energy balance, or circadian rhythm. HFpu and HFs mice also had a similar glucose tolerance, even though HFs mice had more triglycerides in liver and skeletal muscle and larger adipocytes in the eWAT depot. Interestingly, HFs mice were less flexible in their response to both fasting and re-feeding and OxR, which shows the relevance and sensitivity of InCa-based challenge tests. We concluded that InCa-based challenge tests are a valuable contribution to the analysis of metabolic health in mice. Challenge tests in the InCa system may, furthermore, reveal relevant consequences of small changes in metabolic health status, such as adipocyte hypertrophy or ectopic lipid storage.

Chapter 6 describes an in-depth study to the response to OxR both at whole body level using InCa and serum metabolomics (amino acids and (acyl)carnitines) and at WAT level using transcriptomics and the analysis of amino acid and (acyl)carnitine levels. Serum and tissue amino acids levels indicate the level of protein catabolism and certain amino acids are, typically, increased in obese individuals. Serum and tissue (acyl)carnitine levels indicate the rate and completeness of mitochondrial fatty acid oxidation; serum acylcarnitine levels are significantly increased in individuals that suffer from ambient oxygen restriction. The metabolic adaptation to OxR was studied in diet-induced moderately obese mice that received a high-fat diet (HFpu diet, as in chapter 5) for 6 weeks, which is expected to lead to WAT expansion and possibly to reduce oxygen availability in WAT. We found that OxR reduced mitochondrial oxidation at whole-body level, as shown by a reduction in whole-body oxygen consumption and an increase in serum long-chain acylcarnitine levels. WAT did not seem to contribute to this serum profile, since only short-chain acylcarnitines were increased in WAT and gene expression analysis indicated an increase in mitochondrial oxidation, based on

coordinate down-regulation of *Sirt4*, *Gpam* and *Chchd3/Minos3*. In addition, OxR did not induce oxidative stress in WAT, but increased molecular pathways involved in cell growth and proliferation. OxR increased levels of tyrosine, lysine and ornithine in serum and of leucine/isoleucine in WAT. This study shows that OxR limits oxidative phosphorylation at whole-body level, but in WAT compensatory mechanisms seem to operate. The down-regulation of the mitochondria-related genes *Sirt4*, *Gpam,* and *Chchd3* may be considered as a biomarker profile for WAT mitochondrial reprogramming in response to acute exposure to limited oxygen availability.

To conclude, the work presented in this thesis provides more insight in the analysis of metabolic health in mice with the use of transcriptome analysis and InCa-based challenge tests. We show that non-invasive tests using the InCa-system are more likely to reveal differences in metabolic flexibility than invasive challenge tests, such as the oral glucose tolerance test. Furthermore, we show that the challenge approach is more sensitive than analysis of metabolic health under non-challenged (free-feeding) conditions. Transcriptome analysis proved to be very valuable to provide in-depth molecular understanding of the mechanisms underlying reduced or improved metabolic health. Ideally, transciptomic or metabolomic approaches should be integrated with InCa-based challenge tests to further extent physiological understanding of diet-induced health effects.

Samenvatting

Metabole gezondheid is het vermogen om metabole processen steeds adequaat aan te passen aan veranderingen in de omgeving. Vetweefsel speelt een belangrijke rol in het behoud van metabole gezondheid. Gezond vetweefsel zorgt ervoor dat er energie wordt vrij gemaakt in tijden van schaarste en dat energie wordt opgeslagen in tijden van overvloed. Gezond vetweefsel voorkomt ook dat het lichaam ongevoelig wordt voor voedingsgerelateerde signalen en dat vet wordt opgeslagen in andere organen.
Door de wereldwijde toename van overgewicht en obesitas, maar ook door de toename van de gemiddelde en de maximale levensduur, neemt de kans op een zwakke metabole gezondheid toe. Verlaagde metabole gezondheid kan leiden tot ernstige fysieke problemen, zoals diabetes type 2 en hart- en vaatziekten. Om te voorkomen dat veel mensen hier last van krijgen, is het belangrijk om onderzoek te doen naar de factoren die metabole gezondheid kunnen beïnvloeden.
Het doel van het onderzoek beschreven in dit proefschrift, was om metabole gezondheid te onderzoeken met behulp van transcriptoom analyse en met niet-invasieve challenge-testen. Hiervoor werd de muis gebruikt als model voor de mens.
Transcriptoom analyse is een methode waarmee de expressie van alle genen in een bepaald weefsel op een bepaald tijdstip gemeten kan worden. Veranderingen in genexpressie leiden tot veranderingen in de hoeveelheid gecodeerde eiwitten. Dit kan bijvoorbeeld de activiteit van het weefsel veranderen en laat zien hoe het weefsel reageert op een bepaald dieet. In dit onderzoek ging de interesse met name uit naar genexpressie in wit vetweefsel (white adipose tissue; WAT).
Met een challenge-test wordt gemeten in hoeverre het lichaam zich op korte termijn kan aanpassen aan veranderingen in het lichaam of in de omgeving, zoals veranderingen in de aanwezigheid van voedsel, of in de omgevingstemperatuur. Een challenge-test meet hoe flexibel het lichaam is; een gezonde muis kan zich goed aanpassen aan de 'challenge' en voorkomt op deze manier problemen op weefselniveau. Metabole flexibiliteit kan worden gezien als een maat voor metabole gezondheid. De challenge-test maakt op deze manier verschillen in metabole gezondheid zichtbaar die onder normale omstandigheden verborgen blijven.
Voor het onderzoek beschreven in dit proefschrift hebben we metabole flexibiliteit bepaald met twee eerder beschreven challenge-testen: vasten gevolgd door voedselconsumptie en vasten gevolgd door glucoseconsumptie.
Tijdens vasten vertrouwt het lichaam voornamelijk op vetverbranding, terwijl het tijdens voedselconsumptie over moet stappen op koolhydraatverbranding. De efficiëntie van deze overgang is een belangrijke maat voor metabole flexibiliteit.
Beide testen zijn gebaseerd op de veel gebruikte orale glucose tolerantie test. Een groot verschil is dat we voor onze studies geen gebruik hebben gemaakt van invasieve methodes maar de respons op de challenge hebben geanalyseerd met InCa-metingen. De inzet van InCa maakte het mogelijke om niet-invasief het hele proces van metabole

omschakeling te analyseren, wat mogelijk leidt tot een gevoeligere en nauwkeurigere bepaling van metabole gezondheid.
Naast de twee eerder beschreven challenge testen, hebben we ook een nieuwe challenge-test ontwikkeld, waarbij de hoeveelheid zuurstof in de lucht wordt verlaagd (oxygen restriction; OxR). Zuurstof is, net als nutriënten, essentieel voor mitochondriële activiteit en een verlaging in zuurstofbeschikbaarheid vraagt dus om adequate metabole adaptatie om goed te kunnen blijven functioneren.

In **Hoofdstuk 2** beschrijf ik dat de metabole gezondheid van muizen sterk verbeterd kan worden door dieetrestrictie, zelfs terwijl deze restrictie plaats vindt met een, in principe ongezond, hoog-vet dieet (high-fat dietary restriction; HF-DR). Al na 5 weken restrictie hadden HF-DR-muizen lagere serum cholesterol- en leptinewaarden, een betere glucosetolerantie en hogere serum adiponectinewaarden, ten opzichte van muizen die *ad libitum* (HF-AL) van het dieet konden eten. Het lichaamsgewicht van de HF-DR-muizen nam eerst af, maar na 5 weken restrictie bleef het lichaamsgewicht stabiel, net als de eerder genoemde gezondheidsmarkers. Het ontstaan van de stabiele fase geeft aan dat het metabolisme van HF-DR-muizen zich dusdanig heeft aangepast, dat het goed gedijt onder het gebruikte voedingsregime.
Om het mechanisme achter deze aanpassing te begrijpen, hebben we de veranderingen in genexpressie in wit vetweefsel geanalyseerd met transcriptoom analyse. In totaal waren 8643 genen verschillend gereguleerd tussen HF-DR- en HF-AL-muizen. Een groot deel van deze genen was betrokken bij vet metabolisme en mitochondriële functie. Dieetrestrictie verhoogde ook de mitochondriële dichtheid in WAT.
Deze studie suggereert dat dieetrestrictie leidt tot een efficiënter gebruik van specifieke componenten van het dieet; in dit geval de grote hoeveelheid vet in het dieet. Tenslotte zou mitochondriële dichtheid kunnen worden gebruikt als maat voor de gezondheidstoestand van vetweefsel.

Hoofdstuk 3 beschrijft 3 methodes waarop indirecte calorimetrie kan worden ingezet om niet-invasief de metabole flexibiliteit van muizen te meten. Tevens beschrijven we de meetgevoeligheid van de drie methodes en de stabiliteit van de testresultaten tussen twee afzonderlijke meetmomenten. Metabole gezondheid werd bepaald in oude muizen ten opzichte van volwassen muizen. Voor de eerste behandeling werd het dagelijkse patroon van substraatverbruik gevolgd, gedurende 24 uur onder standaardomstandigheden. De tweede en derde behandeling waren beide gebaseerd op een challenge: muizen werden eerst gevast en kregen dan een glucose bolus, of werden blootgesteld aan OxR.
De oude muizen hadden meer vetweefsel en een lagere mitochondriële dichtheid in WAT, vergeleken met volwassen muizen. Dit is een volgende aanwijzing dat mitochondriële dichtheid in WAT gebruikt kan worden als marker voor de

gezondheidsstaat van vetweefsel. De resultaten van de eerste behandeling waren niet stabiel tussen de twee testmomenten, mogelijk door gedragsveranderingen binnen de groep oude muizen.
Met de tweede behandeling werden geen verschillen tussen de twee groepen waargenomen. Behandeling 3, daarentegen, toonde wel significante verschillen aan tussen de oude en volwassen muizen: de volwassen muizen verlaagden hun zuurstofconsumptie tijdens de gehele periode van OxR (6 uur), terwijl de oude muizen dit alleen gedurende het begin van de blootstelling 'volhielden'.
Uit verdere biochemische analyses en analyse van genexpressie in lever en WAT van de volwassen muizen, bleek dat OxR invloed heeft op de glucose en lactaat homeostase, wat mogelijk de waargenomen verlaging in zuurstofverbruik kan verklaren.
Dit is de eerste studie, die aantoont dat OxR in combinatie met InCa een gevoelige en reproduceerbare challenge oplevert, om leeftijdsgebonden veranderingen in metabole gezondheid bij muizen aan te tonen. Verder laat het zien dat InCa-metingen waarbij geen gebruik wordt gemaakt van een challenge-aanpak kunnen worden verstoord door gedragsgeïnduceerde variatie tussen dieren.

De studie beschreven in **hoofdstuk 4** haakt in op de veelbelovende resultaten die werden behaald met de OxR-challenge beschreven in hoofdstuk 3. In deze studie wilden we achterhalen of OxR ook gebruikt kan worden om kleinere, dieet-geïnduceerde gezondheidseffecten aan te tonen in een vroeg stadium van een dierstudie. Als dergelijke gezondheidseffecten eerder kunnen worden aangetoond, kunnen dierexperimenten mogelijk worden verkort, wat weer leidt tot kostenverlaging en minder leeftijdsgebonden variatie tussen dieren. Daarnaast biedt vroege detectie van gezondheidsrisico's meer mogelijkheden tot interventie van verdere gezondheidsproblemen. Voor dit experiment kregen muizen een laag-vet (LF) dieet of een hoog-vet (HF) dieet voor slechts 5 dagen. Daarna werd van beide groepen een deel blootgesteld aan OxR, terwijl het andere deel onder normoxie verbleef. De response op OxR werd gemeten met het InCa-systeem en aansluitend werd het effect op genexpressie in lever en WAT geanalyseerd. In deze studie werden ook markers voor eiwitglycatie en -oxidatie in serum bepaald, om te onderzoeken of er een verschil is in het ontstaan van oxidatieve stress tijdens OxR tussen HF- en LF-muizen.
Hoewel HF-muizen een verhoogd lichaamsgewicht hadden, waren er geen verschillen in substraatverbruik of zuurstofconsumptie onder normale (normoxische) omstandigheden. Tijdens de blootstelling aan OxR daarentegen, hadden HF-muizen een hogere zuurstofconsumptie en meer vetverbranding dan LF-muizen.
Ook de response in genexpressie was verschillend tussen HF- en LF-muizen: OxR verhoogde het proces van gluconeogenese en antioxidant respons in leverweefsel van HF- muizen, maar niet in LF-muizen, terwijl OxR in de LF-muizen leidde tot een

verhoging van *de novo* lipogenese en antioxidant respons in WAT, wat niet werd gezien in de HF-muizen.
OxR leidde ook tot een verhoging van serummarkers voor eiwitglycatie en -oxidatie in HF-muizen, terwijl deze verandering niet werd waargenomen in LF-muizen.
Uit deze studie kunnen we concluderen dat OxR een veelbelovende nieuwe methode is om potentiële gezondheidsbevorderende effecten van voeding aan te tonen.

Het doel van de studie beschreven in **hoofdstuk 5**, was om te bepalen of InCa-gebaseerde challenge-testen ook gebruikt kunnen worden, om verschillen in metabole gezondheid te bepalen, tussen muizen gevoed, met iso-calorische hoog-vet diëten met verschillende vetzuursamenstellingen. Hiervoor hebben we gebruik gemaakt van twee challenge-testen: de OxR-challenge en een challenge, die bestond uit vasten, gevolgd door dieetconsumptie.
Het ene dieet, het Hfpu-dieet, bevatte voornamelijk meervoudig onverzadigde vetzuren (PUFAs). Het tweede dieet, het HFs- dieet, bevatte voornamelijk verzadigde vetzuren (SFAs). PUFAs worden, ten opzichte van SFAs, als gezonder beschouwd. Gezondheidseffecten van een dieet worden ook bepaald door de ratio tussen omega-6 en omega-3 PUFAs (n6/n3 ratio). De n6/n3 ratio werd om deze reden gelijk gehouden tussen beide diëten.
De studie duurde in totaal 6 maanden en tijdens en na afloop van de studie werden steeds verschillende gezondheidsmarkers bepaald. Opvallend genoeg waren er niet veel verschillen tussen Hfpu- en HFs-muizen: beide groepen hadden een vergelijkbaar lichaamsgewicht, evenveel lichaamsvet en er waren geen verschillen in de gezondheidsstatus van vetweefsel, serum adipokines, glucosetolerantie, energieverbruik of circadiaan ritme.
HFs-muizen hadden echter wel meer vetopslag (triglyceriden) in hun lever en spierweefsel en grotere vetcellen in WAT, vergeleken met Hfpu-muizen. HFs-muizen bleken daarnaast minder flexibel in de respons op de vasten- en dieetconsumptie-challenge en de OxR- challenge, wat aantoont dat het HFs-dieet wel degelijk nadelige gezondheidseffecten heeft, ten opzichte van het Hfpu-dieet. Deze studie toont aan dat InCa-gebaseerde challenge-testen een waardevolle aanvulling zijn op de analyse van metabole gezondheid.

Er is tot op heden slechts weinig bekend over de acute metabole adaptatie aan kort durende zuurstofrestrictie. **Hoofdstuk 6** beschrijft daarom een studie waarin we de moleculaire respons op OxR verder hebben onderzocht, met behulp van metaboloom analyse van aminozuren en (acyl)carnitines in serum en wit vetweefsel, en transcriptoom analyse in wit vetweefsel. De niveaus van aminozuren in serum en vetweefsel zijn een maat voor het niveau van eiwitkatabolisme. Bepaalde aminozuren zijn, daarnaast, in verhoogde concentraties aanwezig in individuen met obesitas. Niveaus van (acyl)carnitines in serum en vetweefsel zijn een maat voor het niveau van

mitochondriële vetzuuroxidatie en geven tevens de volledigheid van vetzuuroxidatie weer. Zuurstofrestrictie leidt bijvoorbeeld tot een verhoging van de hoeveelheid acylcarnitines in serum, omdat mitochondriële oxidatie wordt beperkt.
De metabole adaptatie aan OxR werd onderzocht in diëet-geïnduceerde, matig obese muizen, die een hoog-vet dieet (HFpu dieet, als in hoofdstuk 5) ontvingen gedurende 6 weken. De verwachting was dat deze periode van dieetconsumptie zou leiden tot een toename van de hoeveelheid vetweefsel en daarmee mogelijk tot een verlaagde zuurstofspanning in vetweefsel.
OxR verlaagde, net zoals in de voorgaande studies, de zuurstofconsumptie op lichaamsniveau. OxR verhoogde ook de concentratie acylcarnitines (lange ketens) in serum. Hieruit kunnen we opmaken dat de mitochondriële oxidatie op lichaamsniveau omlaag gaat tijdens OxR. In WAT was alleen de concentratie van korte-keten acylcarnitines verhoogd en vonden we een afname in de expressie van drie genen, die betrokken zijn bij mitochondriële functie: *Sirt4*, *Gpam* and *Chchd3*/*Minos3*. Hieruit kunnen we opmaken dat WAT niet bijdraagt aan de verhoogde concentratie lange-keten acylcarnitines in serum en dat WAT eerder mitochondriële activiteit verhoogt, dan verlaagt tijdens de blootstelling aan OxR.
We vonden in WAT ook geen toename van oxidatieve stress, maar wel een toename in expressie van genen, die betrokken zijn bij celgroei en celdeling. OxR verhoogde de concentratie tyrosine, lysine and ornithine in serum en de concentratie van leucine/isoleucine in WAT.
Deze studie toont aan dat OxR de oxidatieve fosforylering op lichaamsniveau remt, maar WAT lijkt op een andere manier te compenseren voor de verlaging in zuurstofspanning. De verlaging in de expressie van de mitochondriële genen *Sirt4*, *Gpam,* and *Chchd3* kan beschouwd worden als een biomarkerprofiel voor mitochondriële herprogrammering in WAT, in reactie op een acute verlaging in zuurstofbeschikbaarheid.

De resultaten, beschreven in dit proefschrift, leveren meer inzicht in de analyse van metabole gezondheid bij muizen met behulp van transcriptoom analyse en InCa-gebaseerde challenge-testen. De InCa-gebaseerde challenge-testen bleken erg geschikt om verschillen in metabole gezondheid aan te tonen. De methodes beschreven in dit proefschrift leken zelfs gevoeliger dan methodes zonder challenge-concept en invasieve methodes, zoals een orale glucose tolerantie test. Daarnaast laten we zien dat OxR een veelbelovende nieuwe methode is om, voedingsonafhankelijk, metabole flexibiliteit in muizen te bepalen.
Transcriptoom analyse bleek erg waardevol om gedetailleerd moleculaire mechanismen achter verbeteringen of verslechteringen in metabole gezondheid in kaart te brengen. Idealiter zouden transcriptoom of metaboloom analyses worden gecombineerd met een challenge-aanpak om de fysiologie achter dieetgeïnduceerde gezondheidseffecten beter te begrijpen.

Dankwoord

Jaap en Evert, als promotor en co-promotor hebben jullie de eer om als eerste bedankt te worden. Ik heb dankzij jullie ontzettend veel geleerd de afgelopen 5 jaar. Ik had in het begin nogal de neiging om als het ware een hengeltje uit te gooien en maar af te wachten wat voor studieresultaten er binnen zouden komen. Ik vond eigenlijk alles wel interessant. Jullie hebben mij geleerd gerichter te werk te gaan en 1 duidelijke vraag op te stellen per experiment (en alle leuke en interessante zijweggetjes even te negeren). Dit heeft ontzettend veel geholpen bij het schrijven van publicaties en het bedenken van nieuwe experimenten; kortom, de reden dat dit boekje hier ligt. Ik wil jullie ook bedanken voor de vele overlegmomenten en de snelle en grondige feedback op mijn manuscripten.

Collega's van HAP, jullie hebben ervoor gezorgd dat ik het erg naar m'n zin heb gehad de afgelopen jaren. In eerste plaats bedankt voor alle gezellige pauzes, uitjes en etentjes! Daarnaast natuurlijk ook veel dank voor alle hulp bij mijn experimenten. Met name Hans, Inge en Annelies bedankt voor al jullie hulp en advies in het lab en bij de dierexperimenten.
Femke en Elise, ik ben blij dat we 5 jaar geleden zo ongeveer gelijk zijn begonnen. Bedankt voor alle gezellige intermezzo's in de AIO-kamer en fijn dat we zoveel aan elkaar hebben gehad om te 'overleven' als AIO.
Li and Wenbiao, thanks for bringing some change into the department. I really appreciated your alternative view and your sense of humour; and of course the Chinese lunches! Good luck with the completion of your thesis.
Marjanne, Lonneke en Jeske; we hebben niet zo heel lang samen kunnen werken, maar ik vond het wel gezellig dat laatste jaar in ons AIO-'gangetje'. Bedankt daarvoor en succes met jullie onderzoek!
I am also thankful for all the MSc students who contributed to my experiments. Dewi, Sanne, Davina, Junyi, Dylan, Esther, Sander, Wuhua and Dimitra; thanks for taking part of the experimental work out of my hands, and thanks for your 'fresh', unbiased ideas on the interpretation of study results.
Finally, I would like to thank the people from the BIOCLAIMS consortium. Our biannual meetings were not only very helpful to discuss scientific progress, but they also had a pleasant and open atmosphere. Thanks to our collaboration I got to know many kind PhD students and other scientists from your labs, which I really appreciated. I hope you will be able to keep on collaborating in the future.

Dan wat betreft het leven buiten het werk. Ik vind het fijn dat ik op deze manier familie en vrienden kan bedanken voor wat ze voor mij betekenen. Jullie hebben inhoudelijk

dan wel niets bijgedragen aan dit proefschrift maar waren wel onmisbaar in het kader daaromheen.
Kim, Inge en Laura; jullie zijn zo veel meer dan alleen jaarclubgenoten. Bedankt voor alle komische momenten, de goede gesprekken en de vele gezellige avondjes, ik hoop dat er nog veel mogen volgen.
Marianne en Susan, ik geloof dat we de afgelopen jaren, alles bij elkaar opgeteld, wel meer dan 900 kilometer samen hebben bewandeld. Dit was werkelijke de perfecte ontspanning na een drukke werkweek en jullie waren daarbij het beste gezelschap. Ik hoop dat we dat nog lang vol blijven houden.
Lieke, Kim en Ilke, ik ken jullie al sinds de basisschool en de middelbare school; SHINTO-ouwe lullen, jullie hebben mijn studententijd zoveel leuker gemaakt: jullie allen bedankt voor alle leuke uitstapjes, weekendjes en etentjes de afgelopen jaren! We zien elkaar niet altijd even frequent, maar als we bij elkaar zijn, is het altijd gezellig.
In het bijzonder wil ik mijn ouders, Bert en Marja Duivenvoorde, maar ook Gijs en Jolien, en de familie van Mark, bedanken. Bedankt voor alle steun, zorg en belangstelling! Wat fijn dat jullie mij af en toe eens uit lieten leggen waarom ik dat nu eigenlijk allemaal deed met die muizen; ik merk dat dat ook belangrijk was om gemotiveerd te blijven. Papa en mama, ik merk nu dankzij Thomas hoeveel invloed je eigenlijk hebt op de capaciteiten van je kind. Dankzij jullie had ik de nieuwsgierigheid, creativiteit en het doorzettingsvermogen om het onderzoek voor dit proefschrift af te ronden. Dank je wel daarvoor!
Tot slot, lieve Mark, wat had ik de afgelopen jaren zonder jou gemoeten. Bedankt voor je relativeringsvermogen, je begrip en alle keren dat jij een stapje harder liep als bij mij het batterijtje leeg was. Ik ben blij dat we over zoveel dingen samen kunnen praten; zelfs over metabole gezondheid, microarrays en zuurstofrestrictie. Thomas, jij bent het mooiste resultaat van de afgelopen 5 jaar. Wat luister ik graag naar je kleurrijke ideeën en verhalen. Ik hoop dat je altijd zo vrolijk en fantasievol blijft.

List of publications

- **Duivenvoorde LP**, van Schothorst EM, Bunschoten A, Keijer J, 2011 *Dietary restriction of mice on a high-fat diet induces substrate efficiency and improves metabolic health*. Journal of Molecular Endocrinology 47:81-97
- **Duivenvoorde LP**, van Schothorst EM, Derous D, van der Stelt I, Masania J, Rabbani N, Thornalley PJ, Keijer J, 2014 *Oxygen restriction as challenge test reveals early high-fat-diet-induced changes in glucose and lipid metabolism*. Pflügers Archive - European Journal of Physiology DOI 10.1007/s00424-014-1553-8
- **Duivenvoorde LP**, van Schothorst EM, Swarts HJ, Keijer J, 2015 *Assessment of Metabolic Flexibility of Old and Adult Mice Using Three Noninvasive, Indirect Calorimetry-Based Treatments.* Journal of Gerontology A. 70: 282-293
- **Duivenvoorde LP**, van Schothorst EM, Swarts HJ, Kuda O, Steenbergh E, Termeulen S, Kopecky J, and Keijer J, *A difference in fatty acid composition of isocaloric high-fat diets alters metabolic flexibility in male C57BL/6JOlaHsd mice.* Revision submitted to PLOS One
- **Duivenvoorde LP**, van Schothorst EM, Kuda O, Cerna M, van der Stelt I, Hoek-van den Hil EF, Mastorakou D, Kopecky J, and Keijer J, *Metabolic adaptation of white adipose tissue to acute short-term oxygen restriction in mice.* Submitted

- van den Berg M, **Duivenvoorde L**, Wang G, Tribuhl S, Bukovinszky T, Vet LEM, Dicke M, Smid HM, 2011 *Natural variation in learning and memory dynamics studied by artificial selection on learning rate in parasitic wasps.* Animal Behaviour 81: 325–333
- Kelder T, Summer G, Caspers M, van Schothorst EM, Keijer J, **Duivenvoorde L**, Klaus S, Voigt A, *et al*., 2014 *White adipose tissue reference network: a knowledge resource for exploring health-relevant relations*. Genes and Nutrition 10: 439-457
- Hoevenaars FPM, Keijer J, van der Stelt I, Široká J, **Duivenvoorde LPM**, Herreman L, van Nes R, Hegeman MA, Friedecký D, van Schothorst EM, *Mild oxygen restriction changes serum adiponectin and metabolite profiles and CCDC3 levels in obese mice white adipose tissue, not triggering adipose tissue inflammation.* Submitted

About the author

Lucinda (Loes) Petronella Maria Duivenvoorde was born on the 16th of November 1984 in Breda, the Netherlands. In 2003 she graduated from the Mencia Mendoza Lyceum in Breda, after which she moved to Wageningen to study Biology at Wageningen University. During her Bachelor studies, Loes obtained a fellowship from the Erasmus Programme to follow part of her Bachelor courses abroad, at the Università di Perugia, Italy. During her Master studies, Loes completed two theses and one internship. Her first thesis was performed at the department of Entomology, Wageningen University. This thesis focused on the molecular and behavioural background of memory retention in parasitic wasps. Her second thesis was performed at the Georg-August-Universität in Göttingen, Germany. In this thesis Loes studied the endocrine regulation of vocalization in grasshoppers. During her internship at the Rudolf Magnus Institute in Utrecht, the Netherlands, she focused on the molecular and behavioral background of the eating disorder Anorexia Nervosa. In January 2010 she started as a PhD student at the department of Human and Animal Physiology, Wageningen University. The PhD project was part of the European Research Consortium BIOCLAIMS and is presented in this dissertation.

Educational statement

WIAS Graduate School Training and Supervision plan

Basic courses
WIAS Introduction course (04-2010)
Course on philosophy of science and/ or ethics (09-2010)

Scientific exposure
International conferences:
Symposium Bioenergetics: live and let die (Nijmegen 11-2010)
BIOCLAIMS symposium (Mallorca 03-2010)
BIOCLAIMS meeting (Potsdam 12-2010)
BIOCLAIMS meeting (Prague 06-2011)
Biennial Colloquium Series Nutrition, Metabolism and the Brain (Groningen 04-2011)
Phenotypic Flexibility Symposium (Madrid 02-2013)
Seminars and workshops:
WIAS science day (Wageningen 02-2010, 2011 and 2013)
NuGO-workshop on obesity and diabetes (Munich, 02-2010)
Poster Presentations:
Phenotypic Flexibility Symposium (Madrid 02-2013)
Mitofood Conference (Wageningen 04-2011)
Oral presentations:
BIOCLAIMS consortium meeting (Potsdam 12-2010)
BIOCLAIMS consortium meeting (Prague 06-2011)
WIAS science day (Wageningen 02-2013)

In-Depth Studies
WIAS Advanced Statistics Course : Design of Experiments (02-2010)
PhD course Measuring mitochondrial function (04-2011)
PhD Summer school Mitochondrial Physiology - Theory & Praxis (09-2013)
HAP scientific meetings (2010-2014)

Statutory Courses
Use of Laboratory Animals (11-2009)
Laboratory Use of Isotopes 5B (05-2010)

Professional Skills Support Courses
Interpersonal communication for PhD students (5/6-10-2011)
Afstudeervak organiseren en begeleiden (05-2011)
Techniques for Writing and Presenting a Scientific Paper (10-2012)
Voice and Presentation Skills Training (04-2012)
High-Impact Writing Course (11-2013)

Research skills and educational skills training
External training period (use and analysis of HPLC-MS) (Prague 07-2014)
Supervision of MSc students (2010-2014; 8 students)

Colophon

The research described in this thesis was financially supported by the European Union's Seventh Framework Program FP7 2007-2013 under grant agreement no. 244995 (BIOCLAIMS Project).

Financial support from the Human and Animal Physiology Group of Wageningen University and TSE Systems GmbH for printing this thesis is gratefully acknowledged.

Cover design, lay out and pictures: Loes Duivenvoorde
Printing: CPI Koninklijke Wöhrmann, Zutphen, the Netherlands